

Transcranial magnetic stimulation
combined with functional magnetic
resonance imaging:
From target identification to prediction of
therapeutic effects in stroke patients

Inaugural-Dissertation

zur

Erlangung des Doktorgrades

der Mathematisch-Naturwissenschaftlichen Fakultät

der Universität zu Köln

vorgelegt von

Svenja Diekhoff

aus Dormagen

2011

Berichterstatter:

Prof. Dr. Ansgar Büschges

(Gutachter)

Prof. Dr. Gereon Fink

PD Dr. Christian Grefkes

Tag der mündlichen Prüfung:

26.10.2011

Table of contents

I List of Abbreviations	1
II List of Figures.....	5
III List of Tables.....	7
IV Abstract	8
V Kurzzusammenfassung.....	12
1 General introduction.....	17
1.1 Stroke	17
1.2 The human motor system	18
1.3 Definition of terms	21
1.3.1 Clinical stages	21
1.3.2 Cerebral hemispheres	21
1.3.3 Cortico-cortical connectivity.....	22
1.4 Transcranial magnetic stimulation (TMS)	23
1.4.1 Stereotaxic frameless neuronavigation.....	25
1.4.2 Single-pulse TMS.....	27
1.4.3 Paired-pulse TMS.....	29
1.4.4 Repetitive transcranial magnetic stimulation (rTMS).....	36
1.5 Functional magnetic resonance imaging (fMRI)	41
1.5.1 Fundamentals of magnetic resonance imaging (MRI) physics	41
1.5.2 MRI signal types	41
1.5.3 fMRI data analysis	45
1.6 Dynamic causal modelling (DCM)	46
2 Objectives and structure of the thesis.....	48
2.1 Summary of the medical problem	48
2.2 Study I & II: Reducing variance across studies	49
2.3 Study III: Reducing variance across patients	50
3 Study I: Spatial congruence of fMRI and TMS in healthy subjects.....	52
3.1 Introduction Study I	52
3.2 Methods Study I	54
3.2.1 Subjects	54
3.2.2 fMRI motor paradigm	54

3.2.3 fMRI data acquisition.....	55
3.2.4 Analysis of individual fMRI data.....	56
3.2.5 Identification of fMRI peak voxel.....	56
3.2.6 Identification of fMRI CoGs	57
3.2.7 Group analysis of fMRI data	57
3.2.8 Neuronavigated TMS apparatus.....	57
3.2.9 Motor hotspot and resting motor threshold	58
3.2.10 TMS motor mapping	58
3.2.11 TMS of peak voxel coordinates at 120 % RMT.....	60
3.3 Results Study I	60
3.3.1 fMRI group analysis.....	60
3.3.2 Individual fMRI peak voxel coordinates.....	62
3.3.3 Individual fMRI CoG coordinates.....	64
3.3.4 Differences in fMRI and TMS positions.....	64
3.3.5 Euclidian distances between fMRI and TMS positions	65
3.3.6 TMS of fMRI peak voxel with 120 % RMT	66
3.3.7 Tests to exclude spatial errors of the TMS equipment.....	68
3.4 Discussion Study I.....	72
3.4.1 Localization differences between fMRI sequences.....	72
3.4.2 Localization differences between fMRI and TMS	76
3.4.3 Possible explanations for the anterior shift of optimal TMS positions.....	77
3.4.4 Implications and limitations	80
4 Study II: Spatial Congruence of fMRI and TMS in stroke patients.....	81
4.1 Introduction Study II	81
4.2 Methods Study II.....	83
4.2.1 Subjects	83
4.2.2 fMRI motor paradigm	85
4.2.3 fMRI data acquisition.....	86
4.2.4 fMRI data analysis	87
4.2.5 Identification of fMRI peak voxel and fMRI CoGs.....	87
4.2.6 Group analysis of fMRI data	88
4.2.7 Neuronavigated TMS apparatus.....	88
4.2.8 Motor hotspot and resting motor threshold	89
4.2.9 TMS Motor Mapping	89

4.2.10 TMS of peak voxel coordinates at 120 % RMT.....	90
4.3 Results Study II.....	90
4.3.1 fMRI group analysis.....	90
4.3.2 Statistical Z-values at individual fMRI peak voxels	98
4.3.3 Differences in fMRI and TMS positions.....	98
4.3.4 Euclidian distances between fMRI and TMS positions	102
4.3.5 TMS of fMRI peak voxel with 120 % RMT	103
4.3.6 Results of TMS motor mappings	104
4.4 Discussion Study II	106
4.4.1 fMRI group analysis.....	106
4.4.2 Statistical Z-values at individual fMRI peak voxels	109
4.4.3 Differences in fMRI and TMS positions.....	109
4.4.4 Euclidian distances between fMRI and TMS positions	110
4.4.5 TMS of fMRI peak voxel with 120 % RMT	111
4.4.6 Results of TMS motor mappings	111
4.4.7 Conclusions Study II	112
5 Study III: Prediction of TBS effects.....	114
5.1 Introduction Study III.....	114
5.2 Methods Study III.....	116
5.2.1 Subjects	116
5.2.2 Clinical impairment score (CIS)	119
5.2.3 Experimental design.....	119
5.2.4 Theta-burst stimulation (TBS) interventions.....	121
5.2.5 TBS effects.....	122
5.2.6 Investigation of electrophysiological TMS parameters at baseline.....	124
5.2.7 Functional magnetic resonance imaging (fMRI) at baseline.....	127
5.2.8 Effects of lesion location, lesion size, and lesion age	138
5.2.9 Statistical analyses.....	139
5.3 Results Study III.....	139
5.3.1 Motor impairment in stroke patients	139
5.3.2 TBS effects	140
5.3.3 Electrophysiological TMS parameters	143
5.3.4 Functional magnetic resonance imaging (fMRI).....	145
5.3.5 Dynamic causal modelling (DCM)	152

5.4 Discussion Study III	164
5.4.1 TBS effects in stroke patients.....	164
5.4.2 Baseline parameters – differences between patients and controls	169
5.4.3 Movement related fMRI signal	175
5.4.4 The functional role of the contralesional hemisphere	177
5.4.5 Dynamic Causal Modelling (DCM)	178
5.4.6 Prediction of TBS effects	183
6 Conclusions and outlook	192
6.1 Study I & II: Reducing variance across studies	192
6.2 Study III: Reducing variance across patients	194
7 References	195
8 Acknowledgements	213
9 Erklärung	214

I List of Abbreviations

AMT: Active motor threshold
ANOVA: Analysis of variance
AP: Anterior-posterior
APB: Abductor pollicis brevis muscle
ARAT: Action Research Arm Test
ASL: Arterial spin labelling
BA: Brodmann area
BET: Brain extraction tool
BMS: Bayesian model selection
BOLD: Blood oxygenation level dependent
CASL: Continuous arterial spin labelling
CBF: Cerebral blood flow
CBV: Cerebral blood volume
CI: Constraint-induced movement therapy
CIS: Clinical impairment score
CoG: Centre of gravity
CS: Conditioning stimulus
CSF: Cerebrospinal fluid
CST: Cortico-spinal tract
cTBS: Continuous theta-burst stimulation
DCM: Dynamic causal modelling
DLPFC: Dorsolateral prefrontal cortex
dPMC: Dorsal premotor cortex
DWI: Diffusion-weighted imaging
EEG: Electroencephalography
EF: Electric field
EHI: Edinburgh Handedness Inventory
EMG: Electromyography
EPI: Echo-planar imaging
EPSP: Excitatory postsynaptic potential
FAIR: Flow sensitive alternating inversion recovery

FDI: First dorsal interosseous muscle
FDR: False discovery rate
FEAT: Functional magnetic resonance imaging expert analysis tool
FILM: FMRIB's improved linear model
FLAME: FMRIB's local analysis of mixed effects
FLIRT: FMRIB's linear image registration tool
fMRI: Functional magnetic resonance imaging
FMRIB: Oxford Centre for Functional Magnetic Resonance Imaging of the Brain
FNIRT: FMRIB's non-linear image registration tool
FOCI: Frequency offset corrected inversion
FOV: Field-of-view
FSL: FMRIB's Software Library
FT: Finger tapping
FWHM: Full width at half maximum
GABA_A: gamma-aminobutyric acid receptor A
GF: Grip force
GLM: General linear model
GRE: Gradient-Echo
HF: High frequency
H-reflex: Hoffmann reflex
HRF: Haemodynamic response function
ICF: Intracortical facilitation
IHF: Interhemispheric facilitation
IHI: Interhemispheric inhibition
ISI: Inter-stimulus interval
iTBS: Intermittent theta-burst stimulation
JTT: Jebsen-Taylor Hand Function Test
LI: Laterality index
LICF: Long-interval intracortical facilitation
LICI: Long-interval intracortical inhibition
LTD: Long-term depression
LTP: Long-term potentiation
M1: Primary motor cortex

M1/S1: Primary sensorimotor cortex
MCA: Middle cerebral artery
MCFLIRT: Motion correction using FMRIB's linear image registration tool
MEP: Motor-evoked potential
MIS: Motor improvement score
MNI: Montreal Neurological Institute
MP-RAGE: Magnetization-prepared rapid acquisition gradient echo
MRI: Magnetic resonance imaging
mRS: Modified Rankin-Scale
MT: Motor threshold
MTAT: Motor threshold assessment tool
NBS: Navigated brain stimulation
NIHSS: National Institutes of Health stroke scale
NMDA: N-methyl-D-aspartate acid
PA: Posterior-anterior
PASL: Pulsed arterial spin labelling
PASW: Predictive Analysis Software
PCA: Principal Component Analysis
PD: Perfusion deficit
PET: Positron emission tomography
PICORE: Proximal inversion with a control for off-resonance effects
PMC: Premotor cortex
PPI: Psychophysiological interactions
Q2TIPS: Quantitative imaging of perfusion using a single subtraction with interleaved thin-slice TI_1 periodic saturation
QUIPSS II: Quantitative imaging of perfusion using a single subtraction
ROI: Region-of-interest
RMT: Resting motor threshold
rTMS: Repetitive transcranial magnetic stimulation
S1: Primary somatosensory cortex
S2: Secondary somatosensory cortex
SE: Spin-Echo
SEM: Structural equation modelling

SICF: Short-interval intracortical facilitation
SICI: Short-interval intracortical inhibition
SMA: Supplementary motor area
SNS: Stereotaxic neuronavigation systems
SNR: Signal-to-noise ratio
SPL: Superior parietal lobule
SPM: Statistical Parametric Mapping
TI: Longitudinal relaxation time
*T2/T2**: Transverse relaxation time
TBS: Theta-burst stimulation
TE: Echo time
TES: Transcranial electric stimulation
TFT: Thin film transistor
TI: Inversion time
TMS: Transcranial magnetic stimulation
TR: Time of repetition
TS: Test stimulus
V1: Primary visual cortex
vPMC: Ventral premotor cortex
VLSM: Voxel-based lesion symptom mapping
WHO: World Health Organization

II List of Figures

Figure 1.1: Introduction: The hand knob formation.....	18
Figure 1.2: Introduction: The transition between BA4 and BA6.....	19
Figure 1.3: Introduction: The human premotor cortex.....	20
Figure 1.4: Introduction: Designation of cerebral hemispheres.....	22
Figure 1.5: Introduction: Principles of transcranial magnetic stimulation.....	24
Figure 1.6: Introduction: Stereotaxic frameless neuronavigation.....	26
Figure 1.7: Introduction: Example TMS motor map.....	29
Figure 1.8: Introduction: Paired-pulse TMS applied to one hemisphere.....	31
Figure 1.9: Introduction: Paired-pulse TMS applied to both hemispheres.....	34
Figure 1.10: Introduction: Repetitive transcranial magnetic stimulation protocols.....	37
Figure 1.11: Introduction: The model of hemispheric competition.....	39
Figure 1.12: Introduction: The haemodynamic response function.....	43
Figure 3.1: Study I: Results of the fMRI group analysis.....	61
Figure 3.2: Study I: Localization of the primary motor cortex with fMRI and TMS.....	63
Figure 3.3: Study I: Stimulation of brain tissue at fMRI peak voxel coordinates with TMS ..	68
Figure 3.4: Study I: Results of TMS motor mappings.....	71
Figure 3.5: Study I: TMS motor mapping with inverted induced current direction.....	71
Figure 4.1: Study II: Results of the fMRI group analysis (fixed movement condition).....	94
Figure 4.2: Study II: Results of the fMRI group analysis (adjusted movement condition).....	96
Figure 4.3: Study II: Localization of the primary motor cortex with fMRI and TMS.....	101
Figure 4.4: Study II: Results of TMS motor mappings in healthy subjects.....	105
Figure 5.1: Study III: Lesion locations.....	117
Figure 5.2: Study III: Experimental design.....	120
Figure 5.3: Study III: Hypothetical models on interregional coupling (models 1-16).....	135
Figure 5.4: Study III: Hypothetical models on interregional coupling (models 17-28).....	136
Figure 5.5: Study III: Hypothetical models on interregional coupling (models 29-36).....	137
Figure 5.6: Study III: Behavioural improvements following theta-burst stimulation.....	141
Figure 5.7: Study III: Movement-related fMRI signal in cortical motor areas.....	148
Figure 5.8: Study III: Correlation between laterality and TBS effects.....	151
Figure 5.9: Study III: Results of the Bayesian model selection procedure.....	153

Figure 5.10: Study III: Significant interregional couplings	156
Figure 5.11: Study III: Significant group differences in effective connectivity	158
Figure 5.12: Study III: Prediction of theta-burst stimulation effects	161
Figure 5.13: Study III: Results of the voxel-based lesion symptom mapping	162

III List of Tables

Table 1.1: Introduction: Designation of clinical stages.....	21
Table 1.2: Introduction: Paired-pulse TMS parameters applied to one hemisphere	30
Table 1.3: Introduction: Paired-pulse TMS parameters assessed over both hemispheres	33
Table 3.1: Study I: Positions of highest fMRI signals and highest TMS effects	64
Table 3.2: Study I: Euclidean distances between fMRI and TMS sites	66
Table 3.3: Study I: Qualitative comparison of different motor mapping approaches	76
Table 4.1: Study II: Demographical, clinical, and behavioural data	84
Table 4.2: Study II: Peak activation cluster of the fMRI group analysis	97
Table 4.3: Study II: Mean fMRI and TMS positions in MNI space	99
Table 4.4: Study II: Mean Euclidean distances between fMRI and TMS positions	103
Table 5.1: Study III: Demographical, clinical, and behavioural data	118
Table 5.2: Study III: Peak voxel coordinates used for ROI analyses and DCM.....	133
Table 5.3: Study III: Summary of previous studies using TBS.....	167
Table 5.4: Study III: Summary of results	170

IV Abstract

Repetitive transcranial magnetic stimulation (rTMS), particularly theta-burst stimulation (TBS), can be applied to modulate cortical excitability beyond the period of stimulation (Huang et al., 2005). Consequently, rTMS is regarded to have high therapeutic potential for treatment of various psychiatric and neurological diseases related to cortical hypo- or hyperexcitability such as stroke (Ridding & Rothwell, 2007). Whether rTMS induced effects are sufficiently robust to be useful in clinical settings is currently under intense investigation. The most challenging problem appears to be considerably high variability in rTMS induced effects both, across studies (Hoogendam et al., 2010) and individual patients (Ameli et al., 2009). Hence, the major goal of the present thesis was to improve rTMS intervention strategies in stroke patients suffering from chronic motor hand deficits by multimodal uses of (repetitive) TMS with state-of-the-art neuroimaging techniques.

Sources of variance across studies are likely to be methodological in origin. They might result from different strategies to identify the cortical rTMS target position. Individual functional magnetic resonance (fMRI) data have been demonstrated to yield best spatial approximations of the most excitable TMS position compared to other techniques (Sparing et al., 2008). However, there is still a considerably large spatial mismatch between the cortical position showing highest movement-related fMRI signal and the cortical position yielding highest muscle responses when stimulated with TMS of up to 14 mm (Bastings et al., 1998; Boroojerdi et al., 1999; Herwig et al., 2002; Krings et al., 1997; Lotze et al., 2003; Sparing et al., 2008; Terao et al., 1998). The underlying cause of this spatial mismatch is unknown. Hence, the aim of the **first study (Study I)** of the present thesis was to test the hypothesis that the spatial mismatch between positions with highest fMRI signal change and positions with highest TMS excitability might be caused by the widely-used Gradient-Echo blood oxygenation level dependent (GRE-BOLD) fMRI technique. GRE-BOLD signal has been demonstrated to occur further downstream from the site of neural activity in large veins running on the cerebral surface (Uludag et al., 2009). Consequently, we tested the hypothesis that alternative fMRI sequences may localize neural activity (i) closer to the anatomical motor hand area, i.e. Brodmann Area 4 (BA4), and (ii) closer to the optimal TMS position than GRE-BOLD. The following alternative fMRI techniques were tested: (i) Spin-Echo (SE-BOLD) assessing blood oxygenation level dependent signal changes with decreased sensitivity for the macrovasculature at high magnetic fields (≥ 3 Tesla, Uludag et al., 2009)

and (ii) arterial spin labelling (ASL), assessing local changes in cerebral blood flow (ASL-CBF) which have been shown to occur in close proximity to synaptic activity (Duong et al., 2000). GRE-BOLD, SE-BOLD, and ASL-CBF signal changes during right thumb abductions were obtained from 15 healthy young subjects at 3 Tesla. In 12 subjects, brain tissue at fMRI peak voxel coordinates was stimulated with neuronavigated TMS to investigate whether spatial differences between fMRI techniques are functionally relevant, i.e. impact on motor-evoked potentials (MEPs) recorded from a contralateral target muscle, which is involved in thumb abductions. A systematic TMS motor mapping was performed to identify the most excitable TMS position (i.e. the TMS *hotspot*) and the *centre-of-gravity* (i.e. the TMS CoG), which considers the spatial distribution of excitability in the pericentral region. Euclidean distances between TMS and fMRI positions were calculated for each fMRI technique. Results indicated that highest SE-BOLD and ASL-CBF signal changes occurred in the anterior wall of the central sulcus (BA4), whereas highest GRE-BOLD signal changes occurred significantly closer to the gyral surface where most large draining veins are located. fMRI techniques were not significantly different from each other in Euclidean distances to optimal TMS positions since optimal TMS positions were located considerably more anterior (and slightly surprisingly in premotor cortex (BA6) and not BA4). Stimulation of brain tissue at GRE-BOLD peak voxel coordinates with TMS resulted in significantly higher MEPs (compared to SE-BOLD and ASL-CBF coordinates). This was probably the case because GRE-BOLD positions tended to be located at the gyral crown, which was slightly (but not significantly) closer to the TMS hotspot position. Taken together, findings of Study I suggest that spatial differences between fMRI and TMS positions are not caused by spatial unspecificity of the widely-used GRE-BOLD fMRI technique. Hence, other factors such as complex interactions between brain tissue and the TMS induced electric field (Opitz et al., 2011), could be the underlying cause.

Identification of the cortical rTMS target position is particularly challenging in stroke patients since reorganization processes after stroke may shift both, fMRI and TMS positions in unknown direction and extend (Rossini et al., 1998). In the **second study (Study II)** of the present thesis, we therefore tested whether findings obtained from healthy young subjects in Study I do also apply to chronic stroke patients and older (i.e. age-matched) healthy control subjects. In this study, arterial spin labelling (ASL) was used to assess CBF and BOLD signal changes simultaneously during thumb abductions with the affected/non-dominant and the unaffected/dominant hand in 15 chronic stroke patients and 13 age-matched healthy control

subjects at 3 Tesla. Brain tissue at fMRI peak voxel coordinates was stimulated with neuronavigated TMS to test whether spatial differences are functionally relevant and impact on MEPs. Systematic TMS motor mappings were performed for both hemispheres in overall 12 subjects (6 stroke patients and 6 healthy subjects). Euclidean distances between fMRI and TMS positions were calculated for each hemisphere and fMRI technique. In line with results of Study I, highest ASL-CBF signal changes were located in the anterior wall of the central sulcus (BA4), whereas highest ASL-BOLD signal changes occurred significantly closer to the gyral surface. In contrast to Study I, there were no significant differences between ASL-CBF and ASL-BOLD positions in MEPs when stimulated with neuronavigated TMS, which suggests that spatial differences (in depth) were not functionally relevant for TMS applications. In line with Study I, there were no significant differences between fMRI techniques in Euclidean distances to optimal TMS positions, since optimal TMS positions were located considerably more anterior than fMRI positions (in premotor cortex, i.e. BA6). Stroke patients showed overall larger displacements (between fMRI and TMS positions) on the ipsilesional (but not the contralesional) hemisphere compared to healthy subjects. However, none of the fMRI techniques yielded positions significantly closer to the optimal TMS position. Hence, functional reorganization may impact on spatial congruence between fMRI and TMS, but the effect is similar for ASL-CBF and ASL-BOLD.

Pathomechanisms underlying stroke induced motor deficits are still poorly understood but a simplified *model of hemispheric competition* has been suggested, which proposes relative hypoexcitability of the ipsilesional hemisphere and hyperexcitability of the contralesional hemisphere leading to pathologically increased interhemispheric inhibition from the contralesional onto the ipsilesional hemisphere during movements of the paretic hand (Duque et al., 2005; Grefkes et al., 2008b, 2010; Murase et al., 2004). In line with the *model of hemispheric competition*, both increasing excitability of the ipsilesional hemisphere (Khedr et al., 2005; Talelli et al., 2007) as well as decreasing excitability of the contralesional hemisphere (Fregni et al., 2006; Di Lazzaro et al., 2008a) have been demonstrated to normalize cortical excitability towards physiological levels and/or ameliorate motor performance of the stroke affected hand. However, there is considerably high inter-individual variance and some patients may even show deteriorations of motor performance after rTMS (Ameli et al., 2009). Therefore, the aim of the **third study (Study III)** was to identify reliable predictors for TBS effects on motor performance of the affected hand in stroke patients, which appears essential for successful implementation of TBS in neurorehabilitation. Overall,

13 chronic stroke patients with unilateral motor hand deficit and 12 age-matched healthy control subjects were included in the study. All patients received 3 different TBS interventions on 3 different days: (i) intermittent TBS (iTBS, facilitatory) over the primary motor cortex (M1) of the ipsilesional hemisphere, (ii) continuous TBS (cTBS, inhibitory) over M1 of the contralesional hemisphere, and (iii) either iTBS or cTBS over a control stimulation site (to control for placebo effects). Motor performance was measured before and after each TBS session with 3 different motor tasks and an overall motor improvement score was calculated. All subjects participated in an fMRI experiment, in which they performed rhythmic fist closures with their affected/non-dominant and unaffected/dominant hand. A laterality index (LI), reflecting laterality of fMRI signal in cortical motor areas was calculated. Effective connectivity, i.e. the direct or indirect causal influence that activity in one area exerts on activity of another area (Friston et al., 1993a), was inferred from fMRI data by means of dynamic causal modelling (DCM). Due to relatively high inter-individual variance, neither iTBS nor cTBS was significantly different from control TBS in terms of average behavioural (or electrophysiological) changes over the group of patients. However, beneficial effects of iTBS over the ipsilesional hemisphere were predicted by a unilateral fMRI activation pattern during movements of the affected hand and by the integrity of the cortical motor network. The more pronounced the promoting influence from the ipsilesional supplementary motor area (SMA) onto ipsilesional M1 and the more pronounced the inhibitory effect originating from ipsilesional M1 onto contralesional M1, the better was the behavioural response to facilitatory iTBS applied to the ipsilesional hemisphere. No significant correlations were found for behavioural improvements following cTBS or behavioural changes of the unaffected hand. Taken together, Study III yielded promising results indicating that laterality of fMRI signal and integrity of the motor network architecture constitute promising predictors for response to iTBS. In patients in whom the connectivity pattern of the ipsilesional motor network resembled physiological network connectivity patterns (i.e. preserved inhibition of the contralesional hemisphere and supportive role of the SMA of the ipsilesional hemisphere), beneficial effects of iTBS over the ipsilesional hemisphere could be observed. In contrast, patients with severely disturbed motor networks did not respond to iTBS or even deteriorated.

V Kurzzusammenfassung

Die repetitive transkranielle Magnetstimulation (rTMS), insbesondere die Theta-Burst Stimulation (TBS), kann dazu verwendet werden, kortikale Erregbarkeit über den Stimulationszeitraum hinaus zu modulieren (Huang et al., 2005). Daher wird der rTMS ein hohes therapeutisches Potenzial für die Behandlung diverser psychiatrischer und neurologischer Erkrankungen zugeschrieben, die mit einer kortikalen Hypo- oder Hyperexzitabilität einhergehen, wie es beispielsweise nach einem Schlaganfall der Fall ist (Ridding & Rothwell, 2007). Ob die durch die rTMS induzierten Effekte ausreichend robust sind, um sich im klinischen Alltag durchzusetzen, wird momentan intensiv untersucht. Die größte Herausforderung besteht möglicherweise darin, die hohe Varianz in rTMS vermittelten Effekten sowohl zwischen Studien (Hoogendam et al., 2010) als auch zwischen einzelnen Patienten (Ameli et al., 2009) zu reduzieren. Daher war das Hauptziel der vorliegenden Doktorarbeit, die Verbesserung von rTMS-Interventionsstrategien für Schlaganfallpatienten mit chronifiziertem motorischem Defizit der Hand durch die multimodale Anwendung der (repetitiven) TMS mit modernsten bildgebenden Verfahren.

Die Quelle hoher Varianz über Studien hinweg ist höchstwahrscheinlich methodischen Ursprungs und könnte daraus resultieren, dass verschiedenen Strategien zur Identifizierung der kortikalen rTMS Zielposition verwendet werden. Individuelle funktionelle Magnetresonanz Tomographie (fMRT) liefert die beste räumliche Annäherung an die Position mit höchster TMS-Erregbarkeit im Vergleich zu anderen Methoden (Sparing et al., 2008). Dennoch gibt es immer noch eine relativ große räumliche Diskrepanz zwischen der kortikalen Position höchster bewegungsabhängiger fMRT-Aktivität und der kortikalen Position, die zu höchsten Muskelantworten führt wenn sie mit TMS stimuliert wird, von bis zu 14 mm (Bastings et al., 1998; Boroojerdi et al., 1999; Herwig et al., 2002; Krings et al., 1997; Lotze et al., 2003; Sparing et al., 2008; Terao et al., 1998). Die Ursache dieser räumlichen Diskrepanz ist unbekannt. Daher war das Ziel der **ersten Studie (Study I)** die Hypothese zu testen, dass die räumliche Diskrepanz zwischen Positionen mit höchster fMRT-Aktivität und Positionen mit höchster TMS-Erregbarkeit durch die Verwendung der weitverbreiteten Gradienten-Echo *blood oxygenation level dependent* (GRE-BOLD) fMRT-Methode zustande kommt. Das GRE-BOLD-Signal entsteht „stromabwärts“ von neuraler Aktivität in großen Venen, die auf der Hirnoberfläche verlaufen (Uludag et al., 2009). Daher testeten wir die Hypothese, dass alternative fMRT-Sequenzen neurale Aktivität (i) näher zum anatomischen

motorischen Handareal, Brodmann Area 4 (BA4) und (ii) näher zur optimalen TMS-Position lokalisieren als GRE-BOLD. Die folgenden fMRT-Sequenzen wurden als Alternativen zu GRE-BOLD getestet: (i) Spin-Echo das den *blood oxygenation level dependent* Effekt (SE-BOLD) bei höheren magnetischen Feldstärken (≥ 3 Tesla) mit verringerter Sensitivität für große Gefäße misst und (ii) die arterielle Spinmarkierung (arterial spin labelling, ASL), die lokale Veränderungen im zerebralen Blutfluss (cerebral blood flow, CBF) misst, die in unmittelbarer Nähe synaptischer Aktivität entstehen (Duong et al., 2000). GRE-BOLD-, SE-BOLD- und ASL-CBF-Signalveränderungen während Abduktionsbewegungen des rechten Daumens wurden von 15 jungen gesunden Probanden bei einer Feldstärke von 3 Tesla erhoben. Bei 12 Probanden wurde außerdem Hirngewebe an der Position des fMRT-Maximums mittels neuronavigierter TMS stimuliert, um zu testen ob räumliche Unterschiede zwischen fMRT-Methoden funktionell relevant sind, das heißt einen messbaren Einfluss auf motorisch evozierte Potentiale (MEPs) haben, die vom einem kontralateralen Zielmuskel abgeleitet wurden, der an der Daumenabduktion maßgeblich beteiligt ist. Mittels TMS wurde eine systematische Kartierung des motorischen Kortex vorgenommen, anhand derer die Position höchster kortikaler Erregbarkeit (TMS *hotspot*) und ein sogenanntes *centre-of-gravity* (TMS CoG) bestimmt wurde, welches die Verteilung kortikaler Erregbarkeit des benachbarten Gewebes mitberücksichtigt. Euklidische Abstände zwischen TMS- und fMRT-Positionen wurden für jede fMRT-Methode berechnet. Die Ergebnisse deuten darauf hin, dass die höchsten SE-BOLD- und ASL-CBF-Signalveränderungen in der Vorderwand des Sulcus centralis auftreten (BA4), während höchste GRE-BOLD-Signalveränderungen signifikant näher zur Hirnoberfläche auftraten, wo die meisten großen Venen verlaufen. Die fMRT-Methoden unterschieden sich nicht signifikant bezüglich ihrer Distanz zur optimalen TMS-Position voneinander, da optimale TMS-Positionen deutlich weiter anterior (und etwas überraschend im prämotorischen Kortex (BA6) und nicht in BA4 lagen). Stimulation des Hirngewebes (das höchste GRE-BOLD-Signalveränderungen zeigte) mittels TMS resultierte in signifikant höheren MEPs im Vergleich zu den anderen beiden fMRT-Methoden. Dies war vermutlich der Fall weil GRE-BOLD-Positionen dazu tendierten auf der Gyriuskrone zu liegen und somit leicht (aber nicht signifikant) näher an der TMS *hotspot* position lagen. Insgesamt konnte also durch die erste Studie gezeigt werden, dass die räumliche Diskrepanz zwischen fMRT- und TMS-Positionen nicht durch die räumliche Unspezifität der weitverbreiteten GRE-BOLD-Methode zustande kommt. Andere Faktoren, wie komplexe

Interaktionen zwischen Hirngewebe und dem durch die TMS induzierten elektrischen Feld (Opitz et al., 2011) könnten stattdessen die Ursache darstellen.

Die Identifizierung der kortikalen Zielregion für die rTMS ist bei Patienten erschwert, da nach einem Schlaganfall Reorganisationsprozesse im Gehirn stattfinden, die dazu führen können, dass sich sowohl fMRT- als auch TMS-Positionen in unbekanntem Ausmaß und in unbekannte Richtung räumlich verschieben (Rossini et al., 1998). In der **zweiten Studie (Study II)** der vorliegenden Doktorarbeit testeten wir daher, ob die Ergebnisse von Study I, die von jungen gesunden Probanden erhoben wurden, auf Schlaganfallpatienten und ältere (d.h. gleichaltrige) gesunde Kontrollprobanden ebenfalls zutreffen. In dieser Studie wurde die arterielle Spinmarkierung (arterial spin labelling, ASL) dazu verwendet, Veränderungen im *blood oxygenation level dependent effect* (BOLD) und im zerebralen Blutfluss (*cerebral blood flow*, CBF) simultan während Daumenabduktionsbewegungen der betroffenen/nicht-dominanten und der nicht-betroffenen/dominanten Hand zu erheben. Die Studie wurde an 15 Patienten im chronischen Stadium und 13 gleichaltrigen gesunden Kontrollprobanden bei einer Feldstärke von 3 Tesla durchgeführt. Hirngewebe an fMRT-Maximums-Positionen wurde mittels neuronavigierter TMS stimuliert, um zu testen ob räumliche Unterschiede funktionell relevant sind und sich auf MEPs auswirken. Eine systematische Kartierung beider motorischer Kortizes wurde bei insgesamt 12 Probanden (6 Schlaganfallpatienten und 6 Kontrollprobanden) mittels TMS erstellt. Euklidische Abstände zwischen fMRT- und TMS-Positionen wurden berechnet. Wie auch in Studie I, traten höchste ASL-CBF-Signalveränderungen in der Vorderwand des Sulcus centralis (BA4) auf, wohingegen höchste ASL-BOLD-Signalveränderungen signifikant näher zur Hirnoberfläche auftraten. Im Gegensatz zur ersten Studie gab es in dieser Studie keinen signifikanten Unterschied zwischen ASL-CBF- und ASL-BOLD-Positionen in durch die direkte TMS-Stimulation resultierenden MEPs, was darauf hinweist, dass signifikante räumliche Unterschiede (in Tiefe) keine funktionelle Relevanz für die TMS besaßen. Wie auch in der ersten Studie, gab es keine signifikanten Unterschiede zwischen den fMRT-Methoden in Euklidischen Abständen zur optimalen TMS-Position, die sich deutlich weiter anterior im prämotorischen Kortex (BA6) befand. Obwohl Patienten auf der ipsiläsionellen Hemisphäre insgesamt größere Distanzen (zwischen fMRT- und TMS-Positionen) im Vergleich zu den gesunden Kontrollprobanden aufwiesen, lieferte keine der fMRT-Methoden Positionen die signifikant näher zur optimalen TMS-Position lagen. Daher scheinen Reorganisationsprozesse einen

Einfluss auf die räumliche Kongruenz von fMRT und TMS zu haben, betreffen aber ASL-CBF ebenso wie ASL-BOLD.

Der Pathomechanismus, der Schlaganfall-induzierten motorischen Defiziten zugrunde liegt, ist größtenteils noch unverstanden. Das stark vereinfachte *Modell der Hemisphärenkonkurrenz* postuliert eine relative Hypoexzitabilität der ipsiläsionellen und Hyperexzitabilität der kontraläsionellen Hemisphäre, was zu einer pathologisch verstärkten Inhibition von der kontraläsionellen Hemisphäre auf die ipsiläsionelle Hemisphäre während Bewegung der betroffenen Hand führt (Duque et al., 2005; Grefkes et al., 2008b, 2010; Murase et al., 2004). Dem *Modell der Hemisphärenkonkurrenz* entsprechend, kann sowohl durch Erhöhung der Exzitabilität der ipsiläsionellen Hemisphäre (Khedr et al., 2005; Talelli et al., 2007) als auch durch Verringerung der Exzitabilität der kontraläsionellen Hemisphäre (Fregni et al., 2006; Di Lazzaro et al., 2008a) eine Normalisierung der kortikalen Exzitabilität hin zu einem physiologischen Gleichgewicht und/oder eine Verbesserung der motorischen Leistung der betroffenen Hand erzielt werden. Es gibt jedoch eine relativ hohe interindividuelle Varianz und einige Patienten können sogar eine verschlechterte motorische Leistung der betroffenen Hand nach rTMS aufweisen (Ameli et al., 2009). Daher war das Ziel der **dritten Studie (Study III)** die Identifizierung zuverlässiger Prädiktoren für die Effekte der TBS auf die motorische Leistung der betroffenen Hand von Schlaganfallpatienten, da dies ein essentieller Schritt für die Implementierung der rTMS in die Neurorehabilitation zu sein scheint. 13 Schlaganfallpatienten mit chronifiziertem motorischem Defizit der Hand und 12 gleichaltrige gesunde Kontrollprobanden nahmen an der Studie teil. Alle Patienten erhielten 3 verschiedene TBS-Interventionen an 3 verschiedenen Tagen: (i) intermittierende TBS (iTBS, fazilitierend) über dem primärmotorischen Kortex (M1) der ipsiläsionellen Hemisphäre, (ii) kontinuierliche (continuous) TBS (cTBS, inhibitorisch) über dem M1 der kontraläsionellen Hemisphäre und (iii) entweder iTBS oder cTBS über einer Kontrollstimulationsposition. Die motorische Leistung wurde vor und nach jeder TBS-Intervention mit 3 unterschiedlichen motorischen Skalen gemessen, auf denen basierend ein allgemeiner Verbesserungswert errechnet wurde. Alle Probanden nahmen an einem fMRT-Experiment teil, in dem sie rhythmische Faustschlussbewegungen mit ihrer betroffenen/nicht-dominanten und ihrer nicht-betroffenen/dominanten Hand durchführten. Ein Lateralitätsindex, der die Lateralität des fMRT-Signals in kortikalen motorischen Arealen widerspiegelt wurde berechnet. Die effektive Konnektivität, also der direkte oder indirekte kausale Einfluss, den Aktivität eines Areals auf die Aktivität eines anderen Areals ausübt (Firston et al., 1993a), wurde mittels

dynamic causal modelling (DCM) aus den fMRT-Zeitreihen geschätzt. Aufgrund einer relativ hohen inter-individuellen Varianz unterschied sich weder die iTBS noch die cTBS signifikant von der Kontrollstimulation bezüglich induzierter Veränderungen in der Leistungsfähigkeit der betroffenen Hand oder Veränderungen in der Exzitabilität der ipsiläsionellen Hemisphäre über die gesamte Gruppe der Patienten hinweg. Positive Effekte der iTBS über der ipsiläsionellen Hemisphäre wurden jedoch signifikant durch ein unilaterales fMRT-Aktivierungsmuster während Bewegung der betroffenen Hand und die Integrität des motorischen Netzwerks prädiziert. Je ausgeprägter der fördernde Einfluss vom ipsiläsionellen supplementär motorischen Areal (SMA) auf den ipsiläsionellen M1 und je ausgeprägter der inhibitorische Einfluss ausgehend vom ipsiläsionellen M1 auf den kontraläsionellen M1, desto höher war die Wahrscheinlichkeit, dass ein Patient von der fazilitierenden iTBS über dem ipsiläsionellen M1 profitierte. Für Verhaltenseffekte nach cTBS und Verhaltenseffekte der nicht-betroffenen Hand wurden keine signifikanten Korrelationen gefunden. Zusammenfassend weisen die Ergebnisse der dritten Studie darauf hin, dass die Lateralität des fMRT-Signals und die Integrität des motorischen Netzwerks vielversprechende Prädiktoren für Verhaltenseffekte nach iTBS darstellen. Bei Patienten bei denen ipsiläsionelle motorische Netzwerkinteraktionen physiologisch auftretenden Netzwerkinteraktionen glichen (erhaltene Inhibition der kontraläsionellen Hemisphäre und unterstützende Rolle des ipsiläsionellen SMA), stellte sich eine Verbesserung der vom Schlaganfall betroffenen Hand ein, wohingegen Patienten mit schwer geschädigtem motorischen Netzwerk keine Veränderungen oder gar eine Verschlechterung nach iTBS zeigten.

1 General introduction

1.1 Stroke

Stroke is caused by an interruption of blood supply to the brain either due to blood vessel blockage (ischaemic stroke, approx. 82%) or blood vessel rupture (haemorrhagic stroke, approx. 14%; Feigin et al., 2009). Both leads to a sudden breakdown in oxygen- and nutrition supply and may cause permanent brain tissue damage. The following World Health Organization (WHO) standard criterion is frequently used to define stroke: “rapidly developing clinical signs of focal (at times global) disturbance of cerebral function, lasting more than 24 hours (if not leading to death) with no apparent cause other than that of vascular origin” (Hatano, 1976). Stroke incidence rates in the years 2000-2008 varied between countries in the range of 74 to 223 (per 100 000 persons per year; Feigin et al., 2009). Spontaneous recovery occurs within three months after stroke until a plateau with relatively stable motor performance is reached after three to six months (Kwakkel et al., 2004). However, clinical outcome after stroke is highly variable across individuals. Data of the German Stroke Database (including 1754 patients) suggest that three months after stroke, 9.5% of patients had died, 58.4% had completely recovered, and 32.1% retained permanent deficits (Weimar et al., 2002). Hemiparesis is the most frequent neurological deficit (occurring in more than 80% of patients), followed by sensory deficits (approx. 45%) and speech deficits (approx. 24%; Rathore et al., 2002). Hemiparesis occurs most often in upper (76%) but also in lower limbs (69%) and the face (55%; Rathore et al., 2002). The ability to live independently after stroke largely depends on reconstitution of motor control. Currently, physical and occupational therapy and at times constraint-induced movement therapy (CI) are used for treatment of stroke-induced hand motor deficits. CI involves immobilization of the unaffected limb to induce “forced use” of the affected limb combined with intense training of the affected limb (Taub et al., 1993). However, additional therapeutic strategies are needed since stroke is the most common cause for permanent disability in adults (Kolominsky-Rabas et al., 2006; Nelles, 2007) and one of the most expensive diseases in industrialised countries (Kolominsky-Rabas et al., 2006).

1.2 The human motor system

The human motor system is composed of cortical and subcortical structures interacting in complex subsystems, which are organized either hierarchically or in parallel (Amunts & Zilles, 2007). Important part of the cortical human motor system is the primary motor cortex (M1; also Brodmann Area (BA) 4; Brodmann, 1909), which is located in the anterior wall of the central sulcus. BA4 is somatotopically organized: foot and leg representations are located in the mesial wall of the precentral gyrus followed by trunk, arm, hand, fingers (from little finger to thumb), face, lips, and tongue representations (from dorsomedial to ventrolateral; Penfield & Rasmussen, 1950). A reliable anatomical landmark for the motor hand representation is the *hand knob* structure, which is shaped like an omega or epsilon in axial slices and hook shaped in sagittal slices (Yousry et al., 1997; Figure 1.1).

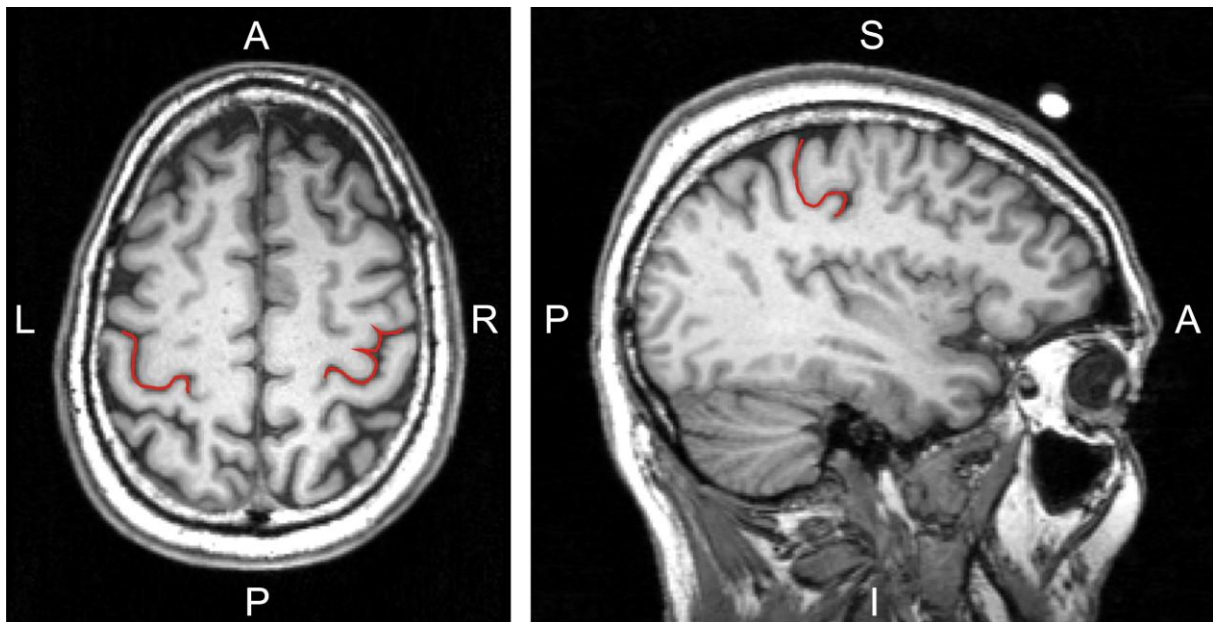


Figure 1.1: Introduction: The hand knob formation. The central sulcus at the hand knob formation is highlighted in red colour on a high-resolution anatomical magnetic resonance image of a healthy volunteer. In the axial slice (image on the left) the hand knob is omega-shaped in the left hemisphere and epsilon-shaped in the right hemisphere. In the sagittal slice (image on the right) the hand knob is shaped like a posteriorly directed hook. (A: anterior; I: inferior; L: left; P: posterior; R: right; S: superior)

The anterior margin of BA4 is the posterior margin of the premotor cortex (PMC; also BA6). Brodmann initially assumed that BA4 extends over the entire surface area of the precentral gyrus (Brodmann, 1909). However, recent histological studies demonstrated that BA4 occupies only a limited part of the exposed surface of the precentral gyrus. The transition

between BA4 and BA6 depends on the lateral position along the central sulcus (Geyer et al., 2000; Rademacher et al., 2001; White et al., 1997). In its dorsomedial part, BA4 covers posterior aspects of the crown of the precentral gyrus, more laterally BA4 tends to submerge inside the central sulcus (Geyer et al., 2000; Figure 1.2).

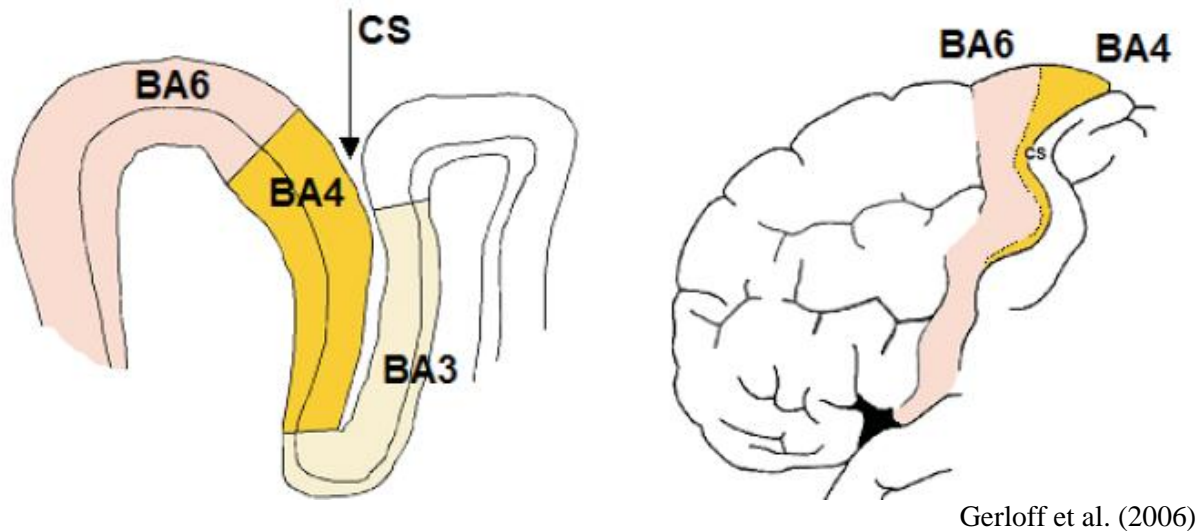


Figure 1.2: Introduction: The transition between BA4 and BA6. As a rule, the primary motor cortex (BA4) occupies only a limited part of the exposed surface of the precentral gyrus, mainly in its dorsomedial part. More laterally, BA4 tends to be buried in the depth of the central sulcus. This latter aspect is depicted in the figure on the right. (BA: Brodmann Area; BA3: primary somatosensory cortex; BA4: primary motor cortex; BA6: premotor cortex; CS: central sulcus)

Cytoarchitecturally, BA4 is characterized by absence of lamina IV and presence of giant Betz cells in lamina V whose axons bend down in the precentral gyrus and form the cortico-spinal tract (CST). The CST passes through the posterior limb of the internal capsule and the cerebral peduncle before 80-85% of the fibres cross at the decussation of pyramids in the medulla oblongata to the contralateral side (referred to as lateral CST). Fibres not crossing in the brain stem (referred to as ventral CST) cross in the spinal cord segment of their target cells. Pyramidal cells enervate motoneurons in the anterior horn of the spinal cord either directly or indirectly via interneurons (Amunts & Zilles, 2007). Finally, spinal cord motoneurons terminate onto skeletal muscles. The human extra-pyramidal motor system is composed of the basal ganglia, cerebellum, and extra-pyramidal fibre tracts connecting the motor cortex with motor brain stem nuclei and the spinal cord respectively. These fibre tracts may act as alternative pathways in the case of severe CST damage after stroke.

The PMC (BA6) is an important cortical motor area engaged in both movement preparation and movement execution. BA6 can be subdivided into at least three distinctive functional areas: (i) the supplementary motor area (SMA), (ii) the dorsal premotor cortex (dPMC), and (iii) the ventral premotor cortex (vPMC). The anterior limit of BA6 is at an individually variable distance anterior to the precentral sulcus and does not correspond to a specific anatomical landmark (Geyer et al., 2004). However, the extent of BA6 is greater in dorsomedial parts of the hemispheres and recedes caudally in ventrolateral parts merging with the precentral sulcus close to the Sylvian fissure (Amunts et al., 1999; Figure 1.3).

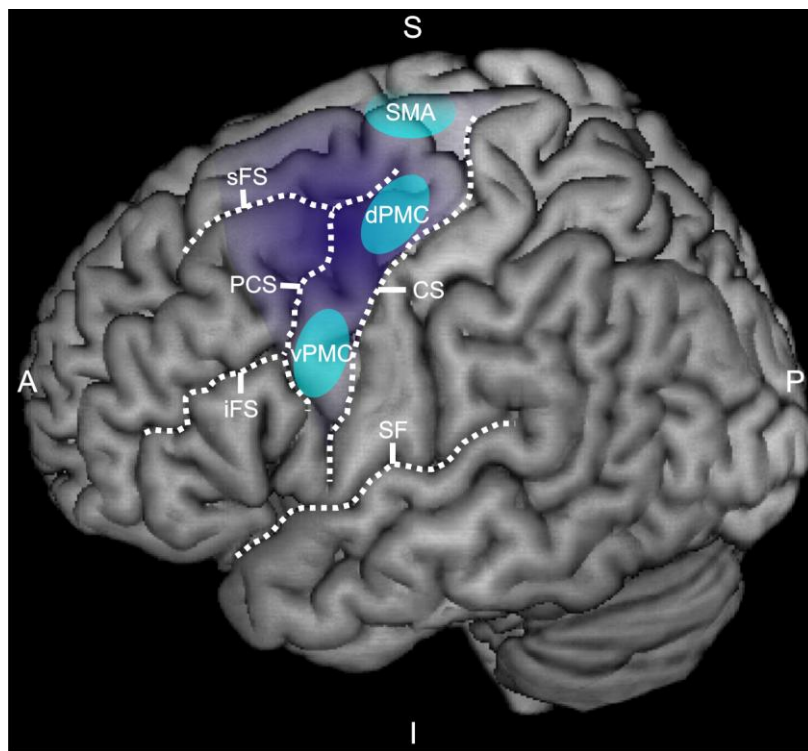


Figure 1.3: Introduction: The human premotor cortex. The lateral view on the left cerebral hemisphere shows the extent of the premotor cortex (in dark purple) and representative areas (in light blue) corresponding to the dorsal premotor cortex (dPMC), ventral premotor cortex (vPMC), and the supplementary motor area (SMA). (A: anterior; CS: central sulcus; I: inferior; iFS: inferior frontal sulcus; P: posterior; PCS: precentral sulcus; S: superior; SF: Sylvian fissure; sFS: superior frontal sulcus)

The SMA is mainly situated in the mesial wall of the hemisphere. Its boundaries are usually located at the *Mantelkante* of the hemisphere (Grafton et al., 1996) but may extend slightly in dorsolateral direction (Mayka et al., 2006; Tanji & Hoshi, 2009). The ventrolateral limit of the SMA is the dorsomedial border of the dPMC. Although SMA and dPMC constitute two functionally distinct regions (Penfield & Welch, 1951), data allowing differentiation of those

two regions based on anatomical grounds are scarce (Matelli et al., 1985). The border between dPMC and vPMC has traditionally been assigned to the intersection of the precentral sulcus and the inferior frontal sulcus (Grezes & Decety, 2001; Picard & Strick, 2001). However, more recent studies based on structural imaging suggest that it is much more dorsal, namely between superior and inferior frontal sulcus (average Z coordinate: 48; Tomassini et al., 2007). Similar to BA4, premotor areas are somatotopically organized and have direct projections to spinal cord motoneurons (He at al., 1993). Additionally, premotor areas send efferent connections to functionally related representations in BA4 (Dum & Strick, 2002). Homotopic transcallosal connections between M1, SMA, vPMC, and dPMC as well as heterotopic transcallosal connections between M1, SMA, and lateral premotor cortex (dPMC and vPMC) have been demonstrated in anatomical tracer studies in macaque monkeys (McGuire et al., 1991; Rouiller et al., 1994).

1.3 Definition of terms

1.3.1 Clinical stages

Based on a recent review article summarizing mechanisms of spontaneous recovery after stroke, the following definitions for clinical stages of the disease are used throughout the manuscript (Cramer, 2008; Table 1.1).

Table 1.1: Introduction: Designation of clinical stages

Acute stage	≤ 3 days after stroke
Subacute stage	4 days to 3 months after stroke
Early chronic stage	3 to 6 months after stroke
Chronic stage	≥ 6 months after stroke

1.3.2 Cerebral hemispheres

Throughout the manuscript, the term **ipsilesional** will be used to refer to the side of the stroke lesion and the term **contralesional** will be used to refer to the side opposite to the stroke lesion. Hence, the **ipsilesional hemisphere** is ipsilateral to the stroke lesion and the **contralesional hemisphere** is contralateral to the stroke lesion. Although, in principle, the ipsilesional hemisphere corresponds to the affected hemisphere and the contralesional

hemisphere corresponds to the unaffected hemisphere these terms may be misleading, since stroke lesions may also impact on the “unaffected” hemisphere (Grefkes et al., 2008b; Loubinoux et al., 2003; Ward et al., 2003a, 2003b), and hence these terms will not be used. The terms ipsilesional hemisphere and contralesional hemisphere should not be confused with the terms **ipsilateral hemisphere** and **contralateral hemisphere** which are used to refer to the hemisphere which is ipsi- or contralateral to an event such as hand movements or an intervention. During movements of the **affected hand** (sometimes referred to as the **paretic hand**) the ipsilateral hemisphere refers to the contralesional hemisphere and the contralateral hemisphere refers to the ipsilesional hemisphere (Figure 1.4).

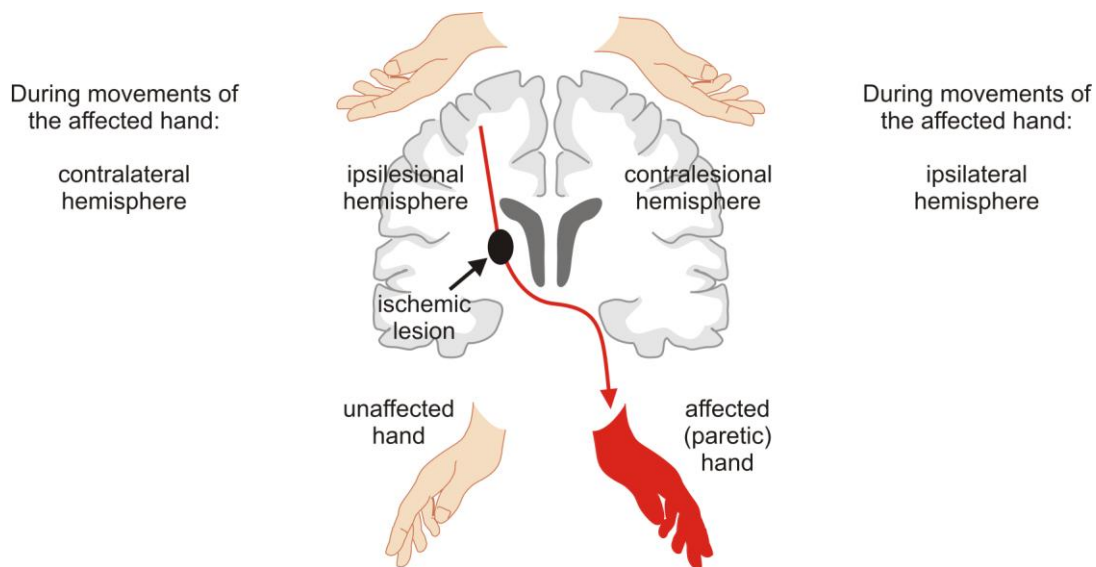


Figure 1.4: Introduction: Designation of cerebral hemispheres. The ipsilesional hemisphere is on the same side as the stroke lesion, whereas the contralesional hemisphere is the hemisphere opposite to the stroke lesion. During movements of the paretic (i.e. affected) hand, the contralateral hemisphere corresponds to the ipsilesional hemisphere and the ipsilateral hemisphere corresponds to the contralesional hemisphere.

1.3.3 Cortico-cortical connectivity

Two important concepts of current brain research are the concept of functional segregation and the concept of functional integration (Friston, 2002; Friston, 1994). **Functional segregation** refers to the finding that in the human brain, particularly in the cerebral cortex, different areas take over different specific tasks, whereas **functional integration** relies on observations that brain functions are not localized in a specific brain region but rely on coordinated exchange of information between different areas with distinct functions (Friston,

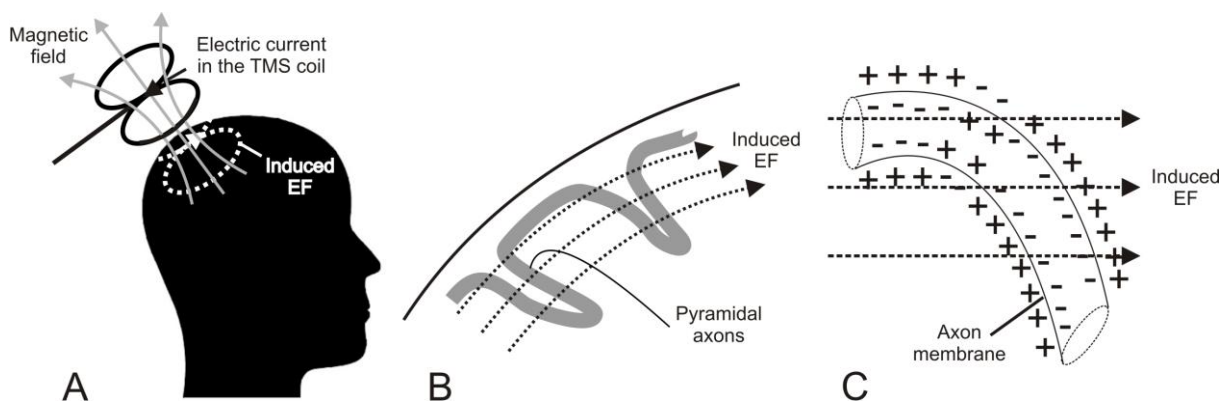
2002). Hence, functional segregation and functional integration are not competing concepts since functional integration is based on the concept of functional segregation, which postulates interactions between areas with distinct functions.

Connectivity describes structural and functional properties of brain networks. Three different subtypes can be distinguished: (i) anatomical connectivity, (ii) functional connectivity, and (iii) effective connectivity. **Anatomical connectivity** refers to anatomical fibre tracts connecting brain regions and providing the neuronal basis for cortico-cortical connectivity. By contrast, **functional connectivity** refers to temporal coherence between remote neurophysiological events (Friston et al., 1993b) whereas **effective connectivity** refers to either direct or indirect *causal* influences that activity in one neuronal system exerts on activity of another neuronal system (Friston et al., 1993a). Effective connectivity can be inferred from functional magnetic resonance imaging (fMRI) data by means of dynamic causal modelling (DCM). Although not considered a measure of effective connectivity *per se*, transcranial magnetic stimulation (TMS) can be employed to probe intra- and intercortical physiology and causal changes in functional circuits of the brain (Reis et al., 2008; Westlake & Nagarajan, 2011).

1.4 Transcranial magnetic stimulation (TMS)

TMS was introduced in 1985 by Barker et al. and has since then gained recognition as safe technique to stimulate the human cerebral cortex non-invasively and pain-free (Barker et al., 1985). TMS makes use of Faraday's principle of electromagnetic induction, which states that electrical energy can be converted into magnetic fields and vice versa (Faraday, 1832). During TMS, a copper stimulation coil is held tangentially to the subject's scalp. The electric current in the stimulation coil produces a strong magnetic pulse of short duration (~2 Tesla, ~50-100 μ s) which passes the skull nearly unhindered and induces an electric field (EF) in the underlying brain tissue (Figure 1.5A). The induced EF causes depolarization of fast conducting large pyramidal cells, which have excitatory monosynaptic connections to spinal cord motoneurons. Hence, TMS pulses may finally result in motor-evoked potentials (MEPs) in contralateral peripheral muscles which can be recorded by means of electromyography (EMG). There is evidence that TMS excites pyramidal cells either directly at the axon membrane or indirectly via transsynaptic input from interneurons (Di Lazzaro et al., 1998a).

Evidence for this suggestion comes from so-called *descending waves* or *descending volleys* recorded from a bipolar electrode inserted into the cervical epidural space of conscious human subjects (Di Lazzaro et al., 1998a). Descending waves are rapidly transmitted (60-70 m/s) synchronized action potentials in fast conducting axons of pyramidal cells, which innervate motoneurons in the spinal cord (Amassian et al., 1987). The first of these descending waves is referred to as *direct wave* or *D-wave*, which is thought to reflect direct excitation of axons in white matter due to its short latency (Amassian et al., 1987). The early D-wave is followed by several later *indirect waves* or *I-waves* which follow in constant intervals of ~ 1.5 ms and correlate with excitatory postsynaptic potentials (EPSP) of fast conducting pyramidal cells (Amassian et al., 1987) and hence are thought to reflect indirect excitation of pyramidal cells by transsynaptic input from excitatory interneurons. TMS may induce both, D-waves and I-waves indicating that the induced EF may excite motoneurons either directly at the axon membrane or indirectly via transsynaptic input (Di Lazzaro et al., 1998a). Axons are preferentially excited if the induced EF changes relative to their trajectory (Figure 1.5B). Since the EF in the brain tissue is horizontal, particularly axons which bend downwards will be locally depolarised at the axon membrane (Basser, 1994; Ilmoniemi et al., 1999; Roth & Basser, 1990; Figure 1.5C).



Modified from: <http://www.biomag.hus.fi/tms/Thesis/Fig1.jpg> (19.10.2011)

Figure 1.5: Introduction: Principles of transcranial magnetic stimulation (TMS). A: The electric current in the TMS coil (solid black line; flowing in posterior-anterior direction) generates a transient magnetic field (solid grey line), which induces an electric field (EF) in the brain (dashed white line; in posterior-anterior direction). B: Motor cortex stimulation and trajectory of pyramidal axons. The induced EF runs in posterior-anterior direction and approximately parallel to the gyral surface. C: Direct axonal excitation at the microscopic level. The induced EF causes local depolarisation of the axon membrane at the position where the pyramidal axon bends downwards.

Excitation of motoneurons has been demonstrated to be maximal if the induced EF is approximately perpendicular to the central sulcus and in posterior-anterior (PA) direction (Mills et al., 1992). Traditional circular-shaped TMS coils induce strong electric fields whereas figure-of-eight TMS coils offer the advantage of increased focality since maximal current is induced in a relatively small area at the intersection of the two round components (Lontis et al., 2006). A recent study of Thielscher and colleagues suggests that TMS has a spatial resolution of at least 7.7 mm (Thielscher & Wichmann, 2009). Since the EF strength decreases exponentially as a function of distance from the TMS coil (Eaton, 1992), TMS is restricted to stimulation of more superficial cortical areas (1-6 cm distant from the TMS coil; Weyh & Siebner, 2007).

Two major approaches can be pursued with TMS:

- 1) Investigation of physiological properties of neuronal tissue by means of several pulses applied at low frequencies (< 1 Hz):

Two different subtypes are:

- a) Single-pulse TMS (to assess e.g. corticospinal excitability; cf. 1.4.2)
 - b) Paired-pulse TMS (to assess intra- or intercortical neuronal pathways; cf. 1.4.3)
- 2) Modulating corticospinal excitability beyond the period of stimulation by means of *repetitive* transcranial magnetic stimulation (rTMS), i.e. many pulses (usually > 500) applied at higher stimulation frequencies (≥ 1 Hz)

The following paragraph gives an overview of TMS techniques with emphasis on the methods applied in the present thesis.

1.4.1 Stereotaxic frameless neuronavigation

Although exact coil positioning is crucial for correct interpretation of TMS effects, accurate positioning of the TMS coil over the cortical target area represents one of the most challenging aspects of the experimental procedure (Sparing et al., 2010). Two conventional strategies have been used before the introduction of stereotaxic frameless neuronavigation for TMS: (i) the international 10-20 electroencephalography (EEG) electrode system and (ii) standardized function guided procedures (Sparing et al., 2008). The former strategy assumes consistent correlation between scalp positions and underlying brain structures and may lead to spatial variations of up to 20 mm with some electrode positions showing larger variability

than others (Herwig et al., 2003). The latter strategy assumes that brain areas are subsequently located in a certain spatial relation to a reference point (e.g. M1 leading to MEPs when stimulated). Accuracy of this procedure falls off with increasing distance from the reference point (Herwig et al., 2001). Since the early 1990s, image-guided frameless stereotaxic neuronavigation systems (SNS) have been used for presurgery evaluation as well as online navigation during neurosurgery (Herwig & Schonfeldt-Lecuona, 2007). Since 1997, SNS is also available for coil guidance during TMS and three different strategies have been suggested, which make use of: (i) the subject's individual structural (anatomical) magnetic resonance imaging (MRI) scan allowing navigation after subject-image coregistration based on facial and/or cranial landmarks, (ii) individual fMRI data, and (iii) probabilistic (group) fMRI data. Highest precision can be achieved with the latter two strategies in which task-related fMRI signal is used as functional landmark for coil positioning (Sparing et al., 2008; Figure 1.6). The probabilistic approach might be particularly useful if reliable fMRI activations cannot be obtained on the single-subject level. Nonetheless, a spatial mismatch of up to 14 mm between the individual position yielding highest MEPs when stimulated with TMS and the position with highest individual fMRI signal has consistently been reported for the human motor cortex (Bastings et al., 1998; Boroojerdi et al., 1999; Herwig et al., 2002; Krings et al., 1997; Lotze et al., 2003; Sparing et al., 2008; Terao et al., 1998). The underlying cause of this spatial mismatch between fMRI and TMS is unknown and will be matter of investigation in the present thesis (Study I & II).

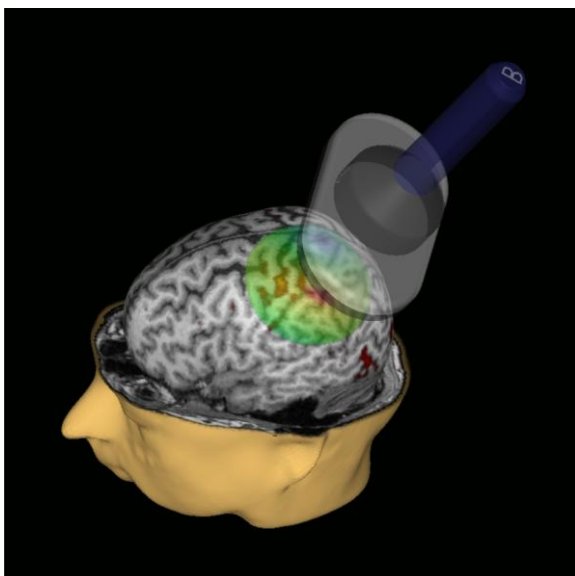


Figure 1.6: Introduction: Stereotaxic frameless neuronavigation for transcranial magnetic stimulation (TMS). The screenshot of the eXimia software (Nexstim, Helsinki) shows a 3D head reconstruction model based on a volunteer's individual high-resolution anatomical magnetic resonance imaging (MRI) scan. The position of the TMS coil and the position of the subject's head are tracked via an infrared camera which allows online navigation. The anatomical MRI scan is overlaid with the subject's individual functional magnetic resonance imaging (fMRI) data during index finger tapping (red/yellow activation cluster in the motor hand area). The electric field (EF) is colour coded (highest EF strength depicted in red).

1.4.2 Single-pulse TMS

1.4.2.1 Motor-evoked potentials (MEPs) and motor thresholds (MTs)

When investigating the human motor system, TMS effects are usually probed by inducing MEPs measured at contralateral peripheral target muscles by means of EMG recordings. Two small hand muscles served as target muscles in the present thesis: (i) the first dorsal interosseous (FDI) muscle involved in index finger abduction, and (ii) the abductor pollicis brevis (APB) muscle involved in thumb abduction. Both muscles, particularly the FDI muscle, have the advantage of relatively large representation areas in M1 and are well suitable for EMG recordings due to their superficial anatomical position. Motor thresholds (MTs) and peak-to-peak amplitudes of MEPs are measures of corticospinal excitability involving both, excitation of cortical neurons (either directly or transsynaptically) and synaptic mechanisms at the level of the spinal cord (Hallett, 2007). The MT is defined as the minimum TMS stimulator output intensity needed to generate MEPs in the target muscle and can be obtained either at rest (resting motor threshold = RMT) or during permanent low-level contraction of the target muscle (active motor threshold = AMT). The RMT depends on at least three different independent factors: (i) excitability of corticospinal axons, (ii) excitability of intracortical synapses, and (iii) excitability of synapses in the spinal cord. The AMT is usually lower than the RMT of the same subject since tonic muscle contraction pre-activates synapses in the spinal cord which lowers their threshold to generate an MEP if a TMS pulse is simultaneously applied (Hess et al., 1987; Rosler et al., 2008). Since synapses in the spinal cord are pre-activated, AMT is assumed to depend mostly on the excitability of cortical axons and intracortical synapses. Hence, AMT is thought to be a measure of cortical rather than corticospinal excitability (Talelli et al., 2006).

1.4.2.1.1 MEPs and MTs early after stroke

In some stroke patients, single-pulse TMS applied to the ipsilesional hemisphere fails to elicit any MEPs in the acute phase (Foltys et al., 2003; Manganotti et al., 2002; Trompetto et al., 2000). According to a systematic review, absence of MEPs in the affected limb in the acute phase is a strong predictor for poor motor recovery (Hendricks et al., 1997). In patients in whom MEPs can be elicited, the RMT of the ipsilesional hemisphere is usually increased (i.e. corticospinal excitability is decreased) compared to healthy subjects and compared to the contralesional hemisphere both in the acute (Manganotti et al., 2002) and sub-acute phase

(Cicinelli et al., 1997). Likewise, AMT which has been suggested to be less sensitive to changes in spinal cord excitability was found to be increased in the sub-acute phase (Cicinelli et al., 2003) indicating reduced cortical excitability. Excitability increases (i.e. MEPs increase and MTs decrease) gradually over time concomitant to motor recovery (Manganotti et al., 2002; Thickbroom et al., 2002; Traversa et al., 2000). MTs of the contralesional hemisphere are usually within normal limits even in the acute phase (Foltys et al., 2003; Manganotti et al., 2002; Shimizu et al., 2002).

1.4.2.2 TMS motor mapping

TMS motor mappings are used to define the position and extend of the cortical representation of a particular peripheral muscle. During this procedure, a focal figure-of-eight TMS coil is systematically moved (usually in 5-10 mm increments) to scalp positions. As a result, a cortical excitability map is generated based on muscle responses (i.e. MEPs) recorded from the target muscle (Figure 1.7). The most important parameters which can be obtained by TMS motor mappings are: (i) the geometric centre-of-gravity (CoG; i.e. the MEP amplitude weighted centre of the map) and (ii) the size of the cortical representation (i.e. the number of excitable scalp positions). The area of tissue which can be excited by means of TMS is considerably larger than the actual representation in M1. This might be due to several reasons including geometry of the EF causing excitation of neurons not only exclusively directly underneath the TMS coil and excitation of axons running horizontally and terminating onto distant neurons. The size of the map area is highly dependent on the stimulation intensity used. By contrast, the CoG is relatively insensitive to stimulation intensity and coil shape (Brasil-Neto et al., 1992; Wassermann et al., 1992).

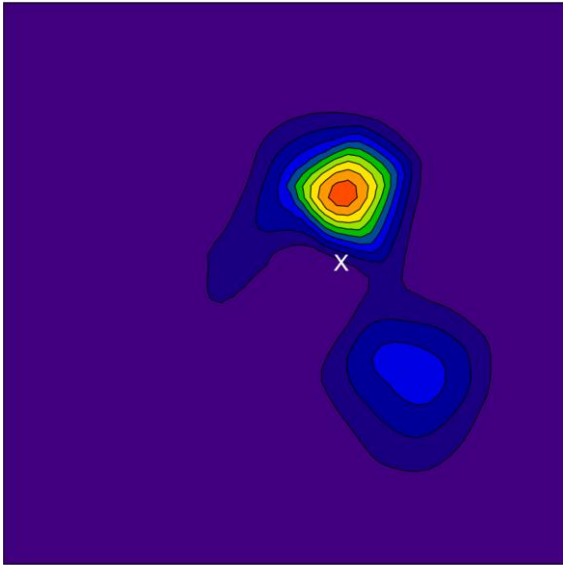


Figure 1.7: Introduction: Example TMS motor map of a healthy volunteer generated with transcranial magnetic stimulation (TMS). Single-pulse suprathreshold TMS (120% resting motor threshold) pulses were applied at different scalp positions spaced at intervals of 5 mm (7 pulses per position). Resulting motor-evoked potentials (MEPs) of the abductor pollicis brevis (APB) muscle were used to generate a colour coded excitability map (purple: lowest MEP; red: highest MEP) and calculate the MEP amplitude weighted centre of the map (i.e. the centre-of-gravity; CoG) which is marked with a white cross.

1.4.2.2.1 TMS motor maps early after stroke

In the acute phase, cortical representations of paretic hand muscles in the ipsilesional hemisphere are significantly smaller than cortical representations of homologue muscles in the contralesional hemisphere (Foltys et al., 2003). The map area increases concomitant with motor recovery (Cicinelli et al., 1997; Traversa et al., 1997). However, stimulation intensities were not adjusted in these studies, and therefore, the results might be confounded by decreases in MT while patients recovered. Analyses on map area would anyway only allow conclusions on a general increase of corticospinal excitability whereas a spatial shift of the CoG suggests changes in somatotopy of motor cortical projections. In the acute phase, the CoG is within the normal range but spatial shifts may occur later during recovery either in the anterior-posterior or medial-lateral direction (Bastings et al., 2002; Thickbroom et al., 2002). Such spatial shifts may range from several millimetres (Byrnes et al., 2001; Thickbroom et al., 2002) up to few centimetres (Bastings et al., 2002; Delvaux et al., 2003), which is well beyond the normal variation range of 2-3 mm in healthy subjects (Wassermann et al., 1996). Motor maps of the contralesional hemisphere usually remain unchanged (Bastings et al., 2002; Liepert et al., 1998).

1.4.3 Paired-pulse TMS

Paired-pulse TMS paradigms can be used to investigate inhibitory and excitatory neuronal circuits either within or between hemispheres with high temporal resolution. What all paired-

pulse TMS paradigms share is the concept of a conditioning TMS pulse (conditioning stimulus = CS) preceding a second test TMS pulse (test stimulus = TS) applied to M1. Although the CS is usually applied to M1, it might also be delivered to other cortical brain areas, for example dPMC (Koch et al., 2006). The intensity of the TS is usually adjusted to generate MEPs of 0.5-1.5 mV in the contralateral target muscle. Trials with paired pulses (CS+TS) and single pulses (TS) are applied in randomized or alternating order within one session and inhibitory or facilitatory effects are inferred from MEP amplitudes resulting from single- compared to paired-pulse trials. Two main protocol types can be distinguished: (i) both stimuli are applied via the same TMS coil at the same position or (ii) stimuli are applied via two different coils at two different positions. The first approach allows investigation of inhibitory and excitatory neuronal circuits within one hemisphere whereas the second approach allows investigation of neuronal circuits between hemispheres, for example between both primary motor cortices.

1.4.3.1 Paired-pulse TMS applied to one hemisphere

Three different types of protocols allow investigation of excitatory and inhibitory neuronal circuits within one hemisphere: (i) protocols with two suprathreshold stimuli of similar intensity separated by long interstimulus intervals (ISIs) of 10-200 ms, (ii) protocols with a subthreshold CS and a suprathreshold TS and short ISIs of 1-15 ms, and (iii) protocols with a suprathreshold CS and a subthreshold TS and very short ISIs of 0.5-5 ms (Table 1.2).

Table 1.2: Introduction: Paired-pulse TMS parameters applied to one hemisphere

CS intensity	TS intensity	ISI	Paired-pulse TMS parameter		First description
Supra-threshold	Supra-threshold	10-40 ms	LICF	Long-interval intracortical facilitation	Claus et al. (1992)
		60-200 ms	LICI	Long-interval intracortical inhibition	
Sub-threshold	Supra-threshold	1-5 ms	SICI	Short-interval intracortical inhibition	Kujirai et al. (1993)
		10-15 ms	ICF	Intracortical facilitation	
Supra-threshold	Sub-threshold	0.5-5 ms	SICF	Short-interval intracortical facilitation	Ziemann et al. (1998b)

CS: Conditioning stimulus; ISI: Inter-stimulus interval; TMS: Transcranial magnetic stimulation; TS: Test stimulus

1.4.3.1.1 Short-interval intracortical inhibition (SICI)

SICI refers to the phenomenon that a suprathreshold TS applied to the motor hand area is suppressed by a subthreshold CS applied at the same position 1 to 5 ms before the TS (Figure 1.8). Maximum inhibition is seen if the TS intensity is adjusted to generate MEPs of 1 mV and the CS intensity is around 80% AMT (Talelli et al., 2006).

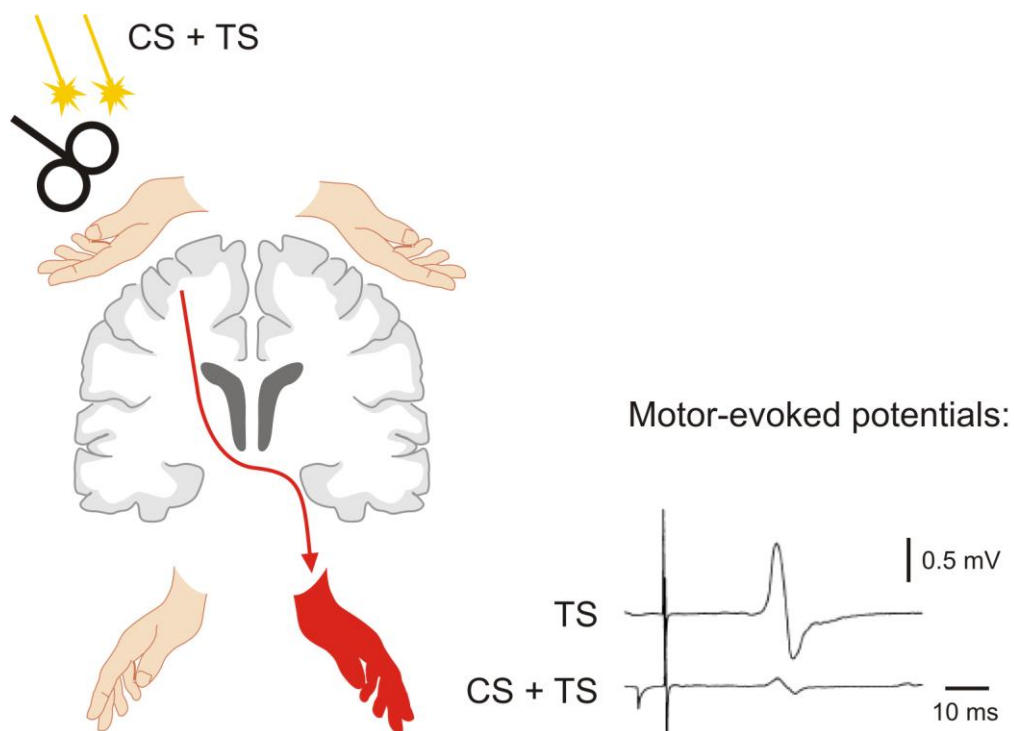


Figure 1.8: Introduction: Paired-pulse transcranial magnetic stimulation (TMS) applied to one hemisphere. During assessment of short-interval intracortical inhibition (SICI) a subthreshold conditioning stimulus (CS; 80% of the active motor threshold) is applied 1-5 ms before a suprathreshold test stimulus (TS) via the same TMS coil positioned over the motor hand area. Stimulation intensity of the TS is adjusted to generate motor-evoked potentials (MEPs) of 1 mV in the contralateral target muscle if applied alone. If the CS precedes the TS, MEPs of the target muscle (contralateral to the TS) are significantly reduced compared to MEPs resulting from single-pulse trials (i.e. application of the TS alone).

Compared to other paired-pulse parameters, relatively much is known about the neurophysiological mechanisms underlying SICI. For instance, there is evidence that SICI is a measure of *intracortical* inhibition, i.e. suppression is likely to occur at the cortical level rather than at the level of the spinal cord. This conclusion was mainly drawn from two

experiments: (i) cortical CS pulses (suppressing cortical TS pulses during SICI) have no effect on Hoffmann reflexes (H-reflexes) generated in spinal cord segments (Kujirai et al., 1993; Ziemann et al., 1996b) and (ii) electrical recordings of descending volleys produced by paired-pulse TMS by means of high cervical epidural electrodes implanted in patients for pain relief demonstrated a significant reduction of later I-waves which suggests involvement of local cortical inhibitory circuits (Di Lazzaro et al., 1998b). If a longer ISI is applied, ICF instead of SICI is induced (cf. Table 1.2). Presumably different neuronal circuits are involved in the generation of SICI and ICF, since SICI can be induced with lower CS intensities than ICF (Kujirai et al., 1993; Ziemann et al., 1996b) and SICI and ICF are differentially affected by neuropharmacological agents. ICF is likely to act on glutaminergic N-methyl-D-aspartate (NMDA) receptors since administration of NMDA-receptor antagonists decreases ICF (Schwenkreis et al., 1999; Ziemann et al., 1998a). By contrast, SICI is mediated by gamma-aminobutyric acid A (GABA_A) receptors since GABA_A agonists have been demonstrated to enhance SICI (Di Lazzaro et al., 2000; Ilic et al., 2002; Ziemann et al., 1996a). SICI is modulated by muscle contraction, i.e. SICI is reduced during contraction of the target muscle (Ridding et al., 1995) and increased during contraction of nearby muscles (Stinear & Byblow, 2003). Therefore, SICI has been suggested to play an important role in selecting the most appropriate muscles for a specific movement. SICI at very short ISI (~ 1 ms) is probably mediated by a different mechanism than SICI at longer ISI (2-5 ms) since it requires much lower CS intensities and is insensitive to voluntary contraction (Fisher et al., 2002). It has been suggested that SICI at very short ISI (~ 1 ms) is most likely caused by relative refractoriness of cortical neural elements activated by the CS whereas SICI at longer ISI reflects GABA_A-mediated intracortical inhibition (Fisher et al., 2002; Hanajima et al., 2003). The present thesis focuses on SICI to assess *intrahemispheric inhibition* because (i) it is a very robust paradigm, (ii) its neurophysiological mechanisms are better understood than those of any other paired-pulse TMS parameter, (iii) it is well characterized in healthy subjects, and (iv) it is of particular relevance for stroke since stroke patients may show abnormal SICI compared to healthy subjects.

1.4.3.1.1.1 SICI early after stroke

In the first days (Di Lazzaro et al., 2010) and weeks after stroke, SICI on the ipsilesional hemisphere tends to be reduced (Cicinelli et al., 2003; Liepert et al., 2000; Manganotti et al., 2002). Although ICF is generally unchanged (Cicinelli et al., 2003; Liepert et al., 2000;

Manganotti et al., 2002) there is a tendency for ICF to occur at shorter ISIs (Liepert et al., 2000; Shimizu et al., 2002) and lower CS intensities (Butefisch et al., 2003), which induce SICI in healthy subjects. These findings suggest that intracortical excitability of the ipsilesional hemisphere is shifted towards facilitation. Interestingly, also excitability of the contralesional hemisphere was found to be changed towards facilitation, i.e. SICI was reduced in the first weeks after stroke in the majority of studies (Butefisch et al., 2003; Liepert et al., 2000; Manganotti et al., 2002; Shimizu et al., 2002). Hence, stroke lesions appear to have differential effects on *corticospinal* excitability (MEPs, MTs) and *intracortical* excitability (SICI, ICF) of the contralesional hemisphere (since MTs of the contralesional hemisphere were found to be unchanged in the majority of studies).

1.4.3.2 Paired-pulse TMS applied to both hemispheres

Two different types of protocols allow investigation of inhibitory and facilitatory neuronal circuits between hemispheres: (i) protocols with two suprathreshold stimuli of similar intensity separated by ISIs of 7-50 ms, (ii) protocols with a subthreshold CS and a suprathreshold TS (applied with anterior-posterior (AP) instead of the standard posterior-anterior (PA) induced current in the brain) and an ISI of 8 ms (Table 1.3).

Table 1.3: Introduction: Paired-pulse TMS parameters assessed over both hemispheres

CS intensity	TS intensity	ISI	Paired-pulse TMS parameter		First description
Supra-threshold	Supra-threshold	7-50 ms	IHI	Interhemispheric inhibition	Ferbert et al. (1992)
Sub-threshold	Supra-threshold (AP induced current)	8 ms	IHF	Interhemispheric facilitation	Baumer et al. (2006)

AP: Anterior-posterior; CS: Conditioning stimulus; ISI: Inter-stimulus interval; TMS: Transcranial magnetic stimulation; TS: Test stimulus

1.4.3.2.1 Interhemispheric inhibition (IHI)

IHI refers to the phenomenon that a suprathreshold TS (yielding MEPs of 0.5-1 mV when applied alone) applied to the motor hand area is suppressed by a suprathreshold CS (0.5-1 mV) applied to the homologue motor hand area of the contralateral hemisphere resulting in a decrease of the MEP recorded from a target muscle contralateral to the TS and ipsilateral to the CS (Figure 1.9).

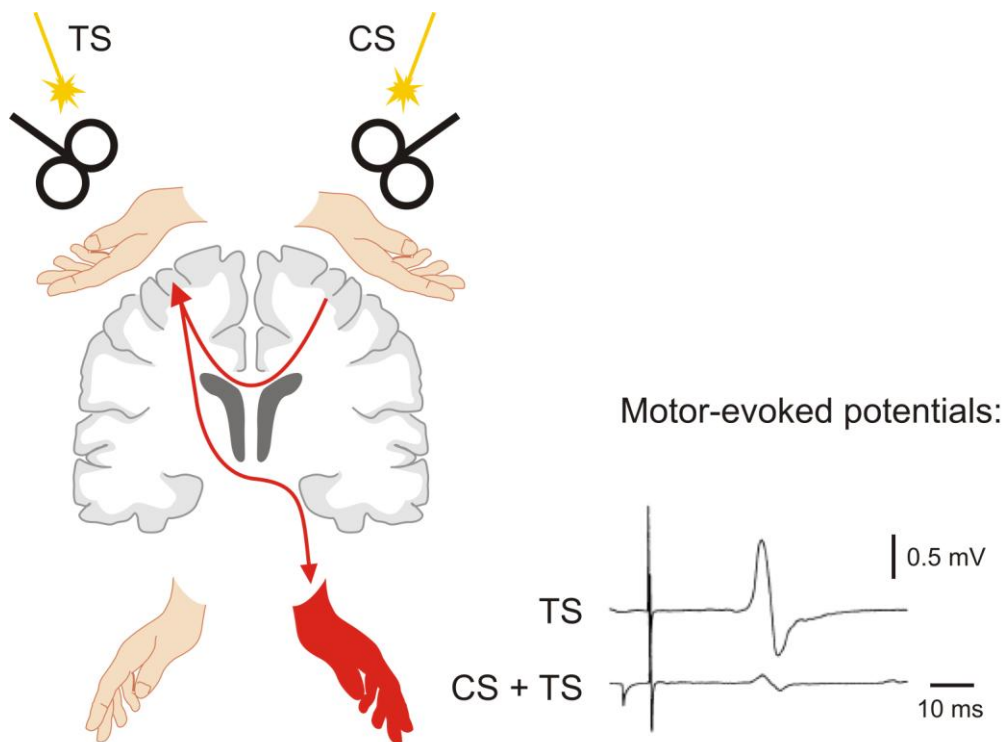


Figure 1.9: Introduction: Paired-pulse transcranial magnetic stimulation (TMS) applied to both hemispheres. During assessment of interhemispheric inhibition (IHI) a suprathreshold conditioning stimulus (CS) is applied to the motor hand area 7-50 ms before a suprathreshold test stimulus (TS) is applied to the homologue motor hand area of the contralateral hemisphere. Stimulation intensities of both CS and TS are adjusted to generate motor-evoked potentials (MEPs) of 1 mV in contralateral target muscle if applied alone. If the CS precedes the TS, MEPs of the target muscle (contralateral to the TS and ipsilateral to the CS) are significantly reduced compared to MEPs resulting from single-pulse trials (i.e. application of the TS alone).

Although the exact mechanisms underlying IHI are still under investigation, involvement of transcallosal glutamatergic pathways linking with CST neurons through inhibitory GABA-ergic interneurons has been suggested (Reis et al., 2008). IHI can be induced in relaxed and voluntary contracted hand muscles (Chen et al., 2003; Ferbert et al., 1992). The higher the intensity of the CS, the more pronounced is IHI. By contrast, high TS amplitudes (~ 2mV)

decrease IHI compared to standard amplitudes of 0.5 to 1mV. Higher stimulation intensities are needed to generate IHI compared to single-pulse MEPs from the same hemisphere, suggesting involvement of different neuronal populations. Under certain constraints IHF could be demonstrated in the healthy brain at rest. However, ICF is considerably less robust than IHI (Ferber et al., 1992; Hanajima et al., 2001; Baumer et al., 2006) and occurs only at an ISI of 8 ms when the TS is applied with AP instead of standard PA induced current in the brain. IHI is thought to consist of two phases: an early phase with ISIs of 7-10 ms and a later phase with intervals > 15 ms (Talelli et al., 2006). The early but not the late phase of IHI is influenced by voluntary muscle contraction. Already the original work by Ferbert et al. (1992), who first described IHI, demonstrated that IHI was increased if the target muscle contralateral to the CS and ipsilateral to the TS was tonically contracted compared to IHI at rest. This finding indicates that voluntary activation of M1 leads to increased inhibition of the contralateral M1. In line with these suggestions, contraction of the hand contralateral to the TS and ipsilateral to the CS has been demonstrated to reduce IHI (Chen et al., 2003). The present thesis focuses on IHI (measured at rest) to assess *interhemispheric inhibition* because it is (i) a very robust paradigm, (ii) well characterized in healthy subjects, and (iii) of particular relevance for stroke since stroke patients may show abnormal IHI compared to healthy subjects.

1.4.3.2.1.1 IHI (measured at rest) early after stroke

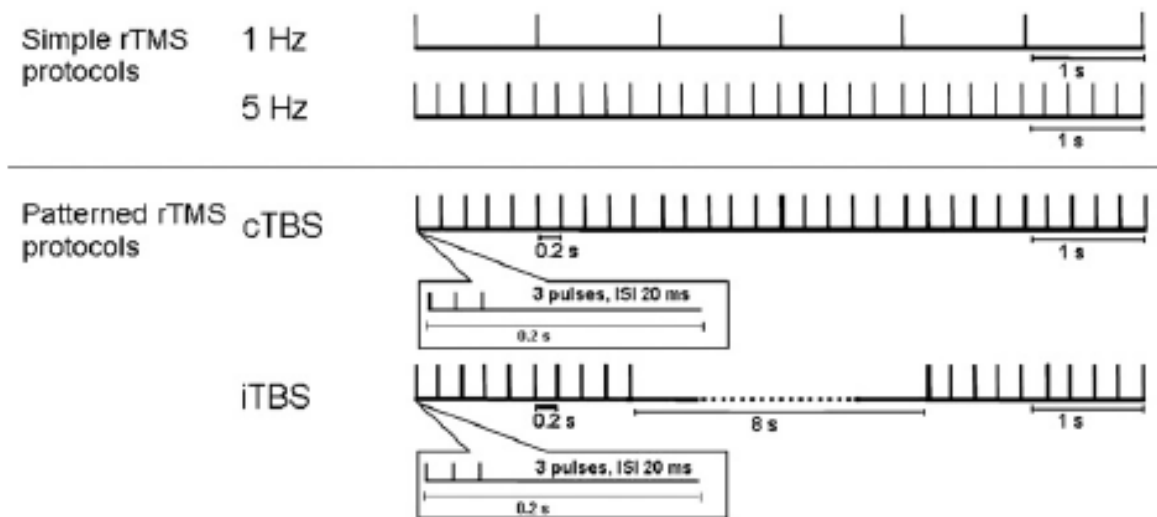
In the subacute stage, IHI from the contralesional onto the ipsilesional hemisphere (CS: contralesional hemisphere; TS: ipsilesional hemisphere) is unchanged (Butefisch et al., 2008). In contrast, IHI from the ipsilesional onto the contralesional hemisphere (CS: ipsilesional hemisphere; TS: contralesional hemisphere) has been shown to be significantly reduced in stroke patients in the subacute stage (Butefisch et al., 2008). IHI targeting the contralesional hemisphere was found to be decreased independent of the lesion site (i.e. cortical-subcortical or purely subcortical) in the study of Butefisch et al. (2008). However, two studies suggest that IHI targeting the contralesional hemisphere might be unchanged if the lesion is purely subcortical and below the centrum semiovale containing transcallosal fibres (Borojerdi et al., 1996; Shimizu et al., 2002). Hence, IHI targeting the contralesional hemisphere might be only reduced if transcallosal fibres are injured.

1.4.4 Repetitive transcranial magnetic stimulation (rTMS)

Repetitive transcranial magnetic stimulation (rTMS) can be used to modulate corticospinal excitability beyond the stimulation period. Stimulation intensities used for rTMS are usually defined as a percentage of the individual MT and are subthreshold in the majority of studies (Hoogendam et al., 2010).

1.4.4.1 rTMS protocols

During rTMS, stimuli are repetitively applied in a specific temporal pattern. Conventional, so called *simple rTMS protocols* are characterized by many (usually > 500) stimuli applied at constant ISIs. By contrast, *patterned rTMS protocols* are characterized by varying ISIs. Effects of *simple rTMS protocols* are bidirectional, depending on the frequency applied: low-frequency rTMS (most frequently used: 1 Hz) produces inhibition whereas high-frequency rTMS (≥ 3 Hz, most frequently used: 5 Hz) produces facilitation of cortical excitability (Chen et al., 1997; Houdayer et al., 2008; Pascual-Leone et al., 1994). Numerous studies demonstrated effects of *simple rTMS protocols* on motor cortex excitability, that is on MEP size (Hoogendam et al., 2010), but durations of after-effects are highly variable across studies and rarely last longer than 30 min despite of relatively long stimulation periods (~ 10–25 min). Theta-burst stimulation (TBS) is a *patterned rTMS protocol* resembling the naturally occurring firing pattern of neurons in the hippocampus (i.e. 5 Hz = theta rhythm; Albensi et al., 2007; Larson et al., 1986). It was developed following the example of the theta-burst protocol used to induce phenomena of synaptic plasticity such as long-term potentiation (LTP) and long-term depression (LTD) in animal studies by means of repetitive electrical stimulation (Hess et al., 1996; Huemmeke et al., 2002; Larson & Lynch, 1986; Vickery et al., 1997). Huang et al. (2005) were the first who used rTMS with a theta-burst stimulation pattern to modulate motor cortex excitability non-invasively in humans. The basic element of TBS patterns are *bursts* (3 pulses given at 50 Hz), which are applied at 5 Hz. Huang et al. (2005) demonstrated that 40 s of *continuous TBS (cTBS)* significantly suppressed motor cortex excitability for nearly 60 min, whereas *intermittent TBS (iTBS)*, in which a 2s-train of stimulation (10 bursts) is followed by 8 s pause, significantly increased motor cortex excitability for about 15 min (Figure 1.10).



Hoogendam et al. (2010)

Figure 1.10: Introduction: Repetitive transcranial magnetic stimulation protocols. Several repetitive transcranial magnetic stimulation (rTMS) protocols are available to modulate cortical excitability beyond the period of stimulation. *Simple rTMS protocols* are characterized by constant inter-stimulus intervals (ISIs). Low-frequency rTMS (most frequently used: 1 Hz) induces inhibition, whereas high-frequency rTMS (≥ 3 Hz; most frequently used: 5 Hz) induces facilitation. Modern *patterned rTMS protocols* are characterized by varying ISIs. The basic elements of theta-burst stimulation (TBS) patterns are bursts (i.e. 3 pulses given at 50 Hz or an ISI of 20 ms respectively). Bursts are repeated at 5 Hz (i.e. with an ISI of 200 ms). Continuous TBS (cTBS) for 40 s induces inhibition, whereas intermittent TBS (iTBS), in which 2 s of stimulation are followed by 8 s pause, induces facilitation. Overall 600 pulses are usually applied during both cTBS and iTBS.

iTBS has facilitatory and cTBS inhibitory effects on cortical excitability, although both protocols contain equivalent number of pulses, namely 600 pulses in total. To explain this finding, Huang et al. (2005) suggested a theoretical model which is based on the following assumptions: (i) TBS induces both facilitatory and inhibitory effects simultaneously in the human brain, (ii) inhibitory effects build up slower than facilitatory effects, and (iii) inhibitory effects dominate over facilitatory effects when both have reached saturation. According to this model, short trains of stimulation (as during iTBS) would favour facilitatory effects which built up faster than inhibitory effects. However, during longer stimulation periods (as during cTBS) inhibitory effects build up and dominate over facilitatory effects on the long run since facilitatory effects saturate at lower levels. However, this is still a hypothetical model. An alternative would be that iTBS and cTBS act on different neuronal circuits. This hypothesis is supported by findings of differential effects on corticospinal activity probed by recordings from patients with electrodes implanted in the epidural space of the spinal cord (Di Lazzaro et al., 2005, 2008b). Huang et al., (2005) did not only probe motor cortex excitability by means

of MEP sizes but additionally demonstrated that TBS may have significant impact on motor performance. Interestingly, behavioural TBS effects were not restricted to the hand contralateral to the stimulated hemisphere but were also found in the hand ipsilateral to the stimulated hemisphere. Reaction times of the contralateral hand were prolonged 10 min after cTBS, whereas reaction times of the ipsilateral hand were significantly shorter 30 min after cTBS. TBS has several advantages over *simple rTMS protocols*, among them low stimulation intensities (reducing the risk to induce seizures; Bezard et al., 1999), robust and long-lasting effects which are more consistent across studies (Hoogendam et al., 2010), and short stimulation duration of only 1-3 min.

1.4.4.2 The neurophysiological basis of rTMS effects

The neurophysiological mechanisms underlying rTMS effects are incompletely understood but there are several lines of evidence supporting the hypothesis that rTMS acts on the level of individual synapses by mechanisms such as LTP and LTD. For instance, there are various characteristics of rTMS induced effects which follow key features of synaptic plasticity: (i) effects outlast the period of stimulation, (ii) direction and duration of effects depend on temporal patterns of the stimuli applied, (iii) induced changes depend on physiologic activity and the history of activation, and (iv) effects interact with skill learning (Hoogendam et al., 2010). Apart from these indirect lines of evidence based on observed similarities, pharmacological and genetical studies suggest a more direct link between rTMS effects and synaptic plasticity such as LTP and LTD. For instance, Aydin-Abidin and colleagues (2008) demonstrated that iTBS increases the expression of Zif268 in the rat brain. Zif268 is a mammalian transcription factor, which is essential for the induction and persistence of LTP (Jones et al., 2001). There is also some evidence that the NMDA receptor, which plays a key role in synaptic plasticity (Cooke & Bliss, 2006), is involved in rTMS mediated effects, since the NMDA receptor antagonist memantine blocks both, the facilitatory effect of iTBS and the inhibitory effect of cTBS in humans (Huang et al., 2007). However, although several lines of evidence suggest that rTMS effects are mediated by synaptic plasticity, a direct proof for the involvement of LTP and LTD in rTMS effectiveness has not yet been demonstrated.

1.4.4.3 Therapeutic potential of rTMS

Since rTMS induces long-lasting changes in cortical excitability or activity, it has therapeutic potential for treatment of various neurological and psychiatric diseases in which the pathomechanism is related to either decreased or increased cortical excitability. Examples for diseases in which inhibitory rTMS is used to suppress abnormal hyperexcitability are epilepsy, hyperkinetic movement disorders, chronic pain, tinnitus, and hallucinations whereas facilitatory rTMS is used to enhance abnormally low excitability in depression and hypokinetic movement disorders (Karim et al., 2007). The therapeutic potential of rTMS for treatment of stroke induced motor deficits seems to be particularly high (Talelli & Rothwell, 2006; Ziemann, 2005). In most cases, rTMS causes no pain and is well tolerated. Although there is a residual risk to cause seizures with rTMS, this is considered low if safety-guidelines are met (Oberman et al., 2011; Wassermann, 1998).

1.4.4.4 The model of hemispheric competition

Although the pathomechanism underlying stroke induced motor deficits is incompletely understood, some studies suggest disturbed hemispheric balance which led to the suggestion of a simplified *model of hemispheric competition* (Figure 1.11).

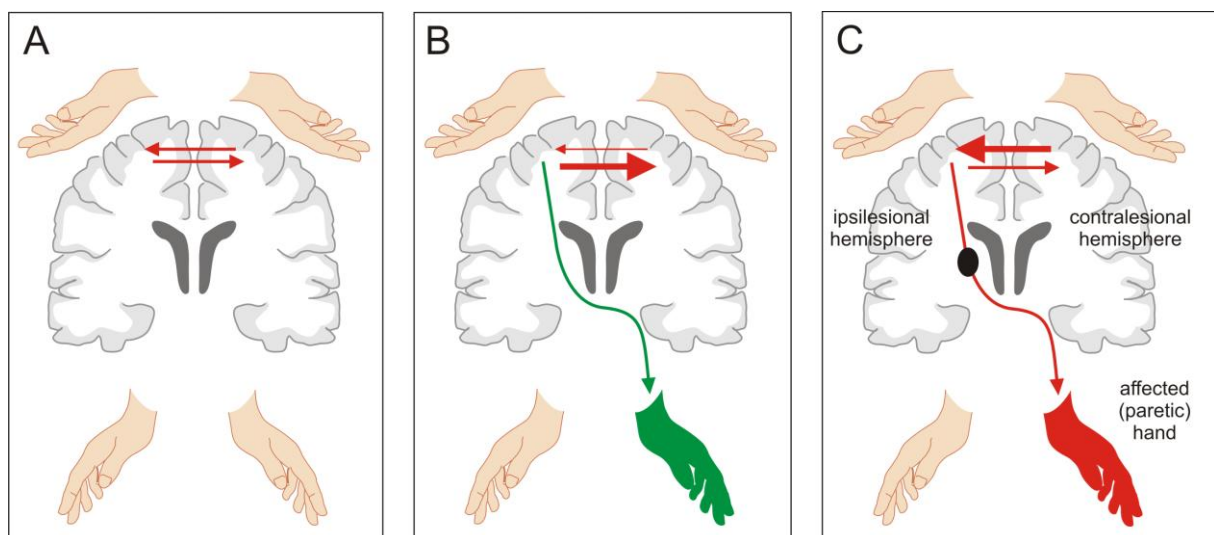


Figure 1.11: Introduction: The model of hemispheric competition. A: There is balanced reciprocal interhemispheric inhibition (IHI) between both primary motor cortices via transcallosal fibre tracts in the healthy human brain at rest. B: In healthy subjects, reciprocal IHI is modulated by the state of activation. During unilateral hand movements, the “active” primary motor cortex (M1) contralateral to hand movements exerts increased IHI onto the M1 ipsilateral to hand movements. C: Modulation of IHI is abnormal in stroke patients. During movements of the paretic hand, the contralesional

hemisphere (ipsilateral to paretic hand movements) exerts pathologically increased IHI onto the “active” ipsilesional M1 (contralateral to paretic hand movements).

In line with the *model of hemispheric competition*, two rTMS intervention strategies have been demonstrated to yield significant transient improvements in motor performance of the affected hand in stroke patients: (i) increasing cortical excitability of the ipsilesional hemisphere by means of high-frequency simple rTMS protocols (Khedr et al., 2005; Kim et al., 2006) and (ii) decreasing cortical excitability of the contralesional hemisphere by means of low-frequency simple rTMS protocols (Fregni et al., 2006; Mansur et al., 2005; Takeuchi et al., 2005). Both stimulation strategies seem to be equally effective and induce improvements of approximately 10-20%. Effects of a single rTMS session rarely last longer than 30-60 min (Hoogendam et al., 2010), whereas effects of multiple sessions have been demonstrated to last for hours and up to 2 weeks (Fregni et al., 2006). This implies that non-invasive brain stimulation techniques could in future be used to promote neural plasticity and to improve clinical outcome of stroke patients in combination with physical training currently used in neurorehabilitation. Whether effects are sufficiently robust in clinical settings is currently under intensive investigation as are questions regarding the optimal stimulation site and protocol. The most important problem that needs to be solved is the considerably high inter-individual variability in rTMS mediated effects, which is seen in healthy subjects (Daskalakis et al., 2006; Van Der Werf & Paus, 2006; Muller-Dahlhaus et al., 2008) as well as stroke patients (Ameli et al., 2009). The latter study by Ameli and colleagues (2009) demonstrated that some stroke patients may even show transient deteriorations of motor performance after rTMS. Hence, for the implementation of rTMS in stroke therapy it seems essential to identify reliable predictors for the therapeutic success of a specific rTMS intervention. Factors which are likely to impact on rTMS induced effects are: (i) time since stroke, (ii) lesion location, and (iii) underlying pathology. Study III of the present thesis focusses on identification of reliable neuroimaging predictors for behavioural response to facilitatory and inhibitory TBS in chronic stroke patients.

1.5 Functional magnetic resonance imaging (fMRI)

1.5.1 Fundamentals of magnetic resonance imaging (MRI) physics

MRI is based on the absorption and emission of radio waves by tissue placed in magnetic fields and was independently developed by different authors in 1973 (Lauterbur 1973; Mansfield & Grannell, 1973). MRI pictures tissue by hydrogen atoms which have a single proton as atomic nucleus and a single electron as atomic shell. Like all elementary particles the proton has a basic property called “spin”, i.e. it rotates along its own axis (Weishaupt et al., 2006). Since the proton is positively charged, it also has a magnetic moment (B). In other words, protons act as small magnets. They are therefore influenced by magnetic fields and electromagnetic waves and induce voltage in the receiving magnetic resonance (MR) coil if the rotation axis of their spin moves. If human tissue is brought into the high magnetic field of the MR scanner (B_0), spins realign with B_0 . Spins show a weak preference for parallel compared to antiparallel realignment with B_0 and hence there is a measureable longitudinal magnetization M_z (Weishaupt et al., 2006). Now radio frequency (RF), also called high frequency (HF) pulses, can be used to deflect spins into the transversal plane (transversal magnetization M_{xy}). After this excitation, the spins start to realign again with B_0 and this induces an electrical voltage in the receiving coil of the MR scanner. This process requires both longitudinal relaxation and transverse relaxation, which are independent processes running in parallel. The longitudinal relaxation time $T1$ (0.5-5 s) is the time needed for full longitudinal relaxation, i.e. the transformation of M_{xy} back to M_z . $T1$ -weighted images are frequently used for high-resolution anatomical images (Weishaupt et al., 2006). The transverse relaxation time $T2$ (100-300ms) is the time needed until transversal magnetization has disappeared because spins started to rotate with different velocities (also referred to as dephasing). Dephasing occurs due to spin-spin interactions ($T2$) as well as field inhomogeneities ($T2^*$; Weishaupt et al., 2006). Generally speaking, small changes in field inhomogeneities are utilized to measure changes in neural activity by means of fMRI.

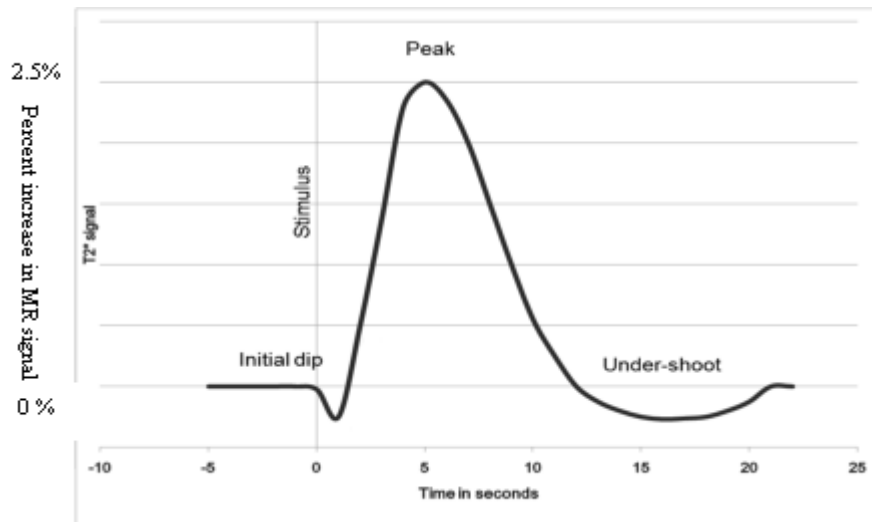
1.5.2 MRI signal types

fMRI measures neural activity indirectly by imaging vascular signals driven by neurovascular coupling. Two different types of neurovascular fMRI signals can be assessed non-invasively: (i) the blood oxygenation level dependent (BOLD) effect and (ii) cerebral blood flow (CBF).

Both fMRI signal types were used in the present thesis and will be introduced in the following sections.

1.5.2.1 The blood oxygenation level dependent (BOLD) effect

It was discovered in 1935 that oxyhaemoglobin is diamagnetic whereas deoxyhaemoglobin is paramagnetic since the iron atom is not shielded by oxygen atoms (Pauling, 1935). Hence, deoxyhaemoglobin causes local field inhomogeneities which formed the basis for fMRI based on T_2^* . The BOLD effect measures neuronal activity indirectly by measuring changes in blood oxygenation but also relies on changes in CBF and cerebral blood volume (CBV) and hence is a rather heterogeneous signal and not a pure measure of one parameter. The temporal time course of the BOLD signal is described by the haemodynamic response function (HRF) which has been validated experimentally for many human brain regions and can be subdivided into three stages (Figure 1.12). Due to increased metabolic demands of firing neurons, deoxyhaemoglobin initially increases slightly, which causes the “initial dip” of the HRF. Following this initial decrease, vasodilatation occurs after a short period of time, which results in local increases in CBF, CBV and an oversupply of oxyhaemoglobin relative to deoxyhaemoglobin. Since oxyhaemoglobin is diamagnetic, the relative increase of oxyhaemoglobin is associated with an increase in MR signal. Finally, the blood oxygenation level returns to normal and the BOLD signal decays to levels slightly below baseline (undershoot) before returning to its initial baseline level (Heeger & Ress, 2002). This neurovascular response is regionally variable and has been demonstrated to relate to local field potentials (which result from various synaptic and cellular mechanisms) with a delay of 3-6 s (Logothetis et al., 2001). BOLD is the by far most widely-used fMRI technique and offers high sensitivity: the BOLD response typically consists of a 0.5-5% increase in regional image intensity which increases further with higher magnetic field strength of the MR scanner (Detre & Wang, 2002). While BOLD fMRI has become a widely accepted brain mapping tool, it is subject to the fact that activation signals come from larger vessels further downstream from the actual site of neuronal activity. The underlying cause is local field inhomogeneity around large draining veins. And hence spatial specificity of BOLD fMRI signal is low compared to CBF techniques (Duong et al., 2000; Luh et al., 2000; Silva et al., 1997; Tjandra et al., 2005).



<http://openwetware.org/wiki/Beauchamp:NIRS> (12.08.2011)

Figure 1.12: Introduction: The haemodynamic response function. The haemodynamic response function (HRF) has been validated experimentally and describes the temporal time course of the BOLD (blood oxygenation level dependent) magnetic resonance imaging (MRI) signal. (T_2^* : transverse relaxation time)

1.5.2.1.1 BOLD fMRI sequences

There are numerous different MRI pulse sequences available among which Gradient-Echo (GRE) and Spin-Echo (SE) are the most important pulse sequences for measuring the BOLD effect. GRE uses a single slice-sensitive RF excitation pulse (deflecting spins by usually 90° = flip angle). Due to static field inhomogeneities spins are dephasing, i.e. some spins run faster than others. In SE, the 90° excitation pulse is therefore followed by a 180° pulse after half echo time (TE). This additional pulse reverses all spins. Now all spins have to travel the same distance to reach their original position which they had already been travelled. Fast moving spins that had already travelled long distances now have to travel long distances to reach their original position whereas slowly moving spins that had travelled only short distances have to travel only short distances to reach their original position. Since the field inhomogeneities that caused differences in travel velocities are still present, all spins are again in-phase after another half TE. This difference makes SE pulse sequences less sensitive to field inhomogeneities around large draining veins than GRE pulse sequences and consequently SE signal has been demonstrated to have higher spatial specificity compared to GRE signal (Goense & Logothetis, 2006; Harel et al., 2006).

1.5.2.2 Perfusion fMRI measuring cerebral blood flow (CBF)

An alternative to fMRI techniques assessing the BOLD effect are perfusion fMRI techniques which are a nearly pure measure of local increases in CBF. Perfusion fMRI has been demonstrated to show excellent co-localization with neuronal activity at the expense of lower sensitivity (~ 1% change in regional image intensity; Wintermark et al., 2005). CBF can be assessed by means of arterial spin labelling (ASL) pulse sequences in which arterial blood water is magnetically labelled (most frequently by inversion of longitudinal magnetization) in an imaging slice proximal to the tissue of interest. This labelling procedure is non-invasive and is achieved by means HF pulses. Control images without blood labelling are additionally acquired to yield images with identical tissue signal but without the signal arising from inflowing blood. Signal from inflowing blood can be inferred from pair-wise subtraction of images acquired with and without blood tagging. Labelled arterial spins flowing into the brain tissue elicit local signal changes (either an increase or decrease depending on the specific technique applied), which are proportional to CBF (i.e. magnetically labelled blood acts as internal diffusible tracer during perfusion MRI).

1.5.2.2.1 CBF fMRI sequences

Numerous different ASL techniques are available, which can be broadly divided into continuous ASL (CASL) and pulsed ASL (PASL). In CASL inversion of blood magnetization is achieved by a continuous RF pulse (lasting a few seconds) delivered at the level of the internal carotid artery (Williams et al., 1992) whereas in PASL inversion of blood magnetization is performed in tissue located next to the slices of interest using a short RF pulse (lasting only a few milliseconds). PASL has several advantages over CASL and is the most frequently used technique (Monet et al., 2009). Numerous different PASL techniques have been developed to minimize artefacts such as magnetization transfer effects (transfer of longitudinal magnetization between free hydrogen atoms and hydrogen atoms bound to macromolecules) by optimising blood water labelling and control image acquisition techniques. In the PICORE (Proximal Inversion with a Control for Off-Resonance Effects) method the inversion pulse, which is used for blood labelling is selectively applied to a region beneath the slices of interest. In the control condition, a non-selective inversion pulse over the entire brain is utilized, which generates the same magnetization transfer effect in the imaging slice as during the tag condition. Hence, magnetization transfer effects cancel each other out when tagged and control images are subtracted. Additionally, saturation pulses can be applied

on both tagged and control images to better define the tail of the inverted blood bolus which is achieved by the QUIPSS II (Quantitative Imaging of Perfusion using a Single Subtraction; Wong et al., 1998) saturation module for PASL. Numerous pulse sequences have been developed based on QUIPSS II. In the present thesis we used PICORE-Q2TIPS, that is the PICORE labelling scheme with Q2TIPS (QUIPSS-II with thin-slice $T1$ periodic saturation), which is a modified version of QUIPSS II eliminating residual errors remaining due to incomplete saturation of spins and minimizing the spatial mismatch of saturation and inversion slice profiles (Luh et al., 1999).

1.5.3 fMRI data analysis

fMRI data analysis usually comprises two main steps, i.e. data preprocessing and subsequent statistical analysis. fMRI data consist of time series of 3D volumes, whereas one volume refers to one image of the brain at a given time point. One volume consists of several subsequently acquired brain slices and each slice consists of rows of voxels. Most frequently applied steps in fMRI data preprocessing are: (i) spatial realignment (of volumes to a mean image by translation and rotation along the three spatial axes to correct for spatial displacements induced by head movements during scanning), (ii) slice timing correction (interpolation of intensity at a specific time point to correct for different acquisition time of slices), (iii) anatomical co-registration (spatial alignment of echo-planar imaging (EPI) volumes with high-resolution anatomical $T1$ -weighted images), (iv) spatial normalization (changing orientation and shape of EPI volumes to match a standard brain template allowing voxel-wise comparison between subjects in group-analyses), and (v) spatial smoothing (to increase statistical power and correct for residual inter-individual differences (Smith, 2001; Wohlschlagel et al., 2007)). For statistical analysis of fMRI data, an univariate General Linear Model (GLM) is used which models the variation of fMRI signal in each voxel as a linear combination of weighted regressors (i.e. experimental conditions) and an error term (Kiebel & Holmes, 2007). Regressors consist of onsets of experimental conditions convolved with the HRF to account for the temporal delay of the haemodynamic response. Regression weights are parameters that are separately estimated for each voxel and experimental condition. Statistical analyses on estimated parameters are performed based on T- or F-contrasts. The result is a statistical map showing significantly activated voxels given a certain linear combination of regressors.

1.6 Dynamic causal modelling (DCM)

Dynamic causal modelling (DCM) was introduced in 2003 to investigate effective connectivity by means of fMRI (Friston et al., 2003). DCM is a systems theory oriented approach (Stephan, 2004). Elements of the modelled system correspond to different brain areas. The direct effect of experimental conditions on activity in brain areas and causal interactions between areas (modulated by experimental conditions) are investigated within the framework of a bilinear model. Dynamic changes within the system are given by measured fMRI data and the thereof estimated parameters θ are interpreted as effective connectivity, i.e. as the causal influence that activity in one area exerts on activity in another area (Friston et al., 2003). DCM is a simplified model for interregional coupling of n interacting brain regions of which each is described by a “neuronal state” (reflecting changes in neuronal activity over time). A particular advantage of DCM over other techniques, which are available to investigate effective connectivity (such as structural equation modelling (SEM), Buchel & Friston, 1997; psychophysiological interactions (PPI), Friston et al., 1997, and Granger causality, Roebroeck et al., 2005) is that effective connectivity is estimated on the neuronal level. Neuronal states are “translated” into BOLD signal by means of a haemodynamic forward model (Friston et al., 2003). Within the same combined model, neuronal interactions between areas as well as parameters of neurovascular coupling of each brain area are estimated (within experimentally validated physiological ranges) to fit the measured data as well as possible. Although neuronal state vectors do not have a direct neurophysiological correlate they follow concepts of local field potentials and neuronal firing rates (Eickhoff & Grefkes, 2011). Neuronal dynamics within the system are approximated by the following bilinear differential neuronal state equation which was proposed based on a general state equation for non-autonomous deterministic systems (non-autonomous systems are systems which exchange energy or matter with their environment; deterministic indicates that external inputs change neuronal activity within the system; Friston et al., 2003; Stephan et al., 2007):

$$\frac{dz}{dt} = Az + \sum_j u_j B^j z + Cu$$

where dz/dt is the change in neuronal activity in one area over time, z is the neuronal state, u is the experimental input, and j refers to the j th input. A , B , and C are matrices of unknown coupling parameters θ_n reflecting effective connectivity between areas. The parameter matrices describe different components of effective connectivity. The DCM-A matrix refers to endogenous connectivity that describes network interactions independent of experimental

conditions. Experimental conditions can impact on the system in two ways, either by modulating coupling strength between areas (which is referred to as task-dependent connectivity described by the DCM-B matrix) or by increasing activity in one or more areas directly, which is referred to as “driving inputs” and is described by the DCM-C matrix (for example visual stimulus presentation increases activity in early visual cortex). Please note that endogenous connectivity may not be mistaken as baseline connectivity. It rather reflects the task-independent component of effective connectivity across the entire time course of the experiment onto which task-modulated changes may add during presence of a certain experimental condition (as can be inferred from the neuronal state equation). Coupling parameters are expressed in the unit Hertz (influence per time). Positive coupling parameters indicate that activity in the source region increases activity in the target region and can be interpreted as facilitation. By contrast, negative coupling parameters indicate that activity in the source region decreases activity in the target region which can be interpreted as inhibition (Friston et al., 2003; Stephan et al., 2010). Please note that coupling parameters also implicitly capture the influence of possible relay regions such as e.g. the basal ganglia or the cerebellum and do not necessarily reflect direct axonal projections between areas. Since task-dependent modulations do not necessarily impact on all endogenous connections, different connectivity models reflecting biologically plausible hypotheses on interregional coupling are usually tested against each other in a Bayesian model selection (BMS) procedure which determines the most likely model given the measured data. This model is characterized by providing the best trade-off between accuracy (in explaining the data) and complexity (in terms of network architecture; Penny et al., 2004).

2 Objectives and structure of the thesis

2.1 Summary of the medical problem

As outlined in section 1 (General introduction), stroke is the most common cause for permanent disability in adults despite physical and occupational therapy (Kolominsky-Rabas et al., 2006). Hence, there is great need for new therapeutic strategies supplementing physical therapy in stroke rehabilitation. Interestingly, physical training is associated with an increase in cortical excitability (Adkins et al., 2006; Butefisch et al., 2000; Perez et al., 2004; Rosenkranz et al. 2007). However, an increase in cortical excitability can also be induced by repetitive transcranial magnetic stimulation (rTMS), and particularly theta-burst stimulation (TBS; Huang et al., 2005). Consequently, TBS is regarded to have high therapeutic potential for treatment of stroke-induced motor deficits if applied alone (Di Lazzaro et al., 2008a, 2010; Talelli et al., 2007) or in combination with physical therapy (Ackerley et al., 2010).

In line with the so-called *model of hemispheric competition*, increasing excitability of the ipsilesional hemisphere (Khedr et al., 2005; Kim et al., 2006; Talelli et al., 2007) as well as decreasing excitability of the contralesional hemisphere (Fregni et al., 2006; Mansur et al., 2005; Takeuchi et al., 2005), has been shown to improve motor performance of the stroke-affected hand. The underlying mechanism for the latter stimulation strategy appears to be reduced interhemispheric inhibition from the contralesional hemisphere onto the ipsilesional hemisphere after inhibitory rTMS applied to the contralesional hemisphere (Grefkes et al., 2010). However, there is considerably high variability in rTMS effects both, across studies (Hoogendam et al., 2010) and across individual patients (Ameli et al., 2009), which puts in question whether rTMS effects are sufficiently robust to be useful in clinical settings. Hence, the major goal of the present thesis was to develop novel strategies to reduce variability in rTMS induced effects in stroke patients with motor deficits. For this purpose, overall three studies, combining (repetitive) TMS with state-of-the-art neuroimaging techniques (such as ASL and DCM), were designed to (i) reduce variance of rTMS effects across studies and (ii) reduce variance of rTMS effects across patients.

2.2 Study I & II: Reducing variance across studies

Sources of variance across studies are likely to be methodological in origin. They might result from differences in rTMS protocols and different strategies to identify the cortical rTMS target position. It is becoming increasingly apparent that effects are more consistent across studies when TBS is used instead of *simple rTMS protocols* and that more and more studies will use TBS in the future (Hoogendam et al., 2010). Therefore, the present thesis focusses on the problem of identifying the most suitable cortical rTMS target position.

Studies which aim to improve motor function after stroke predominantly use the primary motor cortex (BA4) as target area. However, numerous different strategies exist to identify BA4 (Sparing et al., 2008). Compared to other techniques, individual fMRI data yield best approximations of the most excitable TMS position (Sparing et al., 2008). Nevertheless, a considerably large spatial mismatch between the cortical position showing highest movement-related fMRI signal and the cortical position yielding highest muscle responses when stimulated with TMS (of up to 14 mm) has frequently been reported (Bastings et al., 1998; Boroojerdi et al., 1999; Herwig et al., 2002; Krings et al., 1997; Lotze et al., 2003; Sparing et al., 2008; Terao et al., 1998).

The cause for this spatial mismatch is only poorly understood. Hence, the first study (Study I) was designed to increase knowledge of the underlying cause for the spatial mismatch between fMRI and TMS. We tested the hypothesis that high sensitivity of the widely-used Gradient-Echo blood oxygenation level dependent (GRE-BOLD) fMRI technique for large draining veins is responsible for low spatial congruence between fMRI and TMS. For this purpose, positions obtained by the “standard” GRE-BOLD technique were compared to positions obtained by two alternative fMRI techniques, which have been suggested to yield activations closer to the actual site of neuronal activity, i.e. Spin-Echo (SE-BOLD) and arterial spin labelling (ASL-CBF). TMS motor mappings were performed to identify the optimal TMS position and Euclidean distances between the individual optimal TMS position and individual GRE-BOLD, SE-BOLD, and ASL-CBF positions were compared. Our hypothesis was that SE-BOLD and ASL-CBF may localize neural activity significantly closer to both BA4 and the optimal TMS position (since it is assumed that the position with highest TMS excitability corresponds to the position with highest density of motoneurons in BA4 (Talelli et al., 2006)). Hence, SE-BOLD and ASL-CBF could in future be used to achieve more reliable estimates of the most excitable TMS position and lead to more consistent results across studies. Study I

was performed in healthy young subjects and results were recently accepted for publication (Diekhoff et al., 2011).

Identification of the cortical target position for TMS appears particularly challenging in stroke patients because reorganization processes may shift highest movement-related fMRI signal and most excitable TMS positions in unknown extent and direction (Bastings et al., 2002; Rossini et al., 1998; Thickbroom et al., 2002). Whether such shifts increase or decrease spatial congruence between fMRI and TMS is unknown and was matter of investigation in Study II. Results could also be different from healthy subjects because stroke patients may show vascular abnormalities (such as stenoses) and it is unknown differentially impact on conventional BOLD and perfusion MRI techniques (i.e. ASL-CBF). Therefore, similar measurements as in Study I were performed in chronic stroke patients in Study II to investigate whether findings obtained from healthy young subjects do also apply to stroke patients despite spatial shifts induced by functional reorganization and vascular abnormalities. fMRI and TMS positions were obtained from both hemispheres (to investigate differences between the ipsilesional and the contralesional hemisphere in stroke patients) and results of stroke patients were compared to results of a group of age-matched healthy control subjects.

2.3 Study III: Reducing variance across patients

Variance in rTMS effectiveness across patients is likely to result from patient characteristics such as lesion location, time since stroke, severity of deficit, and underlying pathomechanism causing motor hand deficits. The *model of hemispheric competition* is certainly useful as a model but is unlikely to apply uniformly to all stroke patients. It seems more likely that different stroke lesions (affecting different neuronal substrates) produce different subtypes of pathomechanisms. Hence, different patients may benefit from different rTMS intervention strategies. For example, patients with reduced effective connectivity within the ipsilesional hemisphere (Grefkes et al., 2008b; Grefkes & Fink, 2011; Mintzopoulos et al., 2009; Sharma et al., 2009) might benefit from facilitation of the ipsilesional hemisphere whereas patients with pathologically increased inhibition from the contralesional M1 onto the ipsilesional M1 (Grefkes et al., 2008b, 2010; Duque et al., 2005; Murase et al. 2004) might benefit from inhibition of the contralesional hemisphere. The aim of Study III was to identify reliable predictors for behavioural effects of facilitatory iTBS applied to the ipsilesional hemisphere and inhibitory cTBS applied to the contralesional hemisphere (compared to control

stimulation). In a multimodal approach, single-pulse and paired-pulse TMS parameters, movement-related fMRI signal, laterality of fMRI signal, and effective connectivity within the cortical motor network (assessed by means of DCM) were used to identify potential predictors for effects of TBS on motor performance.

3 Study I: Spatial congruence of fMRI and TMS in healthy subjects

3.1 Introduction Study I

As stated above, Gradient-Echo (GRE) is by far the most widely used technique for fMRI due to high data acquisition efficiency and high sensitivity to $T2^*$ effects (Liu & Brown, 2007). The underlying blood oxygenation level dependent (BOLD) contrast relies on alterations of local magnetic susceptibility mainly caused by changes in deoxyhaemoglobin level reflecting the increased metabolic demands due to enhanced neural activity (Logothetis, 2008). However, such changes do not only occur in small blood vessels in brain parenchyma (i.e. grey matter) but also in large draining veins (Buxton et al., 1998). GRE-BOLD signal has been shown to be sensitive to both $T2^*$ changes in parenchyma as well as in and around large draining veins (Boxerman et al., 1995; Frahm et al., 1994; Uludag et al., 2009) and hence GRE-BOLD signal changes may show a spatial displacement from actual neuronal activities, reducing the specificity for functional localization. SE EPI is an alternative BOLD sequence which is sensitive to $T2$ and has been suggested to be more accurate in functional localization at higher field strengths, i.e. from 3 Tesla upwards (Duong et al., 2002; Lee et al., 2002; Norris, 2003; Thulborn et al., 1997; Uludag et al., 2009). Along with SE-BOLD, ASL is an attractive alternative to GRE-BOLD. ASL allows measuring both, CBF as well as BOLD signal simultaneously. The signal type depends on the contrast calculated in the subsequent analysis, i.e. the BOLD contrast is the standard “movement vs. rest” contrast, whereas the ASL-CBF contrast is the interaction between ASL-CBF time series (created by calculating control - tag differences) and the “movement vs. rest” contrast. The ASL signal related to CBF (ASL-CBF) arises from magnetically labelled (i.e. tagged) arterial blood that has passed through the capillary walls into the tissue or is still located within capillaries (Silva et al., 1997). A number of studies demonstrated that ASL-CBF is well co-localized with neuronal activity (Duong et al., 2000; Liu & Brown, 2007; Luh et al., 2000; Silva, 2005; Tjandra et al., 2005; Zappe et al., 2008).

Spatial accuracy of fMRI is especially important for fMRI informed (i.e. stereotaxically neuronavigated) TMS. TMS is a well established tool in neurosciences allowing non-invasive focal brain stimulation via externally applied magnetic fields (Barker et al., 1985). Within the last decade, neuronavigation systems emerged allowing precise online monitoring of coil

positions with reference to underlying brain structures and their functional properties assessed with anatomical or functional MRI, respectively. The potential of TMS in combination with fMRI is regarded to be high, especially for identification of TMS targets in the *virtual lesion approach* or in therapeutic intervention studies (Walsh & Cowey, 2000).

Several studies have already investigated the spatial congruence between positions yielding highest TMS effects, i.e. MEPs, and positions with highest neural activity, i.e. highest statistical t-values, during hand movements measured by neuroimaging techniques such as positron emission tomography (PET, Classen et al. 1998; Wassermann et al., 1996) or fMRI (Bastings et al., 1998; Boroojerdi et al., 1999; Herwig et al., 2002; Krings et al., 1997; Lotze et al., 2003; Sparing et al., 2008; Terao et al., 1998). All studies reported good gross spatial correspondence between TMS and neuroimaging techniques since both techniques localized neural activity during hand movements within the precentral gyrus. However, if mean Euclidean distances between optimal TMS positions and highest neuroimaging signal were reported, they were often relatively large, i.e. 13 (\pm 8.8) mm for ^{15}O (oxygen) PET (4 subjects; Wassermann et al., 1998), 9.8 mm (8 subjects; Herwig et al., 2002) and 13.9 mm (5 subjects; Lotze et al. 2003) for fMRI. Only one study reported relatively short mean 3D distances, i.e. 3.3 ± 0.8 mm (5 subjects; Terao et al., 1998) between TMS and fMRI. Hence, although all studies reported fairly good correspondence between TMS and fMRI, a considerably large residual mismatch has consistently been demonstrated rising the question whether these differences can be solely attributed to technical issues (e.g. coregistration inaccuracy or spatial low specificity of fMRI signal) or if both techniques probe different underlying (neuronal) processes. Although technical limitations due to unavailability of neuronavigated stimulation systems (Lotze et al., 2003; Terao et al., 1998; Wassermann et al., 1998) might have influenced spatial accuracy, the exact cause of the spatial mismatch remains unknown.

In the present study, we aimed to investigate whether displacements between TMS and fMRI might rely on the fMRI sequence used. All studies mentioned above used GRE-BOLD at 1.5 Tesla (except for Krings et al. (1997) who used SE-BOLD at 1.5 Tesla). Thus, all studies employed fMRI sequences that are susceptible to shifts towards large vessels at the field strength used. Hence, the observed mismatch between fMRI and TMS might, at least partially, be explained by inaccurate localization of the motor hand area by the fMRI sequences applied.

We, therefore, hypothesized that at 3 Tesla, SE-BOLD and ASL-CBF may provide more accurate information in terms of functional localization of the motor hand area than GRE-BOLD. In particular, we aimed to test the hypothesis that spatial differences are functionally relevant by stimulating brain tissue at fMRI peak voxel coordinates with single-pulse neuronavigated TMS. Finally, we aimed to answer the question whether the spatially more accurate fMRI sequences better match with optimal TMS sites for evoking highest motor responses.

3.2 Methods Study I

3.2.1 Subjects

MRI measurements were performed on 15 healthy subjects (8 males; 21-31 years old; mean age 24.9 ± 2.7). 14 subjects were right-handed and one subject was left-handed according to the Edinburgh Handedness Inventory (Oldfield, 1971). We did not exclude left-handers as we did not expect that handedness impacts on spatial localization accuracy of fMRI sequences. 12 subjects participated in a subsequent TMS session (7 males; 23-31 years old; mean age 25.1 ± 2.7 ; all right-handed). None of the subjects had any history of medical or psychiatric disease or contraindication to TMS (Wassermann, 1998). All subjects gave informed written consent to participate in this study, which was approved by the ethics committee of the Medical Faculty, University of Cologne, Germany (file-no 08-062). All experiments conformed to the Declaration of Helsinki, sixth revision 2008.

3.2.2 fMRI motor paradigm

Subjects were asked to perform visually paced rhythmic right thumb abductions at a frequency of 1.55 Hz. The movement frequency was paced by a red blinking circle on white background presented on a shielded thin film transistor (TFT) screen at the rear end of the MR scanner visible via a mirror mounted on the MR head coil. Blocks of thumb movements (20 s) were separated by resting baselines (40 s plus 0-6 s jitter) in which a black screen instructed the subjects to rest still until the next block of movements commenced. One fMRI session consisted of 10 cycles of baseline and movement blocks and lasted approximately 11 min. Each subject underwent three fMRI sessions, i.e. one for each fMRI sequence. The order

of fMRI sequences was counterbalanced across subjects. Prior to scanning, subjects were trained until a stable performance was reached, which was monitored by visual inspection.

3.2.3 fMRI data acquisition

MR images were acquired on a 3 Tesla Siemens MAGNETOM TimTrio scanner (Siemens, Erlangen, Germany). High-resolution anatomical $T1$ -weighted images were acquired using a 3D MP-RAGE (magnetization-prepared, rapid acquisition gradient echo) sequence with the following imaging parameters: TR = 2000 ms, TE = 3.25 ms, FOV = 256 mm, 176 sagittal slices, slice thickness = 1 mm, in-plane resolution = $1 \times 1 \text{ mm}^2$, flip angle = 9° . Although CBF and BOLD signal changes can be measured simultaneously using ASL, this approach has been shown to result in a reduction of the BOLD signal in the order of 15 % compared to conventional BOLD measurements (Luh et al., 2000). Hence, a separate GRE-BOLD session was conducted in the present study to ensure that each fMRI measurement was conducted under optimal conditions. Altogether, we employed three different fMRI sequences: (i) Gradient-Echo (GRE-BOLD) echo planar imaging (EPI) sequence with the following parameters: TR = 2200 ms, TE = 30 ms, FOV = 192 mm, 15 axial slices, slice thickness = 3 mm, in-plane resolution = $3 \times 3 \text{ mm}^2$, distance factor = 10 %, flip angle = 90° , (ii) Spin-Echo (SE-BOLD) EPI sequence with identical imaging parameters except for a longer TE of 80 ms, and (iii) PICORE-Q2TIPS (quantitative imaging of perfusion using a single subtraction with thin slice $T1$ periodic saturation – proximal inversion with a control for off-resonance effects) ASL-CBF sequence (Luh et al., 1999) using a FOCI pulse for inversion with the following parameters: $T1_1 = 700 \text{ ms}$, $T1_s = 900 \text{ ms}$, and $T1_2 = 1400 \text{ ms}$, TR = 2200 ms, TE = 30 ms, FOV = 192 mm, 15 axial slices, slice thickness = 3 mm, in-plane resolution = $3 \times 3 \text{ mm}^2$, distance factor = 10 %, flip angle = 90° . The tag was 10 cm in width positioned at a 1 cm gap inferior to the imaging slices. Two presaturation pulses were applied in the imaging planes immediately before the inversion tag to minimize the impact of the static tissue. A 20 mm thick saturation slab was repeatedly applied for the bolus cut-off (Cavusoglu et al., 2009). Images were acquired sequentially in ascending direction using a single-shot EPI technique. Slices covered a region extending from the body of the corpus callosum to the top of the parietofrontal vertex, thereby ensuring full coverage of the primary motor cortex along the central sulcus. Each fMRI session consisted of 310 EPI volumes including four “dummy” scans ensuring a steady-state in tissue contrast. 10 whole brain EPI volumes (35 slices) were

additionally acquired to improve the co-registration with the anatomical *T1* volume in data preprocessing (see below).

3.2.4 Analysis of individual fMRI data

For ASL sessions, ASL-CBF time series were created by calculating control-tag difference images (resulting in a total of 153 subtraction images) using surround subtraction (i.e. computing the difference between each image and the average of its two nearest neighbours), thereby reducing BOLD signal contamination of the ASL-CBF time course (see Cavusoglu et al., 2009). For image preprocessing and statistical analysis of GRE-BOLD, SE-BOLD and ASL-CBF data, we used FEAT (FMRI Expert Analysis Tool) version 5.98, part of FSL (FMRIB's Software Library, www.fmrib.ox.ac.uk/fsl). The following prestatistics processing was applied: motion correction using MCFLIRT (Jenkinson et al., 2002), non-brain removal using the brain extraction tool (BET; Smith, 2002), and spatial smoothing using a Gaussian kernel of 4 mm full width half maximum (FWHM). Time-series statistical analysis was carried out using FILM (FMRIB's Improved Linear Model) with local autocorrelation correction (Woolrich et al., 2001) and a high pass filter of 1/60 Hz to remove low frequency drifts. Head motion parameters were included as covariates into the model. Z (Gaussianised T/F) statistic images were thresholded using a voxel-wise corrected significance threshold of $P < 0.001$ (Forman et al., 1995; Friston et al., 1994; Worsley et al., 1992). ASL-CBF provided much weaker signal intensities than BOLD signal and thus, no correction for multiple comparisons was applied for the identification of peak voxel coordinates ($P < 0.001$, uncorrected). Coregistration to high resolution images was carried out using FLIRT (Jenkinson et al., 2001, 2002).

3.2.5 Identification of fMRI peak voxel

The voxel with the highest statistical t-value located within the precentral gyrus near or at the hand knob was identified for each of the three fMRI sessions per subject. The hand knob is shaped like an omega or epsilon in the axial plane and hook-shaped in the sagittal plane, and has been shown to constitute a reliable anatomical landmark for the motor hand area (Yousry et al., 1997). In two subjects no significant voxel could be observed in the precentral gyrus for the SE-BOLD session after correcting for multiple comparisons, and thus no correction was applied for identification of the peak voxel in these subjects ($P < 0.001$, uncorrected).

3.2.6 Identification of fMRI CoGs

While the peak voxel represents the site of maximal regional activity, the centre-of-gravity (CoG) of an fMRI activation cluster considers the spatial distribution of activity in the pericentral region and hence might be less prone to a spatial shift towards large veins which usually produce high levels of activation (Luh et al., 2000). Therefore, CoGs were computed for each of the three fMRI sessions per subject. In contrast to peak voxel coordinates, CoG coordinates are influenced by the threshold applied and hence a uniform threshold of $P < 0.001$ (uncorrected) was applied to all fMRI data (lower thresholds were found to yield very large activation cluster for BOLD sessions, whereas higher statistical thresholds could not be passed by ASL-CBF activation clusters). After thresholding, the fMRI activation cluster comprising the peak voxel was identified and the CoG was calculated as t-value weighted position.

3.2.7 Group analysis of fMRI data

EPI volumes were normalized to the standard template (MNI152 at 2 mm resolution) of the Montreal Neurological Institute (MNI, Canada) using FNIRT (FMRIB's Non-linear Image Registration Tool). A Gaussian kernel of 4 mm FWHM was used for spatial smoothing. For statistical analysis we applied FLAME 1 (FMRIB's Local Analysis of Mixed Effects). Z (Gaussianised T/F) statistic images were thresholded using clusters determined by $Z > 2.3$ and a corrected cluster significance threshold of $P < 0.001$. For anatomical assignment, statistics for the contrast “movement versus baseline” were overlaid with cytoarchitectonic probability maps of the Juelich Histological Atlas (Eickhoff et al., 2005, 2007).

3.2.8 Neuronavigated TMS apparatus

Stereotaxic frameless neuronavigation was performed with the eXimia navigated brain stimulation (NBS) system version 2.1.1 (Nexstim, Helsinki, Finland). Since subjects performed a thumb abduction task during the fMRI experiment, the right abductor pollicis brevis (APB) muscle, involved in thumb abduction movements served as target muscle. Simultaneous electromyography (EMG) recordings were additionally obtained from the right first dorsal interosseous (FDI) muscle. EMG signals were recorded by Ag/AgCl surface electrodes (Tyco Healthcare, Neustadt, Germany) placed in a belly-tendon montage. The

EMG signal was amplified, filtered with a 0.5 Hz high pass filter and digitized using a PowerLab 26 T Myograph and the “Scope” software package version 3 (ADInstruments Ltd, Dunedin, New Zealand). Prior to the study, TMS coils were x-rayed. Displacements between central positions of the outer plastic case and the inner copper wings occurred solely in anterior-posterior direction and did not exceed 1 mm for any of the TMS coils used.

3.2.9 Motor hotspot and resting motor threshold

Subjects were comfortably seated in an adjustable armchair with head-rest. The head of the subject was co-registered with the individual high-resolution anatomical MR image via anatomical landmarks (e.g., nasion and crus heliis). Prior to the study, the accuracy of the coregistration procedure was verified by small vitamin E capsules (providing a good MRI *T1* contrast) attached to a volunteer’s head at different anatomical positions. The software-depicted and true positions of the capsules did not show mismatches larger than 1 mm for any position. Furthermore, the root mean square difference between positions of landmarks in the MRI volume and at the subjects head was reported to be less than 2 mm for any TMS session of this study (reported by the neuronavigation software). After anatomical coregistration, the motor “hotspot”, i.e. the coil position providing highest MEPs of the APB muscle with shortest latencies during single pulse supra-threshold TMS, was identified. Hotspot coil orientations were (nearly) perpendicular ($90 \pm 10^\circ$) to the central sulcus and tangential to the scalp in all investigated subjects (information provided by the neuronavigation software). The resting motor threshold (RMT) was assessed by means of the TMS Motor Threshold Assessment Tool (MTAT) 2.0 (<http://www.clinicalresearcher.org/software.htm>) suggested by Awiszus (2003). The software starts with 45 % as stimulator output intensity. After being informed via button press whether a TMS effect (in the present study: a MEP with a peak-to-peak amplitude of at least 50 μ V) was induced by the applied stimulus or not, the software suggests a new threshold intensity based on maximum likelihood calculations. In the present study, the procedure was repeated 12 times ensuring a reliable estimation of the motor threshold.

3.2.10 TMS motor mapping

TMS mapping of the dominant, i.e. left motor cortex and the surrounding tissue was obtained by stimulation of an area determined by 8 (anterior-posterior) x 7 (medial-lateral) positions

spaced at intervals of 10 mm. The hand knob structure (Yousry et al., 1997) was located approximately in the centre of the grid, and the anterior-posterior axis was oriented in parallel to the interhemispheric fissure. Classen et al. (1998) showed that increasing the grid size considerably improves the motor mapping accuracy. Hence, we used a relatively large grid resulting in an area of 7 x 6 cm in size being stimulated. With such a large area stimulated we expected that stimulation of several positions at the margins of the grid would not result in MEPs. Classen et al. (1998) demonstrated that 5-6 stimuli per position are sufficient to achieve stable mapping results. Hence, positions not resulting in a MEP after 5 trials (peak-to-peak amplitude > 50 μ V) were stimulated with 5 stimuli, whereas positions resulting in at least one MEP after 5 trials were stimulated with 10 stimuli to achieve a good trade-off between mapping time and accuracy. The order of stimulation was randomized across the 56 positions (120 % RMT; ISI = 1500 ms). During the mapping procedure coil tilting was tangentially to the scalp and the TMS coil orientation was identical to coil orientation during RMT identification and stimulation at fMRI maxima coordinates. Both parameters were maintained throughout the mapping procedure.

The mean peak-to-peak MEP amplitude of the APB was calculated for each grid position using all EMG recordings obtained from this position (i.e. either 5 or 10) and divided by the largest amplitude obtained within the stimulation area. Based on these data, the centre-of-gravity (CoG) of the APB was calculated using the following formula:

$$CoG = \left[\sum_i \frac{\bar{a}(x_i, y_i) x_i}{a_{i,max}}, \sum_i \frac{\bar{a}(x_i, y_i) y_i}{a_{i,max}} \right]$$

with a_i being the mean amplitude at position x_i or y_i (Classen et al., 1998). While the TMS motor hotspot represents the site of maximal neuronal excitability, the CoG takes into account the spatial distribution of excitability in the pericentral region. Spatial differences between hotspot and CoG locations occur if there is an asymmetrical distribution of excitability around the hotspot. Therefore, the information provided by a CoG is not the location of highest excitability, but the weighted average of excitability of the region of interest. Hence, CoG coordinates might be less prone to artefacts. Since it is unknown at which position, superficial or deep, TMS-induced neuronal excitation occurs, we projected TMS identified positions (i.e. hotspot and CoG positions) onto the cerebral surface. This was done by identifying the individual depth of the cerebral surface by surface peeling of the software generated 3D head model (mean distance from the scalp: 24.5 ± 2.7 mm). Positions with highest EF strength at the cerebral surface were recorded during hotspot identification and TMS mapping and used

for later analyses. EF_{\max} positions were also marked on the individual structural *T1* image and transferred into MNI space by applying the respective nonlinear normalization transform that was also used to transfer individual fMRI activation maps into MNI space.

3.2.11 TMS of peak voxel coordinates at 120 % RMT

Brain tissue at fMRI peak voxel coordinates was stimulated with 120 % RMT (15 stimuli; interstimulus interval (ISI) = 3000 ms). The order of peak voxels obtained by the three different fMRI sequences was counterbalanced across subjects. The experimenter was blinded to the fMRI sequence. The target entry point for stimulation was identified by bringing the TMS coil in a position in which the distance between fMRI target and EF_{\max} value position was found to be minimal (0-2 mm, computed by the software). Then, tilting of the coil was adjusted until the coil was tangential to the scalp (computation and visual feedback provided by the software). TMS coil orientation coincided with TMS coil orientation during RMT identification. In this final position, one stimulus was applied. The coil positioning parameters of this stimulus were used as reference for all subsequent stimuli at this particular target (by means of the “aiming tool” implemented in the neuronavigation software).

3.3 Results Study I

3.3.1 fMRI group analysis

The fMRI group analysis of the contrast “right thumb movement versus baseline” revealed a left-lateralized network of cortical areas in left sensorimotor cortex located on the precentral and postcentral gyrus (Figure 3.1, $P < 0.001$, cluster-level corrected). SE-BOLD and GRE-BOLD sequences showed additional bilateral activation of the supplementary motor area (SMA), pre-SMA, cingulate motor area, dorsal and superior ventral premotor cortex, and anterior intraparietal cortex. More voxels were activated in the GRE-BOLD cluster as compared to the SE-BOLD cluster, and more for SE-BOLD than for ASL-CBF. The voxel with highest t-value at the precentral gyrus assessed in the voxel-wise group analysis of the spatially normalised GRE-BOLD session was close to the crown of the precentral gyrus (Figure 3.1, top right) and assigned to Brodmann Area (BA) 6 by the Juelich Histological Atlas (MNI coordinates: -38, -22, 62). In contrast, the peak voxel of the SE-BOLD group analysis was 6 mm deeper within the central sulcus and assigned to area BA4a, i.e. the

anterior primary motor cortex (MNI coordinates: -38, -22, 56; Geyer et al., 1996). The peak voxel of the ASL-CBF group analysis was located even deeper in the central sulcus (14 mm deeper than GRE-BOLD, 8 mm deeper than SE-BOLD group fMRI peak voxels) and assigned to area BA4p, i.e. the posterior part of the primary motor cortex (MNI coordinates: -40, -18, 48).

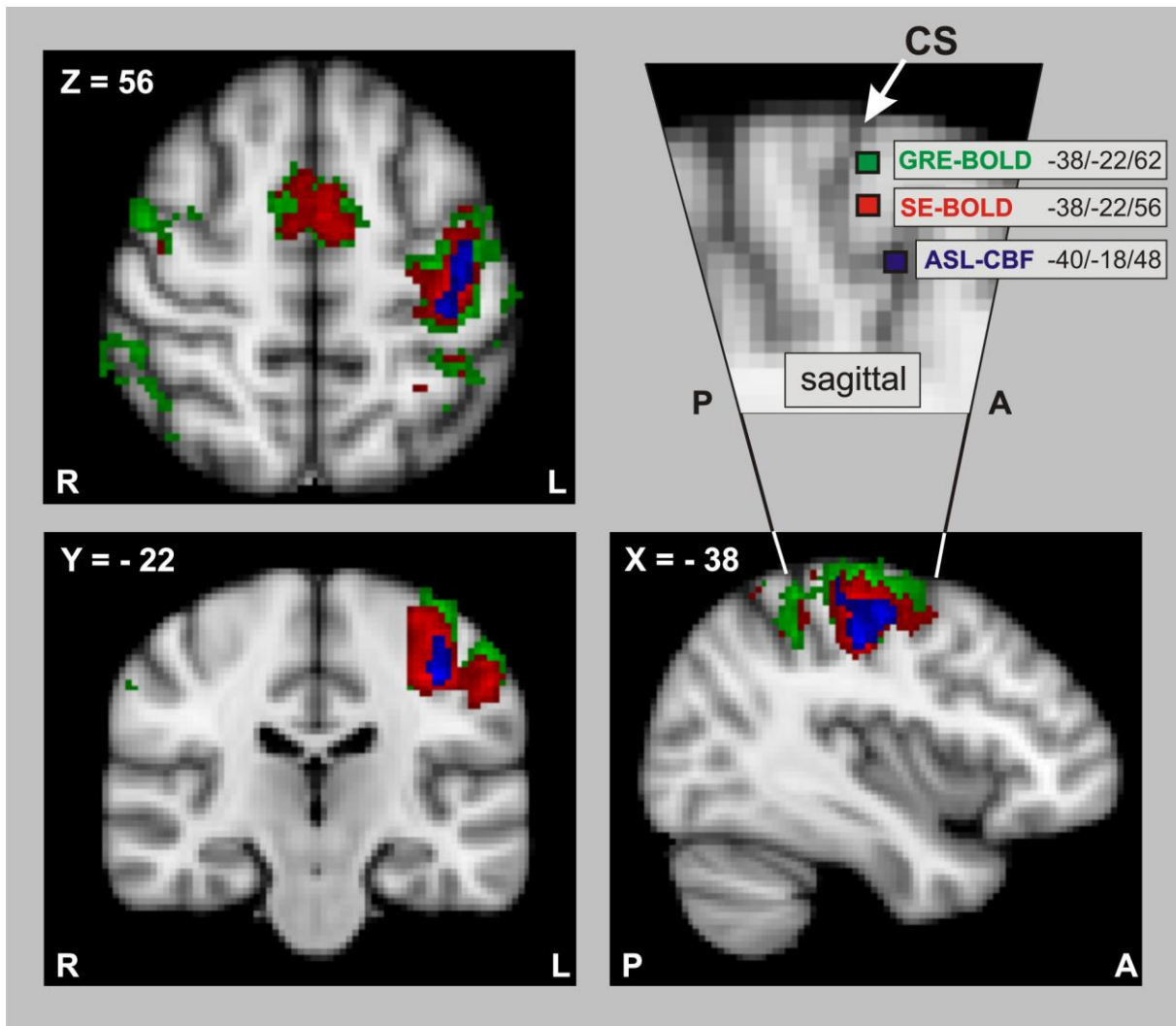


Figure 3.1: Study I: Results of the fMRI group analysis. Functional magnetic resonance imaging (fMRI) was performed in 15 healthy subjects during right thumb abductions with three different fMRI techniques, i.e. Gradient-Echo (GRE-BOLD, green), Spin-Echo (SE-BOLD, red), and arterial spin labelling (ASL-CBF, blue). GRE-BOLD and SE-BOLD rely on blood oxygenation level dependent (BOLD) contrast, whereas ASL-CBF measures changes in cerebral blood flow (CBF). “Movement versus rest” contrasts were superimposed onto the MNI standard template ($P < 0.001$, cluster-level corrected; only voxels exceeding a t-threshold of 3.0 are shown). The detail of the sagittal view (top right) shows the voxel with highest statistical t-value located within the precentral gyrus for each of the three different fMRI techniques (voxels were projected into plane $X = -38$). In line with our hypotheses, SE-BOLD and ASL-CBF yielded more focussed activation with higher specificity than GRE-BOLD. The voxel with highest GRE-BOLD signal change was closest to the gyral surface and was assigned to the premotor cortex (Juelich Histological Atlas). Highest SE-BOLD and ASL-CBF

signal changes occurred 6 and 14 mm deeper within the central sulcus, respectively and were assigned to the primary motor cortex (Juelich Histological Atlas). (A: anterior; CS: central sulcus; L: left; P: posterior; R: right)

3.3.2 Individual fMRI peak voxel coordinates

The differences found for the fMRI sequences in the fMRI group analysis were confirmed by analyses based on individual activation maps. Movement related neural activity could be observed with all three fMRI sequences in all subjects. However, sensitivity in terms of t-values of local maxima at the hand knob was significantly different across fMRI sequences (repeated measures ANOVA ($n = 15$) with the factor APPROACH (levels: GRE-BOLD, SE-BOLD, ASL-CBF; $F(2, 28) = 64.003$; $P < 0.001$). GRE-BOLD peak voxels had significantly higher t-values (11.4 ± 3.8) than SE-BOLD (5.7 ± 2.3) and ASL-CBF (1.6 ± 0.9) peak voxels. SE-BOLD peak voxels had significantly higher t-values than ASL-CBF peak voxels (post-hoc paired sample t-test, $P < 0.001$, each comparison). However, also the position of the peak voxel coordinates was significantly different across sequences: A repeated measures ANOVA ($n = 15$) with the factor APPROACH (levels: GRE-BOLD, SE-BOLD, ASL-CBF) showed significant differences between fMRI peak voxel coordinates in MNI coordinate Z ($F(2, 28) = 3.542$, $P < 0.05$; Figure 3.2; Table 3.1), i.e. in inferior-superior direction. Post-hoc t-tests revealed that GRE-BOLD coordinates (mean MNI coordinate Z: 60.7 ± 6.3) were significantly more superficial than SE-BOLD coordinates (56.4 ± 5.0) and ASL-CBF coordinates (55.5 ± 6.6), which were on average 4.3 mm and 5.2 mm deeper within the central sulcus, respectively ($P < 0.05$, each comparison). SE-BOLD and ASL-CBF peak voxel coordinates were not statistically different in MNI coordinate Z ($P > 0.05$). There were no significant differences between sequences in the other two dimensions, i.e. in the medial-lateral (MNI coordinate X; ANOVA, $F(2, 28) = 1.053$; $P > 0.05$) or posterior-anterior direction (MNI coordinate Y; ANOVA, $F(2, 28) = 0.829$; $P > 0.05$).

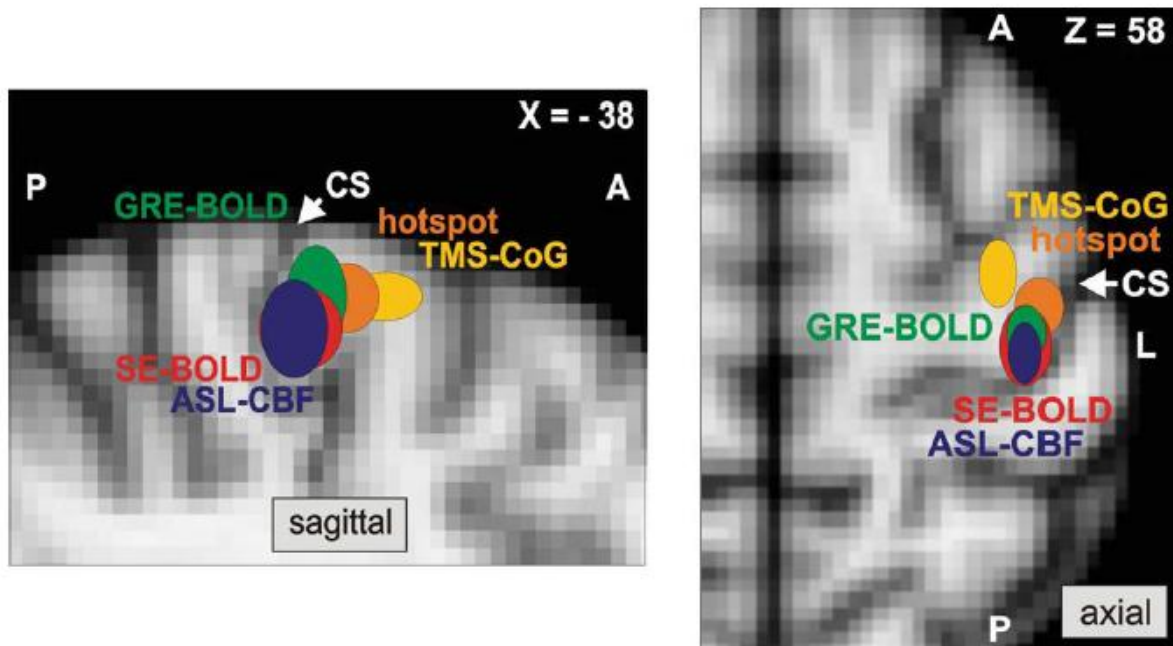


Figure 3.2: Study I: Localization of the primary motor cortex with fMRI and TMS. Coloured ellipsoids indicate mean MNI coordinates (\pm SD) of fMRI peak voxels and optimal TMS positions located within the precentral gyrus of the left hemisphere ($n = 12$ subjects). fMRI peak voxels were defined as voxel with highest statistical t-value during right thumb abductions measured with GRE-BOLD (green), SE-BOLD (red), and ASL-CBF (blue). Hotspot coordinates refer to stimulation sites resulting in highest abductor pollicis brevis (APB) muscle responses with shortest latencies (orange). CoG coordinates were calculated from a systematic TMS motor mapping, and reflect the motor evoked potential weighted maximum electric field coordinate (yellow). All coordinates were projected into sagittal plane $X = -38$ for the figure on the left showing the sagittal view and plane $Z = 58$ for the right figure on the right showing the axial view. GRE-BOLD coordinates were significantly more superficial than SE-BOLD and ASL-CBF coordinates (paired-sample t-test, $P < 0.05$, each comparison). Hotspot and CoG coordinates were significantly more anterior than fMRI maxima (paired-sample t-test, $P < 0.05$, each comparison). Euclidian distances to hotspot or CoG coordinates were not statistically different for GRE-BOLD, SE-BOLD, and ASL-CBF coordinates (paired-sample t-test, $P > 0.05$, each comparison). (A: anterior; ASL: arterial spin labelling; BOLD: blood oxygenation level dependent; CBF: cerebral blood flow; CoG: Centre-of-gravity; CS: central sulcus; fMRI: functional magnetic resonance imaging; GRE: Gradient-Echo; L: left; P: posterior; SD: standard deviation; SE: Spin-Echo; TMS: transcranial magnetic stimulation)

Table 3.1: Study I: Positions of highest fMRI signals and highest TMS effects individually identified in 12 subjects and transferred into MNI space using nonlinear normalization

	X	Y	Z
GRE-BOLD	-38.4 ± 3.2	-20.6 ± 4.2	60.7 ± 6.3
SE-BOLD	-37.9 ± 3.9	-21.5 ± 5.6	56.4 ± 5.0
ASL-CBF	-37.6 ± 2.6	-22.9 ± 4.5	55.5 ± 6.6
TMS hotspot	-40.7 ± 4.3	-15.7 ± 3.8	59.7 ± 3.7
TMS CoG _{APB}	-33.4 ± 2.7	-10.9 ± 5.0	60.0 ± 2.6

APB: Abductor pollicis brevis; ASL: arterial spin labelling; BOLD: blood oxygenation level dependent; CBF: cerebral blood flow; CoG: Centre-of-gravity; GRE: Gradient-Echo; SE: Spin-Echo; TMS: transcranial magnetic stimulation; X: lateral-medial; Y: anterior-posterior; Z: inferior-superior

3.3.3 Individual fMRI CoG coordinates

Significant spatial differences in depth (i.e. in MNI coordinate Z) were preserved when similar analyses (repeated measures ANOVA with the factor APPROACH) were performed on fMRI CoGs instead of fMRI peak voxels ($F(2, 28) = 4.662, P < 0.05$). Post-hoc t-tests revealed that GRE-BOLD CoG coordinates (mean MNI coordinate Z: 56.5 ± 2.5) were significantly more superficial than SE-BOLD (50.9 ± 5.5) and ASL-CBF (52.2 ± 6.9) CoG coordinates ($P < 0.05$, each comparison), whereas SE-BOLD and ASL-CBF CoG coordinates were not statistically different (paired sample t-test; $P > 0.05$). In addition, there was a significant difference in medial-lateral direction (i.e. in MNI coordinate X; $F(2, 28) = 5.948, P < 0.05$) since GRE-BOLD CoGs were significantly more medial than SE-BOLD and ASL-CBF CoG coordinates (paired sample t-tests; $P < 0.05$, each comparison). SE-BOLD and ASL-CBF CoG coordinates were not statistically different in medial-lateral direction (paired sample test; $P > 0.05$). There were no statistically significant differences between sequences in anterior-posterior localization (i.e. MNI coordinate Y) of CoGs ($F(2, 28) = 0.572; P > 0.05$).

3.3.4 Differences in fMRI and TMS positions

For each subject, the TMS coordinate of the motor “hotspot” (i.e. the coil position and tilt for evoking a MEP of 50 μ V peak-to-peak amplitude with lowest stimulator output intensity) and the centre-of-gravity (CoG) of a systematic TMS mapping of the motor cortex were projected

into MNI space by applying the individual FNIRT registration transform. MNI coordinates were then compared with the fMRI peak voxel coordinates by computing a repeated measures ANOVA ($n = 12$) with the factor APPROACH (levels: CoG_{APB}, hotspot, GRE-BOLD, SE-BOLD, ASL-CBF). The analyses revealed significant differences in medial-lateral direction, i.e. in MNI coordinate X ($F(4, 44) = 8.705$; $P < 0.001$) and in anterior-posterior direction, i.e. in MNI coordinate Y ($F(4, 44) = 14.168$; $P < 0.001$). Differences in inferior-superior direction, i.e. MNI coordinate Z showed a statistical trend ($F(4, 44) = 2.353$; $P = 0.069$; Table 3.1). Bonferroni-corrected post-hoc t-tests revealed that the motor hotspot was significantly anterior to GRE-BOLD, SE-BOLD, and ASL-CBF coordinates ($P < 0.05$, each comparison; Figure 3.2). Displacements between fMRI maxima and the hotspot in medial-lateral direction were less pronounced but there was a statistical trend for hotspot coordinates to be laterally of fMRI maxima ($P < 0.100$, each comparison). Hotspot coordinates were assigned to BA6 in all 12 subjects (Juelich Histological Atlas). The CoG_{APB} was significantly anterior to hotspot, GRE-BOLD, SE-BOLD, and ASL-CBF coordinates ($P < 0.05$, each comparison). In addition, CoG_{APB} coordinates were significantly more medial than ASL-CBF, GRE-BOLD, and hotspot coordinates ($P < 0.05$, each comparison) whereas the comparison to SE-BOLD coordinates failed the corrected P-threshold of $P < 0.007$ only marginally ($P = 0.011$, uncorrected). In all 12 subjects the CoG_{APB} was assigned to BA6.

3.3.5 Euclidian distances between fMRI and TMS positions

Although we found spatial differences between fMRI maxima obtained by different fMRI sequences, Euclidean distances between these maxima and the TMS hotspot were not statistically different across sequences (GRE-BOLD: 10.5 ± 3.0 mm; SE-BOLD: 11.2 ± 4.1 mm; ASL-CBF: 12.8 ± 3.7 mm; $F(2, 22) = 1.360$; $P > 0.05$, repeated measures ANOVA; see also Table 3.2). The same was true for Euclidean distances between fMRI maxima and the TMS mapping CoG_{APB}, which were also not significantly different across sequences (GRE-BOLD: 13.4 ± 5.5 mm; SE-BOLD: 15.3 ± 5.7 mm; ASL-CBF 15.3 ± 7.0 mm; $F(2, 22) = 1.115$; $P > 0.05$, repeated measures ANOVA). In other words, none of the fMRI sequences localized neural activity systematically closer to the TMS hotspot or the TMS CoG_{APB}. If identical analyses were conducted with fMRI CoGs instead of fMRI peak voxels, results were similar, i.e. none of the fMRI sequences yielded CoG positions systematically closer to the

TMS hotspot ($F(2, 22) = 1.151$; $P > 0.05$) or CoG_{APB} ($F(2, 22) = 0.191$; $P > 0.05$; see also Table 3.2).

Table 3.2: Study I: Euclidean distances between fMRI and TMS sites in single subject space

Subject	fMRI peak voxel vs. TMS hotspot			fMRI CoG vs. TMS CoG		
	GRE	SE	ASL	GRE	SE	ASL
1	11.49	15.10	13.75	42.89	17.80	21.29
2	12.81	4.90	13.56	8.50	14.73	21.00
3	14.59	14.59	13.00	14.18	14.56	15.98
4	13.75	13.75	9.43	14.49	18.60	8.95
5	7.48	7.48	17.80	17.68	24.49	19.78
6	11.00	6.32	11.49	23.86	12.66	3.84
7	8.72	14.70	13.75	25.54	12.22	11.17
8	5.48	17.15	18.47	22.22	25.30	24.58
9	13.19	13.19	16.67	19.25	25.87	23.75
10	11.45	10.77	10.05	5.20	5.85	17.56
11	6.40	6.32	8.94	5.75	11.77	8.89
12	9.38	10.20	6.32	17.93	22.11	20.53
Mean	10.5	11.2	12.8	18.1	17.2	16.4
SD	3.0	4.1	3.7	10.3	6.3	6.7

ASL: arterial spin labelling; CoG: Centre-of-gravity; fMRI: functional magnetic resonance imaging; GRE: Gradient-Echo; SD: Standard deviation; SE: Spin-Echo; TMS: transcranial magnetic stimulation; vs: versus

3.3.6 TMS of fMRI peak voxel with 120 % RMT

We stimulated brain tissue at the fMRI peak voxel coordinate with single-pulse neuronavigated TMS to investigate whether the spatial differences found for the three different fMRI sequences are functionally relevant, i.e. impact on MEP size of the respective peripheral target muscle (APB) and an adjacent small hand muscle not involved in thumb abductions (FDI). A repeated measures ANOVA ($n = 12$) with the factors APPROACH and MUSCLE (levels: APB, FDI) yielded a significant main effect of APPROACH ($F(22, 2) = 4.797$; $P < 0.05$) and MUSCLE ($F(11, 1) = 8.506$; $P < 0.05$) but no significant interaction ($F(22, 2) = 0.131$; $P > 0.05$). Post-hoc t-tests revealed that mean peak-to-peak MEP amplitudes of the APB and the FDI were higher for GRE-BOLD coordinates compared to both SE-

BOLD coordinates and ASL-CBF coordinates ($P < 0.05$, each comparison; Figure 3.3A). Muscle responses during TMS of SE-BOLD and ASL-CBF coordinates were not statistically different ($P > 0.05$). MEPs of the APB were statistically higher than MEPs of the FDI during stimulation of SE-BOLD and ASL-CBF coordinates ($P < 0.05$, each comparison) but not during stimulation of GRE-BOLD coordinates ($P > 0.05$). In summary, spatial differences of local maxima were matched by functional differences in MEP amplitudes. TMS at GRE-BOLD coordinates was probably more effective than TMS at SE-BOLD or ASL-CBF coordinates because GRE-BOLD coordinates were more superficial and anterior, and hence closer to optimal TMS positions than SE-BOLD and ASL-CBF sites. We correlated individual differences in mean MEPs obtained by stimulation of GRE-BOLD vs. SE-BOLD positions with individual spatial differences of GRE-BOLD vs. SE-BOLD positions in anterior-posterior direction. The result suggests that TMS over the GRE-BOLD site evoked larger MEPs the more anterior the GRE-BOLD coordinate was (APB: Pearson's $r = 0.67$, $P < 0.05$; FDI: Pearson's $r = 0.63$, $P < 0.05$). However, correlations for differences of GRE-BOLD vs. ASL-CBF positions and SE-BOLD vs. ASL-CBF positions were not statistically significant ($P > 0.05$, each correlation). Differences in medial-lateral or inferior-superior direction were also not significantly correlated with differences in MEP amplitudes between the three different fMRI sites ($P > 0.05$, each correlation). However, a significant main effect of sequence in the repeated measures ANOVA on mean EF_{\max} values at the target position during TMS ($F(22, 2) = 5.779$; $P < 0.05$) indicates that due to the physical constraints of TMS, superficial GRE-BOLD coordinates were stimulated with significantly higher mean EF_{\max} values (77.4 ± 23.2 V/m) compared to deeper SE-BOLD (61.7 ± 26.5 V/m) and ASL-CBF coordinates (59.2 ± 25.9 V/m; paired sample t-tests, $P < 0.05$, each comparison; Figure 3.3B). Differences between SE-BOLD and ASL-CBF coordinates in EF_{\max} values were not statistically significant (paired sample t-test, $P > 0.05$).

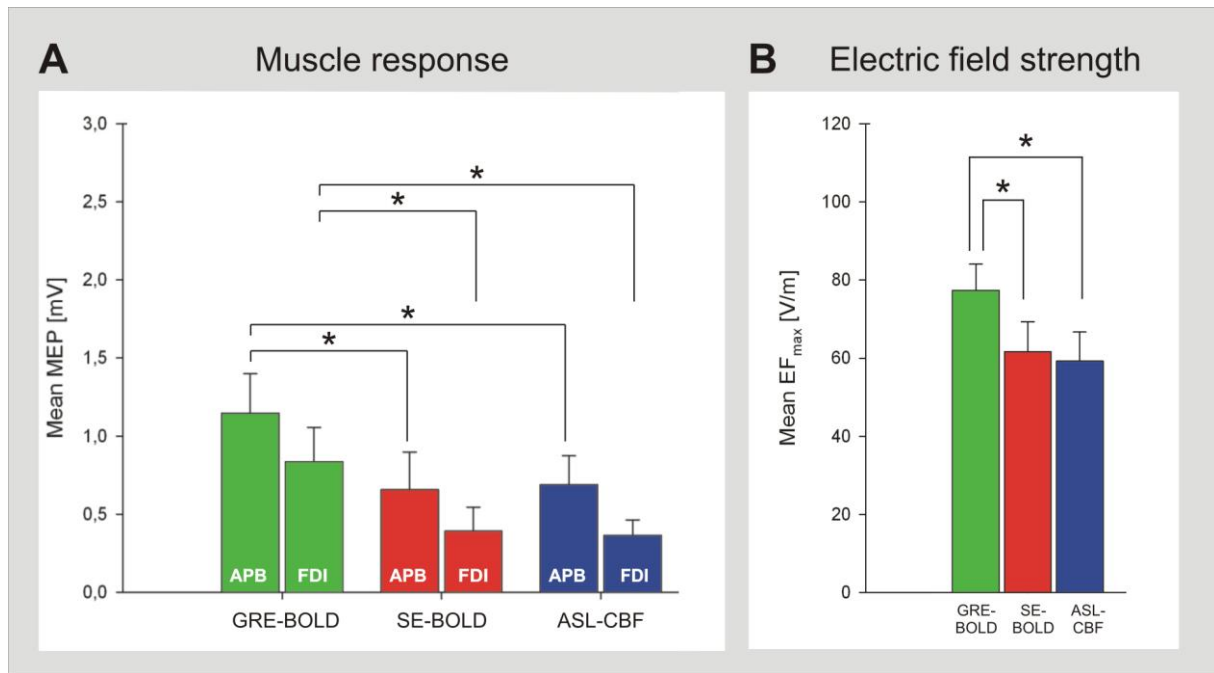


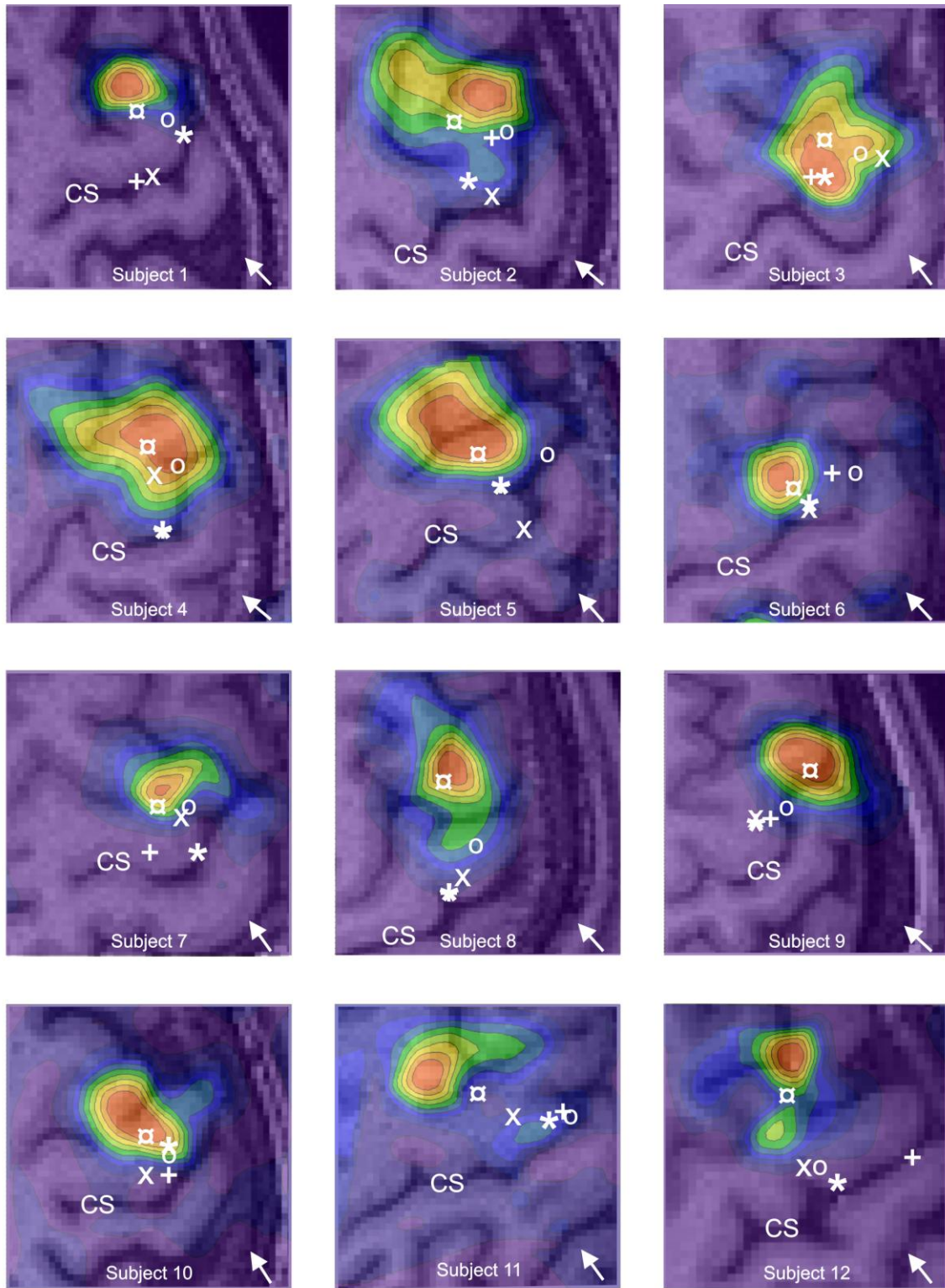
Figure 3.3: Study I: Stimulation of brain tissue at fMRI peak voxel coordinates with TMS. Neuronavigated TMS (120% resting motor threshold) was used to stimulate brain tissue at fMRI peak voxel coordinates to investigate whether localization differences between fMRI sequences are functionally relevant, i.e. impact on muscle responses ($n = 12$ subjects). **A:** Muscle responses. Peak-to-peak motor-evoked potentials (MEPs) of the abductor pollicis brevis (APB) and the first dorsal interosseus (FDI) hand muscle are shown. MEPs resulting of stimulation at GRE-BOLD coordinates were significantly higher than MEPs resulting of stimulation at SE-BOLD and ASL-CBF coordinates. **B:** Electric field strength at target position. Maximum electric field values (EF_{max}) reaching the fMRI target position during stimulation are shown. GRE-BOLD coordinates were stimulated with significantly higher EF_{max} values than SE-BOLD and ASL-CBF coordinates which were significantly deeper in the central sulcus and hence further away from the TMS coil. Mean EF_{max} values during stimulation at SE-BOLD and ASL-CBF coordinates were not statistically different (paired-samples t-test, $P > 0.05$) Error bars indicate standard errors. Asterisks indicate significant differences in paired sample t-tests (paired-sample t-test, $P < 0.05$, each comparison). (ASL: arterial spin labelling; BOLD: blood oxygenation level dependent; CBF: cerebral blood flow; fMRI: functional magnetic resonance imaging; GRE: Gradient-Echo; SE: Spin-Echo; TMS: transcranial magnetic stimulation)

3.3.7 Tests to exclude spatial errors of the TMS equipment

Coregistration quality was verified prior to the study and after each session (to verify that the head tracker depicting the subject's head position had not changed its position during the TMS session). Furthermore, for one subject with pronounced anterior shift of the optimal TMS position (Subject 1; Figure 3.4), the complete motor mapping was repeated with the induced current direction as applied before (i.e. posterior-anterior (PA), perpendicular to the central sulcus) and additionally with inverted induced current direction (i.e. anterior-posterior (AP), perpendicular to the central sulcus). If systematic anterior EF distortions due to coil failure or inaccurate computerized modelling accounted for the anterior shift of the optimal

TMS position, then the CoG of the mapping with inverted coil orientation (AP induced current direction) should be located considerably more posterior (i.e. to the amount of the displacement) than with standard coil orientation. The results showed that except for a drop in maximum MEP size, we basically replicated the map recorded with PA induced current direction with almost identical location of peak excitability and CoG (Figure 3.5). Therefore, technical confounds cannot explain the systematic anterior shift of optimal TMS positions when compared to fMRI peak voxels.

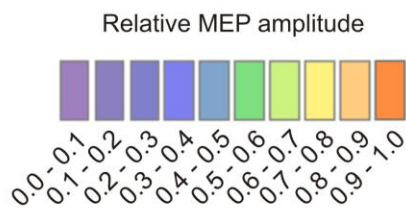
Study I: Congruence of fMRI and TMS in healthy subjects



fMRI:
 X ASL-CBF
 + SE-BOLD
 * GRE-BOLD

TMS:
 □ CoG
 ○ hotspot

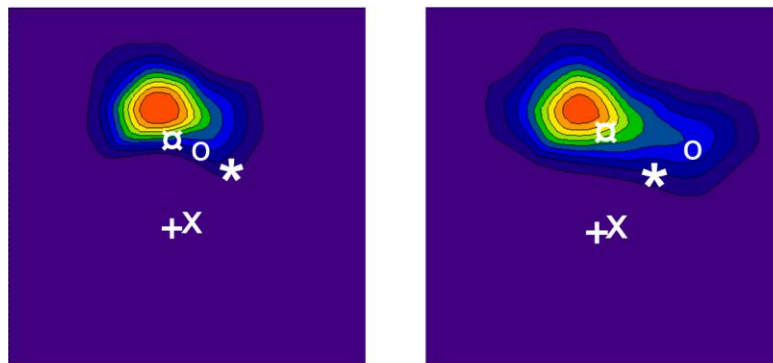
cs central sulcus



anterior
 medial

Figure 3.4: Study I: Results of TMS motor mappings. 8 (anterior-posterior) x 7 (medial-lateral) positions spaced at intervals of 10 mm were stimulated with neuronavigated TMS in randomized order (10 stimuli if at least one motor-evoked potential (MEP) > 50 μ V were recorded after 5 stimuli; otherwise 5 stimuli; 120% RMT (resting motor threshold); ISI (interstimulus interval) = 1500 ms). The hand knob was located approximately in the centre of the grid, and the anterior-posterior axis was oriented in parallel to the interhemispheric fissure. Positions refer to electric field maximum (EF_{max}) positions within the cerebral cortex calculated by computerized modelling. Contours represent 10 percentiles of the averaged maximal response of the abductor pollicis brevis (APB) muscle viewed from above. Background images refer to individual structural images showing the corresponding underlying cerebral anatomy. All fMRI and TMS positions (depicted as white symbols) were projected into the slice corresponding to the mean axial depth of all five individual sites (i.e. GRE-BOLD, SE-BOLD, ASL-CBF, TMS hotspot, and TMS CoG). (ASL: arterial spin labelling; BOLD: blood oxygenation level dependent; CBF: cerebral blood flow; CoG: Centre-of-gravity; fMRI: functional magnetic resonance imaging; GRE: Gradient-Echo; SE: Spin-Echo; TMS: transcranial magnetic stimulation)

Posterior-anterior (PA) current direction



Anterior-posterior (AP) current direction

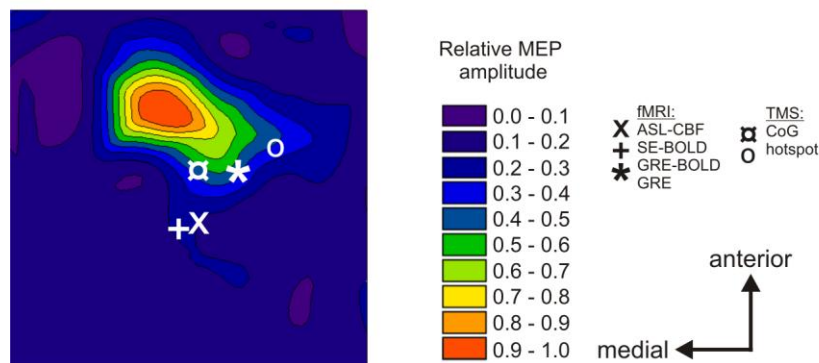


Figure 3.5: Study I: TMS motor mapping with inverted induced current direction. Upper Figures show results of the TMS motor mapping of one subject (Subject 1) with posterior-anterior (PA) induced current direction (perpendicular to the central sulcus). The upper left contour map is the initial mapping result; the upper right map is the result of the repeated mapping. Cortical excitability maps are very similar and demonstrate high reproducibility. The lower left figure shows the result of the mapping with reversed induced current direction pointing in anterior-posterior (AP) direction (perpendicular to the central sulcus). The map recorded with AP current direction replicated results of the mapping with PA current direction with almost identical location of peak excitability and CoG.

(ASL: arterial spin labelling; BOLD: blood oxygenation level dependent; CBF: cerebral blood flow; CoG: Centre-of-gravity; fMRI: functional magnetic resonance imaging; GRE: Gradient-Echo; MEP: Motor-evoked potential; SE: Spin-Echo; TMS: transcranial magnetic stimulation)

3.4 Discussion Study I

3.4.1 Localization differences between fMRI sequences

3.4.1.1 Localization of the motor hand area

The primary motor cortex constitutes a key area for the execution of voluntary movements (Dum & Strick, 2002; Grefkes et al., 2008a; Sanes & Donoghue, 2000). This region is structurally well defined: Human post-mortem studies showed that the primary motor cortex (Brodmann area 4, BA4) is a distinct cytoarchitectonic area characterized by the absence of layer IV and presence of giant Betz cells in layer V (Brodmann, 1909). At the hand representation area, BA4 is buried within the central sulcus and rarely extends to the gyral surface (cf. 1.2 and Figure 1.2), where it forms a boundary with the premotor cortex. Since ASL-CBF and SE-BOLD showed highest signal increase during isolated thumb abductions in the rostral wall of the central sulcus, i.e. the location where BA4 has to be expected (Eickhoff et al., 2005, 2007), our data suggest that at 3 Tesla these fMRI sequences may correctly locate the primary motor hand area. By contrast, signal increases for the GRE-BOLD sequence were shifted towards the crown of the precentral gyrus, and thus, towards BA6.

3.4.1.2 Systematic superior shift of GRE-BOLD

Both, fMRI group analysis as well as single subject fMRI analyses, demonstrated that highest GRE-BOLD signal changes showed a systematic shift in superior direction. These findings suggest that the underlying cause is, at least partially, subject-independent. High susceptibility of GRE-BOLD for large draining veins (Boxerman et al., 1995; Uludag et al., 2009), which mainly run on the cerebral surface (Duong et al., 2000), seems to be the most likely explanation for this finding.

3.4.1.3 Spatial localization of ASL-CBF (vs. GRE-BOLD) signal

ASL sequences measure cerebral blood flow (CBF) by means of magnetically labeled arterial water that has either passed the capillary wall into tissue or is still located within capillaries

(Silva et al. 1997). Due to the tight neurovascular coupling, CBF changes have been shown to occur in close proximity to neuronal activity (Duong et al. 2000; Luh et al. 2000; Tjandra et al. 2005). Duong et al. (2000) compared BOLD and CBF signal changes during forepaw stimulation in anesthetized rats at 9.4 Tesla. Additionally, calcium-dependent synaptic activity was measured by means of manganese ion (Mn^{2+}) acting as calcium analogue and MRI contrast agent. Results were comparable to our findings, i.e. clusters assessed with GRE signal were more expanded and diffuse compared to CBF. Importantly, voxels with highest BOLD percent signal change were located at the cortical surface, whereas voxels with highest CBF percent signal change showed excellent spatial co-localization with synaptic activity within deeper cortical layers, i.e. within layer IV, where neuronal activity was expected during sensory stimulation.

Our findings are also in line with the study of Luh et al. (2000) who identified tissue types by means of *T1* maps, which were correlated on a voxelwise basis with BOLD and CBF signal changes during bilateral finger tapping in 5 healthy subjects at 3 Tesla. This study demonstrated that GRE-BOLD voxels with highest t-values predominantly contained cerebrospinal fluid (CSF) and/or blood. In contrast, highest relative CBF signal changes were located in voxels with *T1*-values similar to voxels containing predominantly grey matter independent of t-score thresholds applied. Hence, CBF activation maps were better localized than BOLD maps, which is compatible with our data. In addition, Luh and colleagues (2000) calculated the fractional overlap of BOLD and CBF activation maps. As a result, the overlap was only in the order of 40%, which indicates that different signals were captured by BOLD and CBF. Tjandra et al. (2005) found no statistical spatial displacement between GRE and CBF statistical t-maps at 3 Tesla during visually cued finger tapping in 5 healthy subjects. However, Tjandra et al. (2005) used center-of-gravities (CoGs) instead of peak voxel coordinates for their comparison. A venous shift might have been evident when using peak voxel instead of CoGs, based on the findings reported by Luh et al. (2000) that especially voxels with high statistical values may contain signal from large veins and CSF. However, Tjandra et al. (2005) provided additional evidence for a shift of GRE signal towards veins. They defined the nearest draining vein by MR venograms and found that the group mean Euclidean distance to the nearest draining vein for GRE was significantly smaller compared to CBF. Thus, our data are supported by growing body of evidence that CBF is better co-localized to neural activity, whereas GRE is susceptible to shifts towards large veins or CSF.

3.4.1.4 Spatial localization of SE-BOLD (vs. GRE-BOLD) signal

SE and GRE fMRI sequences are both sensitive to the BOLD effect - a joint combination of changes in cerebral blood volume, CBF, and de-oxygenation level of blood (Buxton et al. 1998). Several studies demonstrated that both sequences have high susceptibility for large vessels at low magnetic fields, but in contrast to GRE signal, SE signal becomes selectively sensitive to microvasculature with increasing field strength (Kennan et al. 1994; Boxerman et al. 1995; Oja et al. 1999; Uludağ et al. 2009). Recently, Uludağ et al. (2009) proposed a model for assessing the amount of intra- and extravascular contributions to SE and GRE signal for magnetic field strengths ranging from 1.5 to 16.4 Tesla based on Monte-Carlo simulations. At 1.5 and 3 Tesla, intravascular contributions are higher than extravascular contributions for both sequences. Intravascular contributions mainly arise from veins to which GRE is more sensitive than SE. From 3 Tesla upwards, intravascular signal from veins vanishes for SE, but not GRE. Intra- and extravascular contributions to SE signal changes are equal at 3 Tesla (Norris et al. 2002) but intravascular signals mainly arise from the microvasculature (i.e., capillaries, arterioles, and venules), shifting towards blood vessels with high blood oxygenation (i.e., arterioles, capillaries) at higher field strengths. Although intravascular signal also decreases with increasing field strength for GRE, there is no field strength at which the BOLD signal from the microvasculature is larger than from the macrovasculature (Uludağ et al. 2009).

Recent experimental data from high magnetic field studies in animals (Lee et al. 2002) and humans (Duong et al. 2002) support these findings. Lee et al. (2002) compared neural activity during forepaw stimulation measured by SE and CBF in 10 anesthetized rats at 9.4 Tesla and found that both signal types were well correlated and localized in the middle of the cortex. Duong et al. (2002) compared SE and CBF signal changes during visual stimulation and voluntary movements at 4 and 7 Tesla in human subjects and found that both located neural activity within grey matter with good spatial correspondence. Hence, there is good evidence that at high field strengths, SE signal changes have comparable high spatial specificity as CBF signal changes. For example, several studies investigated the laminar specificity of high-resolution SE and GRE fMRI in primary visual cortex of macaque monkeys (Goense & Logothetis, 2006) or cats (Harel et al. 2006) at high magnetic fields, i.e. at 4.7 or 9.4 Tesla, respectively and found that laminar specific activation could be clearly demonstrated for SE yielding highest signal changes in cortical layer IV whereas highest GRE signal changes occurred at the cerebral surface. However, studies in humans at 3 Tesla are scarce (Thulborn

et al. 1997). Thulborn et al. (1997) measured neural activity during stimulation with different visual stimuli in human subjects at 3 Tesla with two different in-plane resolutions ($3.1 \times 3.1 \text{ mm}^2$ and $0.8 \times 1.6 \text{ mm}^2$; slice thickness: 3.0 mm). The authors found that the 10 most significant voxels obtained with SE and GRE overlapped by only 30% (low resolution) and 40% (high resolution) respectively. This result suggests that SE signal is not just a subset of the more sensitive GRE activation, but that both are detecting spatially different effects. This finding is in good agreement with our data suggesting that already from 3 Tesla on, SE signal changes are well localized with primary motor cortex activity. Uludağ et al. (2009) showed that reduced macro-vasculature weighting is achieved if large vessels predominantly run parallel to the main magnetic field as the susceptibility effect equals to zero for this condition. This is for example true for the central sulcus and hence for parts of the motor cortex but not, e.g., for the calcarine sulcus where the large vessels are mainly oriented perpendicular to the magnetic field. Therefore, in our study, SE might be more sensitive to gray matter than large vessels.

Taken together our findings strongly encourage considering alternative fMRI sequences such as ASL and (under certain conditions) SE when spatial localization is of high priority. However, decisions may depend on multiple aspects and not only on localization (Table 3.3). For example, CBF is superior to GRE in spatial accuracy, provides lower inter-session and inter-subject variation (Tjandra et al. 2005). However, GRE offers highest sensitivity (in terms of contrast-to-noise ratio), temporal resolution (due to faster data acquisition) and finally, a larger number of slices can readily measured with GRE, whereas ASL is limited to fewer slices (Liu and Brown, 2007).

Table 3.3: Study I: Qualitative comparison of different motor mapping approaches

	fMRI			TMS
Aim	Identification of position with highest task-related neural activity			Identification of position with lowest electrophysiological threshold to elicit MEPs of the respective peripheral muscle
Assessed via	Neurovascular coupling			Cortico-spinal excitability
	GRE-BOLD	SE-BOLD	ASL-CBF	
Measured variable(s)	BOLD (Deoxy-Hb, CBF, CBV)	BOLD (Deoxy-Hb, CBF, CBV)	CBF	Peripheral EMG signals
Main advantages	High CNR	High spatial specificity	High spatial specificity	Independent of vascular effects
Main disadvantages	Low spatial specificity	Low CNR	Low CNR	Restricted to superficial areas (limited penetration depth)
Main source of signal	Macrovasculature (mainly veins)	Arterioles and capillaries (≥ 3 Tesla)	Capillaries and brain parenchyma	Indirect transsynaptic excitation of cell bodies and direct excitation of axons
Localized structure	BA6	BA4a	BA4p	BA6
Distance to surface	+	++	+++	n/a

ASL: arterial spin labelling; BA: Brodmann area; BA4a: anterior primary motor cortex; BA4p: posterior primary motor cortex; BA6: premotor cortex; BOLD: blood oxygenation level dependent; CBF: cerebral blood flow; CBV: cerebral blood volume; CNR: contrast-to-noise ratio; Deoxy-Hb: deoxyhaemoglobin; EMG: electromyography; fMRI: functional magnetic resonance imaging; GRE: Gradient-Echo; SE: Spin-Echo; n/a: information is not available; TMS: transcranial magnetic stimulation

3.4.2 Localization differences between fMRI and TMS

Surprisingly, although SE-BOLD and ASL-CBF were more accurate in anatomical localization of the primary motor hand area, they provided significantly lower muscle responses than GRE-BOLD when stimulated with TMS. One explanation may be found in the properties of the EF induced by the magnetic pulse which declines exponentially with increasing distance from the TMS coil (Eaton, 1992). As GRE-BOLD peak voxel coordinates were significantly more superior (i.e. closer to the TMS coil), they were stimulated with

significantly higher EF strengths than SE-BOLD and ASL-CBF peak voxels. In this case, stimulation under equal conditions seems impossible to achieve with TMS, since stimulation of maxima with similar EF values would require stimulation with highly different stimulator output intensities, thereby enlarging the stimulated area. However, since it is unknown at which position, superficial or deep, excitation occurs, which accounts for highest TMS effects (Fox et al., 2004; Salinas et al., 2009; Thielscher et al. 2009), the most likely explanation for our findings is that the GRE-BOLD site was located more anterior (i.e. closer to the TMS hotspot) and thus TMS at the GRE-BOLD site was more effective. However, spatial distances between fMRI peak voxels and optimal TMS positions, i.e. hotspots and mapping CoGs, were not statistically different across fMRI sequences. This finding demonstrates that the mismatch between TMS and fMRI persists even if fMRI sequences with high anatomical accuracy such as ASL-CBF or SE-BOLD are used. Hence, a potential shift of GRE-BOLD towards superficial veins cannot explain the spatial mismatch observed between TMS and fMRI. Although fMRI and TMS were not expected to yield exactly identical positions due to apparent technical differences underlying these two brain mapping approaches, spatial mismatches were considerably large, i.e. 11.9 mm and optimal TMS positions were located within premotor areas in all 12 subjects (Eickhoff et al., 2005, 2007). These differences are not likely to be caused by technical issues, such as systematic coregistration errors or systematic EF distortions in posterior direction, since the magnitude of displacements were highly different across subjects (e.g. low in Subject 6, and high in Subject 8; Figure 3.4). Furthermore, similar anterior displacements were also reported in previous studies investigating spatial congruency of TMS and neuroimaging data such as PET (Classen et al., 1998) and fMRI (Herwig et al., 2002; Lotze et al., 2003). Even if no precise specifications were made, published figures often suggested anterior displacements of optimal TMS positions relative to PET (Wassermann et al., 1996; Figure 2) or fMRI (Bastings et al., 1998; Figure 2 and 3) activations.

3.4.3 Possible explanations for the anterior shift of optimal TMS positions

Muscle responses evoked by TMS typically have up to 3 ms longer latencies than muscle responses evoked by electrical stimulation, which led to the assumption that TMS activates cortical cells predominantly transsynaptically, whereas electrical stimuli excite cortical cell bodies or axons directly (Day et al., 1989; Hess et al., 1987; Mills et al., 1992; Rothwell et al.,

1991). However, it is unknown whether the entire synaptic chain (from optimal stimulation position to descending motoneurons) is located within the primary motor cortex or whether it includes (inter-) neurons in other regions, e.g. premotor cortex projecting onto BA4 neurons. Hence, it cannot be ruled out that indirect stimulation of BA4 neurons via transsynaptic input from BA6 accounts for anterior positions of optimal TMS sites.

Although fMRI and TMS sessions were performed under different functional motor states, (“active” during fMRI sessions, “passive” during TMS sessions) this difference seems unlikely to account for the spatial mismatch observed since previous studies demonstrated that TMS mappings under low-level voluntary contraction (10-20 % of maximum contraction) yield CoGs significantly anterior (and non-significantly medial) of CoGs obtained at rest (Lewko et al., 1996; Wilson et al., 1995). This anterior-medial shift (in the range of 6.6 to 20 mm) could be caused by decreased thresholds for surrounding premotor and supplementary motor areas during muscle pre-activation (Lewko et al., 1996). However, this anterior-medial shift would have more likely enlarged than shortened the distance between fMRI and TMS positions in the present study, since TMS mapping CoGs showed already (predominantly) anterior displacements.

We rather assume that EF effects are likely to account for the anterior shift of optimal TMS positions. Like the neuronavigation system used in the present study, most systems compute EF strength based on spherical head models which assume that EF is maximal directly under the junction of the wings and declines exponentially with distance from the coil (Eaton, 1992). However, there is growing evidence that this simplified model is insufficient, since different tissue types of the head have different conductivities which change the EF considerably. Realistic head models such as tissue-segmented MR images with realistic anatomical features like gyri and sulci demonstrated that the EF forms a complex pattern onto the folded cerebral cortex (Salinas et al., 2009). For instance, secondary EFs with either decreasing or increasing effects of varying magnitude (20-35 % of primary EF) and direction (often opposing the primary EF) occur especially near tissue boundaries (Salinas et al., 2009). These data show that stimulation with highest EF intensities does not necessarily occur directly under the junction of the coil as proposed by spherical head models. Therefore, it might be that stimulation with highest EF strength did not necessarily occur directly at the CoG position.

The neurophysiology of TMS is still incompletely understood but there is some evidence that lateral-medial (LM) induced current directions activate cortical motor neurons predominantly

directly leading to D-waves whereas posterior-anterior (PA) induced current directions, as used in the present study, activate cortical motor neurons predominantly indirectly via interneurons leading to I-waves (Di Lazzaro et al., 1998a). However, at stimulus intensities above the motor threshold (MT), as applied in the present study, induced PA current direction can also excite neurons directly generating D-waves (Di Lazzaro et al. 1998a). Hence, for the coil orientation and stimulus intensity used in the present study both types of neuronal excitation (direct and indirect) should be considered. I-wave generation relies on short distance (inter)neuron or even microscopic (dendrite, cell body) geometry (Herbsman et al., 2009), and there is some evidence that especially these short distance neuronal structures are subject to orientation-specific effects (Amassian et al., 1998). For instance, Fox et al. (2004) demonstrated that the orientation of the EF relative to cortical columns outweighs highest absolute EF strengths, i.e. TMS excitation was optimal within sulci where cortical columns run parallel to EF direction, although the absolute EF was higher at gyral crowns (where orientation to cortical columns is less optimal). Direct excitation on the other hand is mediated by longer neuronal structures, i.e. axons. Here, inhomogenities of the applied electric field caused by changes of the axonal trajectory relative to the EF are the most dominant factor in TMS-induced neuronal excitability (Abdeen & Stuchly, 1994; Amassian et al., 1992; Maccabee et al., 1993). Axons originating from BA4 first run perpendicular and anterior to the sulcal wall, and then turn approximately 90° downwards to form the cord fibres and the subcortical bundle in the centre of the precentral gyrus (Schmahmann & Pandya, 2006). Therefore, if for some subjects axonal thresholds were lower due to more abrupt white matter bendings (Fox et al., 2004), these subjects would show an anterior shift of optimal TMS excitation spots. In line with this suggestion are also the results of a very recent study by Herbsman et al. (2009) who investigated the relation between TMS excitability (i.e. motor threshold = MT) and several anatomical parameters in 17 subjects. Approximately 50-60 % of the inter-subject variability in MT can be explained by the subjects' individual skull-to-cortex distance (Kozel et al., 2000) but there is also strong evidence that the anterior component of the corticospinal tract is an additional important predictor for MT accounting for ~ 48 % of the variance observed (Herbsman et al., 2009). Pronounced anterior components of the corticospinal tract were associated with low MT (Herbsman et al., 2009) suggesting that TMS with PA induced current direction may act directly on axons running anterior of BA4 and changing their trajectory relative to the EF.

3.4.4 Implications and limitations

In summary, we conclude from the findings of the current study that the spatial mismatch between fMRI and TMS is not caused by the venous shift of GRE-BOLD signal. Spatial differences between fMRI and TMS are likely to result from different underlying physiological processes, i.e. (perfusion) fMRI predominantly reflects the position with highest task-related synaptic activity (Duong et al., 2000) at cell bodies, i.e. within grey matter, whereas TMS mappings yield optimal positions for neuronal excitation with applied EFs. These two positions might be different for several reasons including (i) EF distortion (caused by tissue boundaries etc.), and (ii) direct excitation of axons (Di Lazzaro et al., 1998a) which might be distant from cell bodies in white matter. One limitation of the present study might be the fact that effects are EF orientation (and hence coil orientation) specific. Our finding that optimal TMS were more anterior might not apply to TMS mappings with other coil orientations. EFs in the coronal plane are more likely to act on medial-lateral fibre tract components, and hence might show displacements in medial-lateral direction in contrast to EFs in PA (or AP) directions which predominantly act on anterior-posterior fibre tract components (Herbsman et al., 2009). Another limitation of the present study might be that fMRI and TMS sessions were not matched in functional state although fMRI informed TMS lesion studies usually use the same task for the MRI localizer and the TMS experiment. Although this limitation is unlikely to account for the mismatch between fMRI and TMS sites observed in the present study, it might limit the significance of our findings with respect to previous fMRI-informed (r)TMS studies. Nevertheless, our findings also have implications for studies in which optimal TMS positions cannot be identified as easily as for the motor or visual cortex. Although fMRI-informed TMS might not reflect the optimal position to generate TMS effects, our data indicate that it provides at least a position resulting in measurable TMS effects, and hence fMRI informed TMS should be preferred to the use of structural landmarks solely. Furthermore, our data imply that when behavioural effects are absent after rTMS over fMRI-based coordinates (e.g., in attention or language experiments), missing effects might also result from ineffective stimulation of the target region due to the spatial mismatch of fMRI coordinates and maximal TMS effects as demonstrated for the motor system in the present study.

4 Study II: Spatial Congruence of fMRI and TMS in stroke patients

4.1 Introduction Study II

Results of Study I indicate that in healthy young subjects, movement-related changes in CBF signal occur close to the anatomical motor hand area, i.e. Brodmann Area 4 (BA4), whereas movement-related changes in BOLD signal occur closer to the gyral surface. However, spatial differences between neuroimaging techniques did not impact on Euclidean distances to optimal TMS positions, since optimal TMS positions were considerably more anterior compared to fMRI positions (and differences between CBF and BOLD signal occurred mainly in cortical depth). Hence, in healthy young subjects, the use of CBF (instead of BOLD) did not improve spatial congruence between fMRI and TMS.

However, the main goal of the present thesis was to improve rTMS intervention strategies in stroke patients and stroke patients in the chronic phase may show several abnormalities compared to healthy subjects. First of all, reorganization processes which take place during the first weeks and months after stroke (Cramer et al., 1997) may shift task-related fMRI signal as well as optimal TMS positions in unknown extent and direction (Bastings et al., 2002; Rossini et al., 1998; Thickbroom et al., 2002). Which influence such shifts may have on congruence between fMRI and TMS is however unknown. Additionally, stroke patients may show vascular abnormalities (e.g. stenoses), but it is unknown whether these abnormalities have stronger effects on BOLD signal (arising from the macrovasculature) compared to CBF (arising from capillaries and smaller vessels). Therefore, we tested whether results obtained from healthy young subjects in Study I do also apply to chronic stroke patients despite of spatial shifts of fMRI and TMS positions caused by reorganization and vascular abnormalities.

Hypoperfusion is the most proximate cause of ischemic stroke. Therefore, CBF measurements have been suggested to have high potential for clinical neuroimaging (Detre et al., 1998). Initially, presence of stenoses and the resulting prolonged transit times in stroke patients were thought to be potential sources of error or artefact in perfusion imaging using ASL. However, in 1998, Detre and colleagues were able to demonstrate that good-quality CBF images can be obtained from patients with chronic cerebrovascular disease at rest (Detre et al., 1998). Nowadays, ASL is predominantly used to assess global perfusion deficits in acute stroke

patients in clinical settings. These measurements are performed in absence of a specific task (“resting state”) and allow identification of the ischemic penumbra (tissue potentially destined for infarction but not yet irreversibly injured; Fisher, 1997), if combined with diffusion weighted imaging (DWI). According to the *diffusion-perfusion mismatch model*, the ischemic penumbra represents the area which shows perfusion deficits assessed by ASL but normal diffusion measured by DWI (Chalela et al., 2004). However, until now, no study has been published using ASL to assess *task-related* changes in CBF in stroke patients. Therefore, an additional aim of the present study was, to demonstrate that meaningful task-related CBF signal changes can be obtained from chronic stroke patients.

Numerous studies used BOLD fMRI to assess movement-related activity in stroke patients and many of these studies reported bilaterally enhanced BOLD signal during movements of the affected hand in stroke patients compared to healthy subjects (Binkofski & Seitz, 2004; Cao et al., 1998; Chollet et al., 1991; Cramer et al., 1997; Grefkes et al., 2008b; Jaillard et al., 2005; Loubinoux et al., 2003; Seitz et al., 1998; Weiller et al., 1992; Ward et al., 2003b). The functional role of enhanced neural activity in the contralesional hemisphere (e.g. supportive, compensatory or detrimental) is currently under intensive debate (cf. sections 4.4, 5.4.3 and 5.4.4). The second aim of the present study was to exclude the possibility that bilaterally organized BOLD signal is simply caused by vascular artefacts (such as local magnetic susceptibility around large draining veins). We hypothesized that bilaterally organized neural activity during movements of the affected hand is also indicated by CBF (and not only by BOLD). Since CBF signal changes exclusively occur in capillaries and brain parenchyma (Duong et al., 2000; Luh et al., 2000; Silva et al., 1997; Tjandra et al., 2005), this finding would strongly argue against artefacts from veins (and for neuronal processes) as underlying cause of bilaterally enhanced BOLD signal in the contralesional hemisphere ipsilateral to movements of the affected hand.

Hence, in the present study we tested on both hemispheres of chronic stroke patients and age-matched healthy controls: (i) whether meaningful movement-related changes in CBF can be obtained from chronic stroke patients, (ii) whether bilaterally enhanced neural activity can be obtained by BOLD as well as CBF, (iii) whether highest task-related CBF signal changes occur closer to the anatomical motor hand area (BA4) than highest task-related BOLD signal changes, (iv) whether spatial differences between neuroimaging techniques are functionally relevant (i.e. impact on MEPs) if brain tissue is stimulated with TMS, and (v) whether

movement-related CBF signal changes occur significantly closer to optimal TMS positions than movement-related BOLD signal changes.

4.2 Methods Study II

4.2.1 Subjects

MRI measurements were performed on 15 chronic stroke patients (61.4 ± 10.2 years old; 12 males) and 13 healthy control subjects (60.1 ± 8.0 years old; 6 males; Table 4.1). There were no significant differences between groups in age (two-sample t-test, $P > 0.05$) or gender (Pearson's chi-square test, $P > 0.05$). Patients had right-sided ($n = 10$) or left-sided ($n = 5$) lesions due to first-ever cerebral ischemia. Patients were included in the study based on the following criteria: (i) stable unilateral hand motor deficit, (ii) insult at least 12 months ago (chronic stage), (iii) absence of aphasia, neglect, and apraxia, and (iv) no mirror movements of the unaffected hand during movements of the affected hand. Three different scales were used to assess clinical impairment: (i) the modified Rankin scale (mRS), (ii) the National Institutes of Health Stroke Scale (NIHSS), and (iii) the Action Research Arm Test (ARAT). Additionally, maximum index finger tapping frequencies (in Hz) and maximum grip force (in kPa) was obtained (the latter with a vigorimeter: Martin, Tuttlingen, Germany). CST damage was assessed by calculating the overlapping volume between the individual MNI-normalized lesion mask and the probabilistic CST map implemented in the SPM "Anatomy" toolbox (Eickhoff et al., 2005, 2007; http://www.fz-juelich.de/inm/inm-1/spm_anatomy_toolbox) in relation to total CST volume. Healthy control subjects were free of any history of medical or psychiatric disease. One subject in each group was left-handed according to the Edinburgh Handedness Inventory (EHI; Oldfield, 1971). Remaining subjects were right-handed (EHI was assessed for the time before stroke in patients). Overall 12 subjects (6 patients and 6 healthy subjects) agreed to participate in a subsequent TMS session in which a systematic TMS motor mapping was performed. None of the subjects had any contraindication to TMS (Wassermann, 1998) and all subjects gave informed consent to participate in the study, which was approved by the ethics committee of the Medical Faculty, University of Cologne, Germany (file-no 09-108). All experiments conform to the Declaration of Helsinki, sixth revision 2008.

Table 4.1: Study II: Demographical, clinical, and behavioural data

Subject	Age	Sex	Handedness	Lesion side	Lesion size [cm ³]	Lesion age [m]	mRS	NIH SS	ARAT	Affected/non-dominant hand				Unaffected/dominant hand			
										FT [Hz]	GF [kPa]	TA max. [Hz]	TA eff. [Hz]	FT [Hz]	GF [kPa]	TA max. [Hz]	TA eff. [Hz]
P 01*	56	M	R	R	0.1	33	1	1	57	4.8	111.0	2.8	1.9	5.4	119.0	2.9	1.9
P 02	48	M	R	R	251.7	156	2	6	30	2.3	105.0	1.4	0.9	6.7	150.0	2.6	1.7
P 03*	65	M	R	R	0.1	28	1	1	46	3.3	76.7	1.5	1.0	5.5	96.3	3.7	2.5
P 04	70	M	R	R	3.0	100	3	7	24	1.5	16.0	1.9	1.3	5.6	90.0	2.9	1.9
P 05*	68	M	R	R	40.2	32	3	5	32	1.7	43.7	1.0	0.7	5.4	113.7	2.5	1.7
P 06	65	M	R	R	1.3	22	2	3	50	3.5	42.7	1.5	1.0	4.5	70.7	2.3	1.5
P 07*	73	M	L	R	0.2	35	1	4	41	3.9	64.7	2.3	1.5	5.3	76.7	2.7	1.8
P 08	75	M	R	L	0.4	43	1	2	57	5.1	64.7	3.1	2.1	5.3	63.3	3.1	2.1
P 09	43	F	R	R	42.1	18	2	3	32	3.0	7.3	1.0	0.7	5.4	60.7	3.7	2.5
P 10	67	M	R	L	1.6	253	1	3	56	4.2	64.7	2.0	1.3	5.1	77.3	2.0	1.3
P 11	60	M	R	R	2.3	16	1	2	54	2.9	71.7	1.6	1.1	5.7	81.0	2.5	1.7
P 12*	52	F	R	R	26.7	12	1	1	57	3.7	49.3	2.1	1.4	4.6	46.7	2.8	1.9
P 13*	74	F	R	L	0.2	50	1	4	54	3.1	21.3	2.7	1.8	3.3	48.0	2.8	1.9
P 14	51	M	R	L	2.7	38	2	3	21	1.6	10.0	1.0	0.7	6.5	106.7	4.4	2.9
P 15	54	M	R	L	10.5	78	2	4	48	2.0	12.7	1.1	0.7	4.5	86.0	2.2	1.5
Mean	61.4				25.5	60.9	1.6	3.3	43.9	3.1	50.8	1.8	1.2	5.3	85.7	2.9	1.9
SD	10.2				64.3	65.4	0.7	1.8	12.9	1.1	33.2	0.7	0.5	0.8	28.1	0.6	0.4
H 01	50	M	R	-	-	-	-	-	-	5.9	95.0	2.6	1.7	6.4	101.7	3.3	2.2
H 02*	66	M	R	-	-	-	-	-	-	5.5	92.0	2.3	1.5	5.8	104.3	2.4	1.6
H 03	56	F	R	-	-	-	-	-	-	5.3	40.0	2.4	1.6	6.3	48.3	3.2	2.1
H 04	66	M	L	-	-	-	-	-	-	5.9	90.0	2.5	1.7	5.5	82.3	2.7	1.8
H 05*	61	F	R	-	-	-	-	-	-	5.1	59.7	3.4	2.3	5.6	55.3	3.1	2.1
H 06*	64	M	R	-	-	-	-	-	-	5.5	119.7	2.7	1.8	5.0	102.3	2.7	1.8
H 07*	63	F	R	-	-	-	-	-	-	6.0	74.0	2.5	1.7	5.7	78.0	2.6	1.7
H 08*	56	M	R	-	-	-	-	-	-	5.7	102.0	2.4	1.6	6.4	97.3	2.6	1.7
H 09*	50	F	R	-	-	-	-	-	-	5.9	66.7	2.7	1.8	6.7	62.7	2.9	1.9
H 10	53	F	R	-	-	-	-	-	-	4.9	99.7	2.3	1.5	5.5	102.7	2.4	1.6
H 11	55	F	R	-	-	-	-	-	-	5.1	49.7	1.8	1.2	5.5	49.3	2.0	1.3
H 12	62	M	R	-	-	-	-	-	-	5.7	112.7	3.3	2.2	6.1	107.7	3.8	2.5
H 13	79	F	R	-	-	-	-	-	-	3.7	60	1.3	0.9	4.4	63	1.2	0.8
Mean	60.1									5.4	77.5	2.5	1.7	5.8	76.8	2.7	1.8
SD	8.0									0.6	32.3	0.5	0.4	0.6	30.7	0.6	0.4

ARAT = Action Research Arm Test; F = female; FT = maximum index finger tapping frequency; GF = maximum grip force; H = healthy control subject; L = left; M = male; m = months; mRS = modified Rankin Scale; NIHSS= National Institutes of Health stroke scale; P = stroke patient; R = right; SD = standard deviation; TA eff. = thumb abduction frequency performed during the functional magnetic resonance imaging experiment (66% of TA max. = maximum thumb abduction frequency) * Subjects participated in TMS experiments

4.2.2 fMRI motor paradigm

A block design was implemented, in which subjects were asked to perform visually paced rhythmic thumb abductions with their affected hand (corresponding to the non-dominant hand of healthy subjects) and their unaffected hand (corresponding to the dominant hand of healthy subjects). The volunteer's hands were fixated on a flat board with elastic velco straps to ensure a flat hand position throughout the experiment. A vertical cylinder, mounted onto the board, served as lateral margin restricting thumb abductions. The position of the cylinder was adjusted to allow thumb abductions of approximately 45°. This experimental setup specifically facilitated movements of the abductor pollicis brevis (APB) muscle, which was later used as target muscle for TMS. Thumb abductions were performed at two different movement frequencies: (i) a fixed frequency of 1 Hz and (ii) a frequency individually adjusted to motor performance (66% of the maximum frequency). The fixed frequency condition was implemented to compare neural activity (between groups or hands) with similar absolute number of thumb abductions in one movement block resulting in, for example similar amount of re-afferent signal, whereas the adjusted frequency condition was implemented to compare neural activity (between groups or hands) during movements with similar degree of difficulty (but different absolute number of movements). The maximum thumb abduction frequency of each hand was determined immediately before fMRI scanning when subjects resided in their final position for the experiment. For assessment of the maximum thumb abduction frequency, subjects were instructed to move their thumb to the cylinder and back as fast as possible as soon as a "go" signal appeared on a shielded thin-film transistor (TFT) screen at the rear end of the MR scanner. Thumb abductions were counted by visual inspection until a "stop" signal was presented after 10s. The procedure was repeated consecutively 3 times for each hand and the mean across 3 blocks was used as maximum thumb abduction frequency (see Table 4.1). During the fMRI experiment, the movement frequency was paced by a red blinking circle on white background presented on the TFT screen, which was visible via a mirror mounted on the MR head coil. Blocks of hand movements (15 s) were separated by resting baselines (30 s plus 0-1.5 s jitter), in which a black screen instructed subjects to rest still until instructions were displayed for 1.5 s indicating which hand to move in the subsequent movement block. The software "Presentation" (Version 9.9, Neurobehavioral Systems, Inc., CA, www.neurobehavioralsystems.com) was used for visual stimulus presentation. One fMRI

experiment consisted of 6 cycles of baseline and movement blocks for each of the 4 conditions which were pseudo-randomized and counterbalanced across the experiment. Overall, the experiment lasted about 19 min. Subjects were trained outside and again inside the scanner until they had reached stable performances (monitored by visual inspection). During the experiment, motor performance was monitored by an MR compatible camera in the scanner room.

4.2.3 fMRI data acquisition

MR images were acquired on a 3 Tesla Siemens MAGNETOM TimTrio scanner (Siemens, Erlangen, Germany). High-resolution anatomical $T1$ -weighted images were acquired using a 3D MP-RAGE (magnetization prepared, rapid acquisition gradient echo) sequence with the following imaging parameters: TR = 2000 ms, TE = 3.25 ms, FOV = 256 mm, 176 sagittal slices, slice thickness = 1 mm, in-plane resolution = 1 x 1 mm², flip angle = 9°. To avoid discomfort for patients induced by long scanning durations, CBF and BOLD signal changes were simultaneously acquired by means of the PICORE-Q2TIPS (quantitative imaging of perfusion using a single subtraction with thin slice $T1$ periodic saturation – proximal inversion with a control for off-resonance effects) pulse sequence using a FOCI pulse for inversion (Luh et al., 1999) with the following parameters: $T1$ = 1000 ms, $T1s$ = 1200 ms, and $T12$ = 1700 ms, TR = 2500 ms, TE = 22 ms, FOV = 256 mm, 8 axial slices, slice thickness = 5 mm, in-plane resolution = 4 x 4 mm², distance factor = 0%, flip angle = 90°, and a flow limit of 100 cm/s. The tagging region was 10 cm in width positioned at a gap of 1 cm inferior to the imaging slices. Two presaturation pulses were applied in the imaging planes immediately before the inversion tag to minimize the impact of the static tissue. A 20 mm thick saturation slab was repeatedly applied for the bolus cut-off (Cavusoglu et al., 2009). Images were acquired sequentially in ascending direction using a single-shot EPI technique. Slices covered a region extending from the fundus of the central sulcus to the top of the parietofrontal vertex, thereby ensuring full coverage of the primary motor cortex. Each fMRI session consisted of 471 EPI volumes, including three “dummy” scans, ensuring a steady-state in tissue contrast. Seven whole brain EPI volumes (30 axial slices) with identical imaging parameters (except for a longer TR of 4000 ms) were additionally acquired to improve the co-registration with the anatomical $T1$ -weighted volume during data pre-processing (see below).

4.2.4 fMRI data analysis

For image preprocessing and statistical analysis of BOLD and CBF data, we used FEAT (fMRI Expert Analysis Tool) version 5.98, part of FSL (FMRIB's Software Library version 4.1.7, www.fmrib.ox.ac.uk/fsl). Dummy scans were discarded from further analyses. EPIs from patients with left-sided lesions ($n = 5$) were mirrored at the midsagittal plane. To account for possible confounds arising from laterality effects, EPIs of 5 healthy subjects were similarly processed. ASL-CBF time series were created by calculating control-tag difference images (resulting in a total of 234 subtraction images) using surround subtraction (i.e. computing the difference between each image and the average of its two nearest neighbours), thereby reducing BOLD signal contamination of the ASL-CBF time course (Cavusoglu et al., 2009). The following prestatistics processing was applied: motion correction using MCFLIRT (Jenkinson et al., 2002), non-brain removal using the brain extraction tool (BET; Smith, 2002), and spatial smoothing using a Gaussian kernel of 5 mm full width half maximum (FWHM). A highpass filter of 1/290 s (i.e. slightly longer than the maximum interval between two blocks of the same condition) to remove low frequency drifts in MR signal. To ensure good spatial co-registration with the high resolution anatomical *T1* image, EPI volumes (covering the brain only partially) were first co-registered with the whole brain EPI before applying the transformation matrix from whole brain EPI to the brain-extracted *T1* image. For statistical analysis on the single-subject level, box-car vectors of the following four conditions were applied to both CBF and BOLD time series in the framework of a general linear model using FILM (FMRIB's Improved Linear Model) with local autocorrelation correction (Woolrich et al., 2001):

- 1) Movements of the affected (non-dominant) hand at 66% of the maximum frequency
- 2) Movements of the affected (non-dominant) hand at 1 Hz
- 3) Movements of the unaffected (dominant) hand at 66% of the maximum frequency
- 4) Movements of the unaffected (dominant) hand at 1 Hz

Head motion parameters were included as covariates into the model.

4.2.5 Identification of fMRI peak voxel and fMRI CoGs

The voxel with the highest statistical Z-value located within the precentral gyrus near or at the hand knob formation (Yousry et al., 1997) was identified for movements of the affected (non-dominant) and the unaffected (dominant) hand (in the adjusted movement frequency

condition) for both BOLD and CBF using a statistical threshold of $P < 0.001$ (uncorrected). In contrast to peak voxel coordinates, CoG coordinates are influenced by the threshold applied. A uniform threshold of $P < 0.001$ (uncorrected) was applied to all fMRI data (lower thresholds were found to yield very large activation cluster for BOLD sessions, whereas higher statistical thresholds could not be passed by CBF activation clusters). After thresholding, the fMRI activation cluster comprising the peak voxel was identified and the CoG was calculated as Z-value weighted position.

4.2.6 Group analysis of fMRI data

Lesion masks were created based on anatomical *T1* images using MRICron (<http://www.cabiatl.com/micro/mricron/>). EPIs volumes were spatially normalized to the standard template of the Montreal Neurological Institute (MNI152_T1_2mm) with masked lesions using FLIRT (Jenkinson et al., 2001, 2002). For the fMRI group analysis we used FLAME 1 (FMRIB's Local Analysis of Mixed Effects) to compare the parameter estimates of each condition between subjects in a full-factorial ANOVA with the factor GROUP (levels: patients, controls). Z (Gaussianised T/F) statistic images were thresholded using a voxel-wise corrected significance threshold of $Z > 3.0$ and a cluster-wise corrected significance threshold of $P < 0.05$ (Forman et al., 1995; Friston et al., 1994; Worsley et al., 1992). For anatomical assignment, statistical contrasts were overlaid with cytoarchitectonic probability maps of the Juelich Histological Atlas (Eickhoff et al., 2005, 2007).

4.2.7 Neuronavigated TMS apparatus

Stereotaxic frameless neuronavigation was performed with the eXimia navigated brain stimulation (NBS) system version 3.2.1 (Nexstim, Helsinki, Finland). Since subjects performed a thumb abduction task during the fMRI experiment, the left and right abductor pollicis brevis (APB) muscle served as target muscles for TMS. EMG signals were recorded by Ag/AgCl surface electrodes (Tyco Healthcare, Neustadt, Germany) placed in a belly-tendon montage. The EMG signal was amplified, filtered with a 0.5 Hz high pass filter and digitized using a ML856 PowerLab 26T Myograph and the “LabChart” software package version 6.0 (ADInstruments Ltd, Dunedin, New Zealand).

4.2.8 Motor hotspot and resting motor threshold

Subjects were comfortably seated in an adjustable armchair with head-rest. The head of the subject was co-registered with the individual high-resolution anatomical MR image via anatomical landmarks (e.g., nasion and crus heliis). The root mean square difference between positions of landmarks at the subjects head and landmarks in the MRI volume did not exceed 3 mm for any TMS session of the present study (calculated by the neuronavigation software). After anatomical coregistration, the motor “hotspot”, i.e. the coil position providing highest MEPs of the contralateral APB muscle with shortest latencies during single pulse supra-threshold TMS, was identified. Hotspot coil orientations were (nearly) perpendicular ($90 \pm 10^\circ$) to the central sulcus and tangential to the scalp in all subjects investigated (information provided by the neuronavigation software). The RMT was defined as the minimum TMS stimulator output intensity required to produce an MEP (peak-to-peak amplitude $\geq 50 \mu\text{V}$) in at least 5 out of 10 consecutive trials in the contralateral APB muscle at rest (Rossini et al., 1994).

4.2.9 TMS Motor Mapping

TMS motor maps of the ipsilesional (non-dominant) and contralesional (dominant) motor cortex and surrounding tissue were obtained from 12 patients (6 stroke patients and 6 healthy subjects). The TMS coil was navigated to grid positions spaced at intervals of 5 mm. The anterior-posterior axis of the grid was oriented in parallel to the interhemispheric fissure. The mapping procedure started at the hotspot position. Subsequent positions followed a helix around the hotspot position until no MEP (peak-to-peak amplitude $\geq 50 \mu\text{V}$) could be elicited at any outside margin of the map. This mapping procedure included the hand knob formation (Yousry et al., 1997) in all subjects. Classen et al. (1998) demonstrated that 5-6 stimuli per position are sufficient to achieve stable mapping results. In the present study, 7 stimuli (at 120% RMT; ISI = 1500 ms) were delivered to each position. Coil tilting was tangentially to the scalp and the TMS coil orientation was identical to coil orientation during RMT identification and stimulation at fMRI maxima coordinates, i.e. approximately perpendicular to the central sulcus. The mean peak-to-peak MEP amplitude of the APB was calculated for each grid position and divided by the largest amplitude obtained within the stimulation area. Based on these data, the centre-of-gravity (CoG) of the cortical APB representation was calculated (Classen et al., 1998). Since it is unknown at which position, superficial or deep,

TMS-induced neuronal excitation occurs, we projected TMS identified positions (i.e. hotspot and CoG positions) onto the cerebral surface. This was done by identifying the individual depth of the cerebral surface by surface peeling of the software generated 3D head model. Positions with highest EF strength at the cerebral surface (EF_{\max}) were recorded during hotspot identification and TMS mapping and used for later analyses. To compare anatomical positions derived by fMRI and TMS, EF_{\max} positions were marked on the individual structural *T1* image and transferred into MNI space by applying the respective nonlinear normalization transform (which was also used to transfer individual fMRI activation maps into MNI space).

4.2.10 TMS of peak voxel coordinates at 120 % RMT

Brain tissue at fMRI peak voxel coordinates was stimulated with 120 % RMT (15 stimuli; ISI = 3000 ms) in all subjects ($n = 28$). The order of stimulation of BOLD and CBF peak voxels was counterbalanced across subjects. The experimenter was blinded to the fMRI sequence. The target entry point for stimulation was identified by bringing the TMS coil in a position in which the distance between fMRI target and EF_{\max} value position was found to be minimal (0-2 mm, computed by the neuronavigation software). Then, tilting of the TMS coil was adjusted until the coil was tangential to the scalp (computation and visual feedback provided by the neuronavigation software). TMS coil orientation coincided with TMS coil orientation during RMT identification. In this final position, one stimulus was applied. The coil positioning parameters of this stimulus were used as reference for all subsequent stimuli at this particular target (by means of the “aiming tool” implemented in the neuronavigation software).

4.3 Results Study II

4.3.1 fMRI group analysis

4.3.1.1 BOLD signal

Figure 4.1 shows regions significantly activated by visually-paced thumb abductions at a movement frequency of 1 Hz in stroke patients ($n = 15$; all normalized as having right sided lesions) and healthy subjects ($n = 13$) relative to the low-level baseline ($Z > 3.0$, $P < 0.05$ cluster-level corrected). Healthy subjects showed increased BOLD signal in a network comprising contralateral primary motor cortex (M1), contralateral primary somatosensory

cortex (S1), bilateral supplementary motor area (SMA), bilateral ventral and dorsal premotor cortex (vPMC, dPMC), and bilateral superior parietal lobule (SPL) during movements of the dominant (Figure 4.1F) and non-dominant (Figure 4.1B) hand. In stroke patients, movements of the unaffected hand yielded comparable results as movements of the dominant or non-dominant hand in healthy subjects (Figure 4.1E). In contrast, movements of the stroke affected hand were associated with significant neural activity in contralesional M1 ipsilateral to movements of the affected hand (Figure 4.1A). Although healthy subjects also showed significant activation in the dominant hemisphere, ipsilateral to movements of the non-dominant hand, this activation was situated in ipsilateral dPMC (Figure 4.1B) and did not extend into ipsilateral M1 as in stroke patients (Figure 4.1A). Results were comparable if the thumb abduction frequency in the fMRI experiment was adjusted to motor performance (66% of maximum frequency; Figure 4.2).

4.3.1.2 CBF signal

The fMRI group analysis of the contrast “thumb abductions versus baseline” on CBF (instead of BOLD) signal revealed lateralized activation clusters in contralateral sensorimotor cortex (M1/S1) in healthy subjects during movements of the dominant (Figure 4.1H) and non-dominant hand (Figure 4.1D). In stroke patients, movements of the unaffected hand yielded similar results as movements of the dominant or non-dominant hand in healthy subjects (Figure 4.1G). In contrast, movements of the stroke affected hand were associated with additional activation clusters in contralesional M1 ipsilateral to hand movements (Figure 4.1C, highlighted by green circles). This activation was located at the lateral margin of the hand knob formation (Yousry et al., 1997) and was not seen in healthy subjects (Figure 4.1D, Figure 4.1H) or stroke patients moving their unaffected hand (Figure 4.1G). Results were comparable if the thumb abduction frequency in the fMRI experiment was adjusted to motor performance (66% of maximum frequency; Figure 4.2).

4.3.1.3 Peak activation clusters

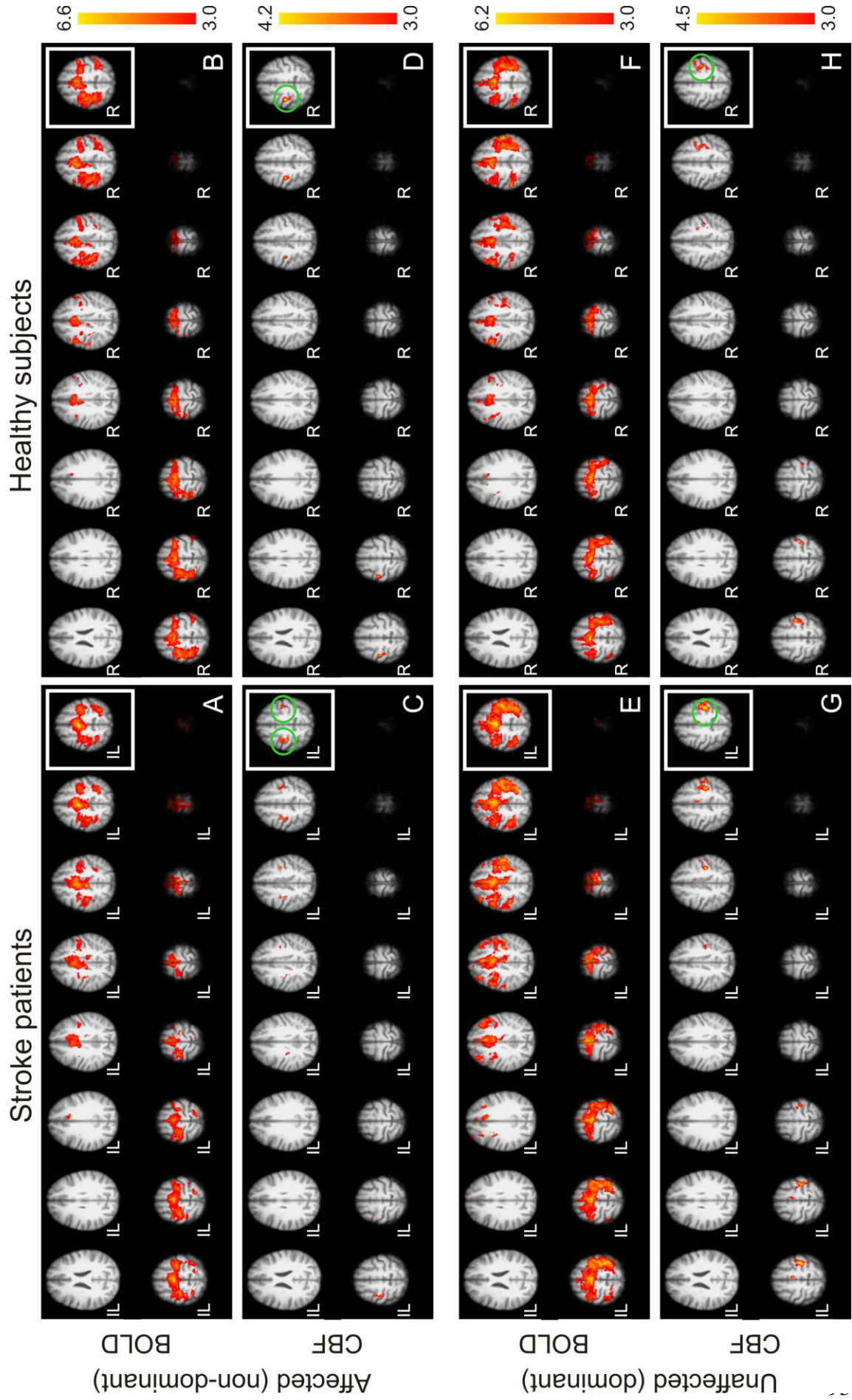
Characteristics of peak activation clusters are given in Table 4.2. CBF peak activation clusters were significantly smaller (i.e. contained significantly fewer voxels) than BOLD peak activation clusters ($P < 0.001$) and had significantly lower statistical Z-values at the peak voxel coordinate ($P < 0.001$). There were no significant differences between stroke patients

and healthy subjects in voxel size or statistical Z-value of peak activation clusters ($P > 0.3$). All peak activation clusters obtained by CBF were located either in the primary motor cortex (M1) or the central sulcus (CS) both in healthy subjects and stroke patients. In contrast, peak activation clusters obtained by BOLD were located in other brain areas (predominantly supplementary motor area, SMA). Only for one of the eight conditions, the BOLD peak activation cluster was located in the CS.

4.3.1.4 Summary fMRI group analysis

In summary, our results demonstrate that meaningful task-related changes (in contralateral M1) can be obtained from chronic stroke patients using ASL-CBF. Additionally to activity in contralateral M1, stroke patients showed enhanced fMRI signal in contralesional (i.e. ipsilateral) M1 during movements of the affected hand (but not during movements of the unaffected hand) compared to healthy subjects. This was the case in both movement conditions. Interestingly, both fMRI signal types, i.e. BOLD *and* CBF, suggested enhanced neural activity in contralesional M1 during movements of the affected hand. CBF peak activation clusters were smaller and had lower statistical Z-values than BOLD peak activation clusters but there were no significant differences between patients and healthy subjects in cluster size or Z-values of peak activation clusters. Highest movement-related CBF signal changes in stroke patients and control subjects were located in M1 or the central sulcus. By contrast, highest movement-related BOLD signal changes were located in other brain areas (such as SMA). There were no differences between stroke patients and healthy subjects in location of peak activation clusters.

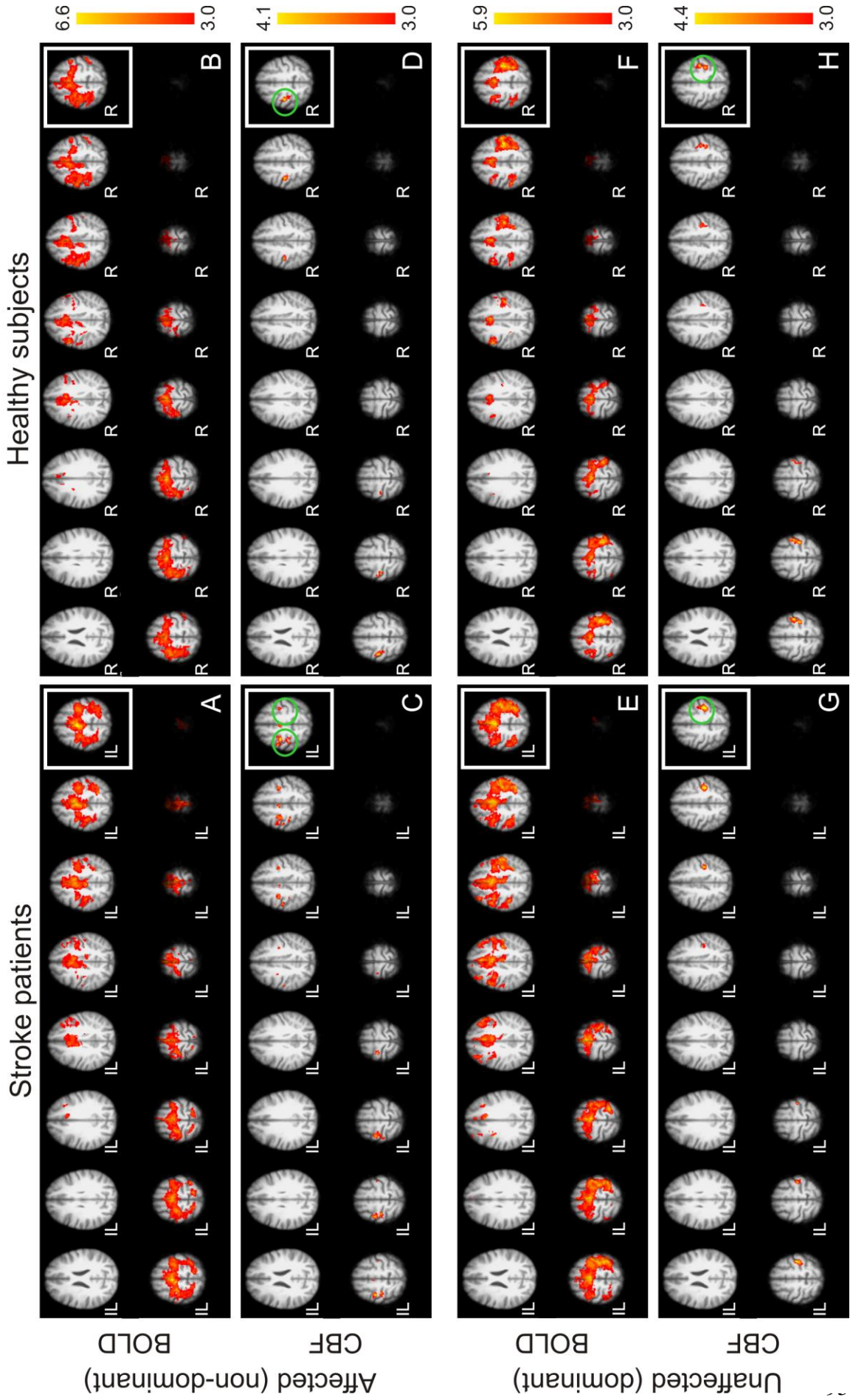
Fixed movement frequency (1 Hz)



Study II: Congruence of fMRI and TMS in stroke patients

Figure 4.1: Study II: Results of the fMRI group analysis (fixed movement condition). Functional magnetic resonance imaging (fMRI) was performed in 15 chronic stroke patients and 13 healthy subjects during visually paced rhythmic thumb abductions of the affected (non-dominant) and unaffected (dominant) hand at a fixed movement frequency of 1 Hz. Arterial spin labelling (ASL) was used as fMRI pulse sequence and blood oxygenation level dependent (BOLD) as well as cerebral blood flow (CBF) fMRI signal was assessed. “Movement versus rest” contrasts were superimposed onto the MNI standard template ($Z > 3.0$; $P < 0.05$, cluster level corrected). Stroke patients showed enhanced BOLD and CBF signal in contralesional M1 (ipsilateral to hand movements) during movements of the affected hand but not during movements of the unaffected hand compared to healthy controls.

Adjusted movement frequency (66% of max.)



Study II: Congruence of fMRI and TMS in stroke patients

Figure 4.2: Study II: Results of the fMRI group analysis (adjusted movement condition). Functional magnetic resonance imaging (fMRI) was performed in 15 chronic stroke patients and 13 healthy subjects during visually paced rhythmic thumb abductions of the affected (non-dominant) and unaffected (dominant) hand at a movement frequency adjusted to motor performance (66% of maximum thumb abduction frequency). Arterial spin labelling (ASL) was used as fMRI pulse sequence and blood oxygenation level dependent (BOLD) as well as cerebral blood flow (CBF) fMRI signal was assessed. “Movement versus rest” contrasts were superimposed onto the MNI standard template ($Z > 3.0$; $P < 0.05$, cluster level corrected). Results were comparable to the fixed movement condition, i.e. stroke patients showed enhanced BOLD and CBF signal in contralesional M1 (ipsilateral to hand movements) during movements of the affected hand (but not during movements of the unaffected hand compared to healthy controls).

Table 4.2: Study II: Peak activation cluster of the fMRI group analysis

Contrast				Voxels	P	Z	Peak X	Peak Y	Peak Z	Area	CoG X	CoG Y	CoG Z	Area
BOLD	Patients	Affected hand	adjusted	14826	0.000	6.66	4	-8	52	SMA	-0.4	-12.7	55.9	SMA
			fixed	10318	0.000	6.67	2	-6	52	SMA	3.7	-9.4	56.0	SMA
		Unaffected hand	adjusted	8675	0.000	5.90	-40	-20	50	CS	-13.8	-10.8	55.7	SMA/WM
			fixed	16379	0.000	6.09	-52	-26	44	S2	-10.1	-7.23	53.9	SMA/WM
	Controls	Non-dom hand	adjusted	12449	0.000	6.16	2	-4	60	SMA	12.2	-6.23	54.5	SMA/WM
			fixed	10378	0.000	5.90	2	-4	58	SMA	12.0	-8.45	55.3	SMA/WM
		Dominant hand	adjusted	10521	0.000	5.91	-44	-12	56	PMC/M1	-17.8	-12.4	56.2	dPMC
			fixed	11172	0.000	6.24	2	-2	56	SMA	-8.21	-6.56	55.2	SMA
CBF	Patients	Affected hand	adjusted	842	0.000	4.15	36	-12	52	M1	37.2	-15.2	54.6	M1
			fixed	305	0.000	5.54	36	-22	54	M1	34.5	-15.6	50.1	M1
		Unaffected hand	adjusted	507	0.000	4.49	-36	-28	50	CS	-37.0	-24.0	51.7	CS
			fixed	844	0.000	4.52	-40	-20	56	M1	-38.7	-22.3	52.6	M1
	Controls	Non-dom hand	adjusted	368	0.000	4.01	42	-20	52	CS	38.4	-20.0	52.7	M1
			fixed	274	0.000	4.24	40	-18	52	M1	39.1	-18.7	53.5	M1
		Dominant hand	adjusted	643	0.000	4.29	-40	-16	58	M1	-36.3	-20.4	53.5	M1
			fixed	515	0.000	4.08	-40	-14	56	M1	-36.1	-15.8	52.4	M1

adjusted: thumb abduction frequency in the fMRI experiment was adjusted to motor performance (66% of maximum frequency); BOLD: blood-oxygenation level dependent; C: control subjects; CBF: cerebral blood flow; CoG: centre-of-gravity coordinate; CS: central sulcus; dPMC: dorsal premotor cortex; fixed: thumb abduction frequency in the fMRI experiment was 1 Hz; fMRI: functional magnetic resonance imaging; M1: primary motor cortex; Non-dom: non-dominant; P: stroke patients; Peak: peak voxel coordinate; S2: secondary somatosensory cortex; PMC: premotor cortex; SMA: supplementary motor area; WM: white matter; X: lateral-medial coordinate; Y: anterior-posterior coordinate; Z: inferior-superior coordinate. Coordinates refer to the standard space of the Montreal Neurological Institute (MNI)

4.3.2 Statistical Z-values at individual fMRI peak voxels

Movement-related neural activity was observed with both ASL-BOLD as well as ASL-CBF in all subjects. However, sensitivity in terms of statistical Z-values of individual local maxima at the hand knob formation was significantly different across fMRI techniques. A repeated measures ANOVA ($n = 28$) with the factors APPROACH (levels: ASL-BOLD, ASL-CBF), HEMISPHERE (levels: ipsilesional/non-dominant, contralesional/dominant), and GROUP (levels: patients, controls) revealed a highly significant main effect of APPROACH ($F(1, 26) = 173.969$; $P < 0.001$). ASL-BOLD peak voxels had significantly higher statistical Z-values (11.8 ± 3.3) than ASL-CBF (4.2 ± 1.0) peak voxels. There was no significant main effect of HEMISPHERE or GROUP and no significant interaction ($P > 0.05$) indicating that statistical Z-values at individual ASL-CBF peak voxels were generally decreased, independent of the hemisphere or group investigated.

4.3.3 Differences in fMRI and TMS positions

Individual TMS hotspot positions were obtained from 15 stroke patients and 13 control subjects ($n = 28$). They were projected into MNI space by applying the individual nonlinear FNIRT registration transform. MNI coordinates of TMS hotspot positions were then compared with MNI coordinates of fMRI peak voxel coordinates by computing a repeated measures ANOVA ($n = 28$) with the factor APPROACH (levels: ASL-BOLD, ASL-CBF, TMS-hotspot) and GROUP (levels: patients, controls) for each hemisphere and dimension (MNI-coordinate X, Y, and Z).

4.3.3.1 Analyses on differences in fMRI and TMS hotspot positions ($n = 28$)

Mean MNI coordinates of ASL-CBF, ASL-BOLD, and TMS hotspots are given in Table 4.3 and depicted in Figure 4.3. In lateral-medial direction (i.e. in MNI coordinate X), there was a significant main effect of APPROACH for both hemispheres (ipsilesional/non-dominant (IL/ND): $F(2, 52) = 7.149$, $P = 0.002$; contralesional/dominant (CL/D): $F(2, 52) = 4.630$, $P = 0.014$). Post-hoc t-test revealed that TMS hotspot positions were significantly more lateral than ASL-CBF positions (IL/ND: $P = 0.001$, FDR-corrected; CL/D: $P = 0.042$, uncorrected) and ASL-BOLD positions (IL/ND: $P = 0.007$, FDR-corrected; CL/D: $P = 0.005$, FDR-corrected). In anterior-posterior direction (i.e. in MNI coordinate Y), there was a highly

significant main effect of APPROACH for both hemispheres (IL/ND: $F(2, 52) = 31.511$, $P < 0.001$; CL/D: $F(2, 52) = 9.661$, $P < 0.001$). Post-hoc t-test revealed that TMS hotspot positions were significantly more anterior than ASL-CBF positions (IL/ND and CL/D: $P < 0.001$, FDR-corrected) and ASL-BOLD positions (IL/ND: $P < 0.001$, FDR-corrected; CL/D: $P = 0.007$, FDR-corrected). As TMS cannot differentiate between superficial and deep targets (due to the physical nature of the magnetic field induced by the TMS coil), analyses in inferior-superior direction (i.e. in MNI coordinate Z) were performed for fMRI approaches without TMS hotspot positions. There was a significant main effect of APPROACH for both hemispheres indicating that ASL-BOLD positions were significantly more superficial than ASL-CBF positions (IL/ND: $F(1, 26) = 4.560$, $P = 0.042$; CL/D: $F(1, 26) = 4.302$, $P = 0.048$). There was no significant main effect of GROUP or significant APPROACH \times GROUP interaction for any of the ANOVAs ($P > 0.05$).

In summary, analyses on differences in ASL-BOLD, ASL-CBF, and TMS-hotspot positions in all 28 subjects indicated that TMS hotspot positions were significantly lateral and anterior of fMRI positions. ASL-BOLD positions were significantly more superficial than ASL-CBF positions. Findings were similar for both hemispheres and there were no significant differences between stroke patients and healthy subjects in ASL-BOLD, ASL-CBF, and TMS-hotspot positions. Results were comparable to results of Study I.

Table 4.3: Study II: Mean fMRI and TMS positions in MNI space

Hemisphere	Approach	Sample size	X	Y	Z	
Contralesional/ dominant	fMRI	BOLD	N = 28	-35.9 ± 6.0	-18.3 ± 8.0	58.9 ± 7.2
		CBF	N = 28	-37.3 ± 5.1	-20.1 ± 6.3	55.7 ± 4.3
	TMS	hotspot	N = 28	-39.9 ± 4.1	-12.3 ± 8.9	$57.8 \pm 4.1^*$
		CoG	N = 12	-35.8 ± 4.8	-5.3 ± 8.6	$57.3 \pm 4.4^*$
Ipsilesional/ non-dom.	fMRI	BOLD	N = 28	38.9 ± 5.1	-19.0 ± 5.9	58.6 ± 8.9
		CBF	N = 28	38.0 ± 4.0	-17.8 ± 5.3	55.0 ± 6.8
	TMS	hotspot	N = 28	42.3 ± 4.5	-8.0 ± 7.7	$57.2 \pm 5.5^*$
		CoG	N = 12	41.2 ± 3.9	-5.8 ± 7.3	$57.2 \pm 4.0^*$

BOLD: blood oxygenation level dependent (fMRI signal type); CBF: cerebral blood flow (fMRI signal type); CoG: TMS centre-of-gravity; fMRI: functional magnetic resonance imaging; MNI: standard space of the Montreal Neurological Institute; non-dom.: non-dominant; TMS: transcranial magnetic stimulation; X: lateral-medial coordinate; Y: anterior-posterior coordinate; Z: inferior-superior coordinate; * Position was projected onto the gyral surface (because TMS has no selectivity for a particular stimulation depth)

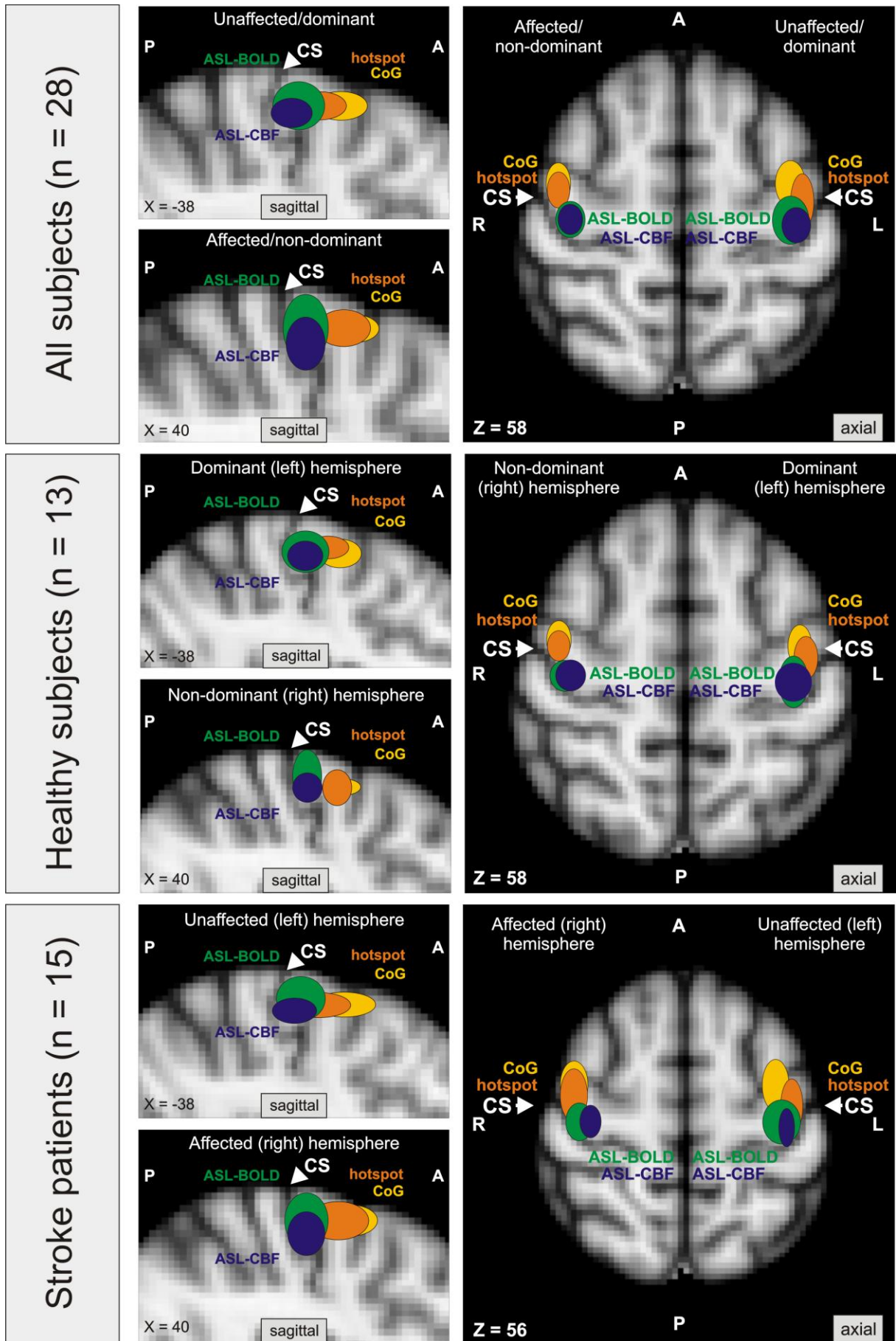


Figure 4.3: Study II: Localization of the primary motor cortex with fMRI and TMS. Coloured ellipsoids indicate mean MNI coordinates (\pm SD) of functional magnetic resonance (fMRI) peak voxels and optimal transcranial magnetic stimulation (TMS) positions located within the precentral gyrus of the contralesional/dominant and ipsilesional/non-dominant hemisphere of stroke patients ($n = 15$) and healthy controls ($n = 13$). Results of stroke patients and healthy controls were pooled since there were no significant differences between groups (ANOVA, $P > 0.05$). fMRI peak voxels were defined as voxel with highest statistical t-value during contralateral thumb abductions measured with ASL-BOLD (green) and ASL-CBF (blue). Hotspot coordinates refer to stimulation sites resulting in highest abductor pollicis brevis (APB) muscle responses when stimulated with TMS (orange). CoG coordinates were calculated from a TMS motor mapping, and reflect the motor evoked potential weighted maximum electric field coordinate (yellow). All coordinates were projected into the sagittal and axial plane corresponding to the mean coordinate across all positions. ASL-BOLD coordinates were significantly more superficial than ASL-CBF coordinates (repeated measures ANOVA, $P < 0.05$). Hotspot and CoG coordinates were significantly more anterior and lateral than fMRI maxima (post-hoc t-tests, $P < 0.05$, FDR-corrected). The white arrow marks the central sulcus (CS).

4.3.3.2 Analyses on differences in fMRI and TMS positions ($n = 12$)

Overall 12 subjects (6 stroke patients and 6 control subjects) agreed to participate in a separate TMS session in which systematic motor mappings of the ipsilesional/non-dominant and contralesional/dominant motor cortex and surrounding tissue was performed. Individual TMS mapping derived CoG positions were projected into MNI space by applying the individual nonlinear FNIRT registration transform. MNI coordinates of TMS CoG positions were then compared with MNI coordinates of fMRI peak voxel coordinates and TMS hotspot positions by computing a repeated measures ANOVA ($n = 12$) with the factor APPROACH (levels: ASL-BOLD, ASL-CBF, TMS-hotspot, TMS-CoG) and GROUP (levels: patients, controls) for each hemisphere and dimension (MNI-coordinate X, Y, and Z).

Mean MNI coordinates of TMS CoG positions are given in Table 4.3 and are depicted in Figure 4.3. In lateral-medial direction (i.e. in MNI coordinate X), there was no significant main effect or interaction ($P > 0.05$). In anterior-posterior direction (i.e. in MNI coordinate Y), there was a highly significant main effect of APPROACH for both hemispheres (IL/ND: $F(3, 30) = 21.798$, $P < 0.001$; CL/D: $F(3, 30) = 24.604$, $P < 0.001$). Post-hoc t-test revealed that both, TMS hotspots and TMS CoGs were significantly more anterior than ASL-BOLD and ASL-CBF positions (IL/ND and CL/D: $P < 0.002$, FDR-corrected). Analyses in inferior-superior direction (i.e. in MNI coordinate Z) were not performed as TMS has no selectivity for a particular stimulation depth. No significant main effect of GROUP or significant APPROACH x GROUP interaction was found for any of the ANOVAs ($P > 0.05$).

In summary, analyses on differences in ASL-BOLD, ASL-CBF, TMS-hotspot, and TMS-CoG positions in all 12 subjects, in whom a systematic TMS motor mapping was performed,

indicated that both TMS-hotspot and TMS-CoG positions are significantly more anterior than fMRI positions. Findings were similar for both hemispheres and there were no significant differences between stroke patients and healthy subjects in TMS-CoG positions. Results were similar to results of Study I.

4.3.4 Euclidian distances between fMRI and TMS positions

To test whether one of the fMRI techniques localizes neural activity significantly closer to the optimal TMS position, Euclidean distances between individual fMRI and TMS positions were calculated (Table 4.4). Two different approaches were pursued: (i) Euclidean distances between fMRI peak voxel positions and the TMS hotspot position ($n = 28$) and (ii) Euclidean distances between the centre-of-gravities (CoGs) of the fMRI activation clusters and the TMS mapping CoG ($n = 12$) were calculated. The CoG approach considers the spatial distribution of fMRI activity (and TMS excitability respectively) in the pericentral region. Hence, the CoG approach has been suggested to be less prone to artefacts (Classen et al., 1998). However, as a drawback, the CoG approach highly depends on the fMRI cluster size and hence on the statistical threshold applied (Duong et al., 2000).

Euclidean distances were entered in repeated measures ANOVAs with the factors APPROACH (levels: ASL-BOLD, ASL-CBF) and GROUP (levels: patients, controls) for each hemisphere. There was no significant main effect or interaction for displacements between fMRI peak voxels and the TMS hotspot indicating that none of the fMRI techniques yielded peak activations significantly closer to the TMS hotspot ($P > 0.05$).

For displacements between fMRI-CoGs and the TMS-CoG, there was a significant main effect of APPROACH for both hemispheres indicating that displacements were significantly larger for ASL-BOLD compared to ASL-CBF if the CoG approach was used (IL/ND: $F(1, 10) = 32.185$, $P < 0.001$; CL/D: $F(1, 10) = 18.294$, $P = 0.002$). For the ipsilesional/non-dominant hemisphere (but not for the contralesional/dominant) hemisphere there was a significant main effect of GROUP for displacements between fMRI-CoGs and the TMS-CoG ($F(1, 10) = 8.432$, $P = 0.016$). This finding indicates that stroke patients show significantly larger displacements between fMRI and TMS positions on the ipsilesional hemisphere (25.3 ± 11.8 mm) compared to the non-dominant hemisphere of healthy subjects (18.0 ± 11.8 mm). However, there was no significant GROUP \times APPROACH interaction, neither on the ipsilesional/non-dominant (IL/ND) nor on the contralesional/dominant (CL/D) hemisphere ($P > 0.05$).

In summary, if Euclidean distances between fMRI peak voxel positions and the TMS hotspot position ($n = 28$) were calculated, there was no statistical difference between fMRI techniques, suggesting that none of the fMRI techniques yielded peak activations significantly closer to the TMS hotspot. Findings were similar for both hemispheres and groups. If however, the CoG approach was used, displacements were overall larger for ASL-BOLD compared to ASL-CBF, but this was the case for both groups. Moreover, displacements were overall larger on the ipsilesional hemisphere of stroke patients (compared to the non-dominant hemisphere of healthy subjects), but this was the case for both fMRI techniques.

Table 4.4: Study II: Euclidean distances between fMRI and TMS positions (single-subject space)

Hemisphere	Approach		Sample size	Euclidean distance [mm]
Contralesional/ dominant	fMRI peak voxel vs. TMS hotspot	BOLD	N = 28	13.2 ± 6.0
		CBF	N = 28	12.6 ± 5.6
	fMRI CoG vs. TMS CoG	BOLD	N = 12	33.1 ± 13.8
		CBF	N = 12	19.1 ± 8.4
Ipsilesional/ non-dom.	fMRI peak voxel vs. TMS hotspot	BOLD	N = 28	15.7 ± 5.8
		CBF	N = 28	13.7 ± 5.8
	fMRI CoG vs. TMS CoG	BOLD	N = 12	29.2 ± 8.8
		CBF	N = 12	14.2 ± 6.0

BOLD: blood oxygenation level dependent (fMRI signal type); CBF: cerebral blood flow (fMRI signal type); CoG: TMS centre-of-gravity; fMRI: functional magnetic resonance imaging; MNI: standard space of the Montreal Neurological Institute; TMS: transcranial magnetic stimulation; X: lateral-medial coordinate; Y: anterior-posterior coordinate; Z: inferior-superior coordinate

4.3.5 TMS of fMRI peak voxel with 120 % RMT

Brain tissue at individual peak voxel coordinates was stimulated with neuronavigated single-pulse suprathreshold TMS to investigate whether spatial differences between ASL-BOLD and ASL-CBF positions (in MNI coordinate Z, i.e. in depth) are functionally relevant, i.e. impact on MEP size of the respective peripheral target muscle (APB). A repeated measures ANOVA ($n = 28$) with the factors APPROACH (levels: ASL-BOLD, ASL-CBF) and GROUP (levels: patients, controls) was performed for each hemisphere. There was no significant main effect or interaction ($P > 0.05$) indicating that there was no significant difference between fMRI techniques in MEPs when stimulated with TMS. Hence, significant differences between fMRI

techniques in depth (i.e. in MNI coordinate Z) were not functionally relevant for TMS applications.

4.3.6 Results of TMS motor mappings

Results of TMS motor mappings can be seen in Figure 4.4 (healthy subjects) and Figure 4.5 (stroke patients). There was considerably high inter-individual difference in cortical excitability maps in healthy subjects as well as stroke patients. As expected, most subjects showed highest excitability in the precentral gyrus (albeit not necessarily at the hand knob formation). In some subjects, highest excitability was found considerably more anterior than the precentral gyrus. However, this finding was not restricted to stroke patients (e.g. see stroke patient 04) but did also occur in healthy subjects (e.g. see healthy subject 06). Interestingly, some subjects showed unusual sites of highest excitability. For example stroke patient 01, showed highest muscle responses when the TMS coil was navigated to an anterior-medial area, which might correspond to the pre-SMA. However, unusual sites of highest excitability were also found among healthy subjects. For instance, highest excitability was found on the postcentral gyrus of the dominant hemisphere in healthy subject 02. Furthermore, in healthy subject 03, highest excitability was likewise found over an anterior-medial area, which might correspond to the pre-SMA.

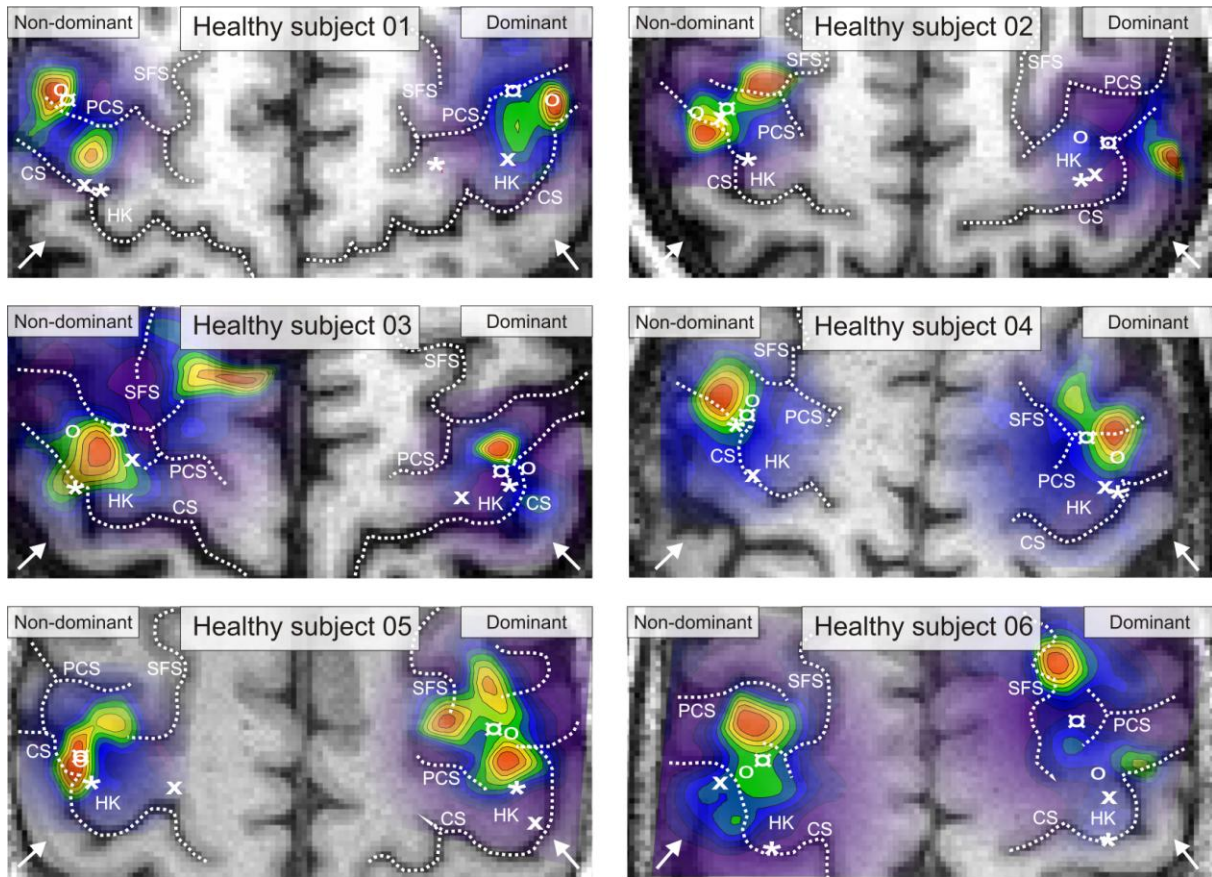


Figure 4.4: Study II: Results of TMS motor mappings of the non-dominant and the dominant motor cortex of six healthy subjects. The TMS coil was navigated to grid positions spaced at intervals of 5 mm starting at the TMS motor hotspot position. Subsequent positions followed a helix around the hotspot position until no MEPs (peak-to-peak amplitude $\geq 50 \mu\text{V}$) could be elicited at any outside margin of the map. This mapping procedure included the hand knob formation (Yousry et al., 1997) in all subjects. Seven stimuli (at 120% RMT; ISI = 1500 ms) were applied at each position. The TMS coil orientation was approximately perpendicular to the central sulcus (cf. white arrows in the lower corners). MEPs were recorded from the APB and a centre-of-gravity (CoG, the weighted average of excitability of the TMS motor map) was calculated. Positions refer to electric field maximum (EF_{\max}) positions within the cerebral cortex calculated by computerized modelling. TMS identified positions (i.e. hotspot and CoG positions) were projected onto the cerebral surface. Coloured contours represent 10 percentiles of the averaged maximal response of the APB muscle viewed from above. The background image is the subject's individual structural MRI scan showing the corresponding underlying cerebral anatomy. All fMRI and TMS positions (depicted as white symbols) were projected into the slice corresponding to the mean axial depth of all individual sites. (CS: central sulcus; HK: hand knob; PCS: precentral sulcus; SFS: superior frontal sulcus).

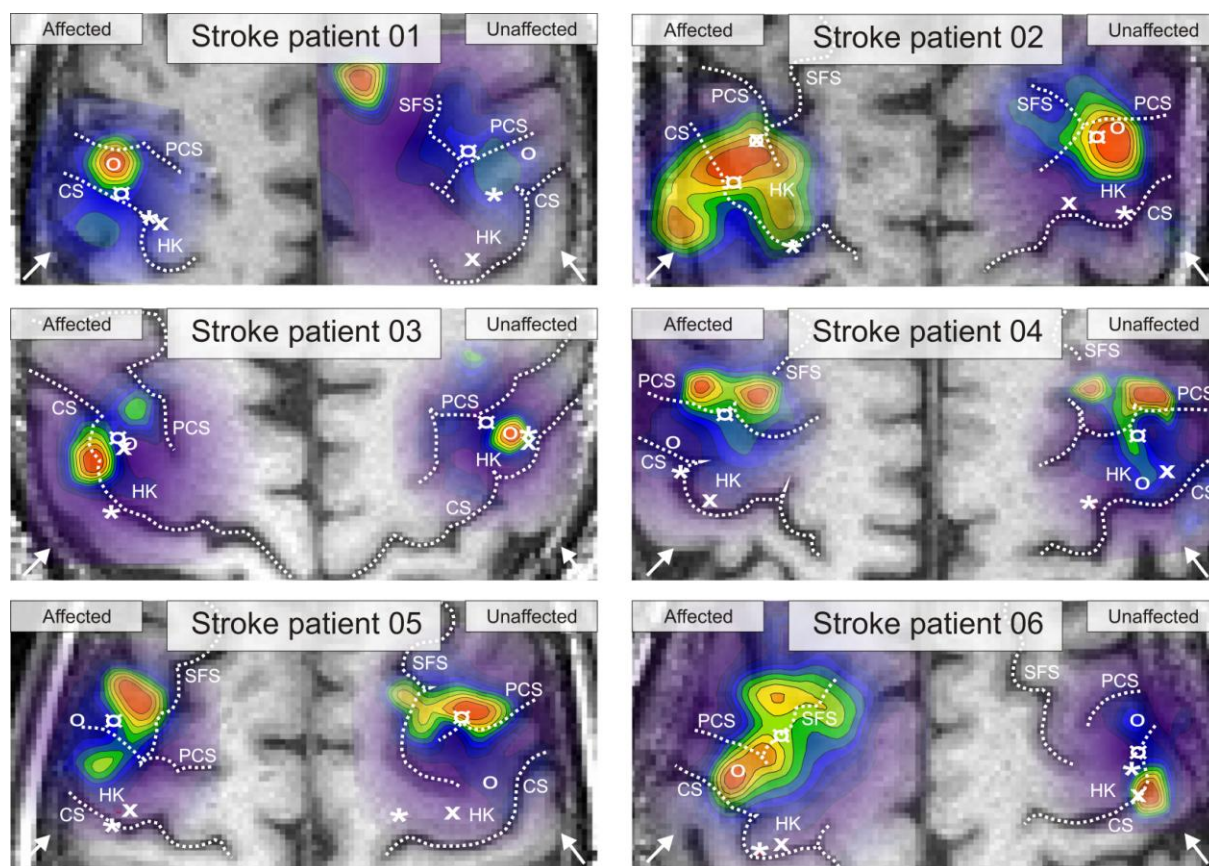


Figure 4.5: Study II: Results of TMS motor mappings of the ipsilesional and the contralesional motor cortex of six chronic stroke patients.

4.4 Discussion Study II

4.4.1 fMRI group analysis

4.4.1.1 fMRI BOLD signal

The fMRI group analysis on BOLD signal change demonstrated that stroke patients show enhanced BOLD signal in contralesional primary motor cortex (M1) during movements of the affected hand (but not during movements of the unaffected hand) compared to healthy controls. This finding is in line with previous studies reporting bilaterally enhanced fMRI BOLD signal in contralesional M1/S1, PMC, ipsilesional cerebellum, bilateral SMA and parietal cortex in stroke patients moving their affected hand compared to control subjects (Chollet et al., 1991; Cramer et al., 1997; Seitz et al., 1998, Ward et al., 2003b; Weiller et al., 1992). The functional role of bilaterally enhanced fMRI signal is still not fully understood but some studies suggest that there is an inverse relationship between enhanced activation and

motor performance, i.e. patients with poorer outcome recruit more regions of the brain (often bilaterally) during movements of the affected hand than less severely affected patients (Ward et al., 2003b). Since SMA and PMC have projections to motoneurons in the spinal cord (Maier et al., 2002), it has been suggested that in patients in whom the cortico-motoneuronal input originating from M1 is lost or severely impaired, there is greater reliance on other parallel motor circuits to generate an alternative input to motoneurons of the spinal cord. This may result in increased task-related activation, however, since alternative projections are less numerous and exert a weaker excitatory effect than those from M1 (Maier et al., 2002), functional recovery is incomplete (Ward et al., 2003b).

Previous studies discussed the possibility that bilaterally enhanced BOLD signal during movements of the affected hand might not exclusively be attributable to neuronal reorganization but may also relate to higher effort in stroke patients (Ward et al., 2003b). The fixed movement condition, in which patients (with impaired motor performance) were asked to perform the motor task with identical parameters (i.e. thumb abduction frequency) as healthy controls, was more effortful and cognitively complex for patients compared to controls. More effortful motor tasks are known to recruit a wider network of motor regions than simple motor tasks (Catalan et al., 1998). In order to control for the degree of effort involved in the thumb abduction task as much as possible, performance levels in the present study were maintained across all subjects (patients and controls) by asking subjects to perform at a percentage (66%) of their individual maximum thumb abduction frequency. Interestingly, stroke patients showed bilaterally enhanced BOLD signal during both, the fixed and the adjusted movement frequency condition compared to control subjects. These findings suggest that bilaterally enhanced BOLD signal during movements of the affected hand is not exclusively caused by increased effort in stroke patients.

4.4.1.2 fMRI CBF signal

Several studies demonstrated that ASL can be successfully used to assess task-related changes in CBF in healthy subjects (Diekhoff et al., 2010; Edelman et al., 1994; Talagala & Noll, 1998; Ye et al., 1997; Yongbi et al., 2002). Although it has been demonstrated that good-quality CBF images can be obtained from stroke patients at rest (Chalela, 2004; Detre et al., 1998), so far no study has been published using ASL to assess *task-related* changes in CBF in stroke patients. Hence, the present study is the first study to demonstrate that meaningful movement-related changes in CBF can be obtained from chronic stroke patients by means of

ASL. By using perfusion MRI, we were able to narrow down the source of fMRI signal to small vessels and capillaries. Vascular abnormalities in stroke patients may result in reduced blood flow (due to artery occlusion or stenoses), which would result in reduced CBF signal (or even absence of CBF signal) due to prolonged transit times which might prevent that blood reaches the imaging slice in due time. However, we were able to find significant CBF signal changes in stroke patients. Additionally, significant CBF signal changes were exclusively located in primary motor cortex and premotor cortex (and nowhere else in the brain; Table 4.2, Figure 4.1), which make artefacts an unlikely cause.

Interestingly, we were able to detect bilaterally organized fMRI activation in chronic stroke patients not only with BOLD but also with perfusion fMRI. The functional role of enhanced BOLD signal in the contralesional hemisphere has been discussed controversially (Butefisch et al., 2005; Fregni et al., 2006; Grefkes et al., 2008b, 2010; Johansen-Berg et al., 2002; Lotze et al., 2006; Murase et al., 2004; Ward et al., 2003b; for a detailed discussion see section 5.4.3 and 5.4.4) and the opportunity that the increased signal might at least in part be attributable to vascular abnormalities (instead of altered neuronal activity) of in the contralesional hemisphere could not entirely be excluded. Our experiments imply that enhanced BOLD signal in the contralesional hemisphere does not exclusively originate from vascular artefacts around large vessels, since bilateral organization of neural activity was suggested by CBF (originating from brain parenchyma and capillaries) as well. Hence, our data support the view that increased fMRI signal in contralesional M1 reflects increased neuronal activity and is not simply caused by vascular artefacts.

All peak activation clusters obtained by ASL-CBF were located either in the primary motor cortex (M1) or the central sulcus (CS). This finding is in agreement with previous studies demonstrating that CBF signal is well co-localized with neural activity (Duong et al., 2000; Luh et al., 2000; Silva et al., 1997; Tjandra et al., 2005). Interestingly, global peak activation obtained by BOLD was located in other brain areas (such as SMA); whereas local BOLD maxima in M1 featured lower statistical Z-values. Hence, CBF suggested highest movement-related neuronal activity in M1, whereas BOLD suggested highest movement-related neural activity in SMA. However, it is difficult to make a clear statement about which fMRI techniques gives a more realistic image of neuronal processes, since it is not precisely known whether neuronal activity in M1 exceeds neuronal activity in SMA (or vice versa) during movement execution in humans.

4.4.2 Statistical Z-values at individual fMRI peak voxels

BOLD activation clusters were larger due to considerably higher sensitivity of BOLD fMRI compared to perfusion fMRI. Statistical Z-values at ASL-BOLD peak voxels were significantly higher compared to statistical Z-values at ASL-CBF peak voxels. This finding is in line with previous reports of reduced sensitivity in perfusion fMRI (~ 1% signal change; Wintermark et al., 2005) compared to BOLD fMRI (up to 5% signal change; Detre & Wang, 2002).

4.4.3 Differences in fMRI and TMS positions

Individual TMS hotspot positions were available for 15 stroke patients and 13 control subjects (n = 28). They were projected into MNI space by applying the individual nonlinear FNIRT registration transform. Analyses on differences in ASL-BOLD, ASL-CBF, and TMS-hotspot positions in all 28 subjects indicated that TMS hotspot positions are more lateral and anterior compared to fMRI positions and that ASL-BOLD positions are significantly closer to the gyral surface than ASL-CBF positions. Individual TMS CoG positions (derived from a systematic TMS motor mapping) were available from 12 subjects (6 stroke patients and 6 control subjects). They were projected into MNI space by applying the individual nonlinear FNIRT registration transform. Analyses on differences in ASL-BOLD, ASL-CBF, TMS-hotspot, and TMS-CoG positions in all 12 subjects, in whom a systematic TMS motor mapping was performed, indicated that TMS-hotspot and TMS-CoG positions were significantly anterior of fMRI positions. Similar findings were found in healthy young subjects in Study I. There were no significant differences between hemispheres or groups regarding ASL-BOLD, ASL-CBF, TMS-hotspot, and TMS-CoG positions in the present study. Hence, results suggest that functional reorganization in stroke patients did not lead to a systematic shift of fMRI or TMS positions in stroke patients compared to control subjects.

In the acute phase after stroke, the TMS CoG (i.e. the amplitude weighted centre of the TMS excitability map) is usually within the normal range (Talelli et al., 2006). However, spatial shifts may occur later during recovery. They may range from several millimetres (Byrnes et al., 2001; Thickbroom et al., 2002) up to few centimetres (Bastings et al., 2002; Delvaux et al., 2003), which is well beyond the normal variation range of 2-3 mm in healthy subjects (Wassermann et al., 1996). However, in line with our findings, such spatial shifts may occur in different directions (Bastings et al., 2002; Byrnes et al., 2001; Delvaux et al., 2003;

Thickbroom et al., 2002), which might explain why we were not able to find a systematic shift over the group of patients. It has been suggested that the underlying cause of a spatial shift in CoG might be: (a) that the corticospinal projection of the muscle has been damaged more in one location than the other, and/or (b) unmasking of additional synaptic inputs to remaining corticospinal output regions (Talelli et al., 2006). Spatial shifts in TMS CoG occur in well-recovered patients (Byrnes et al., 2001), but do not necessarily relate to clinical recovery (Bastings et al., 2002). In the study of Thickbroom et al. (2004) greater map displacement was associated with better motor outcome (i.e. grip strength), but only in a subgroup of patients which showed normal corticospinal conduction in the subacute stage.

4.4.4 Euclidian distances between fMRI and TMS positions

To test whether one of the fMRI techniques localized neural activity significantly closer to optimal TMS positions, Euclidean distances between fMRI maxima and the TMS hotspot ($n = 28$) as well as between fMRI-CoGs and the TMS-CoG ($n = 12$) were calculated. If fMRI maxima and the TMS hotspot were used for analysis, there was no significant difference between fMRI techniques, which suggests that none of the fMRI techniques yielded peak activations significantly closer to the TMS hotspot. This finding is in line with findings of Study I obtained in healthy young subjects. There were no significant differences between hemispheres or groups in the present study, suggesting that functional reorganization after stroke had no significant impact on the spatial congruence between fMRI and TMS.

If however, fMRI-CoGs and the TMS-CoG (instead of peak coordinates) were used for analysis, ASL-CBF showed significantly shorter distances to the TMS-CoG than ASL-BOLD. This was not the case in Study I, which showed no significant difference between BOLD and CBF even if CoGs (instead of peak activations) were used. However, in the present study BOLD activation clusters were larger than BOLD activation clusters of healthy young subjects in Study I (although the same statistical threshold was used). Why BOLD activation clusters in the present study were larger than BOLD activation clusters in Study I is unclear but might be due to increased task difficulty due to the fixation device attached to the subjects hands (cf. 4.2.2). Although the device was useful to standardize movements across subjects, it might have induced additional effort (in order to perform the task “properly”). More demanding tasks have however been demonstrated to induce more widespread fMRI activations (Catalan et al., 1998). However, since BOLD activation clusters were so large, the CoG of

BOLD activation clusters showed a pronounced shift away from the local maximum at the hand knob formation in medial direction (i.e. towards the SMA where highest task-related BOLD signal changes were found in the majority of subjects). CBF activation clusters were much smaller than BOLD activation clusters (due to lower sensitivity) and hence CBF-CoGs showed only small spatial shifts away from the local maximum at the hand knob formation. However, more conservative statistical thresholds, which led to smaller BOLD activation clusters, could not be passed by CBF activation clusters. Hence, although analyses using the CoG approach suggested that ASL-CBF positions were significantly closer to the TMS-CoG than ASL-BOLD positions, this finding can be attributed to enlarged BOLD activation clusters. Due to independence from the statistical threshold applied, we have more confidence in analyses on peak activations (instead of CoGs), which unfortunately suggested no significant difference between fMRI signal types in distance to the TMS hotspot (neither in healthy subjects nor in stroke patients).

Interestingly, stroke patients showed overall larger displacements on the ipsilesional (but not the contralesional) hemisphere compared to healthy controls. Reorganization processes after stroke may cause both, a spatial shift of highest fMRI signal and highest TMS excitability (Rossini et al., 1998). Our data seem to suggest that these processes might further decrease spatial congruence between fMRI and TMS in the ipsilesional hemisphere.

4.4.5 TMS of fMRI peak voxel with 120 % RMT

Although we found significant differences between BOLD and CBF positions, there were no significant differences in MEPs when tissue at fMRI positions was stimulated with neuronavigated single-pulse TMS. This finding indicates that spatial differences between fMRI signal types were not functionally relevant for TMS applications. This might be because CBF and BOLD positions differed from each other only in MNI coordinate Z (i.e. in depth) and TMS cannot differentiate between superficial and deep targets. There were no significant differences between hemispheres or groups and no significant interactions.

4.4.6 Results of TMS motor mappings

Mapping results were highly variable across individuals. However, high inter-individual variability and unusual sites of highest excitability were not restricted to stroke patients but did also occur in healthy subjects. This finding is in line with previous studies demonstrating

high inter-individual variance in TMS motor mapping results in healthy subjects (Classen et al., 1998; Diekhoff et al., 2011; Sparing et al., 2008; Wassermann et al., 1996) and stroke patients (Bastings et al., 2002; Byrnes et al., 2001; Delvaux et al., 2003; Thickbroom et al., 2002). These results strongly suggest that unusual sites of highest TMS excitability (distant from the hand knob formation) are not necessarily caused by reorganization processes in stroke patients but may also be subject to technical issues such as distribution of the TMS induced electric field (EF). For instance a recent study of Opitz and colleagues (2011) demonstrated that EF strength is highest on gyral crowns and lips due to conductivity changes at tissue boundaries. Individual differences in grey matter and white matter anatomy may hence cause considerable differences in TMS mapping results (Opitz et al., 2011).

4.4.7 Conclusions Study II

The present study is the first study to demonstrate that meaningful movement-related changes in CBF signal (located in the primary motor cortex) can be obtained from chronic stroke patients. Enhanced fMRI signal in contralesional primary motor cortex (M1) during movements of the affected hand in stroke patients (compared to healthy subjects) was suggested by both, BOLD *and* CBF signal, which strongly suggests increased neuronal activity (and not vascular artefacts) as underlying cause. Highest movement-related CBF signal changes were located close to the anatomical motor hand area (Brodmann area 4) indicating high spatial specificity of CBF signal. In contrast, highest BOLD signal changes occurred close to the SMA. Similar to findings of Study I, obtained in healthy young subjects, highest BOLD signal changes occurred significantly closer to the cerebral surface than highest CBF signal changes. However, also in line with findings from Study I, this difference between fMRI techniques (in depth) did unfortunately not impact on distances to optimal TMS positions, which were considerably more anterior than fMRI positions. In line with this finding, muscle responses resulting from stimulation of brain tissue at peak voxel positions with TMS was not significantly different for CBF and BOLD positions, indicating that differences in cortical depth are not functionally relevant for TMS applications. Regarding Euclidean distances between fMRI and TMS positions, results of the present study (Study II) were comparable to results of Study I. Hence, findings suggest that neither in healthy young subjects nor in chronic stroke patients (or age-matched healthy controls), ASL-CBF localizes the motor hand area significantly closer to the TMS hotspot than ASL-BOLD. The only

significant group difference, which was found in the present study, suggested significantly larger displacements between fMRI and TMS positions on the ipsilesional hemisphere of stroke patients compared to the non-dominant hemisphere of healthy subjects. This finding might point towards decreased congruence between fMRI and TMS on the ipsilesional hemisphere. However, underlying mechanisms apparently affected both, CBF and BOLD signals to similar extent.

5 Study III: Prediction of TBS effects

5.1 Introduction Study III

The major aim of Study I & II was reduction of variability across studies by improving current strategies to identify the cortical target position for rTMS. The major aim of the present study (Study III) is to identify reliable predictors for effects of rTMS on motor performance of stroke patients to reduce variability across individual patients.

Theta-burst stimulation (TBS) was recently introduced as new rTMS protocol, allowing modulation of cortical excitability outlasting the period of stimulation (Huang et al., 2005). TBS has several advantages over conventional so-called *simple rTMS protocols*: low stimulation intensities, robust and long-lasting effects, which appear to be more consistent across studies (Hoogendam et al., 2010), and short stimulation durations of only a 1-3 minutes. TBS is thought to induce phenomena of synaptic plasticity such as LTP and LTD (Hoogendam et al., 2010), which renders TBS an interesting tool for neurorehabilitation. The pathomechanisms underlying stroke-induced motor deficits do not only depend on direct tissue damage due to ischemia, but may also comprise network disturbances remote from the primary stroke lesion (Feney & Baron, 1986; Grefkes & Fink, 2011; Honey & Sporns, 2008). The simplified *model of hemispheric competition* proposes relative hypoexcitability of the ipsilesional hemisphere and hyperexcitability of the contralesional hemisphere leading to pathologically increased inhibition from the contralesional hemisphere onto the ipsilesional hemisphere (Duque et al., 2005; Grefkes et al., 2008b, 2010; Murase et al., 2004). In line with the *model of hemispheric competition*, both increasing excitability of the ipsilesional hemisphere (Khedr et al., 2005; Talelli et al., 2007) as well as decreasing excitability of the contralesional hemisphere (Fregni et al., 2006; Di Lazzaro et al., 2008) by means of rTMS has been demonstrated to normalize cortical excitability towards levels observed in healthy subjects and/or to ameliorate motor performance of the paretic hand. Interestingly, and in line with the *model of hemispheric competition*, inhibitory 1 Hz rTMS applied to the contralesional hemisphere has been demonstrated to decrease pathologically enhanced interhemispheric inhibition targeting the ipsilesional hemisphere (Grefkes et al., 2010). Effects of a single rTMS session may last several minutes up to one hour, depending on the protocol applied (Huang et al. 2005; Hoogendam et al., 2010). Whether effects are sufficiently robust to be useful in clinical settings is currently under investigation. One of the

most challenging problems that need to be solved is considerably high inter-individual variance in rTMS induced effects, which has been reported for healthy subjects (Daskalakis et al., 2006; Van Der Werf & Paus, 2006; Müller-Dahlhaus et al., 2008) as well as stroke patients (Ameli et al., 2009). Furthermore, stroke patients may even show transient deteriorations of motor performance after rTMS interventions depending on the lesion location (Ameli et al., 2009). Hence, for the implementation of rTMS in stroke rehabilitation, it seems essential to identify reliable predictors for the therapeutic success of a specific rTMS intervention in a specific stroke patient. Factors which are likely to impact on rTMS induced effects are patient characteristics such as time since stroke, lesion location, clinical deficit, and the pathomechanism underlying stroke induced motor hand deficits. The pathomechanism underlying stroke induced motor hand deficits might be best reflected when taking a network perspective (Grefkes & Fink, 2011). It appears likely that the slightly oversimplified *model of hemispheric competition* does not uniformly apply to all stroke patients with motor deficits. It appears conceivable that the variety of lesions in stroke causes a variety of different functional pathologies impacting on the processes of movement planning, execution and feedback control. For example, patients with decreased effective connectivity among cortical motor areas of the ipsilesional hemisphere (Grefkes et al., 2008; Grefkes & Fink, 2009; Mintzopoulos et al., 2009; Sharma et al., 2009) might benefit more likely from facilitation of the ipsilesional hemisphere, whereas patients with pathologically enhanced inhibition from the contralesional primary motor cortex (M1) onto the ipsilesional M1 (Duque et al., 2005; Grefkes et al., 2008b, 2010; Murase et al. 2004) might benefit more likely from inhibition of the contralesional hemisphere. Reducing inter-individual variance and avoiding adverse effects appears crucial to for the implementation of rTMS in stroke rehabilitation. Hence, the aim of the present study was to identify reliable predictors for behavioural effects following facilitatory intermittent TBS (iTBS) applied to ipsilesional M1 and inhibitory continuous TBS (cTBS) applied to contralesional M1 (compared to control stimulation) in chronic stroke patients. We used a multimodal approach consisting of single-pulse and paired-pulse TMS parameters, movement-related fMRI signal in cortical motor areas, laterality of fMRI signal, and effective connectivity within the cortical motor network (assessed by means of dynamic causal modelling, DCM) to identify potential predictors for TBS effects.

5.2 Methods Study III

5.2.1 Subjects

13 stroke patients (62.8 ± 10.3 years old; 10 males) and 12 healthy control subjects (58.5 ± 5.9 years old; 6 males) were investigated (Table 5.1). There were no significant differences between groups in age (two-sample t-test, $P > 0.1$) or gender (Pearson's chi-square test, $P > 0.1$). Patients had right-sided ($n = 10$) or left-sided ($n = 3$) lesions due to first-ever cerebral ischemia. Lesions did not affect the M1 hand representation on the precentral gyrus nor any of the other cortical motor areas used for the DCM analysis (Figure 5.1). Patients were included in the study based on the following criteria: (i) stable unilateral hand motor deficit, (ii) insult at least 12 months ago (chronic stage), (iii) absence of aphasia, neglect, and apraxia, and (iv) absence of mirror movements of the unaffected hand during movements of the affected hand. Healthy control subjects were free of any history of medical or psychiatric disease. One subject in each group was left-handed according to the Edinburgh Handedness Inventory (EHI; Oldfield, 1971). Remaining subjects were right-handed (EHI was assessed for the time before stroke in patients). None of the subjects had any contraindication to TMS (Wassermann, 1998) and all subjects gave informed consent to participate in the study, which was approved by the ethics committee of the Medical Faculty, University of Cologne, Germany (file-no 09-108). All experiments conformed to the Declaration of Helsinki, sixth revision 2008.

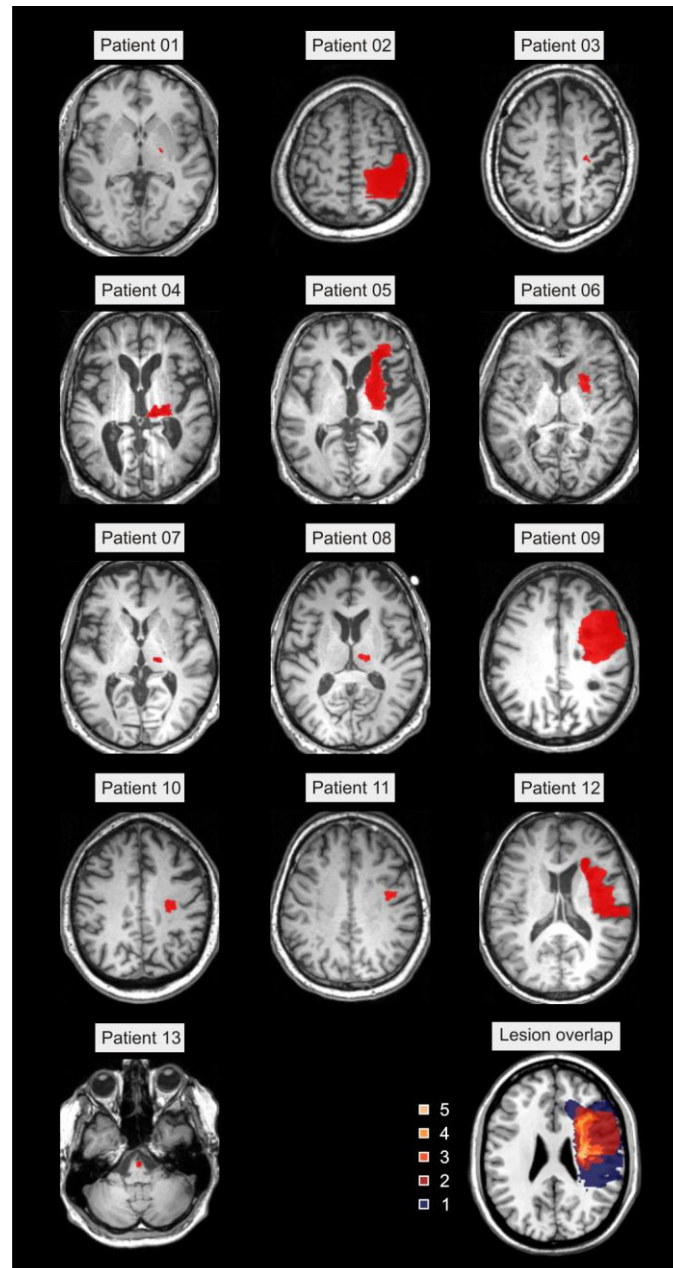


Figure 5.1: Study III: Lesion locations. Individual high-resolution $T1$ -weighted anatomical magnetic resonance (MR) images of 13 chronic stroke patients are shown at the axial depth of the ischaemic lesion (depicted in red colour). MR images of patients with left-sided lesions (Patient 08, 10, and 13) were flipped at the midsagittal plane (see methods section for details). Lesions were spatially normalized to the standard template of the Montreal Neurological Institute (MNI). The colour coded spatial overlap between lesions in MNI standard space can be seen in the lower right corner of the figure.

Study III: Prediction of TBS effects

Table 5.1: Study III Demographical, clinical, and behavioural data

Subject	Age	Sex	Handedness	Lesion side	% CST	Lesion size [cm ³]	Lesion age [m]	mRS	NIH SS	ARAT	CIS	Affected / non-dominant hand					Unaffected / dominant hand					Order of TBS protocols
												JTT [s]	FT [Hz]	GF [kPa]	MIS cTBS	MIS iTBS	JTT [s]	FT [Hz]	GF [kPa]	MIS cTBS	MIS iTBS	
P 01	56	M	R	R	0.0	0.1	33	1	1	57	-1.01	30.7	4.8	111.0	0.51	0.61	27.5	5.4	119.0	1.37	0.85	I – C – Xi
P 02	48	M	R	R	47.7	251.7	156	2	6	30	1.19	120.5	2.3	105.0	-0.46	-0.03	35.9	6.7	150.0	0.76	-0.19	C – Xc – I
P 03	65	M	R	R	0.4	0.1	28	1	1	46	-0.68	64.8	3.3	76.7	-0.13	0.34	36.4	5.5	96.3	-1.18	-0.60	Xc – I – C
P 04	70	M	R	R	2.9	3.0	100	3	7	24	2.01	158.2	1.5	16.0	0.11	-2.42	47.2	5.6	90.0	-0.72	0.04	C – Xc – I
P 05	68	M	R	R	17.9	40.2	32	3	5	32	1.40	165.2	1.7	43.7	-0.50	0.02	39.5	5.4	113.7	0.64	-0.45	I – Xc – C
P 06	65	M	R	R	0.0	1.3	22	2	3	50	0.03	68.5	3.5	42.7	-1.47	-0.98	47.3	4.5	70.7	-0.53	-1.71	Xi – I – C
P 07	73	M	L	R	0.0	0.2	35	1	4	41	0.03	69.4	3.9	64.7	0.14	0.67	37.6	5.3	76.7	0.80	0.89	Xi – C – I
P 08	75	M	R	L	0.0	0.4	43	1	2	57	-0.83	27.7	5.1	64.7	0.13	0.80	26.7	5.3	63.3	-0.83	0.16	Xi – C – I
P 09	43	F	R	R	17.5	42.1	18	2	3	32	0.58	144.8	3.0	7.3	2.89	1.24	33.0	5.4	60.7	0.04	-0.14	C – Xi – I
P 10	67	M	R	L	6.4	1.6	253	1	3	56	-0.61	34.0	4.2	64.7	-0.43	-0.45	32.9	5.1	77.3	-0.52	-1.35	I – Xi – C
P 11	60	M	R	R	7.5	2.3	16	1	2	54	-0.74	46.5	2.9	71.7	0.08	-0.18	43.0	5.7	81.0	-0.21	-0.27	C – Xc – I
P 12	52	F	R	R	7.6	26.7	12	1	1	57	-1.01	38.7	3.7	49.3	-0.70	-0.75	28.6	4.6	46.7	-1.42	0.63	I – Xi – C
P 13	74	F	R	L	0.0	0.2	50	1	4	54	-0.37	41.1	3.1	21.3	-0.15	1.14	33.1	3.3	48.0	1.81	2.15	I – C – Xc
Mean	62.8				8.3	28.4	61.4	1.5	3.2	45.4	0.0	77.7	3.3	56.8	0.0	0.0	36.1	5.2	84.1	0.0	0.0	
SD	10.3				13.4	68.9	70.1	0.8	1.9	12.1	1.0	51.0	1.1	31.4	1.0	1.0	6.8	0.8	29.7	1.0	1.0	
H 01	50	M	R	-	-	-	-	-	-	-	-	22.2	5.9	95.0	-	-	23.7	6.4	101.7	-	-	-
H 02	66	M	R	-	-	-	-	-	-	-	-	28.5	5.5	92.0	-	-	28.6	5.8	104.3	-	-	-
H 03	56	F	R	-	-	-	-	-	-	-	-	26.9	5.3	40.0	-	-	25.9	6.3	48.3	-	-	-
H 04	66	M	L	-	-	-	-	-	-	-	-	31.4	5.9	90.0	-	-	27.2	5.5	82.3	-	-	-
H 05	61	F	R	-	-	-	-	-	-	-	-	33.7	5.1	59.7	-	-	32.0	5.6	55.3	-	-	-
H 06	64	M	R	-	-	-	-	-	-	-	-	28.3	5.5	119.7	-	-	32.5	5.0	102.3	-	-	-
H 07	63	F	R	-	-	-	-	-	-	-	-	25.2	6.0	74.0	-	-	25.7	5.7	78.0	-	-	-
H 08	56	M	R	-	-	-	-	-	-	-	-	26.4	5.7	102.0	-	-	26.7	6.4	97.3	-	-	-
H 09	50	F	R	-	-	-	-	-	-	-	-	27.2	5.9	66.7	-	-	28.6	6.7	62.7	-	-	-
H 10	53	F	R	-	-	-	-	-	-	-	-	30.0	4.9	99.7	-	-	27.5	5.5	102.7	-	-	-
H 11	55	F	R	-	-	-	-	-	-	-	-	29.1	5.1	49.7	-	-	25.4	5.5	49.3	-	-	-
H 12	62	M	R	-	-	-	-	-	-	-	-	29.8	5.7	112.7	-	-	28.6	6.1	107.7	-	-	-
Mean	58.5											28.2	5.5	83.4			27.7	5.9	82.7			
SD	5.9											3.0	0.4	25.2			2.6	0.5	23.2			

% CST = percentage of the corticospinal tract (CST) which is affected by the lesion; ARAT = Action Research Arm Test; C = cTBS (inhibitory) applied to contralesional primary motor cortex; CIS = composite clinical impairment score; cTBS = continuous theta-burst stimulation; F = female; FT = maximum index finger tapping frequency; GF = maximum grip force; H = healthy control subject; I = iTBS (facilitatory) applied to ipsilesional primary motor cortex; iTBS = intermittent theta-burst stimulation; JTT = Jebsen Taylor hand function test; L = left; M = male; m = months; MIS = composite motor improvement score; mRS = modified Rankin Scale; NIHSS = National Institutes of Health stroke scale; P = stroke patient; R = right; SD = standard deviation; TBS = Theta-burst stimulation; Xi = iTBS (facilitatory) applied to control stimulation site; Xc = cTBS (inhibitory) applied to control stimulation site

5.2.2 Clinical impairment score (CIS)

We used three different scales to assess clinical impairment: (i) the modified Rankin scale (mRS), (ii) the National Institutes of Health Stroke Scale (NIHSS), and (iii) the Action Research Arm Test (ARAT). To compute a composite clinical impairment score, individual clinical scores were z-standardized using the following standard equation:

$$z_i = \frac{x_i - \bar{x}}{\sigma}$$

where x_i is the patient's individual value, \bar{x} the mean and σ the standard deviation across the group of patients. Z-standardized values were entered as input variables into a factor analysis with principal component extraction (principal component analysis, PCA). The PCA yielded a one-factor solution explaining 86% of the variance of mRS, NIHSS, and ARAT scores. All variables loaded highly on this factor (mRS = 93%; NIHSS = 91%; ARAT = -95%). Factor values of were calculated for each patient and defined as *clinical impairment score (CIS)* reflecting stroke-induced clinical deficits. Negative CIS values reflect less impairment than the average across the group of patients (Table 5.1).

5.2.3 Experimental design

In this study, we implemented a blinded sham-controlled within-subject design in which all patients received three different theta-burst stimulation (TBS) interventions on three different days separated by at least one day (to avoid carry-over effects). Electrophysiological and behavioural parameters were probed for each hemisphere/hand before and after each TBS session. Functional magnetic resonance imaging (fMRI) experiments were conducted in patients as well as healthy control subjects on a separate day before TBS sessions. Motor performance and electrophysiological TMS parameters at baseline were assessed once in healthy controls and overall five times in stroke patients to ensure stable baseline values. Clinical scales were obtained from patients (the time course of experimental procedures is given in Figure 5.2).

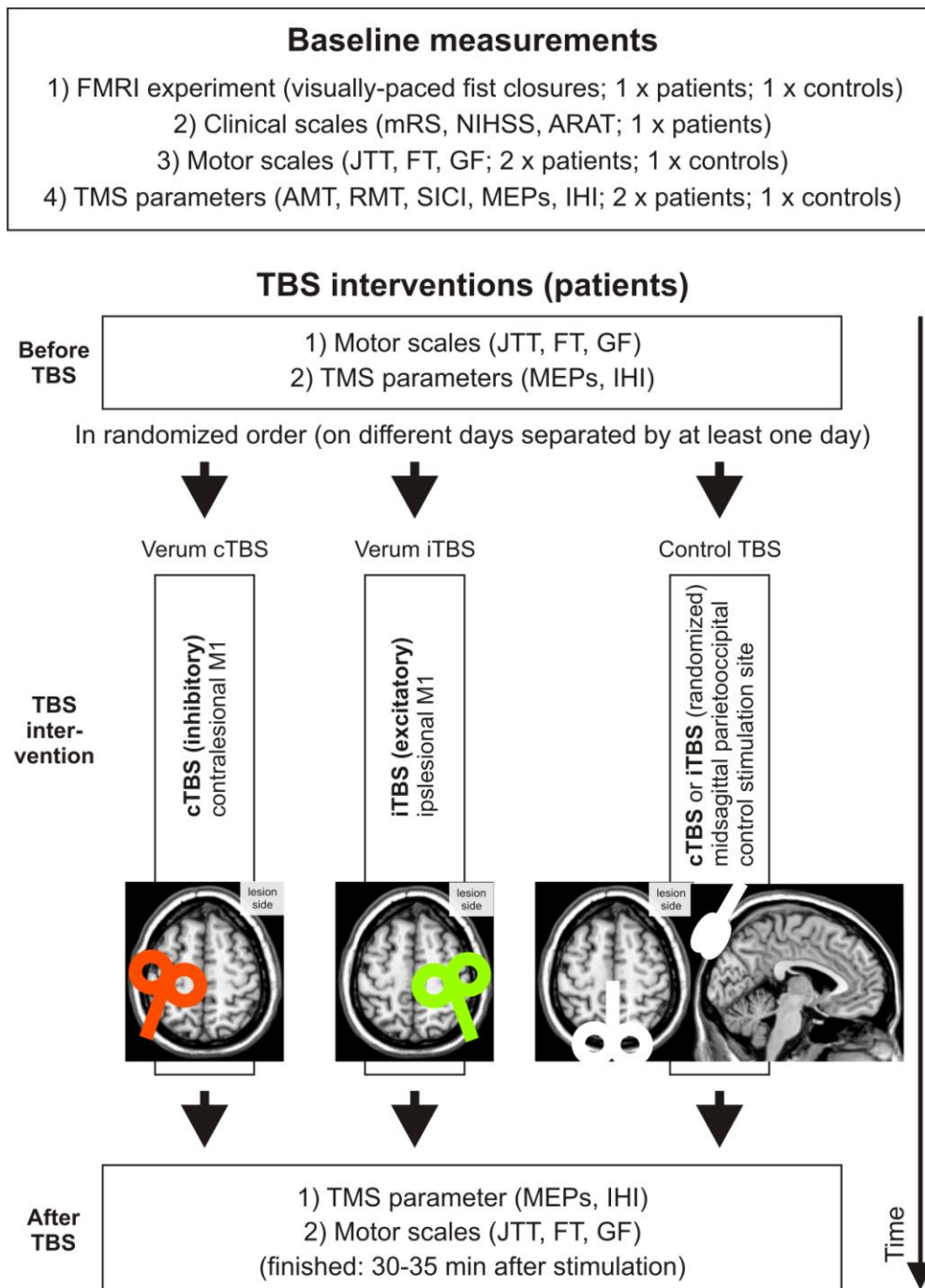


Figure 5.2: Study III: Experimental design of Study III. We implemented a blinded sham-controlled within-subject design in which 13 chronic stroke patients received three different theta-burst stimulation (TBS) interventions on three different days separated by at least one day: (i) inhibitory continuous TBS over the contralateral hemisphere, (ii) facilitatory iTBS over the ipsilesional hemisphere, and (iii) either cTBS or iTBS over the midsagittal parietooccipital control stimulation site (to control for placebo effects). Electrophysiological and behavioural parameters were probed before and after each TBS session for each hemisphere/hand. Baseline measurements including a functional magnetic resonance imaging (fMRI) experiment were conducted in patients as well as 12 age-matched healthy control subjects on a separate day. (AMT: active motor threshold; ARAT: Action Research Arm Test; FT: maximum index finger tapping frequency; GF: maximum grip force; IHI: interhemispheric inhibition; JTT: Jebsen-Taylor Hand Function Test; M1: primary motor cortex;

MEPs: motor-evoked potentials; mRS: modified Rankin scale; NIHSS: National Institutes of Health Stroke Scale; RMT: resting motor threshold; SICI: short-interval intracortical inhibition)

5.2.4 Theta-burst stimulation (TBS) interventions

The following TBS paradigms were applied in stroke patients: (i) facilitatory intermittent theta-burst stimulation (iTBS) applied to the ipsilesional M1, (ii) inhibitory continuous theta-burst stimulation (cTBS) applied to the contralesional M1, and (iii) control TBS applied to the midsagittal line half-way between vertex and protuberantia occipitalis externa (control TBS, Figure 5.2). Each TBS protocol comprised a total of 600 TMS pulses. The cTBS protocol consisted of 200 bursts (one burst refers to 3 pulses given at a frequency of 50 Hz) which were applied continuously at 5 Hz for 40 s. The iTBS protocol consisted of 10 bursts at 5 Hz applied every 10 s. Huang et al. (2005) demonstrated that iTBS may significantly increase motor cortex excitability for about 15 min, whereas cTBS may significantly suppress motor cortex excitability for nearly 60 min. The control stimulation was implemented to control for placebo effects and was either cTBS (n = 7 patients) or iTBS (n = 6 patients). Patients were randomly assigned to the cTBS or iTBS control stimulation group and the order of the three TBS interventions was pseudo-randomized across patients (Table 5.1). TBS was performed using a Magstim Super Rapid² stimulator connected to a standard 70 mm figure-of-eight TMS coil (Magstim, Whitland, U.K.) which was held tangentially to the scalp. The handle of the TMS coil was pointing posterior and approximately 45° away from the midsagittal line during iTBS and cTBS applied to M1 (i.e. verum TBS). Hence, the TMS-induced electric current in the brain was approximately perpendicular to the central sulcus which has been demonstrated to be optimal for excitation of motor neurons (Mills et al., 1992). During control stimulation, the handle of the TMS coil was pointing anterior and parallel to the midsagittal line. The stimulation intensity was defined in relation to the active motor threshold (AMT) and was identical for verum and control stimulation (i.e. 80% AMT). Hence, the control stimulation yielded similar tactile and auditory stimulation as the verum stimulation without stimulating motor areas. The AMT was determined at the motor hotspot position of the hemisphere to be stimulated. For control TBS, the AMT of the ipsilesional hemisphere was used (which is usually higher than the AMT of the contralesional hemisphere; Traversa et al., 2000). Since it has been suggested that muscle contraction before stimulation may reverse TBS effects (Gentner et al., 2008; Iezzi et al., 2008), the AMT was identified at least 10 min before TBS. Moreover, subjects were instructed to avoid any muscle contraction during TBS, which has

been suggested to abolish TBS effects (Huang et al., 2008), and until 5 min after TBS, which has been shown to increase facilitatory after-effects of iTBS but reverses after-effects of cTBS into facilitation (Huang et al., 2008). Muscle relaxation was monitored by online electromyography (EMG) recordings from the peripheral target muscle (i.e. the first dorsal interosseous (FDI) muscle).

5.2.5 TBS effects

TBS-induced effects outlasting the application period were probed on two different levels, i.e. on the behavioural level and on the electrophysiological level. Electrophysiological changes were assessed 5-25 min, and behavioural measurements 25-35 min after application of TBS. Note that in the study of Huang and colleagues (2005) reaction times were found to be significantly decreased 30 min after TBS.

5.2.5.1 Behavioural TBS effects

5.2.5.1.1 Motor tasks

Motor performances of the affected and the unaffected hand of stroke patients were assessed five times at baseline and after each of the three TBS sessions. Motor performance of healthy control subjects was obtained once at baseline. We implemented three different motor tasks to assess different aspects of motor performance: (i) grip force (GF) measurements, (ii) maximum index finger tapping (FT) frequency, and (iii) the Jebsen-Taylor Hand Function Test (JTT). Grip force (in kPa) was measured with a vigorimeter (Martin, Tuttlingen, Germany) in three consecutive trials. The mean across trials was calculated and used for further analyses. Subjects were asked to perform index finger tappings with maximum frequency on a computer keyboard. Mean index finger tapping frequencies (in Hz) across five consecutive blocks of 10 s were calculated and used for further analyses. The Jebsen Taylor Hand Function Test (JTT), mimicking object manipulations of everyday life, was implemented with the following six subtests: (1) turning cards, (2) picking up small objects, (3) spooning kidney beans, (4) stacking checkers, (5) picking up large light objects, and (6) picking up large heavy objects. The time needed to accomplish each subtest was taken with a millisecond precise stopwatch. A time frame of 30 s was given to accomplish each subtest (Jebsen et al., 1969). Some of the more severely impaired patients were not able to perform

all of the six subtests: Patient 04 was not able to perform subtest 2 and 3, Patient 05 was not able to perform subtest 3, and Patient 09 was not able to perform subtest 4. We performed outlier analyses on the five baseline measurements of stroke patients to ensure stable baseline values. Subtests were considered to contain severe outliers if the statistical variance exceeded the statistical mean value, i.e. if $\sigma^2/x > 1$ (where σ^2 is the variance and x is the subject's mean across baselines). Subtests with such high variance were regarded as unstable and were discarded from further analyses in the respective patient. This criterion was only exceeded for the affected hand and only in Patient 02 in subtests 2 and 4, in Patient 04 and Patient 07 in subtest 4, and in Patient 09 in subtest 2. Overall, a total of not more than 4.3% of JTT subtests was unavailable (1.9% due to inability to perform and 2.4% due to unstable performances). The time needed to accomplish all subtests with stable baselines was added up and used for further analyses.

5.2.5.1.2 Motor improvement score (MIS)

To investigate improvements in motor performance after verum compared to control TBS, a composite motor improvement score was calculated based on improvements in JTT, FT, and GF. Overall, four motor improvement scores were calculated for each patient: one for each hand (affected, unaffected) and verum TBS protocol (iTBS applied to ipsilesional M1, cTBS applied to contralesional M1). As a first step, improvements after each TBS session were expressed in percentage terms for each patient, hand, and motor task using the following formula:

$$x = \frac{(pre - post)}{pre} * 100 \%$$

where *pre* is the measured value before and *post* the measured value after TBS. Secondly, behavioural changes after verum TBS in relation to control TBS were calculated by subtracting the behavioural changes following control TBS (in percent) from behavioural changes following verum TBS (in percent). This was again performed for each patient, hand, and motor task. Finally, improvements after verum versus control TBS were z-standardized (cf. 5.2.2). Z-standardized values were entered as variables into factor analyses with principal component extraction (principal component analysis, PCA). Each PCA yielded a one-factor solution explaining 65-67% of the variance of changes in JTT, FT, and GF. All variables loaded positively on this factor (59-97%). Factor values were calculated for each patient and defined as *motor improvement score* (MIS) reflecting changes in general motor performance

following verum TBS compared to control TBS. Negative values reflect less improvement than the average across the group of patients (Table 5.1).

5.2.5.2 Electrophysiological TBS effects

Electrophysiological TBS effects were investigated using single-pulse and paired-pulse transcranial magnetic stimulation (TMS). Two parameters were obtained from both hemispheres before and after each TBS session: (i) motor-evoked potentials (MEPs) elicited by single-pulse supra-threshold TMS (reflecting excitability of the corticospinal motor system) and (ii) interhemispheric inhibition (IHI) between both motor hand representations probed by paired-pulse supra-threshold TMS. Additional TMS protocols were used to obtain electrophysiological parameters at baseline (as potential predictors for therapeutic TBS effects; see section 5.2.6 below).

5.2.6 Investigation of electrophysiological TMS parameters at baseline

Several electrophysiological (TMS) parameters were obtained at baseline and correlated with motor improvement scores (MIS) to investigate their predictive potential regarding therapeutic TBS effects in chronic stroke patients. The following electrophysiological TMS parameters were obtained from both hemispheres at baseline: (i) the resting motor threshold (RMT), (ii) the active motor threshold (AMT), (iii) the 1 mV motor threshold (1mV-MT), (iv) short-interval intracortical inhibition (SICI), and (v) interhemispheric inhibition (IHI).

5.2.6.1 TMS Apparatus

All electrophysiological TMS parameters were assessed with stereotaxic frameless neuronavigation by means of the eXimia NBS system version 3.2.1 (Nexstim, Helsinki, Finland). As the TMS stimulator of the eXimia NBS system cannot be used to apply TBS, the SuperRapid TMS stimulator (Magstim, Whitland, United Kingdom) was used for this purpose. Since assessment of IHI requires the simultaneous use of two TMS coils, and only one TMS coil at a time can be connected to the neuronavigated system, both TMS devices (Nexstim and Magstim) were used for assessment of IHI. A standard monophasic figure-of-eight coil (allowing application of paired-pulses via a single TMS coil) was used to measure SICI, whereas a standard biphasic figure-of-eight coil (allowing higher stimulation intensities)

was used for all other measurements (both TMS coils: Nexstim, Helsinki, Finland). A standard figure-of-eight TMS coil (Magstim, Whitland, United Kingdom) was connected to the Magstim stimulator. Prior to the study, all TMS coils were x-rayed. Displacements between central positions of the outer plastic case and the inner copper wings occurred solely in anterior-posterior direction and did not exceed 1 mm for any of the TMS coils. The neuronavigation software allows tracking of one TMS coil at a time. However, it can additionally track a digitization pen which is usually used for anatomical co-registration. We attached the digitization pen to the handle of the Magstim TMS coil by an in-house built fixation device which allowed maintaining tilting of the coil precisely during assessment of IHI. The correct anterior-posterior and lateral-medial positioning of the Magstim coil was maintained by a mark on the subjects head.

5.2.6.2 Electromyography (EMG) apparatus

Electromyography (EMG) signals were recorded by Ag/AgCl surface electrodes (Tyco Healthcare, Neustadt, Germany) placed in a belly-tendon montage over the left and right first dorsal interosseous (FDI) muscle. The EMG signal was amplified, filtered with a 0.5 Hz high pass filter and digitized using a ML856 PowerLab 26T Myograph and the “LabChart” software package version 6.0 (ADInstruments Ltd, Dunedin, New Zealand).

5.2.6.3 Anatomical co-registration

Subjects were comfortably seated in an adjustable armchair with head-rest. The head of the subject was spatially co-registered with the individual high-resolution anatomical MR image via anatomical landmarks (i.e. nasion and crus helcis of the ears). The root mean square difference between positions of landmarks in the MRI volume and at the subjects head was not more than 3 mm for any TMS session of the present study (information provided by the neuronavigation software).

5.2.6.4 TMS parameters at baseline

5.2.6.4.1 Motor hotspot and motor thresholds

After anatomical co-registration, the motor hotspot, i.e. the coil position providing highest MEPs of the contralateral FDI muscle during single-pulse supra-threshold TMS was

identified for each hemisphere. All electrophysiological TMS parameters were assessed at this hotspot position by means of an “aiming tool” implemented in the neuronavigation software which allows maintaining a certain coil position precisely. Overall, three motor thresholds were assessed: (i) RMT, (ii) AMT, and (iii) 1mV-MT. The RMT was defined as the minimum TMS stimulator output intensity required to produce an MEP (peak-to-peak amplitude $\geq 50 \mu\text{V}$) in at least 5 out of 10 consecutive trials in the contralateral FDI muscle at rest (Rossini et al., 1994). The AMT was defined as the minimum TMS stimulator output intensity required to produce an MEP (peak-to-peak amplitude $\geq 200 \mu\text{V}$) in at least 5 out of 10 consecutive trials from the contralateral FDI muscle while the subject was maintaining tonic voluntary contraction of $20 \pm 5 \%$ of maximum (Rossini et al., 1994). For this purpose, a hand dynamometer (ADInstruments, Ltd, Dunedin, New Zealand; Product Code: MLT003) was placed between the subject’s thumb and index finger and the subject’s individual maximum force was used to calibrate the signal allowing online visual feedback of the force applied on a screen in front of the subject. The 1mV-MT was defined as the TMS stimulator output intensity best suited to produce MEPs with peak-to-peak amplitudes close to 1 mV in the contralateral FDI muscle at rest.

5.2.6.4.2 Motor-evoked potentials (MEP)

Fifteen MEPs elicited by single-pulse TMS (inter-stimulus interval (ISI) = 7s) were recorded from the contralateral FDI at rest (i) at baseline and (ii) 5-15 min after TBS with similar stimulator output intensities determined at baseline (i.e. 100% 1mV-MT at baseline).

5.2.6.4.3 Short-interval intracortical inhibition (SICI)

SICI is a robust paired-pulse paradigm reflecting GABA_A-mediated intracortical inhibition within the primary motor cortex of one hemisphere (Kujirai et al., 1993; Ziemann 2004; cf. 1.4.3.1.1). In this protocol, a supra-threshold test stimulus (TS) is suppressed if a sub-threshold conditioning stimulus (CS) is applied 1-5 ms before the TS via the same TMS coil. The following parameters were applied: CS intensity: 80% AMT, TS intensity: 100% 1mV-MT, 2 ms interval between CS and TS, 7s interval between trials. Ten trials with single (TS) pulses and ten trials with paired (CS+TS) pulses were recorded in alternating order.

5.2.6.4.4 Interhemispheric inhibition (IHI)

IHI is a robust paired-pulse paradigm reflecting the primarily transcallosally mediated interhemispheric inhibition between the primary motor cortex of one hemisphere and the primary motor cortex of the contralateral hemisphere (Ferbert et al., 1992; cf. 1.4.3.2.1). In this protocol, the supra-threshold TS is suppressed if a supra-threshold CS is applied 7-50 ms before the TS on the contralateral hemisphere. Due to spatial restrictions resulting from the size of the two TMS coils we decided to apply TMS with the handle of the TMS coils pointing laterally (i.e. 90° away from the midline) which resulted in an electric field in medial direction induced in the brain tissue. The motor hotspot position and 1mV-MT was re-evaluated for each hemisphere with lateral-medial coil position. Chen et al. (2003) demonstrated that induced current direction of the CS does not impact on IHI if supra-threshold intensities are applied as in the present study. The following parameters were applied for IHI: CS and TS intensity: 1mV-MT of the respective hemisphere, interval between CS and TS: 10 ms, interval between trials: 7s. Ten trials with single (TS) pulses and ten trials with paired (CS+TS) pulses were recorded in alternating order for each direction (i.e. IHI from the ipsilesional onto the contralesional hemisphere and IHI from the contralesional onto the ipsilesional hemisphere).

5.2.6.4.5 Data analysis SICI and IHI

SICI and IHI were expressed as mean peak-to-peak amplitude in conditioned double pulse trials (CS+TS = 100%) relative to mean peak-to-peak amplitude of unconditioned single pulse trials (TS) recorded from the contralateral FDI at rest (CS: conditioning stimulus; TS: Test stimulus):

$$\text{SICI / IHI} = ((\text{TS} - (\text{CS} + \text{TS})) / \text{TS}) * 100\%$$

5.2.7 Functional magnetic resonance imaging (fMRI) at baseline

5.2.7.1 fMRI motor paradigm

We implemented a block design in which subjects were asked to perform visually paced rhythmic fist closures with their affected hand (corresponding to the non-dominant hand of healthy subjects) and their unaffected hand (corresponding to the dominant hand of healthy

subjects). Subjects were instructed to press MR compatible response grips positioned between proximal parts of the thumb and index finger. This experimental setup specifically facilitated movements of the FDI, which was used as target muscle for TMS. The software “Presentation” (Version 9.9, Neurobehavioral Systems, Inc., CA, www.neurobehavioralsystems.com) was used for visual stimulus presentation and movement recordings. Fist closures were performed at two different movement frequencies: (i) a fixed frequency of 0.8 Hz and (ii) a frequency individually adjusted to performance of the hand (40% of the maximum frequency). The fixed frequency condition was implemented to compare neural activity (between groups or hands) with similar absolute number of fist closures in one movement block resulting in, e.g., similar amount of re-afferent signal whereas the adjusted frequency condition was implemented to compare neural activity (between groups or hands) during movements with similar degree of difficulty (but different absolute number of fist closures). The maximum fist closure frequency of each hand was determined immediately before scanning when subjects resided in their final position for the experiment. Subjects were instructed to open and close their hand as fast as possible as soon as a “go” signal appeared until a “stop” signal was presented (after 10s) on a shielded thin-film transistor (TFT) screen at the rear end of the MR scanner. The procedure was repeated consecutively three times for each hand and the mean across three blocks was used as maximum movement frequency. The movement frequency was paced by a red blinking circle on white background presented on the same TFT screen which was visible via a mirror mounted on the MR head coil. Blocks of hand movements (15 s) were separated by resting baselines (13 s plus 0-1.5 s jitter) in which a black screen instructed the subjects to rest still until instructions were displayed for 1.5 s indicating which hand to move in the subsequent movement block. The order of conditions was pseudo-randomized and counterbalanced across the experiment which overall lasted about 18 min. Subjects were trained outside and again inside the scanner until they had reached stable performances (monitored by visual inspection). During the experiment, motor performance was monitored by an MR compatible camera in the scanner room.

5.2.7.2 fMRI data acquisition

MR images were acquired on a 3 Tesla Siemens MAGNETOM TimTrio scanner (Siemens, Erlangen, Germany). High-resolution anatomical *T1*-weighted images were acquired using the following imaging parameters: TR = 2000 ms, TE = 3.25 ms, FOV = 256 mm, 176 sagittal

slices, slice thickness = 1 mm, distance factor = 50%, in-plane resolution = $1 \times 1 \text{ mm}^2$, flip angle = 9° . In order to screen for brain lesions not visible on $T1$ -weighted images and for precise anatomical co-registration in further analysis, high-resolution anatomical $T2$ -weighted images were acquired using the following imaging parameters: TR = 5500 ms, TE = 113 ms, FOV = 220 mm, 48 axial slices, slice thickness = 2 mm, DF = 30%, in-plane resolution = $0.7 \times 0.7 \text{ mm}^2$, flip angle = 90° . For functional imaging a Gradient-Echo blood oxygenation level dependent (GRE-BOLD) EPI sequence with the following parameters was implemented: TR = 2070 ms, TE = 30 ms, FOV = 200 mm, 31 axial slices, slice thickness = 3.1 mm, in-plane resolution = $3.1 \times 3.1 \text{ mm}^2$, distance factor = 20 %, flip angle = 90° . Slices covered the brain from the vertex to lower parts of the cerebellum. Each fMRI session consisted of 537 EPI volumes preceded by three dummy scans ensuring a steady-state in tissue contrast.

5.2.7.3 fMRI data analysis

5.2.7.3.1 Preprocessing

Functional MRI data were analyzed using statistical parametric mapping (SPM8, <http://www.fil.ion.ucl.ac.uk/spm/>). Dummy scans were discarded from further analyses. EPIs from patients with left-sided lesions ($n = 3$) were mirrored at the midsagittal plane. To account for possible confounds arising from laterality effects, EPIs of three healthy subjects were likewise mirrored at the midsagittal plane. The “art_slice” tool, part of the SPM Artefact Repair toolbox (ArtRepair, <http://cibsr.stanford.edu/tools/ArtRepair/ArtRepair.htm>), was used to detect and repair outlier slices (the default threshold was applied to all subjects and resulted in well-tolerable 6.1% of slices being repaired). After spatial realignment of EPI volumes “art_global” was used to detect outlier volumes which either differed considerably in global intensity (i.e. variation in global intensity $> 1.3\%$) or exhibited high scan-to-scan motion (i.e. scan-to-scan motion $> 0.5 \text{ mm/TR}$) due to head movements. Outlier volumes were repaired by interpolation between the nearest non-repaired scans. In two patients and one healthy subject the default threshold had to be slightly increased (to 1.0 mm/TR) to prevent excessive data loss (resulting in well-tolerable 5.7% of volumes being repaired). To ensure good spatial co-registration with the anatomical $T1$ image, EPI volumes were first co-registered with the brain-extracted anatomical $T2$ image (which resembles EPI volumes in MR contrast) before applying the transformation matrix from brain-extracted $T2$ images to the brain-extracted $T1$ images. Lesion masks were created based on anatomical $T1$ images using

MRICron (<http://www.cabiatl.com/mricro/mricron/>). EPIs were spatially normalized to the standard template of the Montreal Neurological Institute (MNI152_T1_2mm) with masked lesions and spatially smoothed with an isotropic Gaussian kernel of 8 mm full-width at half-maximum to compensate for residual variability across subjects after spatial normalization.

5.2.7.3.2 Statistical analysis

For first-level analyses, box-car vectors for each of the four conditions (two for each movement frequency and hand) were convolved with the canonical hemodynamic response function in the framework of a general linear model (GLM). A high-pass filter of 1/300 s (i.e. slightly longer than the maximum interval between two blocks of the same condition) was applied to remove low-frequency drifts in MR signal.

5.2.7.4 Region-of-interest (ROI) analysis

We conducted region-of-interest (ROI) analyses to investigate whether fMRI BOLD signal in motor areas predicted behavioural TBS effects. For this purpose, the first eigenvariate from the time series of voxels surrounding the individual local maximum (in an 8 mm diameter sphere) was extracted from the first-level GLM analysis using the SPM toolbox “MarsBaR” (<http://marsbar.sourceforge.net/>). This procedure was performed for all four conditions and three motor areas per hemisphere, i.e. the primary motor cortex (M1), the ventral premotor cortex (vPMC), and the supplementary motor area (SMA).

5.2.7.5 Laterality index (LI)

To investigate whether laterality of fMRI BOLD signal predicted behavioural response to TBS, we calculated an laterality index (LI) which was first introduced by Cramer et al. (1997) and later used by several stroke fMRI studies as a measure of lateralization of fMRI signal (Carey et al., 2002; Johansen-Berg et al. 2002; Marshall et al., 2000). LI was calculated using the following formula:

$$LI = \frac{CL - IL}{CL + IL}$$

where CL (contralesional) is the number of significantly activated voxels in Brodmann Area (BA) 4 and BA6 of the contralesional/dominant hemisphere and IL (ipsilesional) is the number of voxels in BA4 and BA6 of the ipsilesional/non-dominant hemisphere passing a threshold of $P < 0.001$ (uncorrected). BA4 and BA6 were defined by means of the human post-mortem cytoarchitectonic probability atlas provided by the SPM “Anatomy” toolbox (Eickhoff et al., 2005, 2007; http://www.fz-juelich.de/inm/inm-1/spm_anatomy_toolbox). Positive LI values indicate that the fMRI activation pattern is lateralized towards the contralesional/dominant hemisphere, whereas negative LI values indicate an fMRI activation pattern lateralized towards the ipsilesional/non-dominant hemisphere, and LI values close to zero indicates absence of lateralization. LIs were calculated for each subject and condition based on individual first-level analyses.

5.2.7.6 Dynamic Causal Modelling (DCM)

DCM is a hypotheses-driven approach to model effective connectivity between distinct brain regions, and relies on neurobiologically plausible a priori assumptions regarding hypotheses on relevant brain regions, connections, and context dependent modulations thereof (Friston et al., 2003; cf. 1.6). We performed analyses on core regions of the motor system activated by the fist closure task, namely the primary motor cortex (M1), the ventral premotor cortex (vPMC), and the supplementary motor area (SMA) as well as the striatal and extrastriatal primary visual cortex (V1, as major input region since fist closures were paced by visual cues) bilaterally. BOLD time series were extracted for each of these eight ROIs in first-level fMRI analyses (sphere 8 mm in diameter around the individual activation maximum; see section *Region-of-interest (ROI) analysis* and Table 5.2). ROIs did not overlap with each other nor did they overlap with stroke lesions. Stroke lesions did also not directly interrupt connections between ROIs as inferred from *T1*-weighted images. We first used the fMRI group analysis to define group coordinates (separately for patients and controls) for each region in MNI space. These group coordinates were then used as starting positions for the search of the closest local maximum in the individual SPM map meeting the a priori defined anatomical constraints. The following anatomical landmarks were used: (i) M1: in the rostral wall of the central sulcus at the “hand knob” formation (Yousry et al., 1997), (ii) SMA: in the medial wall of the interhemispheric fissure between the paracentral lobule (posterior margin), the coronal plane cutting the anterior commissure (y-coordinates < 0 , anterior margin), and the cingulate sulcus (inferior margin, Picard & Strick 2001), (iii) vPMC: close to the inferior precentral gyrus and

pars opercularis (Rizzolatti et al., 2002). Invasive tracer studies in macaque monkeys demonstrated that homotopic as well as heterotopic connections between M1, SMA, and PMC exist (McGuire et al., 1991; Rouiller et al., 1994). As we assumed that these connections exist in humans as well, they represent the most likely anatomical (i.e. endogenous) connectivity model (Figure 5.3, upper left corner). Aside from endogenous (i.e. task-independent) coupling, we also investigated how effective connectivity within the network was modulated by fist closures with different movement frequencies. These “task-dependent” modulations do not necessarily impact on all endogenous connections. We therefore constructed 36 different connectivity models (Figure 5.3–5.5) reflecting biologically plausible hypotheses on interregional coupling.

Study III: Prediction of TBS effects

Table 5.2: Study III: Peak voxel coordinates used for region-of-interest (ROI) analyses and dynamic causal modelling (DCM)

Subject	V1 left			V1 right			SMA left			SMA right			vPMC left			vPMC right			M1 left			M1 right		
	X	Y	Z	X	Y	Z	X	Y	Z	X	Y	Z	X	Y	Z	X	Y	Z	X	Y	Z	X	Y	Z
P 01	-14	-100	2	16	-98	-8	-4	-4	74	4	-6	66	-56	0	42	60	0	42	-48	-22	58	36	-24	58
P 02	-16	-100	-10	16	-98	-14	-4	-2	62	6	-8	68	-52	-4	32	52	2	40	-30	-32	60	38	-32	58
P 03	-16	-100	-8	14	-96	-12	-4	2	56	4	-2	60	-52	-8	50	54	-2	46	-38	-22	60	34	-30	70
P 04	-22	-96	4	14	-84	-14	-6	-18	50	10	-6	68	-58	-10	38	58	-6	44	-44	-30	58	36	-28	48
P 05	-30	-92	2	34	-82	0	-6	-12	56	4	-2	74	-54	4	42	62	6	24	-36	-20	66	32	-22	72
P 06	-10	-96	-16	10	-90	-14	-4	-4	62	6	-14	62	-52	-2	34	56	0	34	-42	-32	56	36	-30	58
P 07	-24	-98	2	34	-90	2	-10	-4	66	4	0	68	-62	8	42	58	2	40	-46	-22	60	44	-20	70
P 08	-20	-96	10	28	-92	0	-12	-2	58	4	-10	62	-48	-2	36	58	4	44	-42	-32	58	36	-26	62
P 09	-12	-102	-2	22	-84	-8	-8	-12	58	4	-8	60	-56	0	38	40	20	36	-44	-28	66	36	-18	68
P 10	-22	-94	-2	20	-96	6	-4	-18	70	6	-16	58	-52	-12	46	56	2	40	-36	-34	58	34	-36	50
P 11	-22	-102	4	28	-94	0	-4	-12	64	6	-10	58	-60	6	32	58	6	34	-42	-34	64	40	-34	64
P 12	-18	-98	4	10	-96	2	-8	-8	64	4	-6	66	-44	8	34	60	2	36	-36	-32	74	40	-26	70
P 13	-18	-92	0	30	-88	-8	-4	-10	60	8	-10	62	-58	14	30	54	-10	44	-34	-34	70	40	-30	58
Mean	-18.8	-97.4	-0.8	21.2	-91.4	-5.2	-6.0	-8.0	61.5	5.4	-7.5	64.0	-54.2	0.2	38.2	55.8	2.0	38.8	-39.8	-28.8	62.2	37.1	-27.4	62.0
SD	5.4	3.4	7.0	8.7	5.6	7.1	2.7	6.3	6.3	1.9	4.6	4.8	4.9	7.7	6.0	5.5	7.0	6.0	5.3	5.3	5.4	3.2	5.4	7.8
H 01	-16	-102	-6	20	-96	2	-4	-10	62	8	-8	70	-52	0	32	56	14	40	-42	-34	66	42	-28	58
H 02	-26	-90	-12	20	-100	-2	-6	-4	74	6	-4	62	-48	10	40	56	2	42	-42	-28	62	52	-16	60
H 03	-20	-92	-8	16	-94	-2	-8	-12	68	6	-14	70	-62	10	36	56	8	40	-54	-26	64	40	-28	60
H 04	-24	-96	4	28	-94	-2	-4	-8	66	6	-12	60	-52	0	36	56	0	46	-40	-24	66	44	-26	58
H 05	-24	-96	-4	22	-92	-2	-6	-10	62	4	-8	68	-52	10	44	54	6	44	-42	-26	70	36	-28	58
H 06	-22	-90	2	30	-90	0	-8	-12	66	12	-12	66	-58	6	40	56	0	44	-36	-26	56	46	-28	60
H 07	-16	-96	2	24	-94	2	-10	-6	74	6	-8	66	-54	-4	48	56	-2	48	-42	-22	66	46	-20	62
H 08	-28	-92	-2	26	-94	2	-6	-18	70	4	-2	68	-62	-2	38	58	6	46	-42	-30	54	40	-28	58
H 09	-16	-102	6	18	-92	0	-8	-12	64	6	-6	72	-56	2	38	64	6	34	-40	-26	64	38	-26	64
H 10	-26	-98	2	32	-92	4	-6	-6	66	4	-2	72	-56	6	42	54	14	42	-38	-26	56	36	-24	70
H 11	-20	-96	-2	28	-92	6	-10	-14	68	6	-12	62	-54	-2	44	54	0	46	-42	-32	58	38	-28	56
H 12	-24	-98	4	24	-94	-2	-6	2	62	6	-6	74	-54	0	42	56	-2	48	-38	-28	66	48	-14	62
Mean	-22.3	-96.5	-0.3	23.8	-92.8	0.0	-6.7	-9.5	65.2	6.3	-7.7	69.3	-55.3	2.2	39.7	56.0	5.7	43.0	-43.0	-27.0	62.0	40.2	-25.3	60.5
SD	4.1	3.6	4.2	4.8	1.8	4.1	2.0	5.3	2.8	2.2	4.1	4.8	3.4	4.2	3.7	3.5	5.4	4.1	4.6	3.7	4.8	3.7	4.0	3.8

H = healthy control subject; M1 = primary motor cortex; P = stroke patient; SD = standard deviation; SMA = supplementary motor area; V1: primary visual cortex; vPMC = ventral premotor cortex; X = lateral-medial, Y = anterior-posterior, Z = inferior-superior coordinate in MNI (Montreal Neurological Institute) standard space

Study III: Prediction of TBS effects

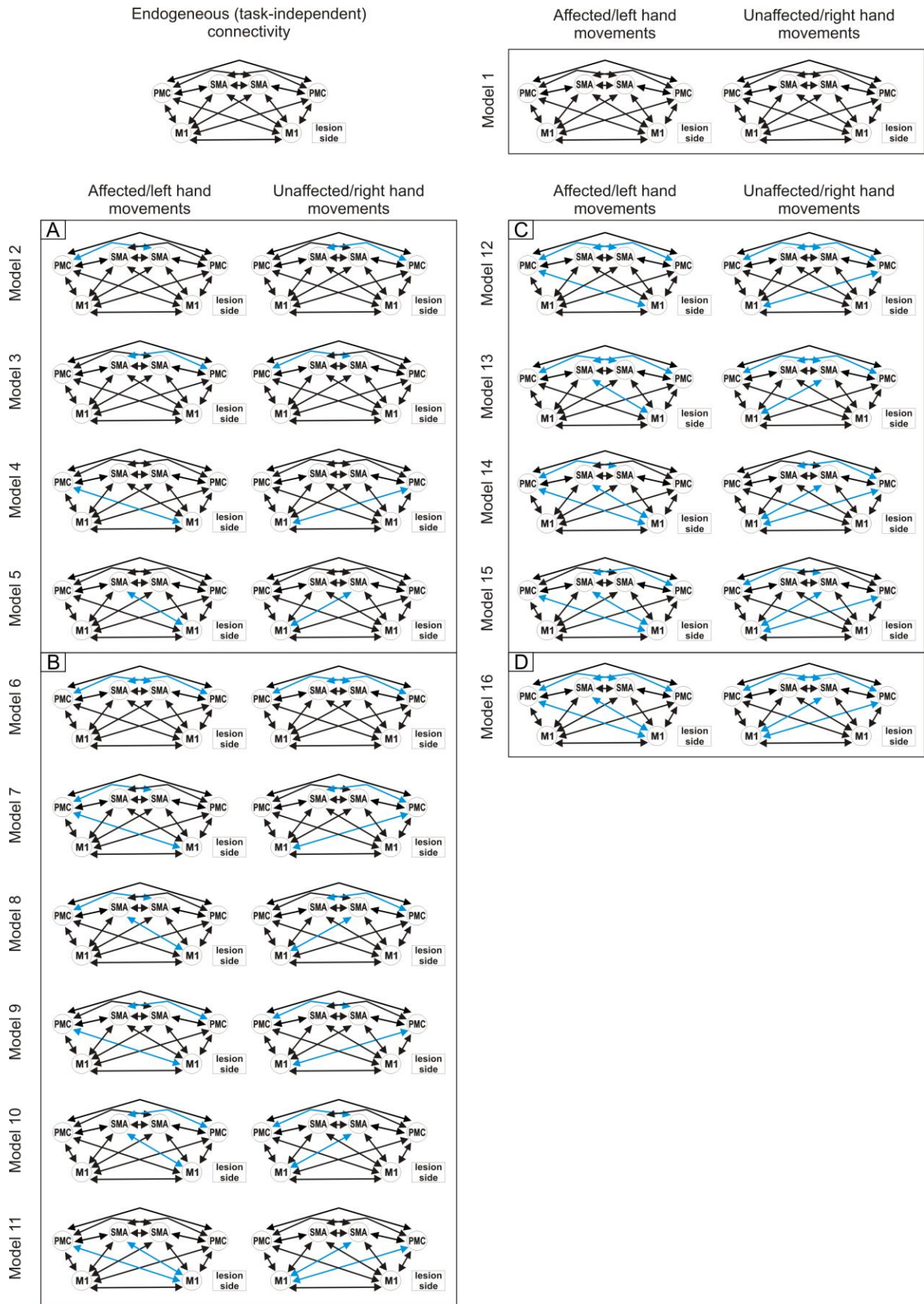


Figure 5.3 - Figure 5.5: Study III: Hypothetical models on interregional coupling. Dynamic causal modelling (DCM) is a hypotheses-driven approach to model effective connectivity between distinct brain regions, and relies on neurobiologically plausible a priori assumptions regarding hypotheses on relevant brain regions, connections, and context dependent modulations thereof (Friston et al., 2003). We performed analyses on core regions of the motor system activated by the fist closure task, namely the primary motor cortex (M1), the ventral premotor cortex (vPMC), and the supplementary motor area (SMA). The primary visual cortex (V1) was used as major input region (not shown). Based on anatomical studies in macaque monkeys (McGuire et al., 1991; Rouiller et al., 1994), reciprocal connections between all six cortical motor areas (M1, SMA, and vPMC bilaterally), can be assumed and hence represent the most likely anatomical (i.e. endogenous) connectivity model (depicted in the upper left corner). “Task-dependent” modulations do not necessarily impact on all endogenous connections. Therefore, we constructed 36 different connectivity models reflecting biologically plausible hypotheses on interregional coupling. We then used random effects Bayesian model selection (BMS) to identify the model with highest evidence given the measured data (Stephan et al., 2009).

Figure 5.3: Study III: Hypothetical models on interregional coupling (Models 1-16). The first model (Model 1) assumed all possible connections between all six cortical motor areas (i.e. 30 connections; upper right corner). Based on this model, connections were systematically varied by subsequently omitting one (Figure 5.3A), two (Figure 5.3B), three (Figure 5.3C) or four (Figure 5.3D) interhemispheric connections. Blue arrows indicate omitted connections. Black arrows indicate remaining connections.

Study III: Prediction of TBS effects

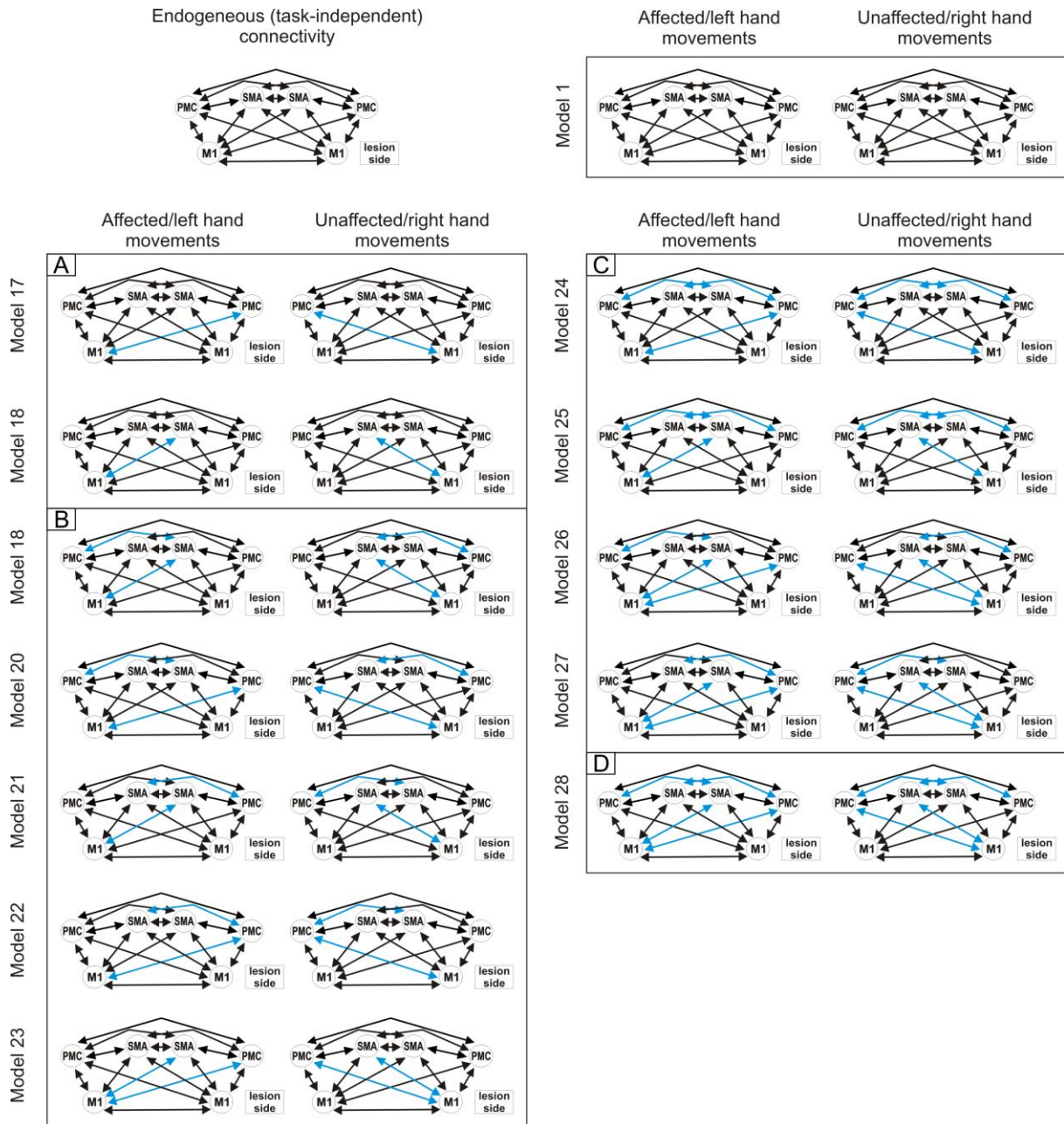


Figure 5.4: Study III: Hypothetical models on interregional coupling (Models 17-28). The first model (Model 1) assumed all possible connections between all six cortical motor areas (i.e. 30 connections; upper right corner). Based on this model, connections were systematically varied by subsequently omitting interhemispheric connections (Models 1-16 in Figure 5.3). All models which assumed asymmetric interregional coupling were mirrored on the midsagittal line (Model 17-28 in the present figure) if the mirrored counterpart was not already included in Figure 5.3. Blue arrows indicate omitted connections. Black arrows indicate remaining connections.

Study III: Prediction of TBS effects

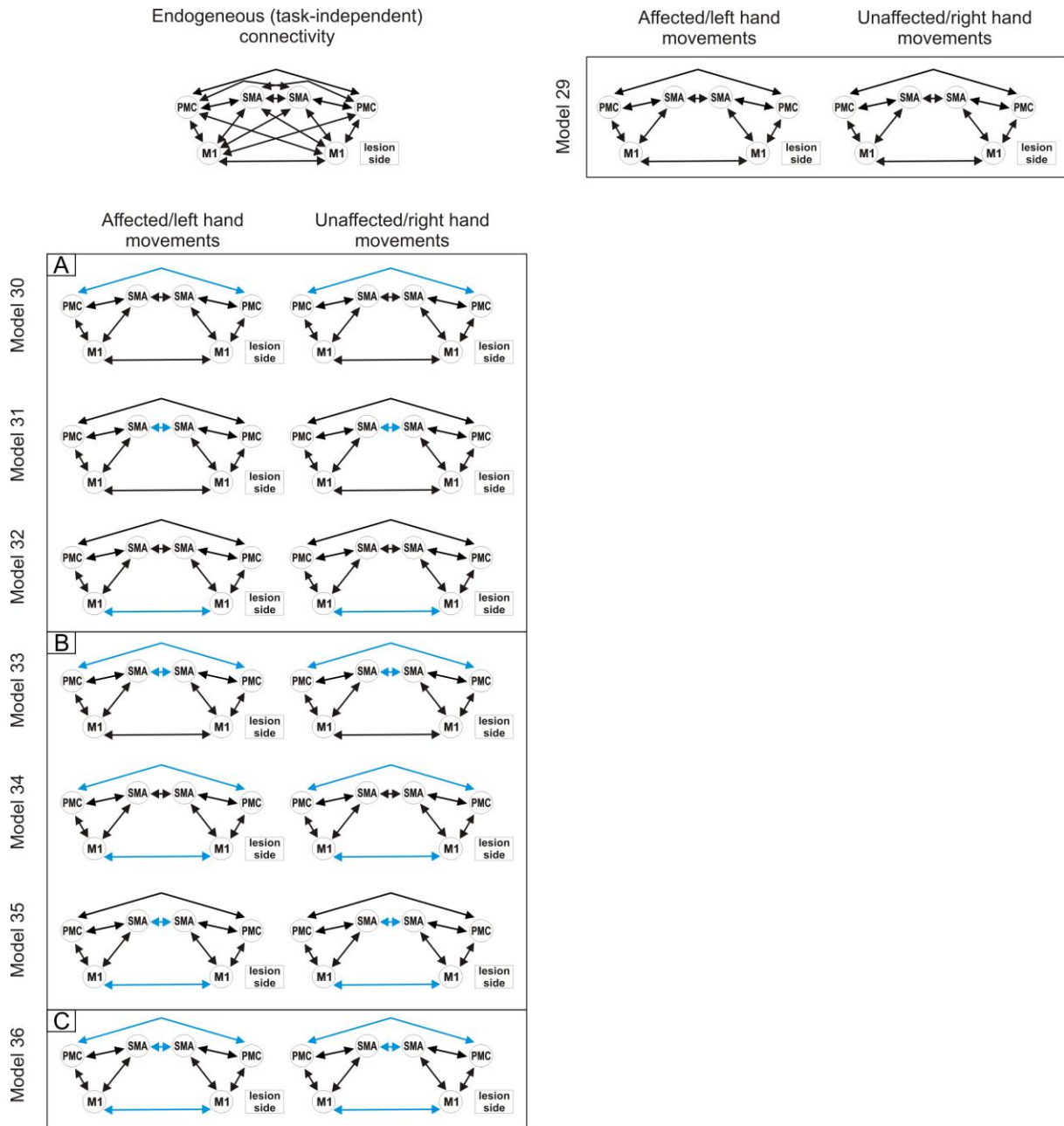


Figure 5.5: Study III: Hypothetical models on interregional coupling (Models 29-36). A less complex model with reciprocal intrahemispheric connections between all three regions and interhemispheric connections between homologous regions was constructed (Model 29; Figure 5.5, upper right corner) and modified by omitting one (Figure 5.5A), two (Figure 5.5B) or all three (Figure 5.5C) interhemispheric connections. Blue arrows indicate omitted connections. Black arrows indicate remaining connections.

The first model (Model 1) assumed all possible connections between all six cortical motor areas (i.e. 30 connections; Figure 5.3 & 5.4, upper right corner). Based on this model, connections were systematically varied by subsequently omitting one (Figure 5.3A), two (Figure 5.3B), three (Figure 5.3C) or four (Figure 5.3D) interhemispheric connections. All models assuming asymmetric interregional coupling were mirrored on the midsagittal line (Figure 5.4) if the mirrored counterpart was not already tested (Figure 5.3). Finally, a less complex model assuming only reciprocal intrahemispheric connections between all three regions and interhemispheric connections between homologous regions was tested (Model 29; Figure 5.5, upper right corner) and modified by omitting one (Figure 5.5A), two (Figure 5.5B) or all three (Figure 5.5C) interhemispheric connections. For all models we assumed that V1 exerts a driving influence onto all premotor areas (i.e. SMA and vPMC bilaterally) as hand movements were paced by a visual cue during fMRI experiments. We then used random effects Bayesian model selection (BMS) to identify the model with highest evidence given the measured data (Stephan et al., 2009).

5.2.8 Effects of lesion location, lesion size, and lesion age

We performed voxel-based lesion symptom mapping (VLSM) analyses by means of MRICron (<http://www.cabiatl.com/micro/micron/install.html>) to investigate the relationship between lesion locations and behavioural TBS effects (Bates et al., 2003; Rorden et al., 2007). Binary lesion masks were constructed based on the high-resolution anatomical *T1*-weighted image of each patient and normalized to MNI space by applying the deformation parameters derived from normalization of the respective *T1*-weighted image into MNI space by means of SPM8. Patients were classified into two groups based on a median split of TBS improvement scores ($n = 7$ patients with scores equal to or less than the median were assigned to the TBS non-responder group; $MIS_{\text{aff}, i\text{TBS}} \leq 0.017$, $MIS_{\text{aff}, c\text{TBS}} \leq -0.128$, $MIS_{\text{unaff}, i\text{TBS}} \leq -0.141$, and $MIS_{\text{unaff}, c\text{TBS}} \leq -0.214$). Behavioural improvements were entered as binary behaviour (responder = 1; non-responder = 0) in separate analyses. Lieberman analysis was performed (which is a more sensitive binomial test than Chi-Squared or Fisher's Exact test; <http://www.cabiatl.com/micro/micron/stats.html>). Additionally, behavioural TBS effects were correlated with lesion characteristics such as lesion size, lesion age, and CST damage. CST damage was defined as overlapping volume between the individual MNI-normalized lesion mask and the probabilistic CST map implemented in the SPM "Anatomy" toolbox

(Eickhoff et al., 2005, 2007; http://www.fz-juelich.de/inm/inm-1/spm_anatomy_toolbox) in relation to total CST volume (Table 5.1).

5.2.9 Statistical analyses

All statistical analyses were performed using the “PASW” software version 18 (<http://www.spss.com>). If not stated otherwise, effects in ANOVAs were considered statistically significant if they passed a threshold of $P < 0.05$. Results from post-hoc t-tests and bivariate Spearman’s ρ correlation analyses were considered statistically significant if they passed a threshold of $P < 0.05$, false discovery rate (FDR)-corrected for multiple comparisons (Benjamini & Hochberg, 1995). Independent-sample t-tests for group comparisons were considered statistically significant if they passed a threshold of $P < 0.05$, corrected with Dunn’s Multiple Comparison Procedure (Dunn, 1961).

5.3 Results Study III

5.3.1 Motor impairment in stroke patients

We performed repeated measures ANOVAs with the factors GROUP (levels: patients, healthy controls) and HAND (levels: affected/non-dominant, unaffected/dominant) for all three motor tasks. There was a significant HAND x GROUP interaction for each task: (i) the Jebsen Taylor Hand Function Test (JTT): $F(1, 23) = 8.751$; $P = 0.007$, (ii) maximum index finger tapping (FT) frequency: $F(1, 23) = 12.714$; $P = 0.002$, and (iii) grip force (GF) measurements: $F(1, 23) = 13.055$; $P = 0.001$. Post-hoc t-tests revealed that stroke patients performed significantly worse with their affected hand compared to healthy subjects performing with their non-dominant hand (JTT: $T(23) = 3.490$; FT: $T(23) = -7.054$, GF: $T(23) = -2.321$; $P < 0.05$, Dunn-corrected). Hence, stroke patients had significant motor hand deficits which were apparent in all three motor tasks that were used as behavioural outcome measures for TBS effects.

5.3.2 TBS effects

5.3.2.1 Behavioural TBS effects

TBS was well tolerated by all patients. There were no adverse events. We performed repeated measures ANOVAs with the factor INTERVENTION (levels: iTBS, cTBS, control TBS) on percentage improvements of each hand (affected, unaffected) and task (JTT, FT, GF). None of the ANOVAs yielded a significant main effect of INTERVENTION ($P > 0.05$). This finding indicates that neither facilitatory iTBS applied to the ipsilesional hemisphere nor inhibitory cTBS applied to the contralesional hemisphere was significantly different from control TBS (over the midsagittal parieto-occipital cortex) in terms of average changes in motor performance of the affected hand across the whole group of patients (Figure 5.6). However, there was a statistical trend for finger tapping of the unaffected hand ($F(2, 24) = 3.354$; $P = 0.052$). Post-hoc t-tests suggested that this trend resulted from decreased performance of the unaffected hand after inhibitory cTBS applied to the contralesional hemisphere ($T(12) = 2.416$, $P = 0.033$, uncorrected) as well as facilitatory iTBS applied to the ipsilesional hemisphere ($T(12) = 2.134$; $P = 0.054$, uncorrected) compared to control stimulation. Analyses performed on absolute improvements (instead of improvements in percentage terms) yielded similar results. These findings suggest that the unaffected hand responded to verum TBS as proposed by the *model of interhemispheric competition* (i.e. with deterioration) whereas the affected hand did not show consistent improvements over the group of patients. However, there was considerable inter-individual variance in behavioural changes following TBS. For example, changes of the affected hand in the JTT ranged between -18.7 and +15.4 % (mean: -0.9 ± 11.2 %) after iTBS and between -23.3 and +19.9 % (mean: -0.8 ± 10.1 %) after cTBS.

Behavioural TBS effects

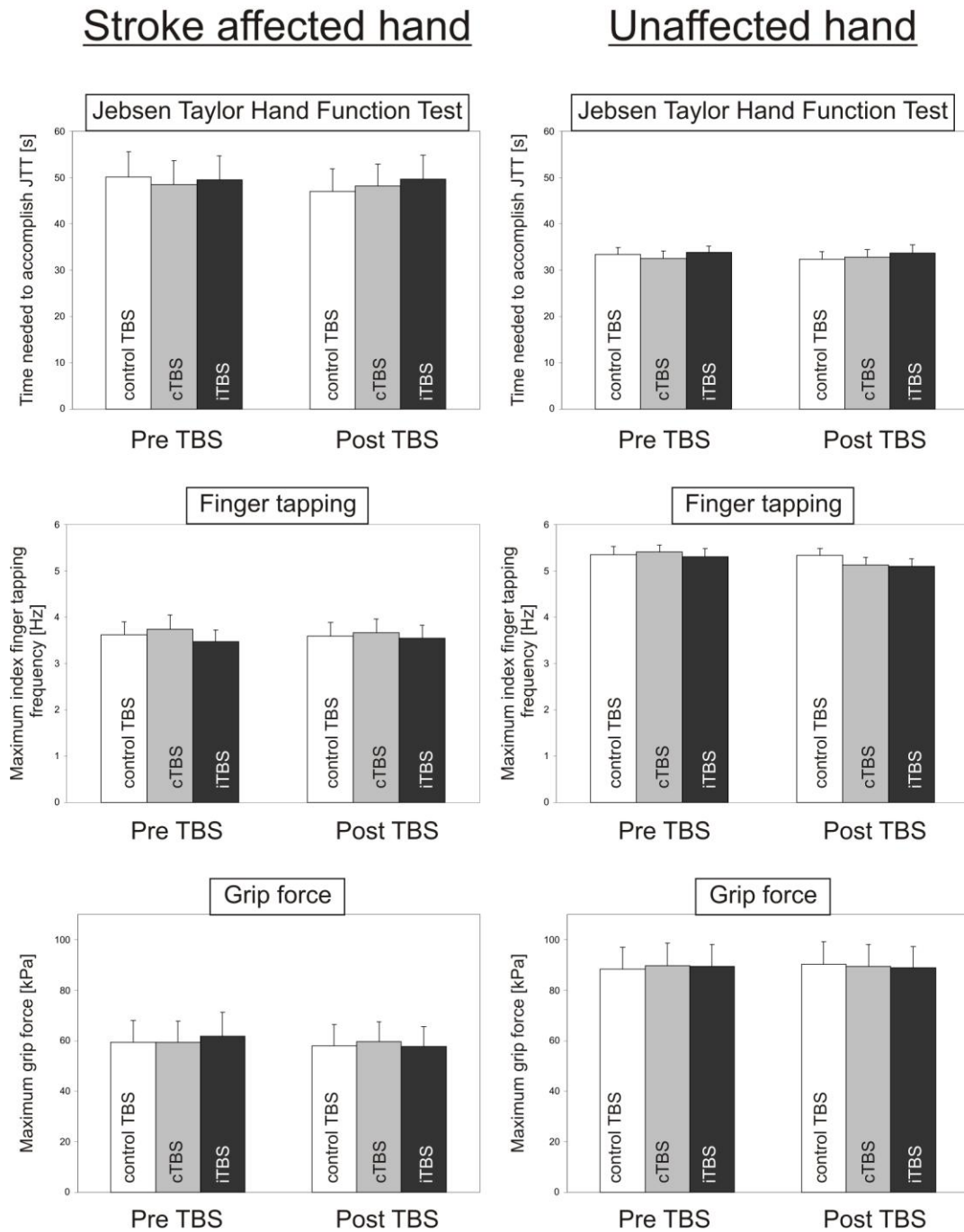


Figure 5.6: Study III: Changes in motor performance following theta-burst stimulation (TBS). Motor performance of the affected hand (left column) and the unaffected hand (right column) was measured before (Pre TBS) and approximately 25 min after (Post TBS) three different TBS interventions in 13 chronic stroke patients: (i) control stimulation, (ii) inhibitory continuous TBS over the contralesional hemisphere, and (iii) facilitatory iTBS over the ipsilesional hemisphere. The following parameters were used to assess motor performance: (i) the time needed to accomplish the Jebsen-Taylor Hand Function Test [s], (ii) the maximum index finger tapping frequency [Hz], and (iii) the maximum grip force [kPa]. Vertical bars reflect the group mean and error bars indicate the standard error of the mean.

Neither facilitatory iTBS applied to the ipsilesional hemisphere nor inhibitory cTBS applied to the contralesional hemisphere was significantly different from control TBS in terms of average changes in motor performance of the affected hand. There was a statistical trend for reduced index finger tapping frequency of the unaffected hand after both inhibitory cTBS applied to the contralesional hemisphere as well as facilitatory iTBS applied to the ipsilesional hemisphere compared to control stimulation. Hence, the unaffected hand responded to verum TBS as hypothesized (i.e. with deterioration) whereas the affected hand did not show consistent improvements over the group of patients.

5.3.2.2 Electrophysiological TBS effects

In line with behavioural TBS effects, there were no significant differences between TBS interventions in terms of average electrophysiological changes across the group of patients. Repeated measures ANOVAs with the factor INTERVENTION (levels: iTBS, cTBS, control TBS) were separately performed on percentaged changes in each TMS parameter (MEP size on each hemisphere and reciprocal IHI). None of the ANOVAs yielded a significant effect of INTERVENTION ($P > 0.05$). In other words, verum TBS was not significantly different from control TBS in terms of average changes in IHI or MEP size of the ipsilesional hemisphere over the group of patients. However, there was a statistical trend for MEPs of the contralesional hemisphere ($F(2, 24) = 3.399$; $P = 0.052$). Post-hoc t-tests suggested that this trend resulted from decreased MEP sizes elicited from the contralesional hemisphere after inhibitory cTBS applied to the contralesional hemisphere ($T(12) = 1.986$; $P = 0.070$, uncorrected) as well as facilitatory iTBS applied to the ipsilesional hemisphere ($T(12) = 2.675$, $P = 0.022$, uncorrected) compared to control stimulation. Analyses performed on absolute changes (instead of changes in percentage terms) yielded similar results. Hence, electrophysiological TBS effects are in line with behavioural TBS effects and suggest that the contralesional hemisphere responded to verum TBS as expected (i.e. with decreased excitability) whereas the ipsilesional hemisphere did not show consistent increases in MEP size over the group of patients. Similar to analyses on behavioural effects, there was considerable inter-individual variance in electrophysiological changes following TBS. For example, changes in MEP size of the ipsilesional hemisphere ranged between -91.8 and +56.5 % (mean: 15.8 ± 65.8 %) after iTBS and between -30.1 and +90.5 % (mean: 16.8 ± 39.2 %) after cTBS.

5.3.2.3 Correlation between behavioural and electrophysiological TBS effects

To investigate whether behavioural TBS effects were related to electrophysiological TBS effects, we correlated improvement scores of cTBS and iTBS with changes in MEP size of both hemispheres and reciprocal IHI. None of the correlations suggested a significant interaction ($P > 0.05$). Hence, although there was a tendency for decreased motor performance of the unaffected hand and decreased MEP size of the contralesional hemisphere after verum TBS, there was no tight relationship between behavioural and electrophysiological TBS effects. This finding suggests that changes observed on the electrophysiological level and changes observed on the behavioural level were not driven by the same subjects.

5.3.2.4 Summary behavioural and electrophysiological TBS effects

In summary, stroke patients had significant motor hand deficits which were evident in all three motor tasks used as outcome measures for behavioural TBS effects. Neither facilitatory iTBS applied to the ipsilesional hemisphere nor inhibitory cTBS applied to the contralesional hemisphere was significantly different from control TBS in terms of average behavioural or electrophysiological changes across the whole group of patients. However, there was a statistical trend for decreased motor performance of the unaffected hand and decreased MEP size of the contralesional hemisphere after cTBS and iTBS compared to control TBS. Hence, the unaffected hand and contralesional hemisphere responded to verum TBS as expected whereas the affected hand and ipsilesional hemisphere did not show consistent changes which was probably due to high inter-individual variability. There was no tight relationship between behavioural and electrophysiological TBS effects suggesting that changes on the behavioural level originated from different patients than changes on the electrophysiological level.

5.3.3 Electrophysiological TMS parameters

5.3.3.1 TMS parameters - differences between groups

To investigate whether stroke patients differed significantly from healthy subjects in terms of TMS electrophysiology at baseline, we computed repeated measures ANOVAs with the factors HEMISPHERE (levels: ipsilesional/non-dominant, contralesional/dominant) and GROUP (levels: patients, healthy subjects) separately for each TMS parameter (AMT, RMT, SICI, IHI). To investigate whether TMS parameters at baseline relate to clinical deficit and

lesion characteristics we correlated TMS parameters with clinical scores (mRS, NIHSS, ARAT), clinical impairment score (CIS), lesion size, lesion age, and CST damage.

5.3.3.1.1 Active and resting motor threshold (AMT & RMT)

ANOVAs on AMT and RMT yielded no significant main effect or interaction ($P > 0.05$) indicating that cortical excitability was not significantly different across the whole group of patients compared to healthy controls. There was a statistical trend for a correlation between AMT assessed over the ipsilesional hemisphere and ARAT scores ($r = -0.543$; $P = 0.055$, uncorrected) indicating that patients with reduced ipsilesional M1 excitability featured more impairment of upper-limb function. To investigate whether motor thresholds differed between mildly and more severely impaired patients we assigned patients to two groups based on a median split of ARAT scores (median of ARAT scores = 50; $n = 7$ patients with ARAT scores ≤ 50 were assigned to the group of more severely impaired patients). Independent-sample t-tests revealed that motor thresholds of the ipsilesional hemisphere were significantly higher in more severely affected patients compared to mildly impaired patients (AMT: $T(11) = 2.515$; RMT: $T(11) = 2.801$; $P > 0.05$, FDR-corrected) whereas motor thresholds assessed over the contralesional hemisphere were not significantly different between groups ($P > 0.2$).

5.3.3.1.2 Short-interval intracortical inhibition (SICI)

There was a statistical trend for a main effect for the factor GROUP for SICI ($F(20, 1) = 3.887$; $P = 0.063$) indicating that patients had decreased SICI compared to healthy controls. Post-hoc t-tests revealed that patients had significantly decreased SICI (i.e. less intracortical inhibition) assessed over the ipsilesional hemisphere ($T(20) = 2.695$; $P < 0.05$, Dunn-corrected) but not over the contralesional hemisphere ($P > 0.05$, Dunn-corrected) compared to healthy controls. SICI was not significantly different between hemispheres, neither in stroke patients nor in healthy subjects ($P > 0.05$). SICI was not significantly associated with lesion characteristics such as lesion size, lesion age, and integrity of the CST ($P > 0.05$). Although correlations between SICI and clinical scores or lesion characteristics were not statistically significant, reduced SICI in the ipsilesional hemisphere was rather associated with better than worse motor performance as indicated by an association with higher ARAT scores ($r = 0.481$; $P = 0.134$) and lower mRS scores ($r = -0.454$; $P = 0.161$). SICI in the contralesional hemisphere was not associated with clinical scores ($P > 0.3$).

5.3.3.1.3 Interhemispheric inhibition (IHI)

There was no significant main effect or interaction in the ANOVA on IHI ($P > 0.05$) indicating that there was no significant difference between groups or hemispheres in IHI. Interhemispheric inhibition was not significantly associated with lesion characteristics ($P > 0.05$). However, clinical scores were associated with the IHI strength targeting the contralesional hemisphere. Patients showing low inhibition from the ipsilesional onto the contralesional hemisphere tended to be more severely affected than patients with preserved IHI ($r = 0.670$; $P = 0.017$, uncorrected).

5.3.3.2 TMS parameters as predictors for TBS effects

To investigate whether motor thresholds (AMT and RMT), short-interval intracortical inhibition (SICI) or interhemispheric inhibition (IHI) predicted behavioural TBS effects, we correlated behavioural improvements following iTBS and cTBS (i.e. overall improvement scores) with electrophysiological TMS parameters obtained at baseline. None of the correlations yielded a significant effect ($P > 0.05$) suggesting that corticospinal excitability and intra- and interhemispheric inhibition probed by TMS have poor predictive value for behavioural improvements following TBS.

5.3.4 Functional magnetic resonance imaging (fMRI)

5.3.4.1 Motor paradigm (maximum fist closure frequencies)

Subjects performed visually-paced fist closures at two different movement frequencies: (i) at a fixed frequency of 0.8 Hz and (ii) at a frequency individually adjusted to 40% of the maximum movement frequency of the respective hand. We computed a repeated measures ANOVA on maximum movement frequencies with the factors HAND (levels: affected/non-dominant, unaffected/dominant) and GROUP (levels: patients, healthy subjects). There was a significant main effect of HAND ($F(23, 1) = 11.457$; $P = 0.003$) which was due to significantly lower movement frequencies for the affected/non-dominant hand compared to the unaffected/dominant hand across groups. The main effect of GROUP ($F(23, 1) = 0.535$; $P = 0.472$) was not significant but there was a significant HAND x GROUP interaction ($F(23, 1) = 9.223$; $P = 0.006$). Post-hoc t-tests revealed that this was due to highly significantly lower movement frequencies of the affected hand compared to the unaffected hand in stroke patients

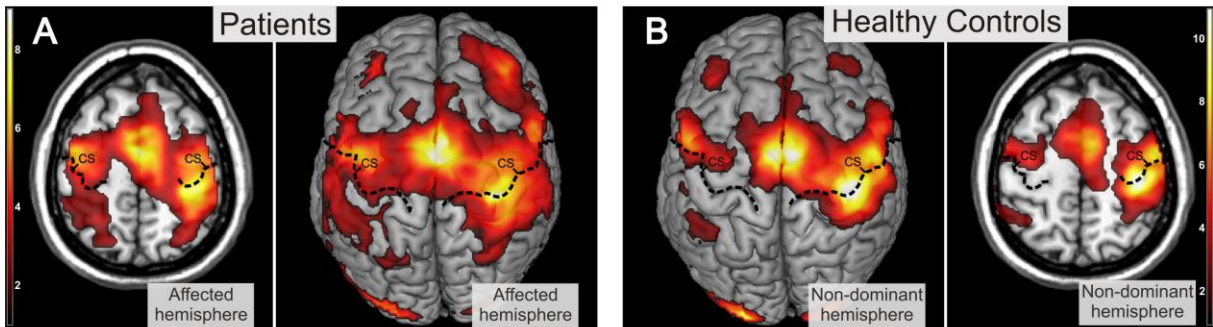
($T(12) = -3.374$; $P < 0.05$, Dunn-corrected). Taken together these results suggest that also in the fMRI task, patients showed a clear unilateral hand motor deficit.

5.3.4.2 fMRI group analysis

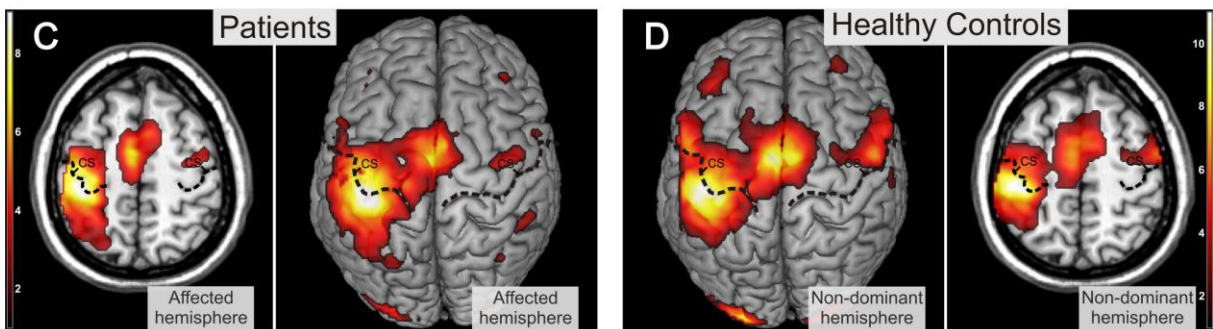
For the fMRI group analysis the parameter estimates of all four conditions were compared in a full-factorial GLM random effects analysis with the within-subject factors HAND (levels: affected/non-dominant, unaffected/dominant) and FREQUENCY (levels: fixed, adjusted). Figure 5.7 shows regions significantly activated by visually-paced fist closures of the affected and the unaffected hand in stroke patients (all normalized as having right sided lesions) as well as movements of the non-dominant and dominant hand in healthy control subjects relative to the low-level baseline. In healthy subjects, dominant and non-dominant hand movements increased neural activity in a network comprising contralateral primary motor cortex (M1), contralateral primary somatosensory cortex (S1), bilateral supplementary motor area (SMA), bilateral ventral and dorsal premotor cortex (vPMC, dPMC), bilateral dorsolateral prefrontal cortex (DLPFC), and bilateral visual cortex ($P < 0.05$, FDR-corrected, Figure 5.7B and 5.7D). In stroke patients, movements of the unaffected hand yielded comparable results as movements of the dominant or non-dominant hand in healthy subjects (Figure 5.7C). However, movements of the stroke affected hand were associated with bilaterally enhanced fMRI signal in a number of cortical regions. Activation clusters in the ipsilesional hemisphere were less focused and extended into frontal and parietal areas (Figure 5.7D). Patients furthermore showed increased activation in the ipsilesional DLPFC, cingulate motor area, and contralateral posterior parietal cortex during movements of the affected hand. Importantly, and in contrast to the healthy control group, movements of the stroke-affected hand were associated with significant neural activity in the contralesional hemisphere (ipsilateral to the performing hand) including activation clusters around the central sulcus, i.e. in M1/S1 (primary sensorimotor cortex). Similar results were found for both fixed and adjusted movement frequencies (Figure 5.7).

Fixed movement frequency (0.8 Hz)

Movements of the stroke affected/non-dominant hand

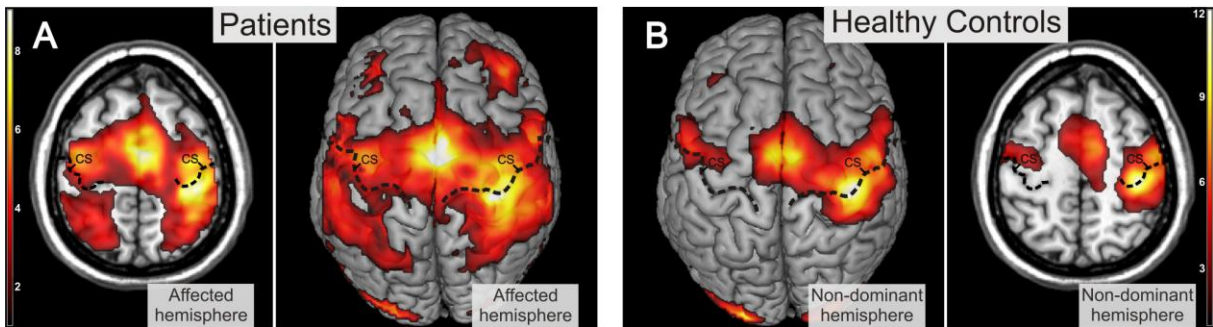


Movements of the unaffected/dominant hand

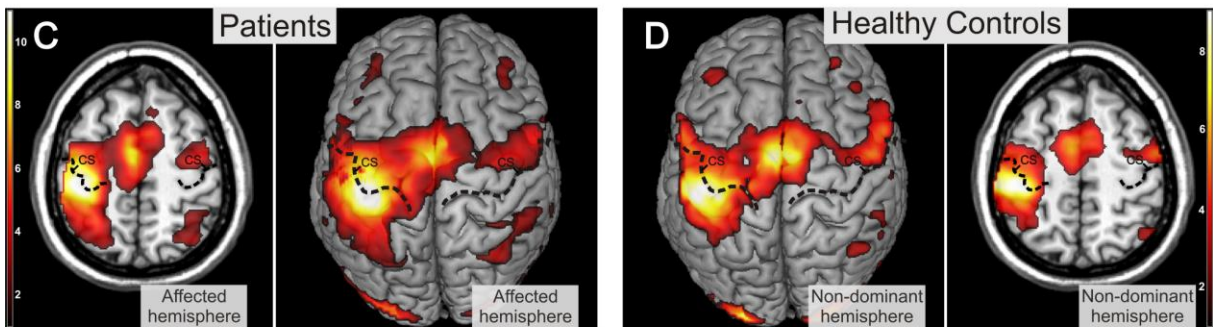


Adjusted movement frequency (40% of max.)

Movements of the stroke affected/non-dominant hand



Movements of the unaffected/dominant hand



FDR corrected ($P < 0.05$)

Figure 5.7: Study III: Movement-related neural signal in cortical motor areas. Functional magnetic resonance imaging (fMRI) was used to measure blood oxygenation level dependent (BOLD) signal in 13 chronic stroke patients and 12 age-matched healthy control subjects. Subjects performed visually-paced rhythmic fist closures at two different movement frequencies: (i) a fixed movement frequency of 0.8 Hz (upper figure), and (ii) a movement frequency individually adjusted to 40% of the maximum movement frequency of the respective hand (lower figure). Regions significantly activated by movements of the affected/non-dominant and the unaffected/dominant hand relative to the low-level baseline are shown ($P < 0.05$, FDR-corrected). In stroke patients, movements of the unaffected hand (Figure 5.7C) yielded comparable results as movements of the dominant (Figure 5.7D) or non-dominant hand (Figure 5.7B) in healthy subjects. However, movements of the stroke affected hand were associated with bilaterally enhanced fMRI signal in a number of cortical regions including contralesional M1/S1 (primary sensorimotor cortex; Figure 5.7A). Similar results were found for fixed and adjusted movement frequencies.

5.3.4.3 Region-of-interest (ROI) analyses

5.3.4.3.1 ROI analysis – differences between groups

To investigate whether neural activity in key motor areas differed significantly between patients and healthy subjects we computed repeated measures ANOVAs with the factor REGION (levels: M1, SMA, vPMC) and GROUP (levels: patients, healthy controls) for each condition and hemisphere on parameter estimates extracted from ROIs. All ANOVAs yielded a significant main effect of REGION ($P < 0.001$) but no main effect of GROUP ($P > 0.05$). A significant REGION \times GROUP interaction was found only for neural activity in the ipsilateral (i.e. contralesional/dominant) hemisphere during movements of the affected/non-dominant hand. This effect was evident for both movement frequencies (fixed: $F(46, 2) = 5.931$; $P = 0.005$; adjusted: $F(46, 2) = 4.589$; $P = 0.015$). Post-hoc t-tests revealed that this effect was due to stroke patients having higher levels of neural activity in M1 of the contralesional hemisphere during movements of the affected hand compared to activity in M1 of the non-dominant hemisphere during movements of the dominant hand in healthy controls (fixed: $T(23) = 3.049$; $P < 0.05$; adjusted: $T(23) = 2.608$; $P < 0.05$; Dunn-corrected). In other words stroke patients had significantly enhanced neural activity in contralesional M1 (but not in contralesional SMA or vPMC) during affected hand movements.

To investigate whether neural activity cortical motor areas relates to clinical deficits and lesion characteristics we correlated parameter estimates extracted from ROIs with the clinical impairment score (CIS), lesion size, lesion age, and CST damage. There were no significant correlations ($P > 0.05$) suggesting that enhanced activity in contralesional M1 was not significantly associated with clinical impairment.

5.3.4.3.2 fMRI signal in ROIs as predictors for TBS effects

To investigate whether behavioural improvements after TBS were predicted by neural activity in key motor areas, we correlated fMRI parameter estimates extracted from ROIs during hand movements with TBS improvement scores of the respective hand. There were no significant correlations between fMRI parameter estimates and improvement scores after cTBS or iTBS indicating that movement-related fMRI signal in distinct motor areas are poor predictors for behavioural improvements after TBS.

5.3.4.4 Lateralization of fMRI signal

5.3.4.4.1 Laterality index (LI) – differences between groups

We calculated laterality indices (LI) based on the number of significantly activated voxels ($P < 0.001$, uncorrected) in both BA4 and BA6 ($LI_{BA4+BA6}$) as well as separately for BA4 and BA6 (LI_{BA4} and LI_{BA6}). Since the ROI analysis revealed that stroke patients had significantly higher activity in contralesional M1 during affected hand movements we had a strong hypothesis that patients would show decreased laterality of fMRI BOLD signal compared to healthy controls. Indeed, LI_{BA4} was significantly different between groups for affected/non-dominant hand movements at both the fixed and adjusted movement frequency. This was due to patients having significantly reduced laterality of fMRI signal due to higher activity in contralesional M1 (fixed: $T = 2.179$; $P < 0.05$; adjusted: $T = 2.345$; $P < 0.05$, Dunn-corrected). However, there were no significant differences between groups in LI_{BA6} or $LI_{BA4+BA6}$ which is in line with results of the ROI analysis that activity was abnormally enhanced only in contralesional M1 but not in SMA or vPMC. Taken together these results suggest that stroke patients showed significantly enhanced neural activity in the contralesional hemisphere during affected hand movements (resulting in significantly reduced laterality) specifically in M1 and not in cortical motor areas in general. To investigate whether reduced laterality relates to clinical deficit or lesion characteristics, we correlated $LI_{BA4+BA6}$, LI_{BA6} , and LI_{BA4} with CIS, lesion size, lesion age and CST damage. No significant correlations were found ($P > 0.05$) suggesting that reduced laterality was not significantly associated with clinical impairment.

5.3.4.4.2 Laterality index (LI) as predictor for TBS effects

To test whether behavioural improvements after TBS were predicted by lateralization of fMRI signal we correlated $LI_{BA4+BA6}$, LI_{BA4} , and LI_{BA6} with improvement after cTBS and iTBS. Interestingly, improvements of the stroke affected hand after iTBS were significantly predicted by $LI_{BA4+BA6}$ and LI_{BA6} . Especially patients with less enhanced neural activity in the contralesional hemisphere during movements of the affected hand (i.e. with reduced laterality as indicated by negative LI values) experienced beneficial effects of facilitatory iTBS applied to the ipsilesional hemisphere. Correlations were highly significant for the fixed movement frequency of 0.8 Hz ($LI_{BA4+BA6}$: $r = -0.735$; LI_{BA6} : $r = -0.714$; $P < 0.05$, FDR-corrected) as well as for the movement frequency adjusted to performance of the affected hand ($LI_{BA4+BA6}$: $r = -0.762$; LI_{BA6} : $r = -0.732$; $P < 0.05$, FDR-corrected; Figure 5.8). This finding indicates that patients with severely reduced lateralisation of fMRI signal were less likely to improve after iTBS applied to the ipsilesional hemisphere. An LI of approximately -0.05 (fixed frequency) and -0.10 (adjusted frequency) respectively was necessary to generate improvements of the affected hand after iTBS. Interestingly, improvements of the affected hand after iTBS were predicted by preserved laterality of fMRI signal in BA4 and BA6 ($LI_{BA4+BA6}$) and in BA6 alone (LI_{BA6}) but not in BA4 alone (LI_{BA4}). Hence, although patients differed significantly from healthy controls only in laterality within BA4 (but not in overall laterality in BA4 and BA6) this was a poorer predictor for behavioural improvements than overall laterality. No correlations were found between laterality indices and improvements of the unaffected hand or between laterality indices and improvements after cTBS.

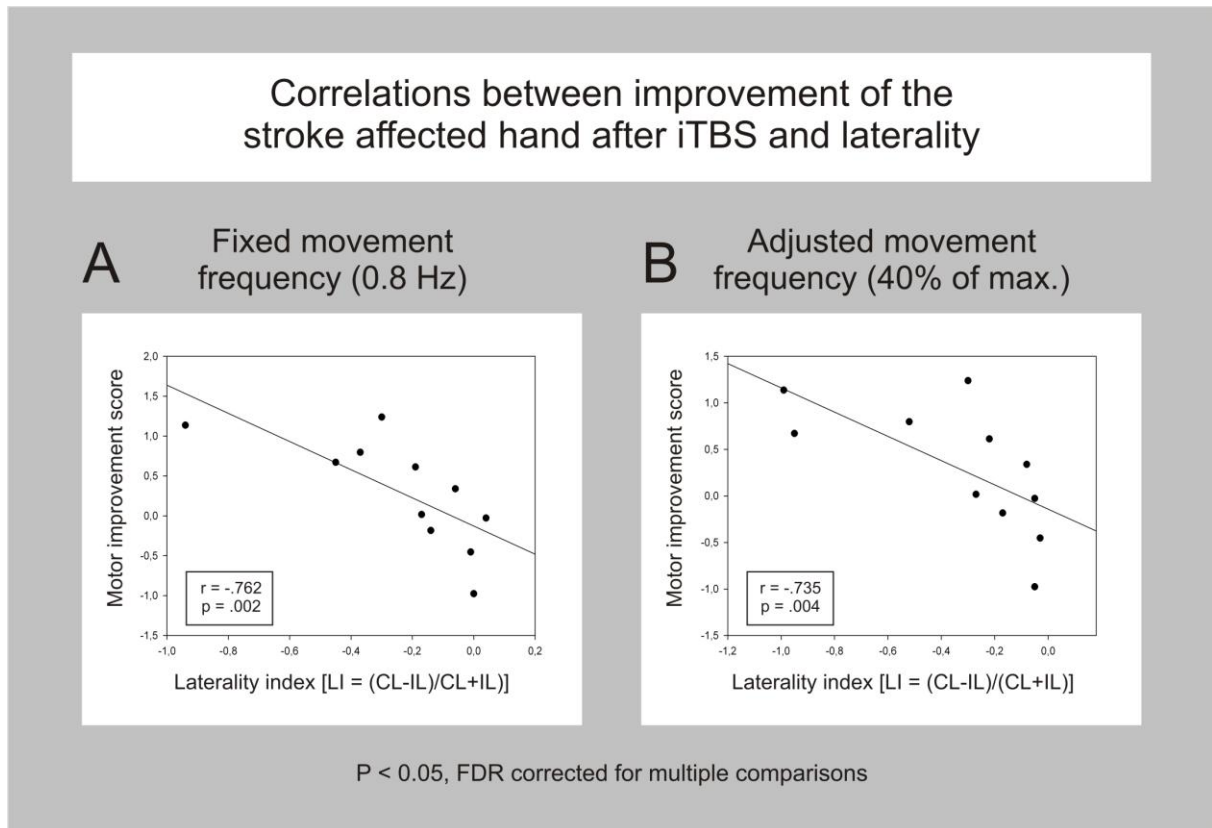


Figure 5.8: Study III: Correlation between laterality and TBS effects. Movement-related functional magnetic resonance imaging (fMRI) signal during visually-paced rhythmic fist closures was obtained from 13 stroke patients. Laterality indices were calculated based on fMRI signal in cortical motor areas (Brodmann area 4 and 6) and correlated with individual changes in motor performance following TBS (motor improvement score). The more negative the LI value of a patient (i.e. the less pronounced neural activity in the contralesional hemisphere) during movements of the affected hand was, the more likely a patient experienced beneficial effects of facilitatory iTBS applied to the ipsilesional hemisphere. No significant correlations were found for changes in motor performance of the unaffected hand or improvements of the affected hand following inhibitory continuous TBS (cTBS) over the contralesional hemisphere. (CL: contralesional; FDR: false-discovery rate; IL: ipsilesional; iTBS: intermittent theta-burst stimulation (iTBS); LI: laterality index)

5.3.4.5 Summary fMRI data

In the fMRI experiment, stroke patients and healthy control subjects performed visually-paced fist closures at 0.8 Hz and 40% of the individual maximum movement frequency. For stroke patients the maximum movement frequencies were significantly different between hands (which was not the case for healthy subjects). The fMRI group analysis revealed that stroke patients had increased fMRI signal in contralesional M1/S1 during movements of the stroke-affected hand but not during movements of the unaffected hand. This finding was supported by ROI analyses demonstrating significantly higher fMRI signal in contralesional M1 during movements of the affected hand. Neural activity in distinct motor areas however did not

predict behavioural TBS effects. Hence, we calculated laterality indices to investigate whether laterality of fMRI signal would predict TBS effects. Patients had decreased laterality of fMRI signal only in BA4, whereas overall laterality in BA4 and BA6 was not significantly different between groups. Interestingly, overall laterality (but not laterality in BA4 alone) was a strong predictor for improvements of the affected after facilitatory iTBS applied to the ipsilesional hemisphere. Patients with more lateralized fMRI signal were more to show improvements of the affected hand after iTBS.

5.3.5 Dynamic causal modelling (DCM)

5.3.5.1 Bayesian Model Selection (BMS)

We performed random effects Bayesian model selection (BMS) analyses to identify the best model, i.e. the model providing the best trade-off between accuracy (in terms of explaining variance in measured data) and simplicity (allowing generalization). Model 1, i.e. the “fully connected” model for interregional coupling during movements of the affected/non-dominant and the unaffected/dominant hand, showed the best model fit in healthy subjects as well as stroke patients given the data. Expected posterior model probabilities (reflecting the likelihood that a specific model generates the data of a randomly chosen subject) as well as model exceedance probabilities (referring to the probability that one model is more likely than any other model) are displayed in Figure 5.9. There was a probability of 99.55 % in healthy subjects and 99.64 % in stroke patients for Model 1 being the most likely model given the data observed.

Bayesian Model Selection Results

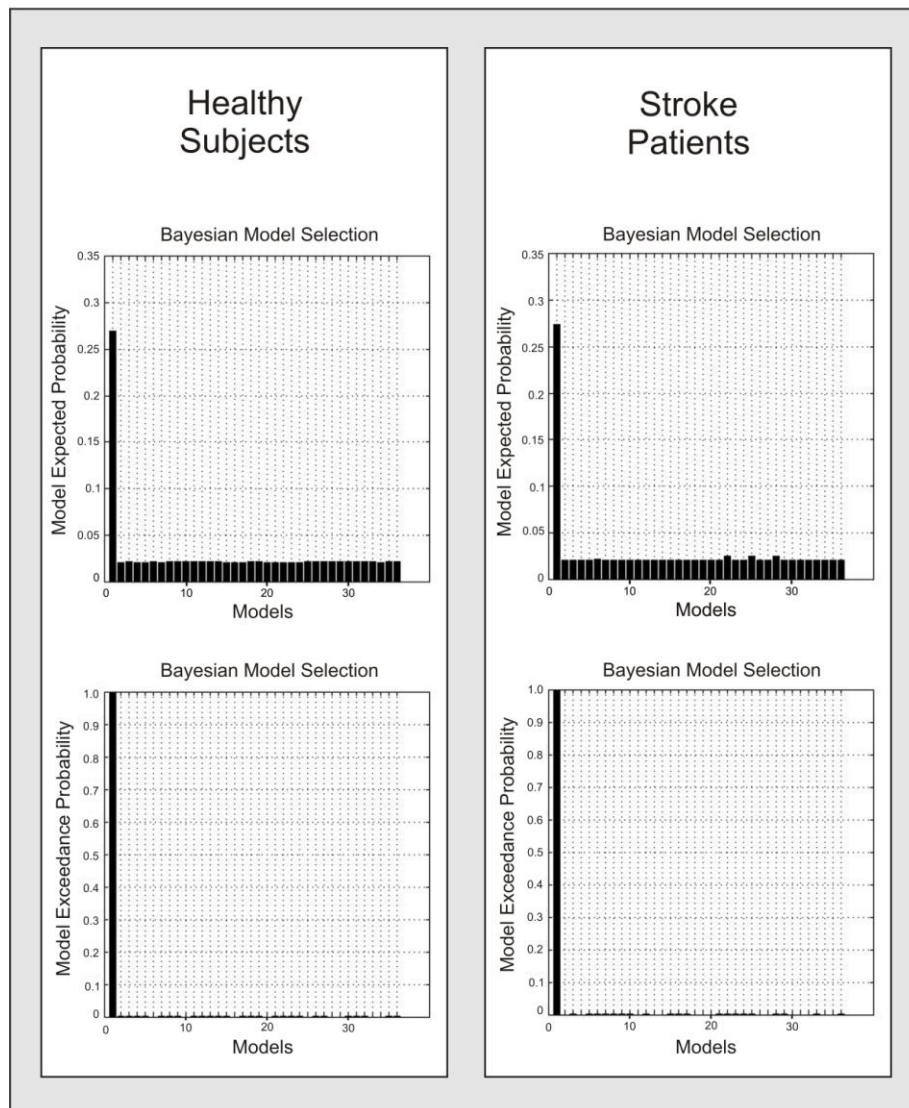


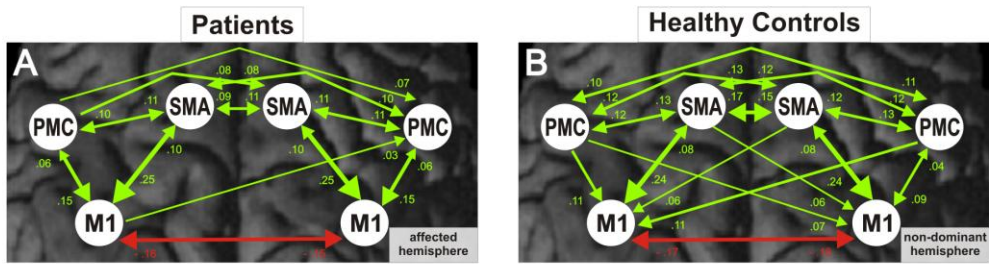
Figure 5.9: Study III: Results of the Bayesian model selection (BMS) procedure. Since “task-dependent” modulations do not necessarily impact on all endogenous connections, we constructed 36 different connectivity models reflecting biologically plausible hypotheses on interregional coupling. We then used random effects BMS to identify the best model, providing the best trade-off between accuracy (in terms of explaining variance in measured data) and simplicity (allowing generalization). Model 1 (the “fully connected” model for interregional coupling during movements of the affected/non-dominant and the unaffected/dominant hand) showed the best model fit in healthy subjects as well as stroke patients given the data. Expected posterior model probabilities (reflecting the likelihood that a specific model generates the data of a randomly chosen subject, upper figure) as well as model exceedance probabilities (referring to the probability that one model is more likely than any other model, lower figure) are displayed. There was a probability of 99.55 % in healthy subjects (left column) and 99.64 % in stroke patients (right column) for Model 1 being the most likely model given the data observed.

5.3.5.2 Significant connections in healthy subjects and patients

5.3.5.2.1 Task-independent (endogenous) connectivity

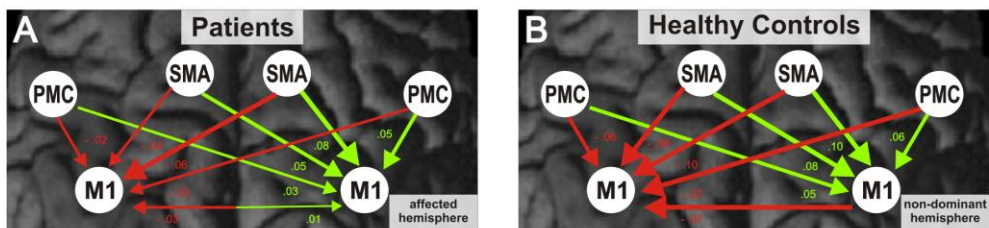
We first investigated endogenous connectivity in healthy subjects and stroke patients separately. Endogenous connectivity reflects the causal influence one area exerts on neural activity of another area independent of a specific experimental condition (Friston et al., 2003). However, endogenous connectivity (DCM A matrix) should not be mistaken as baseline connectivity since it reflects the task-independent component of effective connectivity across the entire time course of the experiment. Figure 5.10 shows significant endogenous connections in patients and healthy controls (one-sample t-tests; $P < 0.05$, FDR-corrected). Green arrows indicate that activity in the source region increased activity in the target region (positive coupling parameter) which can be interpreted as facilitation whereas red arrows indicate that activity in the source region decreased activity in the target region (negative coupling parameter) which can be interpreted as inhibition. Please note that coupling parameters (in Hz) also implicitly capture the influence of possible (subcortical) relay regions such as, e.g., the basal ganglia or the cerebellum. In healthy subjects, endogenous coupling of neural activity among cortical motor areas was almost perfectly symmetrically organized. Almost all influences between motor areas were facilitatory. The most pronounced promoting influence was exerted from the SMA onto the ipsilateral M1. Solely interhemispheric interactions between the two primary motor cortices were inhibitory. Endogenous coupling in stroke patients followed a similar pattern although coupling strength tended to be decreased compared to healthy subjects. Hence, fewer connections passed the statistical threshold (Figure 5.10; $P < 0.05$, FDR-corrected).

Task-independent (endogeneous) connectivity

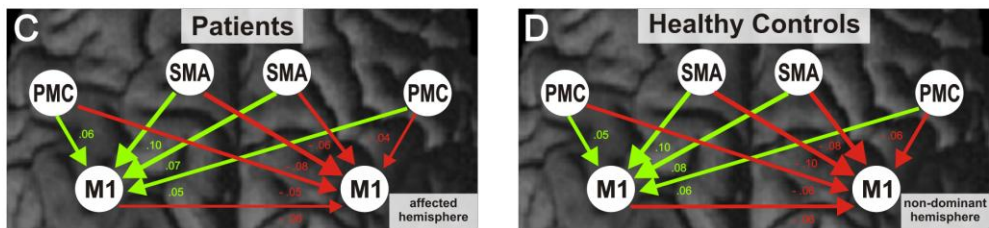


Fixed movement frequency (0.8 Hz)

Movements of the stroke affected/non-dominant hand

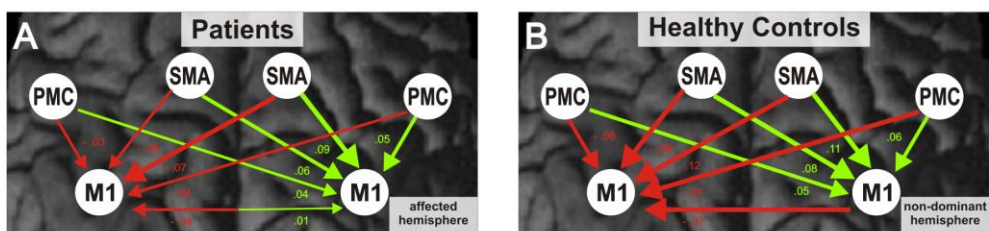


Movements of the unaffected/dominant hand

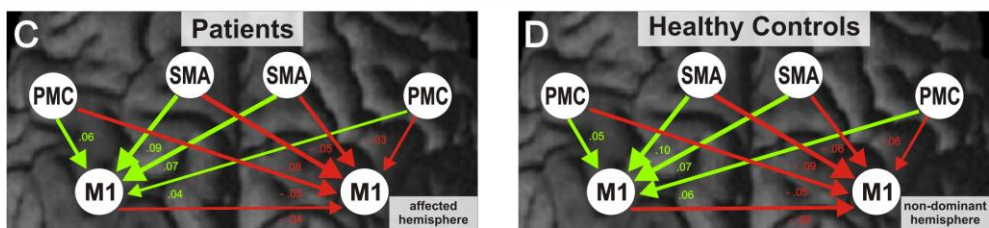


Adjusted movement frequency (40% of max.)

Movements of the stroke affected/non-dominant hand



Movements of the unaffected/dominant hand



FDR corrected ($P < 0.05$)

Figure 5.10: Study III: Significant interregional couplings in healthy subjects and stroke patients. Dynamic causal modelling (DCM) was used to infer task-independent (i.e. endogenous) effective connectivity as well as task-dependent modulations from functional magnetic resonance imaging (fMRI) data of 13 chronic stroke patients (left column) and 12 age-matched healthy subjects (right column). Significant endogenous connections in patients and healthy subjects are shown (one-sample t-tests; $P < 0.05$, FDR-corrected). Numbers refer to coupling strength (in Hz). Green arrows indicate that activity in the source region increased activity in the target region (positive coupling parameter, facilitation) whereas red arrows indicate that activity in the source region decreased activity in the target region (negative coupling parameter, inhibition). Endogenous coupling in stroke patients followed a similar pattern as in healthy subjects although fewer connections passed the statistical threshold. The connectivity pattern of stroke patients moving their unaffected hand (Figure 5.10C) was comparable to motor network connectivity of healthy subjects moving their dominant (Figure 5.10D) or non-dominant hand (Figure 5.10B). By contrast, when patients moved their paretic hand, there was a weak but significant additional positive influence the contralesional M1 exerted onto the ipsilesional M1 which was not found in healthy subjects (Figure 5.10A). Results were similar for the fixed and the adjusted movement frequency. (M1: primary motor cortex; PMC: premotor cortex; SMA: supplementary motor area)

5.3.5.2.1 Task-modulated connectivity

Task-modulated connectivity reflects the influence a specific experimental condition has on interregional coupling. If a certain task (e.g. movements of the affected hand) is performed, task-induced changes in effective connectivity (DCM B matrix) add onto task-independent (endogenous) effective connectivity (DCM A matrix). We first investigated the specific effect of moving the non-dominant or the dominant hand on M1 connections in healthy subjects (Figure 5.10B and 5.10D). In healthy subjects, hand movements were associated with increased promoting influences from all four premotor regions (i.e. SMA and vPMC bilaterally) onto M1 contralateral to the moving hand as well as negative influences from SMA and vPMC bilaterally onto M1 ipsilateral to the moving hand ($P < 0.05$, FDR-corrected). In addition, there was a significant inhibitory influence from the contralateral M1 onto the ipsilateral M1. This connectivity pattern was comparable to motor network connectivity of stroke patients moving their unaffected hand (Figure 5.10C). By contrast, when patients moved their paretic hand, there was a weak but significant additional positive influence the contralesional M1 exerted onto the ipsilesional M1 which was not found in healthy subjects. Results were similar for the fixed and the adjusted movement frequency (Figure 5.10).

5.3.5.3 Effective connectivity – differences between groups

5.3.5.3.1 Task-independent (endogenous) connectivity

In the next step, we investigated differences in effective connectivity between groups by computing repeated measures ANOVAs with the factor CONNECTION (30 connections for endogenous connectivity, 10 connections comprising M1 for task-modulated connectivity) and GROUP (levels: patients, healthy controls). A significant main effect of CONNECTION ($P < 0.001$) but no significant main effect of GROUP ($P > 0.05$) was found in all ANOVAs. Significant CONNECTION \times GROUP interactions were found for endogenous connectivity ($F(667, 29) = 1.508$; $P < 0.05$) and affected/non-dominant hand movements at fixed ($F(667, 29) = 2.235$; $P < 0.001$) and adjusted ($F(667, 29) = 2.668$; $P < 0.001$) movement frequencies but not for movements of the unaffected/non-dominant hand ($P > 0.05$). This finding indicates that stroke patients differed significantly from healthy control subjects (i) in the task-independent component of effective connectivity and (ii) in modulations induced by affected hand movements (but not by modulations induced by unaffected hand movements). Post-hoc t-tests revealed that stroke patients had decreased endogenous connectivity originating from premotor areas of the ipsilesional hemisphere onto areas of the contralesional hemisphere when compared to control subjects (Figure 5.11A; $P < 0.05$, Dunn-corrected). More specifically, patients had reduced positive coupling between the SMA of the ipsilesional hemisphere and SMA as well as vPMC of the contralesional hemisphere. Moreover, there was decreased coupling strength between vPMC of the ipsilesional hemisphere and M1 of the contralesional hemisphere (Figure 5.11A).

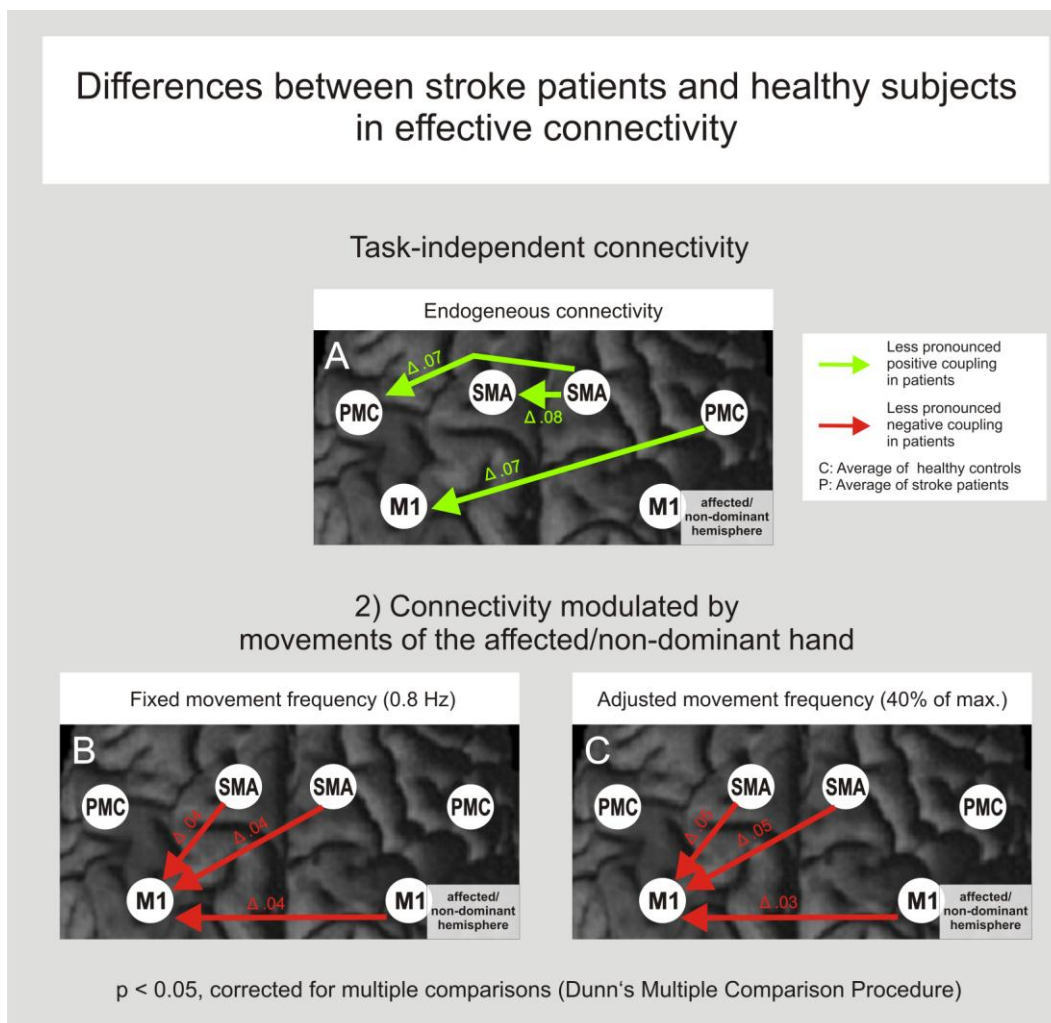


Figure 5.11: Study III: Significant differences between chronic stroke patients ($n = 13$) and age-matched healthy subjects ($n = 12$) in effective connectivity assessed by dynamic causal modelling (DCM) are shown ($P < 0.05$, corrected). Numbers indicate the difference in mean coupling strength (in Hz) between groups. Green arrows indicate that activity in the source region increased activity in the target region (positive coupling parameter, facilitation) whereas red arrows indicate that activity in the source region decreased activity in the target region (negative coupling parameter, inhibition). Stroke patients showed significantly reduced promoting influences originating from premotor areas of the ipsilesional hemisphere onto areas of the contralesional hemisphere in absence of a specific task (Figure 5.11A). Movements of the stroke affected hand were associated with significantly reduced negative coupling, i.e. disinhibition of the contralesional primary motor cortex (M1) ipsilateral to the moving hand. Disinhibition of the contralesional hemisphere was significantly associated with more severe clinical impairment ($P < 0.05$, FDR-corrected). Results were similar for the fixed and the adjusted movement frequency condition (Figure 5.11B and 5.11C).

5.3.5.3.2 Task-modulated connectivity

However, there were also differences between groups in modulations of effective connectivity induced by affected/non-dominant hand movements. Movements of the stroke affected hand were associated with reduced negative coupling, i.e. disinhibition of the contralesional M1 ipsilateral to the moving hand. More specifically, inhibition originating from ipsilesional M1, ipsilesional SMA, and contralesional SMA onto contralesional M1 was significantly reduced compared to healthy controls (Figure 5.11B; $P < 0.05$, Dunn-corrected). Results were similar for the fixed and the adjusted movement frequency condition (Figure 5.11B and 5.11C).

To investigate whether reduced endogenous connectivity or disinhibition of the contralesional M1 during affected hand movements related to clinical deficit or lesion characteristics, we correlated coupling parameters with CIS, lesion size, lesion age, and CST damage. No significant correlations were found for endogenous connectivity suggesting that decreased promoting influences originating from premotor areas of the ipsilesional hemisphere were not associated with clinical deficit. In contrast, coupling parameters modulated by movements of the affected hand were significantly correlated with clinical impairment. All coupling parameters modulated by adjusted hand movements which showed a significant difference between groups (Figure 5.11B) correlated significantly with CIS ($P < 0.05$, FDR-corrected). For the fixed movement frequency condition, only the connection from the ipsilesional M1 onto the contralesional M1 correlated significantly with CIS ($P < 0.05$, FDR-corrected) whereas correlations for the other two connections did not pass correction for multiple comparisons ($P < 0.05$, uncorrected). These findings suggest that disinhibition of the contralesional hemisphere during affected hand movements is associated with more severe clinical impairment.

5.3.5.4 Effective connectivity as predictor for TBS effects

To investigate whether motor network interactions predict behavioural improvements after TBS, we correlated coupling parameters of M1 connections with TBS improvement scores. There were no significant correlations for movement-related modulations of effective connectivity. Hence, although patients showed reduced inhibition of the contralesional hemisphere during movements of the affected hand, movement-related disinhibition of the contralesional hemisphere did not predict behavioural TBS effects. Interestingly, behavioural improvements of the affected hand after iTBS were predicted by endogenous effective

connectivity. The stronger the promoting influence from ipsilesional SMA onto ipsilesional M1 and the stronger the inhibition originating from ipsilesional M1 onto contralesional M1, the more likely a patient showed improvements of the affected hand after facilitatory iTBS applied to the ipsilesional hemisphere. Both correlations were highly significant (SMA-M1: $r = 0.709$; $P < 0.05$, FDR-corrected; M1-M1: $r = -0.764$; $P < 0.05$, FDR-corrected; Figure 5.12) and suggest that both, preserved supportive role of the ipsilesional SMA and preserved inhibition of contralesional M1 might constitute essential pre-conditions which are needed to produce beneficial effects of iTBS over the ipsilesional hemisphere. A coupling strength of approximately +0.24 (SMA-M1 connection) and -0.16 (M1-M1 connection) respectively was necessarily to generate improvements of the affected hand after iTBS. No significant correlations were found for behavioural changes of the unaffected hand or improvements of the affected hand following cTBS.

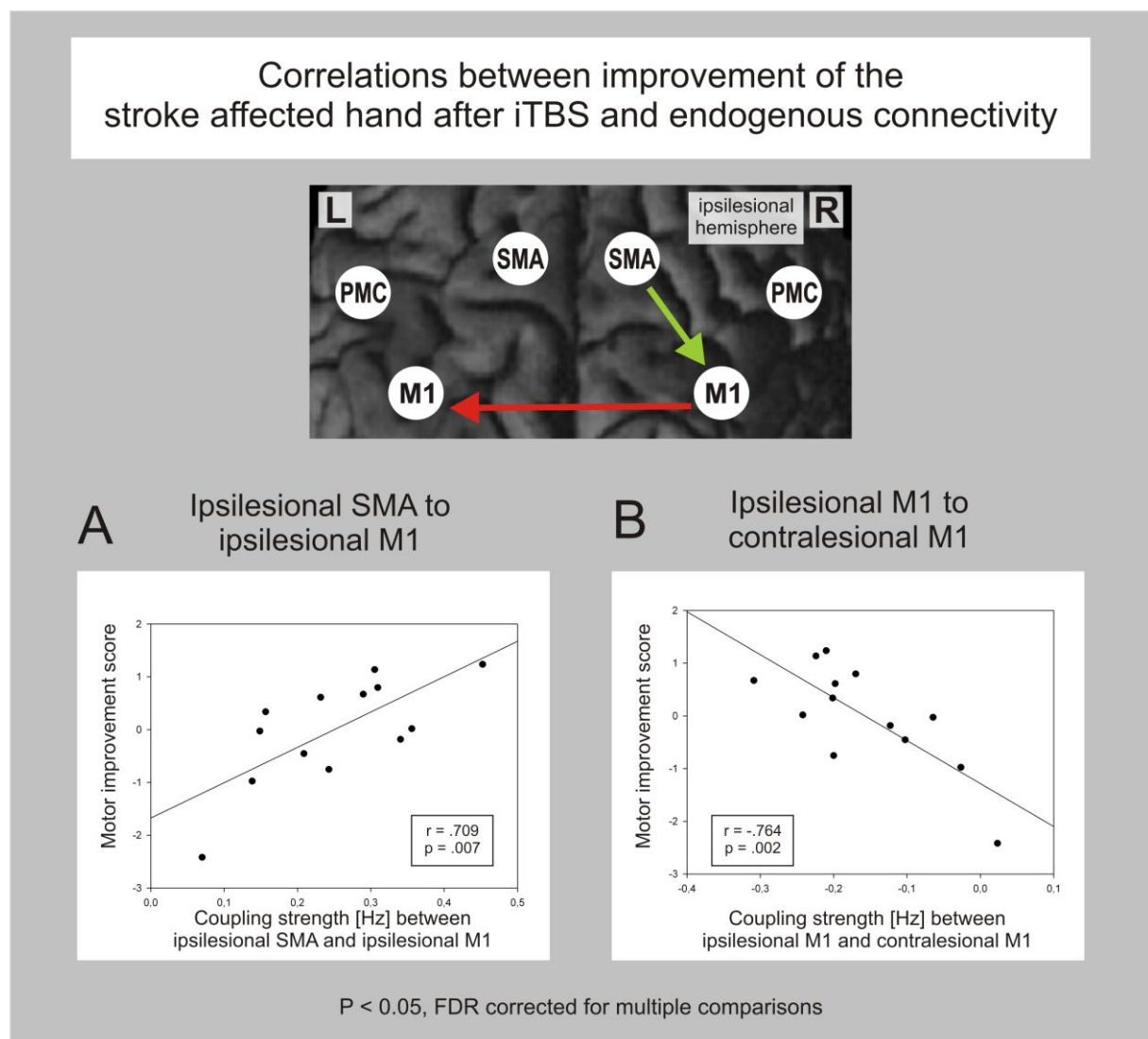


Figure 5.12: Study III: Correlation between endogenous connectivity and theta-burst stimulation (TBS) effects. Task-independent (endogenous) effective connectivity was obtained from 13 chronic stroke patients by means of dynamic causal modelling (DCM). Individual coupling parameters (in Hz) were correlated with individual changes in motor performance following TBS (motor improvement score). The stronger the promoting influence from the ipsilesional supplementary motor area (SMA) onto the ipsilesional primary motor cortex (M1) was, and the stronger the inhibition originating from the ipsilesional M1 onto the contralesional M1 was, the more likely a patient showed improvements of the affected hand after facilitatory iTBS applied to the ipsilesional hemisphere. No significant correlations were found for changes in motor performance of the unaffected hand or improvements of the affected hand following inhibitory continuous TBS (cTBS) over the contralesional hemisphere. (FDR: false-discovery rate; L: left; PMC: premotor cortex; R: right)

5.3.6 Correlation between IHI probed by DCM and paired-pulse TMS

The relationship between effective connectivity probed by DCM and TMS is unknown but one might expect that task-independent (i.e. endogenous) effective connectivity between primary motor cortices probed by DCM (Friston et al., 2003) resembles IHI probed by paired-pulse TMS at rest (Ferbert et al., 1992). We found that TBS effects were significantly predicted by IHI from ipsilesional M1 to contralesional M1 probed by DCM but not by IHI probed by paired-pulse TMS. To investigate the relationship between IHI obtained by these two different approaches we performed correlation analyses in healthy subjects and stroke patients separately. None of the correlations was statistically significant ($P > 0.05$) indicating that DCM and TMS yielded different measures of IHI in healthy subjects and stroke patients.

5.3.7 Clinical impairment as predictor for TBS effects

To investigate whether clinical impairment predicted behavioural TBS effects, we correlated behavioural improvements after TBS with mRS, NIHSS, ARAT, and the overall clinical impairment score (CIS). No relationship was found between clinical scales and behavioural effects in the affected hand after cTBS or for behavioural effects in the unaffected hand. There was a statistical trend for a correlation between improvements of the affected hand after iTBS and mRS ($r = -0.490$; $P = 0.089$) indicating that less impaired patients were more likely to show improvements of the affected hand after iTBS over the ipsilesional hemisphere than more severely affected patients.

5.3.8 Lesion characteristics as predictors for TBS effects

The voxel-based lesion symptom mapping (VLSM) analysis suggested a relationship between lesions in CST and behavioural improvements of the affected hand after iTBS. Patients with lesions comprising a region within the right CST (MNI coordinates: 28, -15, 26; probability for right CST: 81% according to human post-mortem cytoarchitectonic probability maps of the Juelich Histological Atlas; Eickhoff et al., 2005, 2007) were less likely to benefit from facilitatory iTBS applied to the ipsilesional hemisphere ($Z > 2.5$, uncorrected; Figure 5.13). This finding suggests that facilitatory iTBS applied to the ipsilesional hemisphere is less effective in patients in whom descending fibres from ipsilesional M1 are dissected at the level of the CST. No relationship was found between lesion locations and behavioural effects in the unaffected hand or for behavioural effects induced by cTBS. However, the amount of damaged CST volume in relation to the entire CST volume was not significantly correlated with behavioural improvements indicating that not CST damage in general but damage to the CST at this position might predict poor behavioural response to iTBS. No significant correlations were found between behavioural TBS effects and lesion size or lesion age ($P > 0.05$).

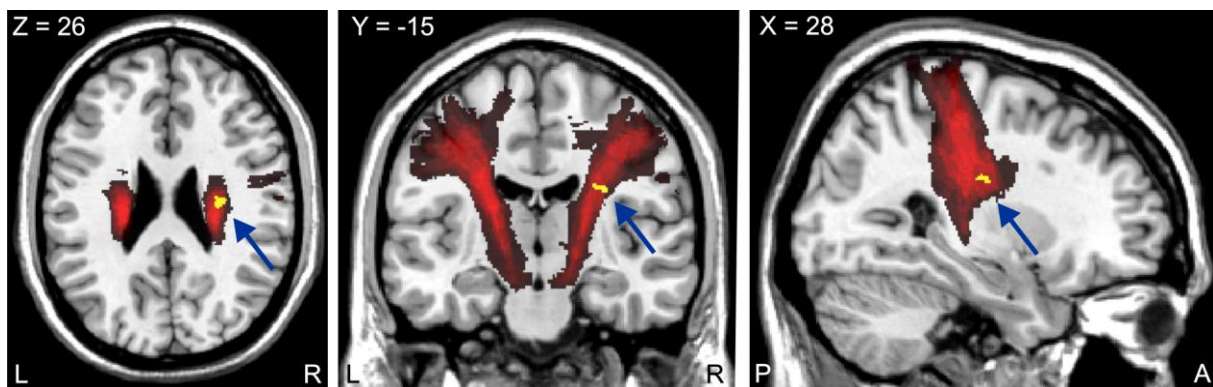


Figure 5.13: Study III: Results of the voxel-based lesion symptom mapping (VLSM). VLSM was performed to assess whether lesion location predicts theta-burst stimulation (TBS) effects on motor performance of the affected hand. Binary lesion masks were constructed based on the high-resolution anatomical *T1*-weighted image of each patient and normalized to MNI space. Patients were classified into two groups based on a median split of motor improvement scores. Behavioural improvements were entered as binary behaviour (responder = 1; non-responder = 0) using Liebermeister analysis. Patients with lesions comprising a region within the right (ipsilesional) cortico-spinal tract (CST), were less likely to benefit from facilitatory intermittent TBS (iTBS) applied to the ipsilesional hemisphere (MNI coordinates: 28, -15, 26; $Z > 2.5$, uncorrected). This finding suggests that iTBS is less effective in patients in whom descending fibres from ipsilesional primary motor cortex are dissected at the level of the CST. No relationship was found between lesion locations and behavioural effects in the unaffected hand or for behavioural effects induced by inhibitory continuous TBS (cTBS) applied to the contralesional hemisphere.

5.3.9 Summary results Study III

The major goal of the present study was to identify reliable predictors for behavioural improvements of the affected hand induced by facilitatory iTBS applied to the ipsilesional hemisphere and inhibitory cTBS applied to the contralesional hemisphere of chronic stroke patients. Neither iTBS nor cTBS was significantly different from control TBS in terms of average behavioural (or electrophysiological) changes over the group of patients. This was due to relatively high inter-individual variability, i.e. some patients showed improvements whereas others showed no improvements or even deterioration. Interestingly, behavioural improvements of the affected hand following iTBS were predicted by lateralization of the fMRI BOLD signal and motor network connectivity. Patients with lateralized fMRI activation patterns during affected hand movements were more likely to benefit from iTBS than patients with enhanced fMRI signal in both hemispheres, i.e. patients with bilateral fMRI activation patterns. Additionally, we found that patients who had a pronounced promoting influence originating from ipsilesional SMA onto ipsilesional M1 and patients who had pronounced inhibition originating from ipsilesional M1 onto contralesional M1 were more likely to benefit from iTBS over the ipsilesional hemisphere. Hence, patients showing improvements after iTBS had fMRI activation patterns and network interactions which can be regarded more physiological. These findings suggest that both intact motor network interactions in the ipsilesional hemisphere (such as supportive role of the ipsilesional SMA) and preserved inhibition of the contralesional hemisphere are crucial for improvements after iTBS. Furthermore we found some evidence that patients with CST lesions were less likely to benefit from iTBS over the ipsilesional hemisphere presumably because integrity of motor neurons descending from ipsilesional M1 is crucial to generate iTBS effects. In line with these suggestions, there was a tendency that more severely affected patients were less likely to experience beneficial effects of iTBS over the ipsilesional hemisphere. Electrophysiological TMS parameters and fMRI signal in discrete brain regions were poor predictors for behavioural TBS effects. No significant correlations were found for behavioural improvements following cTBS or behavioural changes of the unaffected hand.

5.4 Discussion Study III

The major goal of Study III was to identify reliable predictors for therapeutic TBS effects in chronic stroke patients. The main finding of the study was that behavioural improvements of the affected hand after facilitatory iTBS applied to the ipsilesional hemisphere were predicted by a more lateralized (i.e. physiological) fMRI activation pattern (towards the ipsilesional hemisphere during movements of the affected hand) and by motor network interactions such as: (i) pronounced promoting influence from the ipsilesional SMA onto the ipsilesional M1, and (ii) pronounced inhibition from ipsilesional M1 to contralesional M1. In the following, TBS effects on motor performance of the affected hand and motor cortex excitability are discussed first (cf. 5.4.1), followed by differences between stroke patients and healthy subjects in parameters obtained at baseline (cf. 5.4.2). Finally, parameters predicting rTMS effects are discussed (cf. 5.4.3).

5.4.1 TBS effects in stroke patients

According to the *model of hemispheric competition*, we expected that both facilitatory iTBS applied to the ipsilesional hemisphere and inhibitory cTBS applied to the contralesional hemisphere would result in significantly increased excitability of the ipsilesional hemisphere and behavioural improvements of the paretic hand (Khedr & Fetoh, 2010; Nowak et al., 2010). The latter approach relies on observations that in some stroke patients the contralesional hemisphere exerts pathologically increased IHI onto the ipsilesional hemisphere (Grefkes et al., 2008b, 2010; Murase et al., 2004) and that decreasing excitability of one motor cortex increases excitability of the contralateral motor cortex presumably due to a reduction in IHI (Gilio et al., 2003; Schambra et al., 2003; Heide et al., 2006).

However, in the present study we found no significant difference between iTBS, cTBS, and control TBS (over the parieto-occipital midsagittal line) in average behavioural or electrophysiological changes over the group of patients. Also several other studies did not find significant increases in MEP size following low-frequency (Bagnato et al., 2005; Daskalakis et al., 2006; Modugno et al., 2003; Pal et al., 2005) or high-frequency rTMS (Fitzgerald et al. 2007; Suppa et al., 2008) in healthy subjects or in chronic stroke patients (low frequency: Carey et al., 2008; high-frequency: Malcom et al., 2007). In the present study, there was no average improvement over the group of patients due to considerably high

inter-individual variance which was also found in several other rTMS studies (e.g. Daskalakis et al., 2006; Van Der Werf & Paus, 2006; Muller-Dahlhaus et al., 2008).

Until now, studies using TBS to reconstitute hemispheric balance and improve motor performance of the paretic hand are scarce (Table 5.3). Di Lazzaro and colleagues (2010) found that excitability of the ipsilesional hemisphere was significantly increased, whereas excitability of the contralesional hemisphere was significantly decreased following facilitatory iTBS over the ipsilesional hemisphere in 16 acute to subacute stroke patients (< 10 days after stroke; with cortical and subcortical lesions). Interestingly, this study also demonstrated that favourable clinical outcome (as indicated by mRS after 6 months) was associated with relatively low initial excitability of the contralesional hemisphere and pronounced LTP-like effects in the ipsilesional and LTD-like effects in the contralesional hemisphere following iTBS. This finding strongly suggests that spontaneous recovery of function relies on the capability to induce cortical plasticity which seems to be the neurophysiological basis for functional reorganization. Hence, these findings strongly support the use of non-invasive stimulation techniques (which have been demonstrated to enhance cortical plasticity) to promote recovery of function after stroke.

In an earlier study, Di Lazzaro and colleagues (2008a) investigated both facilitatory and inhibitory TBS effects in 12 acute to subacute stroke patients (\leq 10 days after stroke; with cortical and subcortical lesions) and 12 age-matched healthy control subjects. As suggested by the *model of interhemispheric competition*, both iTBS over the ipsilesional hemisphere and cTBS over the contralesional hemisphere increased excitability of the ipsilesional hemisphere and decreased excitability of the contralesional hemisphere in acute to subacute stroke patients. The effect was slightly stronger for iTBS than for cTBS (increase in MEP size after iTBS: 20%, after cTBS: 16%) although this difference between TBS protocols was not statistically significant. Interestingly, TBS effects were comparable in healthy subjects and stroke patients. Unfortunately, behavioural effects were not investigated in neither of the studies published by Di Lazzaro et al. (2008a, 2010). In the present study, excitability of the ipsilesional hemisphere was not significantly increased over the group of patients, but in line with the *model of interhemispheric competition* and results of Di Lazzaro et al. (2008a, 2010) excitability of the contralesional hemisphere tended to be decreased after both iTBS and cTBS. The decrease in corticospinal excitability was mirrored by a tendency for deteriorated motor performance of the unaffected hand after both iTBS and cTBS. This finding indicates that iTBS and cTBS impacted on excitability of the contralesional hemisphere and motor

performance of the unaffected hand, whereas changes in the ipsilesional hemisphere and affected hand were more variable across subjects and hence did not result in a net increase over the group of patients. Why our results differ from findings of Di Lazzaro et al. (2008a, 2010) is unclear but might be due to methodological differences. In studies of Di Lazzaro et al. results were not compared with control stimulation, patients were more severely affected, had exclusively subcortical lesions and were in the acute to subacute stage (< 10 days after stroke).

Study III: Prediction of TBS effects

Table 5.3: Study III: Summary of previous studies using theta-burst stimulation (TBS) to modulate cortical excitability in stroke patients

Study	Subjects	Lesion locations	Clinical phase	TBS protocols	Outcome measures	Results
Ackerley et al. (2010)	10 patients	Subcortical	Chronic phase (> 6 months)	1) iTBS (90% AMT; 600 stimuli) applied to IL 2) cTBS (90% AMT; 600 stimuli) applied to CL 3) Sham TBS (sham coil, applied to IL or CL) Each followed by motor training	- MEP size of AH - Grip-lift kinematics of AH	1) iTBS + training: - MEP AH ↑ - Movement kinematics AH ↑ 2) cTBS + training: - MEP AH ↔ (strong trend for ↓) - Movement kinematics AH ↑ - ARAT AH ↓ 3) Sham + training: - MEP AH ↔ Movement kinematics AH ↓
Di Lazzaro et al. (2008a)	12 patients & 12 age-matched healthy controls	Cortical & subcortical	Acute phase (≤ 10 days)	1) iTBS (80% AMT; 600 stimuli) applied to IL 2) cTBS (80% AMT; 600 stimuli) applied to CL	- MEP size of AH & UH	iTBS: - MEP AH ↑ - MEP UH ↓ cTBS: - MEP AH ↑ - MEP UH ↓
Di Lazzaro et al. (2010)	16 patients	Cortical & subcortical	Acute phase (< 10 days)	1) iTBS (80% AMT; 600 stimuli) applied to IL	- MEP size of AH & UH	iTBS: - MEP AH ↑ - MEP UH ↓
Talelli et al. (2007)	6 patients	Cortical & subcortical	Chronic phase (> 12 months)	1) iTBS (80% AMT; 600 stimuli) applied to IL 2) cTBS (80% AMT; 300 stimuli) applied to CL 3) Control TBS (50% max. output; angulated coil; cTBS or iTBS applied to IL or CL)	- MEP size of AH (cTBS: AH & UH) - Simple reaction time (SRT) of AH - Choice reaction time (CRT) of AH (cTBS: AH & UH)	iTBS: - MEP AH ↑ - SRT AH ↓ - CRT AH ↔ cTBS: - MEP AH ↔ - MEP UH ↓ - SRT AH ↔ - CRT AH ↔ - CRT UH ↔

AH = affected hand; AMT = active motor threshold; ARAT = action research arm test; CL = contralesional hemisphere; CRT = choice reaction time; cTBS = continuous theta-burst stimulation; IL = ipsilesional hemisphere; iTBS = intermittent theta-burst stimulation; MEP = motor-evoked potential; SRT = simple reaction time; TBS = theta-burst stimulation; UH = unaffected hand

However, TBS effects have also been demonstrated for chronic stroke patients although more convincing for iTBS than for cTBS (Ackerley et al., 2010; Talelli et al., 2007). Talelli and colleagues (2007) investigated TBS effects in six chronic stroke patients (> 1 year and up to 9 years after stroke) with motor hand deficits and cortical or subcortical lesions and found that iTBS applied to the ipsilesional hemisphere (but not cTBS or sham stimulation) resulted in significantly increased excitability of the ipsilesional hemisphere and shorter simple reaction times (but not choice reaction times) of the affected hand for up to 30 minutes. This finding suggests that iTBS might be more effective than cTBS in chronic stroke patients, but is more likely to impact on simple rather than complex motor behaviour. In line with our results, cTBS applied to the contralesional hemisphere was successful in decreasing excitability of the contralesional hemisphere in the study of Talelli et al. (2007), but did not increase excitability of the ipsilesional hemisphere or result in significant improvements of the affected hand. The authors suggested that this finding might indicate that the effect of stimulation was not transmitted to the contralateral (i.e. ipsilesional) hemisphere because transcallosal fibres have been suggested to require higher stimulation intensities for excitation than usually used for TBS (Talelli et al., 2007). However, this suggestion is not supported by results in the present study, since we found decreased excitability of the contralesional hemisphere after both cTBS and iTBS (and the latter approach requires interhemispheric transmission to generate this effect). Since we found decreased excitability of the contralesional hemisphere but unchanged excitability of the ipsilesional hemisphere after TBS, our results imply that the contralesional hemisphere responds to TBS as proposed by the *model of hemispheric competition* whereas the ipsilesional hemisphere shows no consistent change. It might be more difficult to induce consistent effects in the less intact ipsilesional hemisphere due to stroke induced changes such as altered synaptic plasticity which might interfere with induction of beneficial TBS effects in some of the patients.

Also in the study of Ackerley and colleagues (2010) iTBS resulted in more convincing results than cTBS when combined with upper-limb training (and compared to sham stimulation combined with training) in 10 chronic stroke patients (> 6 months since stroke; with subcortical lesions). As hypothesized, excitability of the ipsilesional hemisphere was increased after iTBS over the ipsilesional hemisphere, but surprisingly, it was decreased after cTBS over the contralesional hemisphere. Behavioural effects of cTBS were controversial. Although, grip-lift kinematics of the paretic hand improved after training combined with real iTBS or real cTBS (but deteriorated after training combined with sham stimulation), cTBS

combined with training deteriorated overall upper-limb function (as probed by the ARAT). This deterioration was significantly correlated with decreased excitability of the ipsilesional hemisphere. The authors suggested that inhibitory cTBS applied to the contralesional hemisphere might deteriorate motor performance of the affected hand because the contralesional hemisphere might play a pivotal role in stroke recovery. Also we did not find decreased excitability of the ipsilesional hemisphere after TBS in the present study, our results likewise indicate that (at least some) patients might deteriorate after TBS. This finding is also in line with a study of Ameli and colleagues (2009) who found that 7 out of 13 patients with cortico-subcortical lesions (but only one patient with a purely subcortical lesion) deteriorated after facilitatory 10 Hz rTMS applied to the ipsilesional hemisphere.

Taken together, our results suggest high inter-individual variance in TBS induced changes in corticospinal excitability and motor performance, especially in the ipsilesional hemisphere and the paretic hand.

5.4.2 Baseline parameters – differences between patients and controls

Compared to healthy subjects, stroke patients in the chronic stage showed several abnormalities in TMS and fMRI parameters at baseline (Table 5.4) such as:

- 1) Decreased SICI (i.e. less intracortical inhibition) in the ipsilesional hemisphere
- 2) Increased fMRI signal in contralesional M1 (ipsilateral to hand movements) during movements of the affected hand (as suggested by the ROI analysis)
- 3) Decreased laterality (i.e. more bilateral activation) of fMRI signal in M1 during movements of the affected hand (LI_{BA4})
- 4) Decreased inhibitory influence from bilateral SMA and ipsilesional M1 to contralesional M1 during movements of the affected hand (modulatory effective connectivity)
- 5) Decreased promoting influence from ipsilesional SMA and vPMC onto motor areas of the contralesional hemisphere (endogenous effective connectivity)

Differences between stroke patients in the chronic stage compared to healthy subjects in TMS and fMRI parameters at baseline are discussed in front of the literature in the following

section. Additionally, to elucidate the functional role of stroke induced changes further, the relationship between baseline parameters and clinical deficit is discussed.

Table 5.4: Study III: Summary of results

		Mean (SD) for healthy subjects	Mean (SD) for stroke patients	Differences between patients and controls	Correlation with clinical impairment score (CIS)	Correlation with motor improvement score (MIS)
RMT	IL	39.273 (5.101)	40.846 (11.929)	n.s.	n.s.	n.s.
	CL	38.909 (6.685)	36.615 (4.032)	n.s.	n.s.	n.s.
AMT	IL	32.545 (3.882)	33.092 (10.220)	n.s.	n.s.	n.s.
	CL	32.000 (4.472)	27.277 (4.317)	n.s.	n.s.	n.s.
SICI	IL	46.024 (26.887)	75.630 (24.589)	T = 2.695 P = 0.014	n.s.	n.s.
	CL	44.761 (23.046)	46.526 (12.904)	n.s.	n.s.	n.s.
IHI	IL to CL	55.964 (35.693)	45.773 (25.379)	n.s.	r = 0.670 * P = 0.017	n.s.
	CL to IL	51.708 (33.804)	57.932 (36.746)	n.s.	n.s.	n.s.
ROI-CL Fixed	M1	-0.011 (0.313)	0.581 (0.600)	T = 2.608 P = 0.016	n.s.	n.s.
	SMA	1.160 (0.436)	1.259 (0.596)	n.s.	n.s.	n.s.
	vPMC	0.930 (0.477)	0.885 (0.486)	n.s.	n.s.	n.s.
ROI-CL Adjusted	M1	-0.061 (0.377)	0.420 (0.526)	T = 3.049 P = 0.006	n.s.	n.s.
	SMA	1.161 (0.470)	1.104 (0.674)	n.s.	n.s.	n.s.
	vPMC	0.936 (0.640)	0.822 (0.462)	n.s.	n.s.	n.s.
LI Fixed	LI _{BA4}	-0.835 (0.240)	-0.299 (0.780)	T = 2.345 P = 0.029	n.s.	n.s.
	LI _{BA6}	-0.305 (0.257)	-0.175 (0.289)	n.s.	n.s.	r = -0.714 P = 0.006
	LI _{BA4+BA6}	-0.360 (0.249)	-0.200 (0.272)	n.s.	n.s.	r = -0.735 P = 0.004
LI Adjusted	LI _{BA4}	-0.811 (0.292)	-0.302 (0.689)	T = 2.179 P = 0.041	n.s.	n.s.
	LI _{BA6}	-0.311 (0.190)	-0.237 (0.373)	n.s.	n.s.	r = -0.732 P = 0.004
	LI _{BA4+BA6}	-0.385 (0.222)	-0.285 (0.336)	n.s.	n.s.	r = -0.762 P = 0.002
DCM-B Fixed	SMA CL – M1 CL	-0.080 (0.049)	-0.040 (0.044)	T = -2.170 P = 0.041	r = 0.555 * P = 0.049	n.s.
	SMA IL – M1 CL	-0.101 (0.416)	-0.056 (-0.051)	T = -2.383 P = 0.026	r = 0.571 * P = 0.042	n.s.
	M1 IL – M1 CL	-0.066 (0.031)	-0.028 (0.035)	T = -2.873 P = 0.009	r = 0.631 P = 0.021	n.s.
	SMA CL – M1 CL	-0.091 (0.042)	-0.042 (0.032)	T = -3.255 P = 0.003	r = 0.741 P = 0.004	n.s.
DCM-B Adjusted	SMA IL – M1 CL	-0.118 (0.034)	-0.068 (0.037)	T = -3.529 P = 0.002	r = 0.740 P = 0.004	n.s.
	M1 IL – M1 CL	-0.070 (0.023)	-0.036 (0.024)	T = -3.710 P = 0.001	r = 0.717 P = 0.006	n.s.

DCM-A	SMA IL –	0.166	0.089	T = 2.234	n.s.	n.s.
	SMA CL	(0.060)	(0.104)	P = 0.036		
	SMA IL –	0.120	0.052	T = 2.216	n.s.	n.s.
	vPMC CL	(0.063)	(0.089)	P = 0.037		
	vPMC IL –	0.113	0.036	T = 2.497	n.s.	n.s.
	M1 CL	(0.046)	(0.097)	P = 0.020		
	SMA IL –	0.235	0.250		n.s.	r = 0.709
	M1 IL	(0.099)	(0.106)		n.s.	P = 0.007
	M1 IL –	-0.169	-0.163		n.s.	r = 0.764
	M1 CL	(0.084)	(0.087)		n.s.	P = 0.002

* Correlation did not reach significance after correction for multiple comparisons

Adjusted = the movement frequency during the fMRI experiment was adjusted to motor performance (40% of the maximum frequency)

AMT = Active motor threshold (higher value indicate lower excitability)

BA4 = Brodmann area 4 (primary motor cortex)

BA6 = Brodmann area 6 (premotor cortex)

CL = Contralesional hemisphere (dominant hemisphere in healthy subjects)

DCM-A = Endogenous effective connectivity (positive values indicate promoting influences, negative values indicate inhibitory influences)

DCM-B = modulatory effects of movements of the affected/non-dominant hand on effective connectivity (positive values indicate promoting influences, negative values indicate inhibitory influences)

Fixed = the movement frequency during the fMRI experiment was fixed (0.8 Hz)

fMRI = Functional magnetic resonance imaging

IHI = Interhemispheric inhibition (higher value indicates less inhibition)

IL = Ipsilesional hemisphere (non-dominant hemisphere in healthy subjects)

LI = Laterality index during movements of the affected/non-dominant hand

-1 = complete lateralization to the ipsilesional/non-dominant hemisphere

1 = complete lateralization to the contralesional/dominant hemisphere

0 = no lateralization

M1 = Primary motor cortex

n.s. = Not significant ($P > 0.05$, FDR-corrected for multiple comparisons)

RMT = Resting motor threshold (higher values indicate lower excitability)

ROI-CL = fMRI signal in the contralesional/dominant hemisphere during movements of the affected/non-dominant hand (higher values indicate higher signal change)

SD = Standard deviation

SICI = Short-interval intracortical inhibition (higher values indicate less inhibition)

SMA = Supplementary motor area

vPMC = Ventral premotor cortex

5.4.2.1 Electrophysiological TMS parameters

5.4.2.1.1 MEP and MT in chronic stroke patients

Corticospinal excitability of the ipsilesional hemisphere is often decreased (i.e. MT is increased) early after stroke, i.e. in acute to subacute stages (cf. 1.4.2.1.1). However, excitability of the ipsilesional hemisphere increases gradually over time (Catano et al., 1996; Heald et al., 1993; Manganotti et al., 2002; Thickbroom et al., 2002; Traversa et al., 2000; Turton et al., 1996). In the present study, we found no statistically significant difference between chronic stroke patients and healthy control subjects in motor thresholds (i.e. RMT or AMT). This finding is in line with other studies suggesting that motor thresholds of stroke patients tend to normalize in chronic stages (Floel et al., 2008; Murase et al., 2004; Nair et al., 2007). However, motor thresholds have been demonstrated to be higher in patients with more severe deficits (Catano et al., 1996; Heald et al., 1993; Manganotti et al., 2002; Pennisi et al., 2002; Thickbroom et al., 2002; Traversa et al., 2000; Turton et al., 1996; Werhahn et al., 2003). In line with these studies, we found an association between AMT and upper-limb dysfunction as indicated by ARAT scores, i.e. patients with high AMT on the ipsilesional hemisphere were more severely impaired than patients with lower AMT on the ipsilesional hemisphere. When patients were separated in more severely and mildly impaired patients according to a median split on ARAT scores, patients with more severe upper-limb dysfunction had significantly increased motor thresholds assessed for the ipsilesional (but not the contralesional) hemisphere compared to mildly impaired patients. In line with our results, Werhahn and colleagues (2003) found that excitability thresholds were significantly increased only in patients with poor recovery. Also in line with these findings, Byrnes and colleagues (2001) found increased AMT in only 3 of 10 mildly impaired chronic stroke patients. Previous studies suggest that MTs of the contralesional hemisphere are usually within normal limits in the chronic phase (Cicinelli et al., 2003; Pennisi et al., 2002; Traversa et al., 2000) which is in agreement with results of the present study.

5.4.2.1.2 SICI in chronic stroke patients

Early after stroke (i.e. in acute to subacute stages), SICI is decreased not only in the ipsilesional, but also in the contralesional hemisphere (cf. 1.4.3.1.1.1). Data on SICI in chronic patients are scarce but there is some evidence that SICI tends to normalize in chronic stages (Wittenberg et al., 2003). In the present study, we found evidence for reduced SICI in the ipsilesional, but not the contralesional hemisphere, in chronic stroke patients. Our findings are in line with a recent study of Berweck et al. (2008) who found reduced SICI on the ipsilesional hemisphere in patients with congenital cortico-subcortical stroke. Shimizu and colleagues (2002) found that SICI was decreased in 12 patients with cortical lesions but was unchanged in patients with subcortical lesions, whereas, others found that SICI was independent of lesion site (Cicinelli et al., 2003; Manganotti et al., 2002). The functional role or consequences of reduced SICI are still unclear. Neural circuits involved in SICI are thought to focus excitatory motor input onto appropriate outputs, and hence reduced SICI may lead to problems in selecting appropriate combinations of muscles in a particular movement (Talelli et al., 2006). Alternatively, reduced SICI has also been suggested to increase excitability of remaining output immediately after the injury, which might allow functional reorganization in the long run by unmasking alternative pathways. Correlations between SICI and clinical recovery are conflicting. Manganotti et al. (2002) found that normalisation of SICI on the contralesional hemisphere was associated with recovery. However, Butefisch et al. (2003) found that especially patients with good clinical progress showed a shift of intracortical excitability towards facilitation in the contralesional hemisphere and Liepert and colleagues did not find any relation (Liepert et al., 2000; Shimizu et al., 2002). In the present study, reduced SICI in the ipsilesional hemisphere tended to be associated with better performance of the affected hand which supports the hypothesis that decreased SICI might be supportive.

5.4.2.1.3 IHI in chronic stroke patients

In the subacute stage, IHI from the ipsilesional to the contralesional hemisphere was demonstrated to be reduced whereas IHI in the opposite direction remained unchanged (cf. 1.4.3.2.1.1). In the present study, we found no significant difference between chronic stroke patients and healthy control subjects in IHI. In line with this finding, Shimizu and colleagues (2002) found a significant relationship between IHI and duration of the disease, which indicates that IHI targeting the contralesional hemisphere is reduced in patients early after

stroke (< 4 months), but tends to normalize with time. Our finding is also in line with results of Murase and colleagues (2004) who found that IHI was not significantly different between patients in the chronic phase and healthy controls if assessed in resting conditions. Interestingly, Murase et al. (2004) and Duque et al., (2005) also investigated the time-dependent modulation of IHI during movement preparation. Both studies reported significant disturbances in chronic stroke patients with subcortical lesions compared to healthy controls (Duque et al., 2005; Murase et al., 2004). Whereas healthy subjects showed a reversal from IHI into IHF (from the “resting” onto the “active” hemisphere) shortly before movement initiation, IHI targeting the ipsilesional hemisphere persisted uninfluenced from movement preparation of the affected hand in chronic stroke patients (Duque et al., 2005; Murase et al., 2004). This finding was specific for movements of the paretic hand, since IHI targeting the contralesional hemisphere during movement preparation of the unaffected hand was unchanged in stroke patients compared to controls (Duque et al., 2005). Interestingly, persistence of IHI targeting the ipsilesional hemisphere was significantly associated with severity of motor deficits (Murase et al., 2004) suggesting a detrimental role of the contralesional hemisphere during paretic hand movements. The relationship between IHI measured at rest and clinical impairment is unknown but results of the present study suggest that chronic patients with preserved inhibition of the contralesional hemisphere at rest are less severely affected. This finding is in line with growing body evidence suggesting hemispheric imbalance and a detrimental role of the contralesional hemisphere in chronic stroke patients.

In summary, our data suggest that MTs and reciprocal IHI at rest tend to normalize in the chronic phase. However, more severely affected stroke patients may still show decreased excitability (i.e. increased MTs) on the ipsilesional hemisphere and reduced IHI from the ipsilesional to the contralesional hemisphere. Patients had significantly reduced SICI on the ipsilesional hemisphere which was associated with better motor performance of the affected hand suggesting a supportive role of reduced SICI resulting in maximum possible corticospinal output of the ipsilesional hemisphere by unmasking of alternative neuronal pathways.

5.4.3 Movement related fMRI signal

5.4.3.1 Movement related fMRI signal in healthy subjects

In line with previous reports, healthy subjects showed increased fMRI BOLD signal in contralateral primary motor cortex (M1), contralateral primary somatosensory cortex (S1), bilateral supplementary motor area (SMA), and bilateral ventral and dorsal premotor cortex (vPMC, dPMC) during movement execution (Richter et al., 1997). Although neural activity during movement execution might be bilaterally organised in healthy subjects, activity in cortical motor areas is more lateralized to the hemisphere contralateral to the movement (Mattay & Weinberger, 1999; Richter et al., 1997). Activity in M1 is particularly lateralized to the contralateral hemisphere and activity in ipsilateral M1 occurs only at high levels of task complexity (Mattay et al., 1998).

5.4.3.2 Movement related fMRI signal early after stroke

In a very recent study, Rehme and colleagues (2011b) investigated movement-related fMRI BOLD signal in 11 stroke patients from the acute to the subacute phase (starting within 3 days and up to 2 weeks after stroke). Initially mildly impaired patients showed relatively constant motor network activity, and hence did not differ significantly from healthy control subjects at any time point. In contrast, severely affected patients showed a global reduction in movement-related fMRI BOLD signal, followed by a gradual increase, predominantly in motor areas of the contralesional hemisphere. Increases of activity in M1 and PMC of the contralesional hemisphere were significantly associated with recovery of function in severely affected patients, suggesting a supportive role of the contralesional hemisphere in the early phase after stroke. Ward and colleagues (2003a) investigated movement-related fMRI BOLD signal in 8 stroke patients from 9-14 days up to one year after stroke (i.e. from the subacute to the chronic phase). This study can be seen as continuation of the study of Rehme et al. (2011b) since stroke patients had comparable clinical deficits after two weeks (i.e. at the last time point in the study of Rehme et al. and the first time point in the study of Ward et al.). Interestingly, Ward et al. (2003a) found that from two weeks post-stroke on, task-related fMRI BOLD signal showed a decrease over time in similar motor regions that showed an increase in the early phase after stroke, i.e. bilateral M1, dPMC, vPMC, and SMA. This later decrease of activity was significantly associated with recovery of function (Ward et al.,

2003a) which strongly suggests a detrimental role of activity in the contralesional hemisphere in later stages of the disease.

5.4.3.3 Movement related fMRI signal in chronic stroke patients

The fMRI group analysis of the present study indicates that chronic stroke patients with persistent motor hand deficits maintain bilaterally enhanced fMRI BOLD signal in cortical motor areas during movements of the affected hand (but not the unaffected hand) compared to healthy controls. This enhancement led to wide-spread activity in the ipsilesional hemisphere and activity in homologue areas of the contralesional hemisphere (ipsilateral to hand movements) including contralesional M1/S1. This finding is in line with previous reports of bilaterally enhanced fMRI BOLD signal during movements of the affected hand in stroke patients (Binkofski & Seitz, 2004; Cao et al., 1998; Chollet et al., 1991; Cramer et al., 1997; Grefkes et al., 2008b; Jaillard et al., 2005; Loubinoux et al., 2003; Seitz et al., 1998; Weiller et al., 1992; Ward et al., 2003b). Several studies indicate that more bilaterally enhanced fMRI signal is associated with poor motor performance (Calautti et al., 2001; Loubinoux et al., 2003; Ward et al., 2003b; Weder et al., 1994) and more pronounced CST damage (Newton et al., 2006; Schaechter et al., 2008; Stinear et al., 2007; Ward et al., 2006, 2007).

In line with findings from the fMRI group analysis, we found significant differences between healthy subjects and stroke patients in LI depicting lateralization of fMRI signal in BA4 (M1). Stroke patients showed significantly reduced lateralization of fMRI signal during movements of the paretic hand, particularly in M1, due to overactivity in contralesional M1. Presumably, laterality of fMRI signal in stroke patients was particularly decreased in M1 (but did not reach significance in PMC or over both areas) because healthy subjects show neural activity nearly exclusively in (contralateral) M1/S1 during unilateral hand movements (Mattay et al., 1998; Rao et al., 1993), whereas neural activity in PMC tends to be more bilaterally organized, even in healthy subjects (Deiber et al., 1991; Kim et al., 1993; Rao et al., 1993; Shibasaki et al., 1993). In line with these findings, Cramer et al. (1997) found that the region which most frequently showed an increase in stroke patients compared to healthy controls during finger tapping was contralesional M1/S1. Interestingly, there is evidence that reduced lateralization in M1/S1 (depicted by LI) is associated with poor motor performance (Marshall et al., 2000).

5.4.4 The functional role of the contralesional hemisphere

It must be mentioned, however, that the functional role of enhanced neural activity in the contralesional hemisphere is still controversial (Butefisch et al., 2005; Fregni et al., 2006; Grefkes et al., 2008b, 2010; Johansen-Berg et al., 2002; Lotze et al., 2006; Murase et al., 2004; Ward et al., 2003b). It is to a large extent unclear whether stroke induced changes reflect adaptive or maladaptive brain organization, motor performance compensation or merely epiphenomena, such as the release of the contralesional hemisphere from suppression of the ipsilesional hemisphere. Findings which strongly suggest enhanced neural activity in the contralesional hemisphere is detrimental for motor performance of the paretic hand are: (i) the finding that bilateral enhancement of fMRI signal decreases (i.e. LI increases) concomitant to motor recovery (Ward et al., 2003a; Marshall et al., 2000), (ii) findings of pathologically increased IHI from the contralesional M1 onto the ipsilesional M1 suggested by both paired-pulse TMS during movement preparation and DCM (Duque et al., 2005; Grefkes et al., 2008b, 2010; Murase et al., 2004), and (iii) the finding that behavioural improvements of the affected hand have been observed after inhibitory rTMS applied to the contralesional hemisphere (Fregni et al., 2006; Mansur et al., 2005; Takeuchi et al., 2005). However, there are also few studies which suggest that enhanced neural activity in the contralesional hemisphere may be supportive for motor performance of the affected hand. For instance enhanced neural activity was also found in patients with excellent motor recovery in the subacute (Butefisch et al., 2005) or subacute to chronic phase (Weiller et al., 1992). Additionally, several TMS studies suggest a beneficial role of the contralesional hemisphere (Bestmann et al., 2010; Johansen-Berg et al., 2002; Lotze et al., 2006). For instance, TMS pulses (disrupting information processing of the target area; Cohen et al., 1997) deteriorated motor performance of the paretic hand if applied to contralesional dPMC (Johansen-Berg et al., 2002; Lotze et al., 2006), contralesional M1 (Lotze et al., 2006) or contralesional SPL (Lotze et al., 2006) in chronic stroke patients. Interestingly, deteriorations after stimulation over ipsilateral dPMC were not seen in healthy subjects and were more pronounced in more severely affected patients (Johansen-Berg et al., 2002) which suggests that activity in contralesional dPMC might compensate for damaged or disconnected regions particularly in severely affected patients. This suggestion is further supported by a very recent study of Bestmann et al. (2010) who measured the interhemispheric influence between contralesional dPMC and ipsilesional M1 with TMS concurrently with a grip-force task during fMRI examination in chronic stroke patients. The authors observed that severely impaired patients

exerted less inhibitory (i.e. more facilitatory) influences from contralesional dPMC to ipsilesional M1. The level of BOLD response in ipsilesional M1 was depending on the magnitude of this facilitatory TMS influence from contralesional dPMC (Bestmann et al., 2010).

5.4.5 Dynamic Causal Modelling (DCM)

5.4.5.1 Effective connectivity in healthy subjects

5.4.5.1.1 Endogenous (task-independent) effective connectivity

Endogenous effective connectivity reflects interregional coupling in absence of a specific task. It is influenced by the experimental design of the study and hence cannot be directly compared between studies but only between groups within the same study. Nonetheless, there are several features of endogenous effective connectivity in healthy subjects, which are remarkably constant across studies using blocks of unilateral hand movements such as rhythmic fist closures (Rehme et al., 2011a) or index finger tappings (Wang et al., 2011). In line with findings of the present study, previous studies reported a pattern of interregional coupling between cortical motor areas (M1, SMA, vPMC bilaterally) which was symmetrically organized in healthy subjects (Rehme et al., 2011a; Wang et al., 2011). Also in line with data of the present study, the majority of intra- and interhemispheric connections was facilitatory and the promoting influence from the SMA onto the ipsilateral M1 was particularly pronounced (Rehme et al., 2011; Wang et al., 2011). Like in the present study, only reciprocal interhemispheric connections between both primary motor cortices were inhibitory (Rehme et al., 2011; Wang et al., 2011).

5.4.5.1.2 Modulatory effects of hand movements on effective connectivity

Modulatory effects of hand movements on effective connectivity within the cortical motor network depend on the specific task which is performed. However, blocks of unilateral hand movements, such as rhythmic fist closures (Grefkes et al., 2008a) or index finger tappings (Wang et al., 2011) are associated with increased promoting influences from premotor areas (SMA and vPMC) of both hemispheres onto the M1 contralateral to the moving hand. Additionally, there are inhibitory influences from premotor areas (SMA and vPMC) of both hemispheres onto the M1 ipsilateral to the moving hand (Grefkes et al., 2008a; Wang et al.,

2011). Effective connectivity from the ipsilateral M1 onto the contralateral M1 is usually near zero, and hence nonexistent in healthy subjects. In contrast, there is usually significant inhibition from the contralateral M1 onto the ipsilateral M1 during unilateral hand movements (Grefkes et al., 2008a; Wang et al., 2011).

5.4.5.2 Effective connectivity early after stroke

A very recent study investigated changes in effective connectivity from the acute to the early chronic stage in 12 stroke patients and 12 healthy control subjects by means of DCM (Rehme et al., 2011a). In the following, results are separately summarized for endogenous effective connectivity and modulatory effects of hand movements.

5.4.5.2.1 Endogenous (task-independent) effective connectivity

Analyses on endogenous (i.e. task-independent) connectivity suggest that two connections are particularly relevant for stroke recovery: (i) the promoting influence from ipsilesional SMA onto ipsilesional M1, and (ii) the inhibitory influence from ipsilesional M1 onto contralesional M1. Endogenous effective connectivity was significantly reduced in both connections in stroke patients in the acute and the subacute phase compared to healthy controls. More pronounced reductions were seen in patients with more severe initial deficits. Coupling strength in both connections gradually increased from the acute to the early chronic stage concomitant to motor recovery and was not significantly different from healthy subjects in the early chronic stage (3 to 6 months after stroke). These findings strongly suggest motor recovery depends on normalization of effective connectivity in these motor network connections (Rehme et al., 2011a).

5.4.5.2.2 Modulatory effect of hand movements on effective connectivity

Modulations of effective connectivity induced by movements of the non-paretic hand were not significantly different between healthy subjects and stroke patients in the acute or the subacute phase (Rehme et al., 2011a). However, there were significant differences between healthy subjects and stroke patients in modulations of effective connectivity induced by movements of the affected hand. Three connections were particularly relevant: (i) the promoting influence from ipsilesional SMA onto ipsilesional M1, (ii) the inhibitory influence

from ipsilesional M1 onto contralesional M1, and (iii) the inhibitory influence from contralesional M1 onto ipsilesional M1. Results for the first two connections were similar to results of analyses on endogenous connectivity. The inhibitory influence from contralesional M1 to ipsilesional M1, however, showed different time dependent modulations. This connection showed no significant difference to healthy controls in the acute stage. In the subacute phase, there was an additional positive influence from contralesional M1 onto ipsilesional M1 (not seen in healthy subjects), especially in more severely affected patients. This finding suggests a supportive role of the contralesional hemisphere in early stages of the disease. The positive coupling between contralesional M1 and ipsilesional M1 vanished in the early chronic stage, and hence resembled levels observed in healthy subjects. However, patients who developed strong inhibitory influences from the contralesional M1 onto the ipsilesional M1 during transition from the subacute to the early chronic phase had considerably poorer outcome in the early chronic phase. Hence, this finding suggests a detrimental role of the contralesional hemisphere in later stages of the disease.

5.4.5.3 Endogenous connectivity in chronic stroke patients

Stroke patients may show various alterations in motor network interactions, not only within the ipsilesional hemisphere, but also between hemispheres, which demonstrates that stroke lesions have system-wide impact on functional motor network architecture (Grefkes & Fink, 2011; Westlake & Nagarajan, 2011). Connectivity studies in stroke patients with motor deficits seem to reach highest consensus on two findings: (i) effective connectivity within the ipsilesional hemisphere is decreased (particularly from ipsilesional SMA to ipsilesional M1) and (ii) interhemispheric inhibition between primary motor cortices is altered (reduced from ipsilesional M1 to contralesional M1; increased from contralesional M1 to ipsilesional M1; Grefkes & Fink, 2011; Westlake & Nagarajan, 2011). In the present study, chronic stroke patients showed significantly reduced endogenous (i.e. task-independent) effective connectivity originating from ipsilesional premotor areas (ipsilesional SMA and vPMC) when compared to healthy control subjects (Figure 5.11A). Interestingly, this finding is in agreement with a recent study demonstrating decreased endogenous coupling originating from ipsilesional SMA and vPMC in 11 stroke patients (9 in the chronic stage; 2 in the subacute stage) compared to 11 healthy control subjects (Wang et al., 2011). In summary, these findings suggest “hypoconnectivity” of ipsilesional SMA and vPMC in chronic stroke patients in absence of a specific task.

During movements of the paretic hand, patients showed significantly reduced inhibition of the contralesional (i.e. ipsilateral) M1 exerted by contralesional and ipsilesional SMA, and ipsilesional M1 compared to healthy controls (Figure 5.11B, Figure 5.11C). This “disinhibition” of the contralesional hemisphere during movements of the affected hand was found for both movement conditions and correlated inversely with clinical impairment, suggesting that inhibition of the contralesional M1 was particularly reduced in more severely affected patients. Also in the study of Wang et al. (2011), patients in the subacute to chronic stage showed decreased inhibition from ipsilesional M1 and contralesional vPMC to contralesional M1 during index finger tapping with the affected hand compared to healthy controls. Longitudinal observations of effective connectivity from the acute to the early chronic phase indicate that inhibition from ipsilesional M1 to contralesional M1 gradually increases over time and that regains of inhibition are associated with motor recovery (Rehme et al., 2011). This finding strongly suggests that “disinhibition” of the contralesional M1 is associated with poor motor performance. In summary, these findings suggest “disinhibition” of contralesional M1, particularly by ipsilesional M1, during movements of the affected hand, particularly in more severely affected stroke patients.

Two studies strongly suggest that interhemispheric inhibition from contralesional M1 to ipsilesional M1 may be pathologically increased in stroke patients (Grefkes et al. 2008b, 2010). In the first study, Grefkes et al. (2008b) investigated effective connectivity in 12 stroke patients with subcortical lesions in the subacute phase (≥ 5 months after stroke) and 12 healthy control subjects by means of DCM and demonstrated that patients showed significant inhibition from contralesional M1 onto the “active” ipsilesional (i.e. contralateral) M1 during movements of the affected hand which was not present in healthy subjects or stroke patients moving their unaffected hand (Grefkes et al., 2008b). Interestingly, the extent of this inhibition was significantly correlated with the motor deficit, i.e. the more pronounced inhibition from contralesional M1 to ipsilesional M1 was, the stronger the motor hand deficit. This finding suggests a detrimental role of the contralesional hemisphere during movements of the paretic hand as proposed by the *model of interhemispheric competition*. These findings are further supported by a later study investigating the effect of 1 Hz rTMS on motor network interactions by means of DCM (Grefkes et al., 2010). Interestingly, 1 Hz rTMS applied to the contralesional hemisphere (but not control stimulation over vertex) significantly decreased inhibition originating from contralesional M1 onto ipsilesional M1 during paretic hand movements. Furthermore, 1 Hz rTMS was associated with increased endogenous positive

coupling between ipsilesional SMA and ipsilesional M1 suggesting that 1 Hz rTMS acts by reconstituting physiological network interactions in stroke patients (Grefkes et al., 2010).

However, in contrast to Grefkes et al. (2008b, 2010), we did not find pathologically increased interhemispheric inhibition from contralesional M1 to ipsilesional M1 in our group of chronic patients compared to controls. This might be because in studies of Grefkes et al. (2008b, 2010), movement frequencies in the motor task were not matched to decreased motor performance of stroke patients, and hence stroke patients were overstrained by the task. In contrast, in the present study, the adjusted movement condition (40% of max.) as well as the fixed movement condition (0.8 Hz) could be readily performed by all patients. In other words, excessive demands could lead to pathologically increased interhemispheric inhibition observed in studies of Grefkes et al. (2008b, 2010). Another possible explanation might be that the functional role of the contralesional hemisphere depends on the clinical state of the patient. Although activation of the contralesional hemisphere appears to be maladaptive in relatively mildly affected patients it could be beneficial in more severely affected patients. Patients in the study of Grefkes et al. (2008b) were less severely impaired than patients in the present study as indicated by mRS scores (Table 5.1). There was a statistical trend for a correlation between mRS score and inhibition from the contralesional M1 to the ipsilesional M1 ($r = 0.491$; $P = 0.088$) indicating that more severely affected patients showed reduced rather than increased inhibition from contralesional to ipsilesional M1. In fact, the most severely affected patient (Patient 04) even showed a promoting influence from contralesional M1 to ipsilesional M1. Interestingly, patients in the study of Rehme et al. (2011a) showed significant promoting influence from contralesional M1 to ipsilesional M1 compared to healthy controls. However, this was only the case at the time point at which patients had similar deficits as patients in the present study (mean ARAT score: 45 ± 12 ; Rehme et al.: 45 ± 19). The degree of this promoting influence from contralesional M1 to ipsilesional M1 was significantly correlated with clinical impairment and occurred particularly in more severely affected patients. Also in the present study, patients showed a promoting influence from contralesional M1 to ipsilesional M1 (Figure 5.10A). The difference between patients and controls (no such influence) was significant ($P < 0.05$) but did not pass correction for comparisons in the present study. In the study of Rehme et al. (2011a), the promoting influence disappeared in the early chronic phase in which patients had nearly fully recovered (mean ARAT 55 ± 3 ; highest possible score: 57). Taken together these findings suggest that fully recovered patients show interhemispheric balance comparable to healthy subjects,

whereas the impairment of mildly affected patients might be caused by pathologically increased IHI onto the ipsilesional hemisphere. In contrast, more severely affected patients seem to rely on recruitment of the contralesional hemisphere. This suggestion is further strengthened by studies disrupting or inhibiting dPMC by means of TMS (Fridman et al. 2004; Johansen-Berg et al., 2002). Inhibition of contralesional dPMC by means of TMS caused deterioration of motor performance in the affected hand of stroke patients suggesting a supportive role of the contralesional dPMC (Johansen-Berg et al., 2002). However, less affected patients have been demonstrated to preferentially recruit the ipsilesional dPMC if this is spared by the lesion (Fridman et al., 2004).

5.4.6 Prediction of TBS effects

5.4.6.1 Electrophysiological TMS parameters

This is the very first study which investigated the relationship between TMS parameters at baseline and behavioural improvements following TBS in stroke patients. Stroke patients may show decreased corticospinal excitability (i.e. increased MTs) assessed over the ipsilesional hemisphere and there is evidence that higher MTs are associated with poor motor performance (Manganotti et al., 2002; Thickbroom et al., 2002; Traversa et al., 2000). Two causes might account for increased MTs: (i) changes in membrane properties (which are thought to play a major role in primarily cortical stroke) and (ii) severe reductions in number of corticospinal axons (which is thought to play a major role in subcortical stroke; Talelli et al., 2006). AMT is thought to be less influenced by spinal cord activity than RMT. Our results indicate that, both AMT and RMT at baseline are not significantly associated with behavioural improvements after TBS. Hence, our results indicate that motor cortex excitability is a poor predictor for behavioural improvements following TBS. It has been demonstrated that rTMS impacts on areas far beyond the stimulated region and involve various subcortical and cortical regions functionally related to the targeted area (Bestmann et al., 2003; Paus et al., 1997) which makes it likely that excitability of the primary motor cortex alone is not sufficient for improvements after TBS, which might rather rely on motor network interactions within and between hemispheres.

SICI is thought to reflect intracortical inhibition mediated by GABA_A receptors (Di Lazzaro et al., 2000; Ilic et al., 2002; Ziemann et al., 1996) and tends to be decreased both on the

ipsilesional as well as the contralesional hemisphere (Liepert et al., 2000; Manganotti et al., 2002). No consensus has been reached across studies whether decreased SICI is beneficial or detrimental (Talelli et al., 2006). Our results indicate that, SICI at baseline is not significantly associated with behavioural improvements after TBS. This finding indicates that intracortical inhibition within the primary motor cortex constitutes a poor predictor for TBS effects. Hence, generation of TBS effects might rely on the interplay of M1 with other motor areas.

IHI is thought to reflect interhemispheric cortical inhibition mediated by transcallosal glutamatergic pathways linking with pyramidal tract neurons through GABAergic interneurons (Reis et al., 2008). IHI from the ipsilesional to the contralesional hemisphere measured at rest tends to be reduced (especially early after stroke and in patients with damaged transcallosal fibre tracts; Boroojerdi et al., 1996; Butefisch et al., 2008; Shimizu et al., 2002) whereas IHI from the contralesional to the ipsilesional hemisphere is unchanged if measured at rest (Butefisch et al., 2008). Whether disinhibition of the contralesional hemisphere has a supportive or detrimental role has been controversially discussed but we found evidence for the hypothesis that reduced inhibition of the contralesional hemisphere is associated with more severe motor impairment. Our results indicate that, there is no significant association between IHI and behavioural improvements after TBS which indicates that disinhibition of the contralesional hemisphere at rest measured by paired-pulse TMS is a poor predictor for TBS effects. Interestingly, we found that disinhibition of the contralesional hemisphere probed by DCM was a strong predictor for TBS effects. Possible explanations for divergent results will be discussed in paragraph 4.4.6.3.

In summary, TMS studies demonstrated that stroke patients may show increased MTs on the ipsilesional hemisphere, decreased SICI on both hemispheres, and decreased IHI from the ipsilesional onto the contralesional hemisphere (at rest) as well as increased IHI from the contralesional to the ipsilesional hemisphere (during movement preparation). Particularly, increases in MT and imbalance in IHI are associated with poor motor performance. However, none of these TMS parameters could predict behavioural TBS effects in a satisfactory manner.

5.4.6.2 fMRI activation pattern and DCM parameters

The main finding of the present study was that behavioural improvements of the affected hand induced by facilitatory iTBS applied to the ipsilesional hemisphere were predicted by several fMRI parameters at baseline (Table 5.4) indicating more intact functional motor network architecture:

- 1) An fMRI activation pattern which was more lateralized towards the ipsilesional hemisphere during movements of the affected hand ($LI_{BA4+BA6}$ & LI_{BA6})
- 2) More pronounced promoting influence from ipsilesional SMA to ipsilesional M1 in absence of a specific task (endogenous effective connectivity)
- 3) More pronounced inhibitory influence from ipsilesional M1 to contralesional M1 in absence of a specific task (endogenous effective connectivity)

None of the parameters that predicted TBS effects was significantly different between healthy subjects and stroke patients or was significantly correlated with clinical impairment. Or in other words, none of the parameters which were altered in stroke patients compared to controls or which correlated with clinical deficits predicted TBS effects (Table 5.4). Hence, in parameters with relatively low variance we were able to find significant group differences (but variations were too low to explain variations in TBS effects) in contrast parameters with relatively high variance did not result in a group difference but were much more successful in explaining variance in TBS effects since they reflected a broader spectrum from more physiological to more pathological across the group of patients.

There is strong evidence from longitudinal studies that bilaterally enhanced fMRI signal (Ward et al., 2003a) and reduced laterality (Marshall et al., 2000) are associated with poor motor performance. Additionally, reduced promoting influence from ipsilesional SMA to ipsilesional M1 and reduced inhibitory influence from ipsilesional M1 to contralesional M1 are associated with poor motor performance (Rehme et al., 2011a).

Hence, our findings strongly suggest that particularly patients with more physiological motor network interactions experienced beneficial effects of iTBS applied to the ipsilesional hemisphere. Hence, these network interactions might constitute crucial preconditions for the generation of positive TBS effects. This finding appears highly plausible. Nonetheless it is a true gain of knowledge since the alternative could also have turned out, i.e. that particularly patients with severely disturbed motor network interactions improve after TBS, which has

been demonstrated to normalize motor network disturbances (Grefkes et al., 2010). Hence, it could have been that the “network shaping effect” of TBS would have been lower in patients which have already relatively efficient motor network architecture which would correspond to some kind of “ceiling effect”. This suggestion is however contradicted by the finding that TBS may improve motor performance even in healthy subjects (Huang et al., 2005). Taken together, results of the present study strongly suggest that improvements after facilitatory iTBS applied to the ipsilesional hemisphere relies on integrity of the cortical motor network, i.e. preserved supportive role of the ipsilesional SMA and preserved inhibition of the contralesional hemisphere.

Until now, studies investigating predictors for rTMS effects by means of neuroimaging are scarce (Ameli et al., 2009; Grefkes et al., 2010; Nowak et al., 2008). Nowak and colleagues (2008) investigated the effect of inhibitory 1 Hz rTMS applied to the contralesional hemisphere in 15 patients with subcortical lesions in the subacute to early chronic stage (4 weeks to 4 months after stroke) and found that 1 Hz rTMS significantly reduced neural overactivity in the contralesional hemisphere, focussed activity in the ipsilesional hemisphere, and increased the maximum index finger tapping frequency of the affected hand. However, reduction of fMRI BOLD signal in the contralesional hemisphere was not significantly associated with behavioural improvements of the affected hand. This finding appears to be in line with our finding that reduced corticospinal output from the contralesional hemisphere was not significantly associated with behavioural improvements of the affected hand. In line with our findings, there was no significant correlation between fMRI BOLD signal in contralesional M1 and behavioural improvements of the affected hand after rTMS in the study of Nowak et al. (2008). However, overactivity of the adjacent contralesional dPMC, as well as contralesional parietal operculum, and ipsilesional mesial frontal cortex at baseline predicted improvement of the affected hand after rTMS applied to contralesional M1 in the study of Nowak et al. (2008). Ameli and co-workers (2009) investigated the effect of facilitatory 10 Hz rTMS applied to the ipsilesional hemisphere in 16 patients with subcortical and 13 patients with cortico-subcortical stroke lesions. Patients were in the subacute to chronic stage of their disease (1-88 weeks after stroke). Interestingly, the majority of patients with subcortical stroke, but none of the patients with cortico-subcortical stroke, showed improvements of the paretic hand after 10 Hz rTMS applied to the ipsilesional hemisphere. Approximately half of the patients with cortico-subcortical lesions showed deterioration of motor performance of the

affected hand after rTMS applied to the ipsilesional hemisphere. Interestingly, stroke patients, showing no change or even deterioration after facilitatory 10 Hz rTMS applied over ipsilesional M1, had reduced ipsilesional M1 activation levels prior to rTMS and pathologically enhanced activation levels in the contralesional hemisphere after rTMS. The authors argued that stimulation of a dysfunctional M1 may have unexpected or even opposite effects compared to what is observed in healthy subjects or in patients with rather normal M1 activity (Ameli et al., 2009). This conclusion is strongly supported by the findings of the current study, and also explains that only stimulation of the contralesional, i.e. “unaffected”, hemisphere yielded TBS effects which can be observed in healthy subjects (Huang et al., 2005).

5.4.6.3 Correlation between IHI probed by DCM and paired-pulse TMS

Endogenous DCM coupling parameters and paired-pulse TMS at rest yielded measures of IHI which were not significantly related to each other, neither in healthy subjects nor in stroke patients. Behavioural TBS effects were significantly predicted by inhibition from the ipsilesional M1 to the contralesional M1 if probed by DCM but not if probed by paired-pulse TMS. Taken together, these findings underpin methodological differences between approaches. Differences between IHI measured by DCM and TMS might result from several methodological differences such as (i) signal types used as outcome measures, (ii) anatomical structures involved, and (iii) activation state. At first glance, the most striking difference between measures of DCM and TMS seems to be the signal type used as outcome measure. Whereas DCM relies on fMRI data which is a neurovascular signal, TMS uses an EMG response, i.e. a signal from a muscle as outcome measure. Hence, differences between approaches might arise from involvement of haemodynamic mechanisms (in DCM) or spinal cord excitability (in TMS). However, DCM explicitly acts on the neuronal level thereby avoiding confounds arising from neurovascular influences (Friston et al., 2003) and IHI has been demonstrated to act predominantly on the cortical level which reduces confounds arising from spinal cord excitability (Ferber et al., 1992). Two experiments by Ferbert et al. (1992) indicate that IHI measured with paired-pulse TMS acts on the cortical level. These experiments tested whether application of a normal cortical CS applied by TMS impacts on test signals generated more downstream of the cortical level. In the first experiment, the authors found that a CS had no effect on H-reflexes (generated at the level of the spinal cord), which indicates that inhibition (during normal assessment of IHI) is not mediated by activity

in a direct ipsilateral inhibitory pathway to motoneurons of the spinal cord. In a second experiment, Ferbert et al. (1992) demonstrated that a CS had no effect on a cortical TS applied by electric (instead of magnetic) stimulation. The rationale for this second experiment was that TMS excites neurons either directly or transsynaptically, whereas transcranial electric stimulation (TES) excites axons directly in the white matter (Di Lazzaro et al., 1998a). Hence, test responses applied by TMS are much more influenced by cortical excitability (Datta et al., 1989; Day et al., 1991; Ugawa et al., 1991) and the absence of an inhibitory effect on a TS generated by TES suggests that IHI primarily occurs at the cortical level (Ferbart et al., 1992).

Another explanation why TMS and DCM yielded different results for IHI might be that slightly different positions were used. For TMS we used the hotspot position, i.e. the position yielding highest EMG responses when stimulated with TMS. This is the most commonly used procedure and ensures stimulation of the most excitable cortex position (which was necessarily to generate MEPs with peak-to-peak amplitude of 1mV in stroke patients). For DCM however, we used the fMRI activation peak within an anatomically defined landmark for the motor hand region (i.e. the “hand knob” formation; Yousry et al., 1997). This is also the most common procedure and ensures inclusion of the cortical position with highest fMRI BOLD signal. Hence, we optimised procedures for each technical approach but results of Study I & II of the present thesis demonstrate that the hotspot position is not necessarily within M1 but might be more anterior within the PMC. Hence, a functional role of the PMC in generation of IHI measured by TMS cannot be entirely excluded. Since the PMC has anatomical connections to contralateral PMC as well as contralateral M1 (McGuire et al., 1991; Rouiller et al., 1994), transcallosally mediated inhibition could also (at least partially) take place between PMC and the contralateral PMC or contralateral M1. Hence, DCM might reflect a more valid measure of the M1-M1 connection than stimulation of the hotspot position by means of TMS.

The third, and probably most likely, cause for differences observed between IHI measured by DCM and TMS might arise from state of activation. During assessment of IHI by means of TMS subjects were at rest. However, as stated earlier, endogenous effective connectivity may not be mistaken as effective connectivity during the baseline condition. It reflects the effective connectivity over the entire time course of the experiment independent of which experimental condition is currently performed. Hence, endogenous connectivity is always present and task-specific modulations add onto it. However, although it is independent of presence or absence

of a specific task that is (or is not) currently performed, endogenous connectivity is not independent of tasks implemented in the experiment. In other words, endogenous connectivity is always specific to a certain experiment, i.e. the result would be different if different experimental conditions would be implemented (Friston et al., 2003). Hence, it appears reasonable that IHI measured by paired-pulse TMS in the resting condition yielded divergent results compared to endogenous effective connectivity which does not reflect “baseline connectivity”.

5.4.6.4 Clinical impairment as predictor for TBS effects

There was a statistical trend for a negative correlation between mRS-score and improvements of the affected hand after iTBS applied to the ipsilesional hemisphere. This result provides some evidence that patients with less severe general disability were more likely to improve after iTBS than more severely affected patients. Hence, this finding points in a similar direction as results from fMRI and DCM analyses suggesting that patients with physiological motor network interactions are more likely to improve. Note however, that the modified Rankin-Scale (mRS) is a very rough estimate of clinical impairment. Clinical scales which are more specific for *motor* impairment such as the ARAT did not show correlations with TBS effects.

5.4.6.5 Lesion characteristics as predictors for TBS effects

The VBSM analyses suggested an association between lesions comprising a specific region within the CST (MNI coordinates XYZ: 28, -15, 26) and improvements of the affected hand after iTBS. Note, that only positions which are affected by a lesion can show a correlation in VBSM analyses. The reason why particularly this position showed a correlation might be that it showed highest lesion overlap between patients (Figure 5.1). However, this position is also likely to comprise descending motoneurons in high density. Hence, this finding suggests that facilitatory iTBS applied to the ipsilesional hemisphere is less effective in patients in whom descending fibres from ipsilesional M1 are dissected at the level of the CST. Hence, integrity of the CST may be one factor influencing the effectiveness of rTMS applied over ipsilesional M1. Previous studies demonstrated that both, functional integrity of the CST probed by single-pulse TMS (Rapisarda et al., 1996; Stinear et al., 2007) and structural integrity of the CST probed by DTI (Stinear et al., 2007), constitute reliable indicators of motor recovery of

the affected upper limb after stroke. Presence of MEPs in the affected upper limb is a predictor for relevant motor recovery (Stinear et al., 2007). If MEPs are absent in the affected upper extremity, the possibility for relevant motor recovery declines with increasing CST damage assessed by means of DTI (Stinear et al., 2007). Impaired integrity of the CST after stroke has also been demonstrated to be associated with increases in neural activity within the ipsilesional hemisphere (Stinear et al., 2007; Ward et al., 2006) and enhanced recruitment of M1 and premotor areas in the contralesional hemisphere (Rehme et al., 2011b; Schaechter et al., 2008; Ward et al., 2006) during movements of the affected hand.

In summary, our findings that both integrity of the CST and bilaterally enhanced fMRI signal were predictors for motor improvements of the affected hand after iTBS applied to the ipsilesional hemisphere, are supported by previous studies demonstrating a relation between integrity of the CST and motor recovery (Rapisarda et al., 1996; Stinear et al., 2007) and between integrity of the CST and enhanced neural activity in the contralesional hemisphere (Rehme et al., 2011b; Schaechter et al., 2008; Ward et al., 2006).

5.4.6.6 Absence of predictors for effects of cTBS

In the present study we found several reliable predictors for improvements of the affected hand after facilitatory iTBS applied to the ipsilesional hemisphere. In contrast, there were no reliable predictors for improvements of the affected hand after inhibitory cTBS applied to the contralesional hemisphere. At a first glance, one might expect that the reason for this was that iTBS was more effective than cTBS in patients of the present study. Previous studies demonstrated stronger and more consistent effects for iTBS compared to cTBS in stroke patients (cf. 5.4.1). However, we found no support for this hypothesis since iTBS and cTBS were not significantly different from each other in behavioural improvements over the group of patients (mean improvement iTBS: $-0.8 \pm 10.1\%$; cTBS: $-0.9 \pm 11.2\%$). In other words, both stimulation strategies resulted in highly variable responses and none of them was more or less effective than the other. Only effects of iTBS were highly-significantly predicted by laterality of fMRI signal and DCM coupling parameters, whereas effects of cTBS were not. This indicates that there was a tighter relationship between iTBS effects and TMS and fMRI parameters at baseline, whereas cTBS effects were unrelated to these parameters. One possible explanation for this finding might be that iTBS takes effect in a more consistent way than cTBS. It could be that iTBS initiates mechanisms which ultimately result in more effective corticospinal output of the ipsilesional M1, whereas cTBS is a more indirect

stimulation strategy which is more likely than iTBS to act in different ways in different patients. Interestingly, Grefkes et al. (2010) demonstrated that inhibitory 1 Hz rTMS over the contralesional hemisphere modulates motor network connectivity within and between hemispheres in two ways. That is, 1 Hz rTMS increased the promoting influence from ipsilesional SMA to ipsilesional M1 and reduced the inhibitory influence from contralesional M1 to ipsilesional M1, which was significantly associated with motor improvement of the affected hand. Hence, it is conceivable that beneficial cTBS effects are mediated primarily by reducing pathologically increased IHI from contralesional M1 to ipsilesional M1 in some patients, whereas in other patients cTBS might also increase effectiveness of information processing within the ipsilesional hemisphere (i.e. increase SMA-M1 coupling) indirectly. If this would be the case, iTBS would show more consistent associations with motor network preconditions (since it acts more consistent across subjects) than cTBS (which might act in more different ways). This however, cannot be inferred from our data and hence remains speculative. Future studies, are needed to investigate the effect of cTBS and iTBS on effective connectivity within the cortical motor network in stroke patients.

6 Conclusions and outlook

Although rTMS in general and TBS in particular, have been suggested to have high therapeutic potential for treatment of motor deficits induced by stroke (Ridding & Rothwell, 2007), several problems need to be solved before rTMS can be successfully implemented in neurorehabilitation. One of the most urgent problems appears to be high variance in rTMS induced effects both across studies (Hoogendam et al., 2010) and patients (Ameli et al., 2009). Hence, the major goal of the present thesis was to make a contribution to improve rTMS intervention strategies by means of state-of-the-art neuroimaging techniques. More precisely, the aim was to (i) reduce variance across studies by improving strategies to identify the cortical rTMS target position (by means of perfusion MRI assessed with ASL) and (ii) reduce variance across patients by identifying reliable predictors for TBS effects in stroke patients (by means of fMRI and effective connectivity assessed with DCM).

6.1 Study I & II: Reducing variance across studies

The majority of rTMS intervention studies, which aim to improve motor performance in stroke patients, use the primary motor cortex (BA4) as target region (Hoogendam et al., 2010). However, considerably large spatial displacements between fMRI and TMS positions have consistently been reported for the human motor system (cf. Study I). This is surprising because the position with highest TMS excitability might be expected to correspond to the position with highest density of motoneurons, i.e. BA4 (Talelli et al., 2006). We suspected that the spatial mismatch between fMRI and TMS is caused by imperfect functional localization of BA4 by the conventional GRE-BOLD fMRI technique. State-of-the-art perfusion fMRI techniques indeed localized neural activity closer to BA4, but unfortunately not closer to the optimal TMS position, because optimal TMS positions were located further anterior in premotor cortex (BA6). Hence, the spatial mismatch between fMRI and TMS could not be reduced by the use of perfusion fMRI signal (ASL-CBF), i.e. was not caused by vascular artefacts in GRE-BOLD signal. Close examination of previous studies revealed that, in line with our findings, the majority of studies found an anterior shift of optimal TMS positions compared to fMRI positions. Findings might be explained by inhomogeneity of the

TMS-induced electric field and its distinct effects on different tissue types or components (such as axons) depending on their orientation in space.

Future studies are needed to elucidate the spatial mismatch between fMRI and TMS positions further and investigate why TMS positions appear to be located consistently further anterior. Additionally, more research is needed to increase our understanding of the physiological mechanisms leading to rTMS induced effects. Furthermore, it would be interesting to investigate whether stimulation of the anatomical motor hand area or stimulation of the most excitable TMS position (further anterior) is more effective in terms of behavioural improvements following rTMS. However, since mean 3D distances between individual fMRI and TMS positions was found to be between 10-12 mm (cf. Table 3.2) and TMS has a spatial resolution of approximately 7.7 mm (Thielscher & Wichmann, 2009), it might be that TMS cannot sufficiently differentiate between these two positions to result in significant differences on the behavioural level.

Results of Study II in stroke patients were comparable to results of Study I: Although perfusion fMRI signal (ASL-CBF) yielded activations closer to BA4, these were not significantly closer to optimal TMS positions which were located in BA6. Hence, increased spatial specificity of perfusion fMRI did not result in improved spatial congruence between fMRI and TMS, neither in healthy subjects nor in stroke patients. Nevertheless, Study II yielded promising novel insights which demonstrate that (i) meaningful *task-related* perfusion MRI signal can be obtained from patients with cerebrovascular disease by means of ASL-CBF, (ii) task-related perfusion fMRI signal during movements of the affected hand is also bilaterally organized (similar to BOLD fMRI signal), which strongly suggests *neuronal* processes as underlying cause, and (iii) reorganization processes might further decrease congruence between fMRI and TMS.

More studies are needed to explore task-related perfusion MRI signal in stroke patients. For instance, it would be interesting to investigate how (bilateral) movement-related perfusion MRI signal evolves from the acute to the subacute and chronic phase and whether (and how) task-related perfusion MRI signal is changed by rTMS. However, there are also numerous interesting applications conceivable assessing perfusion MRI signal in absence of a specific task (“resting-state”) in stroke patients. This approach might be particularly promising for studies on stroke patients in the acute phase (which might not be able to perform any motor task in the scanner), and could for example be used to identify predictors for spontaneous. Forthcoming results are likely to have high implications for clinical settings.

6.2 Study III: Reducing variance across patients

Inter-individual differences in rTMS effects between stroke patients are likely to result from distinct pathomechanisms causing motor impairments. The aim of Study III was to identify reliable predictors for rTMS mediated effects on motor performance of the affected hand by means of fMRI and DCM assessing effective connectivity. Study III yielded promising results suggesting that integrity of the cortical motor network is an essential requisite to improve motor performance of the affected hand by means of facilitatory iTBS applied to the ipsilesional hemisphere. Patients with severely disturbed motor networks did not respond to iTBS or even deteriorated. It is conceivable that, neuroimaging derived parameters such as the laterality index (LI) or coupling strength (in Hz) between key motor areas assessed by means of dynamic causal modelling (DCM) could in future be used to predict rTMS effects in stroke patients. However, future studies with larger sample sizes are needed to identify reliable cut-off values, which allow making a clear statement on whether or not a patient will improve after rTMS based on the patients' individual measured value. Larger sample sizes might also allow investigation of differential effects of e.g. lesion location, time since stroke or other factors on rTMS responsiveness. Future studies are also needed to investigate the functional role of neural activity in the contralesional hemisphere further. It also needs to be clarified whether multiple sessions of rTMS can be used to yield more robust effects, which might last for a longer period of time. Finally, future studies need to elucidate the most appropriate time point for rTMS with regard to stage of the disease (acute, subacute or chronic phase) and with regard to combination with physical therapy (before, during or after physical training).

7 References

- Abdeen MA, Stuchly MA. Modeling of magnetic field stimulation of bent neurons. *IEEE Trans Biomed Eng.* 1994 Nov;41(11):1092-5.
- Ackerley SJ, Stinear CM, Barber PA, Byblow WD. Combining theta burst stimulation with training after subcortical stroke. *Stroke.* 2010 Jul;41(7):1568-72.
- Adkins DL, Boychuk J, Remple MS, Kleim JA. Motor training induces experience-specific patterns of plasticity across motor cortex and spinal cord. *J Appl Physiol.* 2006 Dec;101(6):1776-82.
- Albensi BC, Oliver DR, Toupin J, Otero G. Electrical stimulation protocols for hippocampal synaptic plasticity and neuronal hyper-excitability: are they effective or relevant? *Exp Neurol.* 2007 Mar;204(1):1-13.
- Amassian VE, Cracco RQ, Maccabee PJ, Cracco JB, Rudell AP, Eberle L. Transcranial magnetic stimulation in study of the visual pathway. *J Clin Neurophysiol.* 1998 Jul;15(4):288-304.
- Amassian VE, Eberle L, Maccabee PJ, Cracco RQ. Modelling magnetic coil excitation of human cerebral cortex with a peripheral nerve immersed in a brain-shaped volume conductor: the significance of fiber bending in excitation. *Electroencephalogr Clin Neurophysiol.* 1992 Oct;85(5):291-301.
- Amassian VE, Stewart M, Quirk GJ, Rosenthal JL. Physiological basis of motor effects of a transient stimulus to cerebral cortex. *Neurosurgery.* 1987 Jan;20(1):74-93.
- Ameli M, Grefkes C, Kemper F, Riegg FP, Rehme AK, Karbe H, et al. Differential effects of high-frequency repetitive transcranial magnetic stimulation over ipsilesional primary motor cortex in cortical and subcortical middle cerebral artery stroke. *Ann Neurol.* 2009 Sep;66(3):298-309.
- Amunts K, Schleicher A, Burgel U, Mohlberg H, Uylings HB, Zilles K. Broca's region revisited: cytoarchitecture and intersubject variability. *J Comp Neurol.* 1999 Sep 20;412(2):319-41.
- Amunts K, Zilles K. Funktionelle Neuroanatomie. In: Schneider F, Fink GR, editors, *Funktionelle MRT in Psychiatrie und Neurologie.* Heidelberg: Springer; 2007. p. 9-59.
- Awiszus F. TMS and threshold hunting. *Suppl Clin Neurophysiol.* 2003;56:13-23.
- Aydin-Abidin S, Trippe J, Funke K, Eysel UT, Benali A. High- and low-frequency repetitive transcranial magnetic stimulation differentially activates c-Fos and zif268 protein expression in the rat brain. *Exp Brain Res.* 2008 Jun;188(2):249-61.
- Bagnato S, Curra A, Modugno N, Gilio F, Quartarone A, Rizzo V, et al. One-hertz subthreshold rTMS increases the threshold for evoking inhibition in the human motor cortex. *Exp Brain Res.* 2005 Jan;160(3):368-74.
- Barker AT, Jalinous R, Freeston IL. Non-invasive magnetic stimulation of human motor cortex. *Lancet.* 1985 May 11;1(8437):1106-7.
- Basser PJ. Focal magnetic stimulation of an axon. *IEEE Trans Biomed Eng.* 1994 Jun;41(6):601-6.
- Bastings EP, Gage HD, Greenberg JP, Hammond G, Hernandez L, Santiago P, et al. Co-registration of cortical magnetic stimulation and functional magnetic resonance imaging. *Neuroreport.* 1998 Jun 22;9(9):1941-6.
- Bastings EP, Greenberg JP, Good DC. Hand motor recovery after stroke: a transcranial magnetic stimulation mapping study of motor output areas and their relation to functional status. *Neurorehabil Neural Repair.* 2002 Sep;16(3):275-82.

- Bates E, Wilson SM, Saygin AP, Dick F, Sereno MI, Knight RT, et al. Voxel-based lesion-symptom mapping. *Nat Neurosci.* 2003 May;6(5):448-50.
- Baumer T, Bock F, Koch G, Lange R, Rothwell JC, Siebner HR, et al. Magnetic stimulation of human premotor or motor cortex produces interhemispheric facilitation through distinct pathways. *J Physiol.* 2006 May 1;572(Pt 3):857-68.
- Benjamini Y, Hochberg Y. Controlling the false discovery rate: a practical and powerful approach to multiple testing. *J R Stat Soc.* 1995;57(1):289-300.
- Berweck S, Walther M, Brodbeck V, Wagner N, Koerte I, Henschel V, et al. Abnormal motor cortex excitability in congenital stroke. *Pediatr Res.* 2008 Jan;63(1):84-8.
- Bestmann S, Baudewig J, Siebner HR, Rothwell JC, Frahm J. Subthreshold high-frequency TMS of human primary motor cortex modulates interconnected frontal motor areas as detected by interleaved fMRI-TMS. *Neuroimage.* 2003 Nov;20(3):1685-96.
- Bestmann S, Swayne O, Blankenburg F, Ruff CC, Teo J, Weiskopf N, et al. The role of contralesional dorsal premotor cortex after stroke as studied with concurrent TMS-fMRI. *J Neurosci.* 2010 Sep 8;30(36):11926-37.
- Bezard E, Boraud T, Nguyen JP, Velasco F, Keravel Y, Gross C. Cortical stimulation and epileptic seizure: a study of the potential risk in primates. *Neurosurgery.* 1999 Aug;45(2):346-50.
- Binkofski F, Seitz RJ. Modulation of the BOLD-response in early recovery from sensorimotor stroke. *Neurology.* 2004 Oct 12;63(7):1223-9.
- Borojerdi B, Diefenbach K, Ferbert A. Transcallosal inhibition in cortical and subcortical cerebral vascular lesions. *J Neurol Sci.* 1996 Dec;144(1-2):160-70.
- Borojerdi B, Foltys H, Krings T, Spetzger U, Thron A, Topper R. Localization of the motor hand area using transcranial magnetic stimulation and functional magnetic resonance imaging. *Clin Neurophysiol.* 1999 Apr;110(4):699-704.
- Boxerman JL, Bandettini PA, Kwong KK, Baker JR, Davis TL, Rosen BR, et al. The intravascular contribution to fMRI signal change: Monte Carlo modeling and diffusion-weighted studies in vivo. *Magn Reson Med.* 1995 Jul;34(1):4-10.
- Brasil-Neto JP, Cohen LG, Panizza M, Nilsson J, Roth BJ, Hallett M. Optimal focal transcranial magnetic activation of the human motor cortex: effects of coil orientation, shape of the induced current pulse, and stimulus intensity. *J Clin Neurophysiol.* 1992 Jan;9(1):132-6.
- Brodmann K. Vergleichende Lokalisationslehre der Großhirnrinde in ihren Prinzipien dargestellt aufgrund des Zellenbaues. Leipzig: Barth; 1909.
- Buchel C, Friston KJ. Modulation of connectivity in visual pathways by attention: cortical interactions evaluated with structural equation modelling and fMRI. *Cereb Cortex.* 1997 Dec;7(8):768-78.
- Butefisch CM, Davis BC, Wise SP, Sawaki L, Kopylev L, Classen J, Cohen LG. Mechanisms of use-dependent plasticity in the human motor cortex. *Proc Natl Acad Sci U S A.* 2000 Mar 28;97(7):3661-5.
- Butefisch CM, Kleiser R, Korber B, Muller K, Wittsack HJ, Homberg V, et al. Recruitment of contralesional motor cortex in stroke patients with recovery of hand function. *Neurology.* 2005 Mar 22;64(6):1067-9.
- Butefisch CM, Netz J, Wessling M, Seitz RJ, Homberg V. Remote changes in cortical excitability after stroke. *Brain.* 2003 Feb;126(Pt 2):470-81.
- Butefisch CM, Wessling M, Netz J, Seitz RJ, Homberg V. Relationship between interhemispheric inhibition and motor cortex excitability in subacute stroke patients. *Neurorehabil Neural Repair.* 2008 Jan-Feb;22(1):4-21.

- Buxton RB, Wong EC, Frank LR. Dynamics of blood flow and oxygenation changes during brain activation: the balloon model. *Magn Reson Med*. 1998 Jun;39(6):855-64.
- Byrnes ML, Thickbroom GW, Phillips BA, Mastaglia FL. Long-term changes in motor cortical organisation after recovery from subcortical stroke. *Brain Res*. 2001 Jan 19;889(1-2):278-87.
- Calautti C, Leroy F, Guincestre JY, Marie RM, Baron JC. Sequential activation brain mapping after subcortical stroke: changes in hemispheric balance and recovery. *Neuroreport*. 2001 Dec 21;12(18):3883-6.
- Cao Y, D'Olhaberriague L, Vikingstad EM, Levine SR, Welch KM. Pilot study of functional MRI to assess cerebral activation of motor function after poststroke hemiparesis. *Stroke*. 1998 Jan;29(1):112-22.
- Carey JR, Evans CD, Anderson DC, Bhatt E, Nagpal A, Kimberley TJ, et al. Safety of 6-Hz primed low-frequency rTMS in stroke. *Neurorehabil Neural Repair*. 2008 Mar-Apr;22(2):185-92.
- Carey JR, Kimberley TJ, Lewis SM, Auerbach EJ, Dorsey L, Rundquist P, et al. Analysis of fMRI and finger tracking training in subjects with chronic stroke. *Brain*. 2002 Apr;125(Pt 4):773-88.
- Catalan MJ, Honda M, Weeks RA, Cohen LG, Hallett M. The functional neuroanatomy of simple and complex sequential finger movements: a PET study. *Brain*. 1998 Feb;121 (Pt 2):253-64.
- Catano A, Houa M, Caroyer JM, Ducarne H, Noel P. Magnetic transcranial stimulation in acute stroke: early excitation threshold and functional prognosis. *Electroencephalogr Clin Neurophysiol*. 1996 Jun;101(3):233-9.
- Cavusoglu M, Pfeuffer J, Ugurbil K, Uludag K. Comparison of pulsed arterial spin labeling encoding schemes and absolute perfusion quantification. *Magn Reson Imaging*. 2009 Oct;27(8):1039-45.
- Chalela JA, Merino JG, Warach S. Update on stroke. *Curr Opin Neurol*. 2004 Aug;17(4):447-51.
- Chen R, Classen J, Gerloff C, Celnik P, Wassermann EM, Hallett M, et al. Depression of motor cortex excitability by low-frequency transcranial magnetic stimulation. *Neurology*. 1997 May;48(5):1398-403.
- Chen R, Yung D, Li JY. Organization of ipsilateral excitatory and inhibitory pathways in the human motor cortex. *J Neurophysiol*. 2003 Mar;89(3):1256-64.
- Chollet F, DiPiero V, Wise RJ, Brooks DJ, Dolan RJ, Frackowiak RS. The functional anatomy of motor recovery after stroke in humans: a study with positron emission tomography. *Ann Neurol*. 1991 Jan;29(1):63-71.
- Cicinelli P, Pasqualetti P, Zaccagnini M, Traversa R, Oliveri M, Rossini PM. Interhemispheric asymmetries of motor cortex excitability in the postacute stroke stage: a paired-pulse transcranial magnetic stimulation study. *Stroke*. 2003 Nov;34(11):2653-8.
- Cicinelli P, Traversa R, Rossini PM. Post-stroke reorganization of brain motor output to the hand: a 2-4 month follow-up with focal magnetic transcranial stimulation. *Electroencephalogr Clin Neurophysiol*. 1997 Dec;105(6):438-50.
- Classen J, Knorr U, Werhahn KJ, Schlaug G, Kunesch E, Cohen LG, et al. Multimodal output mapping of human central motor representation on different spatial scales. *J Physiol*. 1998 Oct 1;512 (Pt 1):163-79.
- Claus D, Weis M, Jahnke U, Plewe A, Brunholzl C. Corticospinal conduction studied with magnetic double stimulation in the intact human. *J Neurol Sci*. 1992 Sep;111(2):180-8.
- Cohen LG, Celnik P, Pascual-Leone A, Corwell B, Falz L, Dambrosia J, et al. Functional relevance of cross-modal plasticity in blind humans. *Nature*. 1997 Sep 11;389(6647):180-3.
- Cooke SF, Bliss TV. Plasticity in the human central nervous system. *Brain*. 2006 Jul;129(Pt 7):1659-73.

- Cramer SC. Repairing the human brain after stroke: I. Mechanisms of spontaneous recovery. *Ann Neurol.* 2008 Mar;63(3):272-87.
- Cramer SC, Nelles G, Benson RR, Kaplan JD, Parker RA, Kwong KK, et al. A functional MRI study of subjects recovered from hemiparetic stroke. *Stroke.* 1997 Dec;28(12):2518-27.
- Daskalakis ZJ, Moller B, Christensen BK, Fitzgerald PB, Gunraj C, Chen R. The effects of repetitive transcranial magnetic stimulation on cortical inhibition in healthy human subjects. *Exp Brain Res.* 2006 Oct;174(3):403-12.
- Datta AK, Harrison LM, Stephens JA. Task-dependent changes in the size of response to magnetic brain stimulation in human first dorsal interosseous muscle. *J Physiol.* 1989 Nov;418:13-23.
- Day BL, Dressler D, Maertens de Noordhout A, Marsden CD, Nakashima K, Rothwell JC, et al. Electric and magnetic stimulation of human motor cortex: surface EMG and single motor unit responses. *J Physiol.* 1989 May;412:449-73.
- Day BL, Riescher H, Struppler A, Rothwell JC, Marsden CD. Changes in the response to magnetic and electrical stimulation of the motor cortex following muscle stretch in man. *J Physiol.* 1991 Feb;433:41-57.
- Deiber MP, Passingham RE, Colebatch JG, Friston KJ, Nixon PD, Frackowiak RS. Cortical areas and the selection of movement: a study with positron emission tomography. *Exp Brain Res.* 1991;84(2):393-402.
- Delvaux V, Alagona G, Gerard P, De Pasqua V, Pennisi G, de Noordhout AM. Post-stroke reorganization of hand motor area: a 1-year prospective follow-up with focal transcranial magnetic stimulation. *Clin Neurophysiol.* 2003 Jul;114(7):1217-25.
- Detre JA, Alsop DC, Vives LR, Maccotta L, Teener JW, Raps EC. Noninvasive MRI evaluation of cerebral blood flow in cerebrovascular disease. *Neurology.* 1998 Mar;50(3):633-41.
- Detre JA, Wang J. Technical aspects and utility of fMRI using BOLD and ASL. *Clin Neurophysiol.* 2002 May;113(5):621-34.
- Di Lazzaro V, Oliviero A, Meglio M, Cioni B, Tamburrini G, Tonali P, et al. Direct demonstration of the effect of lorazepam on the excitability of the human motor cortex. *Clin Neurophysiol.* 2000 May;111(5):794-9.
- Di Lazzaro V, Oliviero A, Profice P, Saturno E, Pilato F, Insola A, et al. Comparison of descending volleys evoked by transcranial magnetic and electric stimulation in conscious humans. *Electroencephalogr Clin Neurophysiol.* 1998a Oct;109(5):397-401.
- Di Lazzaro V, Pilato F, Dileone M, Profice P, Capone F, Ranieri F, et al. Modulating cortical excitability in acute stroke: a repetitive TMS study. *Clin Neurophysiol.* 2008a Mar;119(3):715-23.
- Di Lazzaro V, Pilato F, Dileone M, Profice P, Oliviero A, Mazzone P, et al. The physiological basis of the effects of intermittent theta burst stimulation of the human motor cortex. *J Physiol.* 2008b Aug 15;586(16):3871-9.
- Di Lazzaro V, Pilato F, Saturno E, Oliviero A, Dileone M, Mazzone P, et al. Theta-burst repetitive transcranial magnetic stimulation suppresses specific excitatory circuits in the human motor cortex. *J Physiol.* 2005 Jun 15;565(Pt 3):945-50.
- Di Lazzaro V, Profice P, Pilato F, Capone F, Ranieri F, Pasqualetti P, et al. Motor cortex plasticity predicts recovery in acute stroke. *Cereb Cortex.* 2010 Jul;20(7):1523-8.
- Di Lazzaro V, Restuccia D, Oliviero A, Profice P, Ferrara L, Insola A, et al. Magnetic transcranial stimulation at intensities below active motor threshold activates intracortical inhibitory circuits. *Exp Brain Res.* 1998b Mar;119(2):265-8.

- Diekhoff S, Uludag K, Sparing R, Tittgemeyer M, Cavusoglu M, von Cramon DY, et al. Functional localization in the human brain: Gradient-Echo, Spin-Echo, and arterial spin-labeling fMRI compared with neuronavigated TMS. *Hum Brain Mapp.* 2011 Mar;32(3):341-57.
- Dum RP, Strick PL. Motor areas in the frontal lobe of the primate. *Physiol Behav.* 2002 Dec;77(4-5):677-82.
- Dunn OJ. Multiple comparison among means. *J Am Stat Assoc.* 1961 56:52-64.
- Duong TQ, Silva AC, Lee SP, Kim SG. Functional MRI of calcium-dependent synaptic activity: cross correlation with CBF and BOLD measurements. *Magn Reson Med.* 2000 Mar;43(3):383-92.
- Duong TQ, Yacoub E, Adriany G, Hu X, Ugurbil K, Vaughan JT, et al. High-resolution, spin-echo BOLD, and CBF fMRI at 4 and 7 T. *Magn Reson Med.* 2002 Oct;48(4):589-93.
- Duque J, Hummel F, Celnik P, Murase N, Mazzocchio R, Cohen LG. Transcallosal inhibition in chronic subcortical stroke. *Neuroimage.* 2005 Dec;28(4):940-6.
- Eaton H. Electric field induced in a spherical volume conductor from arbitrary coils: application to magnetic stimulation and MEG. *Med Biol Eng Comput.* 1992 Jul;30(4):433-40.
- Edelman RR, Siewert B, Darby DG, Thangaraj V, Nobre AC, Mesulam MM, et al. Qualitative mapping of cerebral blood flow and functional localization with echo-planar MR imaging and signal targeting with alternating radio frequency. *Radiology.* 1994 Aug;192(2):513-20.
- Eickhoff SB, Paus T, Caspers S, Grosbras MH, Evans AC, Zilles K, et al. Assignment of functional activations to probabilistic cytoarchitectonic areas revisited. *Neuroimage.* 2007 Jul 1;36(3):511-21.
- Eickhoff S, Stephan KE, Mohlberg H, Grefkes C, Fink GR, Amunts K, et al. A new SPM toolbox for combining probabilistic cytoarchitectonic maps and functional imaging data. *Neuroimage.* 2005 May 1;25(4):1325-35.
- Eickhoff SB, Grefkes C. Approaches for the Integrated Analysis of Structure, Function and Connectivity of the Human Brain. *Clin EEG Neurosci.* 2011 Apr;42(2):107-21.
- Faraday M. Experimental research in electricity. *Phil Trans R Soc Lond.* 1832 Jan;122:125-162.
- Feigin VL, Lawes CM, Bennett DA, Barker-Collo SL, Parag V. Worldwide stroke incidence and early case fatality reported in 56 population-based studies: a systematic review. *Lancet Neurol.* 2009 Apr;8(4):355-69.
- Feeney DM, Baron JC. Diaschisis. *Stroke.* 1986 Sep-Oct;17(5):817-30.
- Ferbert A, Priori A, Rothwell JC, Day BL, Colebatch JG, Marsden CD. Interhemispheric inhibition of the human motor cortex. *J Physiol.* 1992;453:525-46.
- Fisher M. The new magnetic resonance techniques of diffusion and perfusion imaging. *Adm Radiol J.* 1997 Aug;16(8):29-30, 35-6.
- Fisher RJ, Nakamura Y, Bestmann S, Rothwell JC, Bostock H. Two phases of intracortical inhibition revealed by transcranial magnetic threshold tracking. *Exp Brain Res.* 2002 Mar;143(2):240-8.
- Fitzgerald PB, Fountain S, Hoy K, Maller J, Enticott P, Laycock R, et al. A comparative study of the effects of repetitive paired transcranial magnetic stimulation on motor cortical excitability. *J Neurosci Methods.* 2007 Sep 30;165(2):265-9.
- Floel A, Hummel F, Duque J, Knecht S, Cohen LG. Influence of somatosensory input on interhemispheric interactions in patients with chronic stroke. *Neurorehabil Neural Repair.* 2008 Sep-Oct;22(5):477-85.

- Foltys H, Krings T, Meister IG, Sparing R, Boroojerdi B, Thron A, et al. Motor representation in patients rapidly recovering after stroke: a functional magnetic resonance imaging and transcranial magnetic stimulation study. *Clin Neurophysiol.* 2003 Dec;114(12):2404-15.
- Forman SD, Cohen JD, Fitzgerald M, Eddy WF, Mintun MA, Noll DC. Improved assessment of significant activation in functional magnetic resonance imaging (fMRI): use of a cluster-size threshold. *Magn Reson Med.* 1995 May;33(5):636-47.
- Fox PT, Narayana S, Tandon N, Sandoval H, Fox SP, Kochunov P, et al. Column-based model of electric field excitation of cerebral cortex. *Hum Brain Mapp.* 2004 May;22(1):1-14.
- Frahm J, Merboldt KD, Hanicke W, Kleinschmidt A, Boecker H. Brain or vein--oxygenation or flow? On signal physiology in functional MRI of human brain activation. *NMR Biomed.* 1994 Mar;7(1-2):45-53.
- Fregni F, Boggio PS, Valle AC, Rocha RR, Duarte J, Ferreira MJ, et al. A sham-controlled trial of a 5-day course of repetitive transcranial magnetic stimulation of the unaffected hemisphere in stroke patients. *Stroke.* 2006 Aug;37(8):2115-22.
- Fridman EA, Hanakawa T, Chung M, Hummel F, Leiguarda RC, Cohen LG. Reorganization of the human ipsilesional premotor cortex after stroke. *Brain.* 2004 Apr;127(Pt 4):747-58.
- Friston K. Functional integration and inference in the brain. *Prog Neurobiol.* 2002 Oct;68(2):113-43.
- Friston KJ. Functional and effective connectivity in neuroimaging: a synthesis. 1994 Oct;2(1-2):56-78.
- Friston KJ, Buechel C, Fink GR, Morris J, Rolls E, Dolan RJ. Psychophysiological and modulatory interactions in neuroimaging. *Neuroimage.* 1997 Oct;6(3):218-29.
- Friston KJ, Firth CD, Frackowiak RSJ. Time-dependent changes in effective connectivity measured with PET. *Hum Brain Mapp.* 1993a Oct;1(1):69-79.
- Friston KJ, Frith CD, Liddle PF, Frackowiak RS. Functional connectivity: the principal-component analysis of large (PET) data sets. *J Cereb Blood Flow Metab.* 1993b Jan;13(1):5-14.
- Friston KJ, Harrison L, Penny W. Dynamic causal modelling. *Neuroimage.* 2003 Aug;19(4):1273-302.
- Friston KJ, Tononi G, Reeke GN, Jr., Sporns O, Edelman GM. Value-dependent selection in the brain: simulation in a synthetic neural model. *Neuroscience.* 1994 Mar;59(2):229-43.
- Gentner R, Wankerl K, Reinsberger C, Zeller D, Classen J. Depression of human corticospinal excitability induced by magnetic theta-burst stimulation: evidence of rapid polarity-reversing metaplasticity. *Cereb Cortex.* 2008 Sep;18(9):2046-53.
- Gerloff C, Bushara K, Sailer A, Wassermann EM, Chen R, Matsuoka T, et al. Multimodal imaging of brain reorganization in motor areas of the contralesional hemisphere of well recovered patients after capsular stroke. *Brain.* 2006 Mar;129(Pt 3):791-808.
- Geyer S. The microstructural border between the motor and the cognitive domain in the human cerebral cortex. *Adv Anat Embryol Cell Biol.* 2004;174:I-VIII, 1-89.
- Geyer S, Ledberg A, Schleicher A, Kinomura S, Schormann T, Burgel U, et al. Two different areas within the primary motor cortex of man. *Nature.* 1996 Aug 29;382(6594):805-7.
- Geyer S, Matelli M, Luppino G, Zilles K. Functional neuroanatomy of the primate isocortical motor system. *Anat Embryol (Berl).* 2000 Dec;202(6):443-74.
- Gilio F, Rizzo V, Siebner HR, Rothwell JC. Effects on the right motor hand-area excitability produced by low-frequency rTMS over human contralateral homologous cortex. *J Physiol.* 2003 Sep 1;551(Pt 2):563-73.

- Goense JB, Logothetis NK. Laminar specificity in monkey V1 using high-resolution SE-fMRI. *Magn Reson Imaging*. 2006 May;24(4):381-92.
- Grafton ST, Fagg AH, Woods RP, Arbib MA. Functional anatomy of pointing and grasping in humans. *Cereb Cortex*. 1996 Mar-Apr;6(2):226-37.
- Grefkes C, Eickhoff SB, Nowak DA, Dafotakis M, Fink GR. Dynamic intra- and interhemispheric interactions during unilateral and bilateral hand movements assessed with fMRI and DCM. *Neuroimage*. 2008a Jul 15;41(4):1382-94.
- Grefkes C, Fink GR. Reorganization of cerebral networks after stroke: new insights from neuroimaging with connectivity approaches. *Brain*. 2011 May;134(Pt 5):1264-76.
- Grefkes C, Nowak DA, Eickhoff SB, Dafotakis M, Kust J, Karbe H, et al. Cortical connectivity after subcortical stroke assessed with functional magnetic resonance imaging. *Ann Neurol*. 2008b Feb;63(2):236-46.
- Grefkes C, Nowak DA, Wang LE, Dafotakis M, Eickhoff SB, Fink GR. Modulating cortical connectivity in stroke patients by rTMS assessed with fMRI and dynamic causal modeling. *Neuroimage*. 2010 Mar;50(1):233-42.
- Grezes J, Decety J. Functional anatomy of execution, mental simulation, observation, and verb generation of actions: a meta-analysis. *Hum Brain Mapp*. 2001 Jan;12(1):1-19.
- Hallett M. Transcranial magnetic stimulation: a primer. *Neuron*. 2007 Jul 19;55(2):187-99.
- Hanajima R, Furubayashi T, Iwata NK, Shio Y, Okabe S, Kanazawa I, et al. Further evidence to support different mechanisms underlying intracortical inhibition of the motor cortex. *Exp Brain Res*. 2003 Aug;151(4):427-34.
- Hanajima R, Ugawa Y, Machii K, Mochizuki H, Terao Y, Enomoto H, et al. Interhemispheric facilitation of the hand motor area in humans. *J Physiol*. 2001 Mar 15;531(Pt 3):849-59.
- Harel N, Lin J, Moeller S, Ugurbil K, Yacoub E. Combined imaging-histological study of cortical laminar specificity of fMRI signals. *Neuroimage*. 2006 Feb 1;29(3):879-87.
- Hatano S. Experience from a multicentre stroke register: a preliminary report. *Bull World Health Organ*. 1976;54(5):541-53.
- He SQ, Dum RP, Strick PL. Topographic organization of corticospinal projections from the frontal lobe: motor areas on the lateral surface of the hemisphere. *J Neurosci*. 1993 Mar;13(3):952-80.
- Heald A, Bates D, Cartlidge NE, French JM, Miller S. Longitudinal study of central motor conduction time following stroke. 2. Central motor conduction measured within 72 h after stroke as a predictor of functional outcome at 12 months. *Brain*. 1993 Dec;116 (Pt 6):1371-85.
- Heeger DJ, Ress D. What does fMRI tell us about neuronal activity? *Nat Rev Neurosci*. 2002 Feb;3(2):142-51.
- Heide G, Witte OW, Ziemann U. Physiology of modulation of motor cortex excitability by low-frequency suprathreshold repetitive transcranial magnetic stimulation. *Exp Brain Res*. 2006 May;171(1):26-34.
- Hendricks HT, Hageman G, van Limbeek J. Prediction of recovery from upper extremity paralysis after stroke by measuring evoked potentials. *Scand J Rehabil Med*. 1997 Sep;29(3):155-9.
- Herbsman T, Forster L, Molnar C, Dougherty R, Christie D, Koola J, et al. Motor threshold in transcranial magnetic stimulation: the impact of white matter fiber orientation and skull-to-cortex distance. *Hum Brain Mapp*. 2009 Jul;30(7):2044-55.
- Herwig U, Kolbel K, Wunderlich AP, Thielscher A, von Tiesenhansen C, Spitzer M, et al. Spatial congruence of neuronavigated transcranial magnetic stimulation and functional neuroimaging. *Clin Neurophysiol*. 2002 Apr;113(4):462-8.

- Herwig U, Padberg F, Unger J, Spitzer M, Schonfeldt-Lecuona C. Transcranial magnetic stimulation in therapy studies: examination of the reliability of "standard" coil positioning by neuronavigation. *Biol Psychiatry*. 2001 Jul 1;50(1):58-61.
- Herwig U, Satrapi P, Schonfeldt-Lecuona C. Using the international 10-20 EEG system for positioning of transcranial magnetic stimulation. *Brain Topogr*. 2003 Winter;16(2):95-9.
- Herwig U, Schonfeldt-Lecuona C. Neuronavigation der transkraniellen Magnetstimulation. In: Siebner HR, Ziemann U, editors. *Das TMS-Buch*. Heidelberg: Springer; 2007. p. 317-21.
- Hess CW, Mills KR, Murray NM. Responses in small hand muscles from magnetic stimulation of the human brain. *J Physiol*. 1987 Jul;388:397-419.
- Hess G, Donoghue JP. Long-term potentiation and long-term depression of horizontal connections in rat motor cortex. *Acta Neurobiol Exp (Wars)*. 1996;56(1):397-405.
- Honey CJ, Sporns O. Dynamical consequences of lesions in cortical networks. *Hum Brain Mapp*. 2008 Jul;29(7):802-9.
- Hoogendam JM, Ramakers GM, Di Lazzaro V. Physiology of repetitive transcranial magnetic stimulation of the human brain. *Brain Stimul*. 2010 Apr;3(2):95-118.
- Houdayer E, Degardin A, Cassim F, Bocquillon P, Derambure P, Devanne H. The effects of low- and high-frequency repetitive TMS on the input/output properties of the human corticospinal pathway. *Exp Brain Res*. 2008 May;187(2):207-17.
- Huang YZ, Chen RS, Rothwell JC, Wen HY. The after-effect of human theta burst stimulation is NMDA receptor dependent. *Clin Neurophysiol*. 2007 May;118(5):1028-32.
- Huang YZ, Edwards MJ, Rounis E, Bhatia KP, Rothwell JC. Theta burst stimulation of the human motor cortex. *Neuron*. 2005 Jan 20;45(2):201-6.
- Huang YZ, Rothwell JC, Edwards MJ, Chen RS. Effect of physiological activity on an NMDA-dependent form of cortical plasticity in human. *Cereb Cortex*. 2008 Mar;18(3):563-70.
- Huemmeke M, Eysel UT, Mittmann T. Metabotropic glutamate receptors mediate expression of LTP in slices of rat visual cortex. *Eur J Neurosci*. 2002 May;15(10):1641-5.
- Iezzi E, Conte A, Suppa A, Agostino R, Dinapoli L, Scontrini A, et al. Phasic voluntary movements reverse the aftereffects of subsequent theta-burst stimulation in humans. *J Neurophysiol*. 2008 Oct;100(4):2070-6.
- Ilic TV, Meintzschel F, Cleff U, Ruge D, Kessler KR, Ziemann U. Short-interval paired-pulse inhibition and facilitation of human motor cortex: the dimension of stimulus intensity. *J Physiol*. 2002 Nov 15;545(Pt 1):153-67.
- Ilmoniemi RJ, Ruohonen J, Karhu J. Transcranial magnetic stimulation--a new tool for functional imaging of the brain. *Crit Rev Biomed Eng*. 1999;27(3-5):241-84.
- Jaillard A, Martin CD, Garambois K, Lebas JF, Hommel M. Vicarious function within the human primary motor cortex? A longitudinal fMRI stroke study. *Brain*. 2005 May;128(Pt 5):1122-38.
- Jebsen RH, Taylor N, Trieschmann RB, Trotter MJ, Howard LA. An objective and standardized test of hand function. *Arch Phys Med Rehabil*. 1969 Jun;50(6):311-9.
- Jenkinson M, Bannister P, Brady M, Smith S. Improved optimization for the robust and accurate linear registration and motion correction of brain images. *Neuroimage*. 2002 Oct;17(2):825-41.
- Jenkinson M, Smith S. A global optimisation method for robust affine registration of brain images. *Med Image Anal*. 2001 Jun;5(2):143-56.

- Johansen-Berg H, Rushworth MF, Bogdanovic MD, Kischka U, Wimalaratna S, Matthews PM. The role of ipsilateral premotor cortex in hand movement after stroke. *Proc Natl Acad Sci U S A*. 2002 Oct 29;99(22):14518-23.
- Jones MW, Errington ML, French PJ, Fine A, Bliss TV, Garel S, et al. A requirement for the immediate early gene Zif268 in the expression of late LTP and long-term memories. *Nat Neurosci*. 2001 Mar;4(3):289-96.
- Karim AA, Birbaumer N, Siebner HR. Transkranielle Kortexstimulation. In: Siebner HR, Ziemann U, editors. *Das TMS-Buch*. Heidelberg: Springer; 2007. p. 555-65.
- Kennan RP, Zhong J, Gore JC. Intravascular susceptibility contrast mechanisms in tissues. *Magn Reson Med*. 1994 Jan;31(1):9-21.
- Khedr EM, Ahmed MA, Fathy N, Rothwell JC. Therapeutic trial of repetitive transcranial magnetic stimulation after acute ischemic stroke. *Neurology*. 2005 Aug 9;65(3):466-8.
- Khedr EM, Fetoh NA. Short- and long-term effect of rTMS on motor function recovery after ischemic stroke. *Restor Neurol Neurosci*. 2010 28(4):545-59.
- Kiebel SJ, Holmes AP. The general linear model. In: Friston KJ, Ashburner JT, Kiebel SJ, Nichols TE, Penny WD, editors. *Statistical parametric mapping: The analysis of functional brain images*. London: Elsevier; 2007. p. 101-25.
- Kim SG, Ashe J, Hendrich K, Ellermann JM, Merkle H, Ugurbil K, et al. Functional magnetic resonance imaging of motor cortex: hemispheric asymmetry and handedness. *Science*. 1993 Jul 30;261(5121):615-7.
- Kim SG, Tsekos NV, Ashe J. Multi-slice perfusion-based functional MRI using the FAIR technique: comparison of CBF and BOLD effects. *NMR Biomed*. 1997 Jun-Aug;10(4-5):191-6.
- Kim YH, You SH, Ko MH, Park JW, Lee KH, Jang SH, et al. Repetitive transcranial magnetic stimulation-induced corticomotor excitability and associated motor skill acquisition in chronic stroke. *Stroke*. 2006 Jun;37(6):1471-6.
- Koch G, Franca M, Del Olmo MF, Cheeran B, Milton R, Alvarez Sauco M, et al. Time course of functional connectivity between dorsal premotor and contralateral motor cortex during movement selection. *J Neurosci*. 2006 Jul 12;26(28):7452-9.
- Kolominsky-Rabas PL, Heuschmann PU, Marschall D, Emmert M, Baltzer N, Neundorfer B, et al. Lifetime cost of ischemic stroke in Germany: results and national projections from a population-based stroke registry: the Erlangen Stroke Project. *Stroke*. 2006 May;37(5):1179-83.
- Kozel FA, Nahas Z, deBrux C, Molloy M, Lorberbaum JP, Bohning D, et al. How coil-cortex distance relates to age, motor threshold, and antidepressant response to repetitive transcranial magnetic stimulation. *J Neuropsychiatry Clin Neurosci*. 2000 Summer;12(3):376-84.
- Krings T, Buchbinder BR, Butler WE, Chiappa KH, Jiang HJ, Cosgrove GR, et al. Functional magnetic resonance imaging and transcranial magnetic stimulation: complementary approaches in the evaluation of cortical motor function. *Neurology*. 1997 May;48(5):1406-16.
- Kujirai T, Caramia MD, Rothwell JC, Day BL, Thompson PD, Ferbert A, et al. Corticocortical inhibition in human motor cortex. *J Physiol*. 1993 Nov;471:501-19.
- Kwakkel G, Kollen B, Lindeman E. Understanding the pattern of functional recovery after stroke: facts and theories. *Restor Neurol Neurosci*. 2004;22(3-5):281-99.
- Larson J, Lynch G. Induction of synaptic potentiation in hippocampus by patterned stimulation involves two events. *Science*. 1986 May 23;232(4753):985-8.

- Larson J, Wong D, Lynch G. Patterned stimulation at the theta frequency is optimal for the induction of hippocampal long-term potentiation. *Brain Res.* 1986 Mar 19;368(2):347-50.
- Lauterbur PC. Image formation by induced local interactions: examples employing Nuclear Magnetic resonance. *Nature.* 1973 Mar 16;242:190-91.
- Lee SP, Silva AC, Kim SG. Comparison of diffusion-weighted high-resolution CBF and spin-echo BOLD fMRI at 9.4 T. *Magn Reson Med.* 2002 Apr;47(4):736-41.
- Lewko JP, Stokić DS, Tarkka IM. Dissociation of cortical areas responsible for evoking excitatory and inhibitory responses in the small hand muscles. *Brain Topogr.* 1996 Summer;8(4):397-405.
- Liepert J, Hamzei F, Weiller C. Motor cortex disinhibition of the unaffected hemisphere after acute stroke. *Muscle Nerve.* 2000 Nov;23(11):1761-3.
- Liepert J, Miltner WH, Bauder H, Sommer M, Dettmers C, Taub E, et al. Motor cortex plasticity during constraint-induced movement therapy in stroke patients. *Neurosci Lett.* 1998 Jun 26;250(1):5-8.
- Liu TT, Brown GG. Measurement of cerebral perfusion with arterial spin labeling: Part 1. Methods. *J Int Neuropsychol Soc.* 2007 May;13(3):517-25.
- Logothetis NK. What we can do and what we cannot do with fMRI. *Nature.* 2008 Jun 12;453(7197):869-78.
- Logothetis NK, Pauls J, Augath M, Trinath T, Oeltermann A. Neurophysiological investigation of the basis of the fMRI signal. *Nature.* 2001 Jul 12;412(6843):150-7.
- Lontis ER, Voigt M, Struijk JJ. Focality assessment in transcranial magnetic stimulation with double and cone coils. *J Clin Neurophysiol.* 2006 Oct;23(5):462-71.
- Lotze M, Kaethner RJ, Erb M, Cohen LG, Grodd W, Topka H. Comparison of representational maps using functional magnetic resonance imaging and transcranial magnetic stimulation. *Clin Neurophysiol.* 2003 Feb;114(2):306-12.
- Lotze M, Markert J, Sauseng P, Hoppe J, Plewnia C, Gerloff C. The role of multiple contralesional motor areas for complex hand movements after internal capsular lesion. *J Neurosci.* 2006 May 31;26(22):6096-102.
- Loubinoux I, Carel C, Pariente J, Dechaumont S, Albucher JF, Marque P, et al. Correlation between cerebral reorganization and motor recovery after subcortical infarcts. *Neuroimage.* 2003 Dec;20(4):2166-80.
- Luh WM, Wong EC, Bandettini PA, Hyde JS. QUIPSS II with thin-slice T1I periodic saturation: a method for improving accuracy of quantitative perfusion imaging using pulsed arterial spin labeling. *Magn Reson Med.* 1999 Jun;41(6):1246-54.
- Luh WM, Wong EC, Bandettini PA, Ward BD, Hyde JS. Comparison of simultaneously measured perfusion and BOLD signal increases during brain activation with T(1)-based tissue identification. *Magn Reson Med.* 2000 Jul;44(1):137-43.
- Maccabee PJ, Amassian VE, Eberle LP, Cracco RQ. Magnetic coil stimulation of straight and bent amphibian and mammalian peripheral nerve in vitro: locus of excitation. *J Physiol.* 1993 Jan;460:201-19.
- Maier MA, Armand J, Kirkwood PA, Yang HW, Davis JN, Lemon RN. Differences in the corticospinal projection from primary motor cortex and supplementary motor area to macaque upper limb motoneurons: an anatomical and electrophysiological study. *Cereb Cortex.* 2002 Mar;12(3):281-96.
- Malcolm MP, Triggs WJ, Light KE, Gonzalez Rothi LJ, Wu S, Reid K, et al. Repetitive transcranial magnetic stimulation as an adjunct to constraint-induced therapy: an exploratory randomized controlled trial. *Am J Phys Med Rehabil.* 2007 Sep;86(9):707-15.

- Manganotti P, Patuzzo S, Cortese F, Palermo A, Smania N, Fiaschi A. Motor disinhibition in affected and unaffected hemisphere in the early period of recovery after stroke. *Clin Neurophysiol.* 2002 Jun;113(6):936-43.
- Mansfield P, Grannell PK. NMR 'diffraction' in solids? *J Phys C: Solid State Phys.* 1973 Nov;22(6):L422-L426.
- Mansur CG, Fregni F, Boggio PS, Riberto M, Gallucci-Neto J, Santos CM, et al. A sham stimulation-controlled trial of rTMS of the unaffected hemisphere in stroke patients. *Neurology.* 2005 May 24;64(10):1802-4.
- Marshall RS, Perera GM, Lazar RM, Krakauer JW, Constantine RC, DeLaPaz RL. Evolution of cortical activation during recovery from corticospinal tract infarction. *Stroke.* 2000 Mar;31(3):656-61.
- Matelli M, Luppino G, Rizzolatti G. Patterns of cytochrome oxidase activity in the frontal agranular cortex of the macaque monkey. *Behav Brain Res.* 1985 Nov-Dec;18(2):125-36.
- Mattay VS, Callicott JH, Bertolino A, Santha AK, Van Horn JD, Tallent KA, et al. Hemispheric control of motor function: a whole brain echo planar fMRI study. *Psychiatry Res.* 1998 Jul 15;83(1):7-22.
- Mattay VS, Weinberger DR. Organization of the human motor system as studied by functional magnetic resonance imaging. *Eur J Radiol.* 1999 May;30(2):105-14.
- Mayka MA, Corcos DM, Leurgans SE, Vaillancourt DE. Three-dimensional locations and boundaries of motor and premotor cortices as defined by functional brain imaging: a meta-analysis. *Neuroimage.* 2006 Jul 15;31(4):1453-74.
- McGuire PK, Bates JF, Goldman-Rakic PS. Interhemispheric integration: I. Symmetry and convergence of the corticocortical connections of the left and the right principal sulcus (PS) and the left and the right supplementary motor area (SMA) in the rhesus monkey. *Cereb Cortex.* 1991 Sep-Oct;1(5):390-407.
- Mills KR, Boniface SJ, Schubert M. Magnetic brain stimulation with a double coil: the importance of coil orientation. *Electroencephalogr Clin Neurophysiol.* 1992 Feb;85(1):17-21.
- Mintzopoulos D, Astrakas LG, Khanicheh A, Konostas AA, Singhal A, Moskowitz MA, et al. Connectivity alterations assessed by combining fMRI and MR-compatible hand robots in chronic stroke. *Neuroimage.* 2009 Aug;47 Suppl 2:T90-7.
- Modugno N, Curra A, Conte A, Inghilleri M, Fofi L, Agostino R, et al. Depressed intracortical inhibition after long trains of subthreshold repetitive magnetic stimuli at low frequency. *Clin Neurophysiol.* 2003 Dec;114(12):2416-22.
- Monet P, Franc J, Brasseur A, Desblache J, Saliou G, Deramond H, et al. [Arterial spin labeling: state of the art]. *J Radiol.* 2009 Sep;90(9 Pt 1):1031-7.
- Muller-Dahlhaus JF, Orekhov Y, Liu Y, Ziemann U. Interindividual variability and age-dependency of motor cortical plasticity induced by paired associative stimulation. *Exp Brain Res.* 2008 May;187(3):467-75.
- Murase N, Duque J, Mazzocchio R, Cohen LG. Influence of interhemispheric interactions on motor function in chronic stroke. *Ann Neurol.* 2004 Mar;55(3):400-9.
- Nair DG, Hutchinson S, Fregni F, Alexander M, Pascual-Leone A, Schlaug G. Imaging correlates of motor recovery from cerebral infarction and their physiological significance in well-recovered patients. *Neuroimage.* 2007 Jan 1;34(1):253-63.
- Nelles G. Funktionserholung nach Schlaganfall. In: Schneider F, Fink GR, editors, *Funktionelle MRT in Psychiatrie und Neurologie.* Heidelberg: Springer; 2007. p. 491-500.
- Newton JM, Ward NS, Parker GJ, Deichmann R, Alexander DC, Friston KJ, et al. Non-invasive mapping of corticofugal fibres from multiple motor areas--relevance to stroke recovery. *Brain.* 2006 Jul;129(Pt 7):1844-58.

- Norris DG. High field human imaging. *J Magn Reson Imaging*. 2003 Nov;18(5):519-29.
- Norris DG, Zysset S, Mildner T, Wiggins CJ. An investigation of the value of spin-echo-based fMRI using a Stroop color-word matching task and EPI at 3 T. *Neuroimage*. 2002 Mar;15(3):719-26.
- Nowak DA, Bosl K, Podubecka J, Carey JR. Noninvasive brain stimulation and motor recovery after stroke. *Restor Neurol Neurosci*. 2010 Aug;28(4):531-44.
- Nowak DA, Grefkes C, Dafotakis M, Eickhoff S, Kust J, Karbe H, et al. Effects of low-frequency repetitive transcranial magnetic stimulation of the contralesional primary motor cortex on movement kinematics and neural activity in subcortical stroke. *Arch Neurol*. 2008 Jun;65(6):741-7.
- Oberman L, Edwards D, Eldaief M, Pascual-Leone A. Safety of Theta Burst Transcranial Magnetic Stimulation: A Systematic Review of the Literature. *J Clin Neurophysiol*. 2011 Feb;28(1):67-74.
- Oja JM, Gillen J, Kauppinen RA, Kraut M, van Zijl PC. Venous blood effects in spin-echo fMRI of human brain. *Magn Reson Med*. 1999 Oct;42(4):617-26.
- Oldfield RC. The assessment and analysis of handedness: the Edinburgh inventory. *Neuropsychologia*. 1971 Mar;9(1):97-113.
- Opitz A, Windhoff M, Heidemann RM, Turner R, Thielscher A. How the brain tissue shapes the electric field induced by transcranial magnetic stimulation. *Neuroimage*. 2011 Jul 1. [Epub ahead of print]
- Pal PK, Hanajima R, Gunraj CA, Li JY, Wagle-Shukla A, Morgante F, et al. Effect of low-frequency repetitive transcranial magnetic stimulation on interhemispheric inhibition. *J Neurophysiol*. 2005 Sep;94(3):1668-75.
- Pascual-Leone A, Valls-Sole J, Wassermann EM, Hallett M. Responses to rapid-rate transcranial magnetic stimulation of the human motor cortex. *Brain*. 1994 Aug;117 (Pt 4):847-58.
- Pauling L. The oxygen equilibrium of hemoglobin and its structural interpretation. *Proc Natl Acad Sci U S A*. 1935 Apr;21(4):186-191.
- Paus T, Jech R, Thompson CJ, Comeau R, Peters T, Evans AC. Transcranial magnetic stimulation during positron emission tomography: a new method for studying connectivity of the human cerebral cortex. *J Neurosci*. 1997 May 1;17(9):3178-84.
- Penfield W, Rasmussen T. *The cerebral cortex of Man: A Clinical Study of Localization of function*. New York: Macmillan; 1950.
- Penfield W, Welch K. The supplementary motor area of the cerebral cortex; a clinical and experimental study. *AMA Arch Neurol Psychiatry*. 1951 Sep;66(3):289-317.
- Pennisi G, Alagona G, Rapisarda G, Nicoletti F, Costanzo E, Ferri R, et al. Transcranial magnetic stimulation after pure motor stroke. *Clin Neurophysiol*. 2002 Oct;113(10):1536-43.
- Penny WD, Stephan KE, Mechelli A, Friston KJ. Comparing dynamic causal models. *Neuroimage*. 2004 Jul;22(3):1157-72.
- Perez MA, Lungholt BK, Nyborg K, Nielsen JB. Motor skill training induces changes in the excitability of the leg cortical area in healthy humans. *Exp Brain Res*. 2004 Nov;159(2):197-205.
- Picard N, Strick PL. Imaging the premotor areas. *Curr Opin Neurobiol*. 2001 Dec;11(6):663-72.
- Rademacher J, Burgel U, Geyer S, Schormann T, Schleicher A, Freund HJ, et al. Variability and asymmetry in the human precentral motor system. A cytoarchitectonic and myeloarchitectonic brain mapping study. *Brain*. 2001 Nov;124(Pt 11):2232-58.

- Rao SM, Binder JR, Bandettini PA, Hammeke TA, Yetkin FZ, Jesmanowicz A, et al. Functional magnetic resonance imaging of complex human movements. *Neurology*. 1993 Nov;43(11):2311-8.
- Rapisarda G, Bastings E, de Noordhout AM, Pennisi G, Delwaide PJ. Can motor recovery in stroke patients be predicted by early transcranial magnetic stimulation? *Stroke* 1996 Dec;27(12):2191-6.
- Rathore SS, Hinn AR, Cooper LS, Tyroler HA, Rosamond WD. Characterization of incident stroke signs and symptoms: findings from the atherosclerosis risk in communities study. *Stroke*. 2002 Nov;33(11):2718-21.
- Rehme AK, Eickhoff SB, Wang LE, Fink GR, Grefkes C. Dynamic causal modeling of cortical activity from the acute to the chronic stage after stroke. *Neuroimage*. 2011a Apr 1;55(3):1147-58.
- Rehme AK, Fink GR, von Cramon DY, Grefkes C. The role of the contralesional motor cortex for motor recovery in the early days after stroke assessed with longitudinal fMRI. *Cereb Cortex*. 2011b Apr;21(4):756-68.
- Reis J, Swayne OB, Vandermeeren Y, Camus M, Dimyan MA, Harris-Love M, et al. Contribution of transcranial magnetic stimulation to the understanding of cortical mechanisms involved in motor control. *J Physiol*. 2008 Jan 15;586(2):325-51.
- Richter W, Andersen PM, Georgopoulos AP, Kim SG. Sequential activity in human motor areas during a delayed cued finger movement task studied by time-resolved fMRI. *Neuroreport*. 1997 Mar 24;8(5):1257-61.
- Ridding MC, Rothwell JC. Is there a future for therapeutic use of transcranial magnetic stimulation? *Nat Rev Neurosci*. 2007 Jul;8(7):559-67.
- Ridding MC, Taylor JL, Rothwell JC. The effect of voluntary contraction on cortico-cortical inhibition in human motor cortex. *J Physiol*. 1995 Sep 1;487 (Pt 2):541-8.
- Rizzolatti G, Fogassi L, Gallese V. Motor and cognitive functions of the ventral premotor cortex. *Curr Opin Neurobiol*. 2002 Apr;12(2):149-54.
- Roebroeck A, Formisano E, Goebel R. Mapping directed influence over the brain using Granger causality and fMRI. *Neuroimage*. 2005 Mar;25(1):230-42.
- Rorden C, Karnath HO, Bonilha L. Improving lesion-symptom mapping. *J Cogn Neurosci*. 2007 Jul;19(7):1081-8.
- Rosenkranz K, Williamon A, Rothwell JC. Motorcortical excitability and synaptic plasticity is enhanced in professional musicians. *J Neurosci*. 2007 May 9;27(19):5200-6.
- Rosler KM, Roth DM, Magistris MR. Trial-to-trial size variability of motor-evoked potentials. A study using the triple stimulation technique. *Exp Brain Res*. 2008 May;187(1):51-9.
- Rossini PM, Barker AT, Berardelli A, Caramia MD, Caruso G, Cracco RQ, et al. Non-invasive electrical and magnetic stimulation of the brain, spinal cord and roots: basic principles and procedures for routine clinical application. Report of an IFCN committee. *Electroencephalogr Clin Neurophysiol*. 1994 Aug;91(2):79-92.
- Rossini PM, Caltagirone C, Castriota-Scanderbeg A, Cicinelli P, Del Gratta C, et al. Hand motor cortical area reorganization in stroke: a study with fMRI, MEG and TCS maps. *Neuroreport*. 1998 Jun 22;9(9):2141-6.
- Roth BJ, Basser PJ. A model of the stimulation of a nerve fiber by electromagnetic induction. *IEEE Trans Biomed Eng*. 1990 Jun;37(6):588-97.
- Rothwell JC, Thompson PD, Day BL, Boyd S, Marsden CD. Stimulation of the human motor cortex through the scalp. *Exp Physiol*. 1991 Mar;76(2):159-200.

- Rouiller EM, Babalian A, Kazennikov O, Moret V, Yu XH, Wiesendanger M. Transcallosal connections of the distal forelimb representations of the primary and supplementary motor cortical areas in macaque monkeys. *Exp Brain Res*. 1994;102(2):227-43.
- Salinas FS, Lancaster JL, Fox PT. 3D modeling of the total electric field induced by transcranial magnetic stimulation using the boundary element method. *Phys Med Biol*. 2009 Jun 21;54(12):3631-47.
- Sanes JN, Donoghue JP. Plasticity and primary motor cortex. *Annu Rev Neurosci*. 2000;23:393-415.
- Schaechter JD, Perdue KL, Wang R. Structural damage to the corticospinal tract correlates with bilateral sensorimotor cortex reorganization in stroke patients. *Neuroimage*. 2008 Feb 1;39(3):1370-82.
- Schambra HM, Sawaki L, Cohen LG. Modulation of excitability of human motor cortex (M1) by 1 Hz transcranial magnetic stimulation of the contralateral M1. *Clin Neurophysiol*. 2003 Jan;114(1):130-3.
- Schmahmann JD, Pandya DN. 2006. *Fiber pathways of the brain*. Oxford: Oxford University Press. 654 p.
- Schwenkreis P, Witscher K, Janssen F, Addo A, Dertwinkel R, Zenz M, et al. Influence of the N-methyl-D-aspartate antagonist memantine on human motor cortex excitability. *Neurosci Lett*. 1999 Aug 6;270(3):137-40.
- Seitz RJ, Hoflich P, Binkofski F, Tellmann L, Herzog H, Freund HJ. Role of the premotor cortex in recovery from middle cerebral artery infarction. *Arch Neurol*. 1998 Aug;55(8):1081-8.
- Sharma N, Baron JC, Rowe JB. Motor imagery after stroke: relating outcome to motor network connectivity. *Ann Neurol*. 2009 Nov;66(5):604-16.
- Shibasaki H, Sadato N, Lyshkow H, Yonekura Y, Honda M, Nagamine T, et al. Both primary motor cortex and supplementary motor area play an important role in complex finger movement. *Brain*. 1993 Dec;116 (Pt 6):1387-98.
- Shimizu T, Hosaki A, Hino T, Sato M, Komori T, Hirai S, et al. Motor cortical disinhibition in the unaffected hemisphere after unilateral cortical stroke. *Brain*. 2002 Aug;125(Pt 8):1896-907.
- Silva AC. Perfusion-based fMRI: insights from animal models. *J Magn Reson Imaging*. 2005 Dec;22(6):745-50.
- Silva AC, Williams DS, Koretsky AP. Evidence for the exchange of arterial spin-labeled water with tissue water in rat brain from diffusion-sensitized measurements of perfusion. *Magn Reson Med*. 1997 Aug;38(2):232-7.
- Smith SB. Preparing fMRI data for statistical analysis. In: Jezzard P, Matthews PM, Smith SB, editors. *Functional MRI: an introduction to methods*. New York: Oxford University Press; 2001. p. 229-41.
- Smith SM. Fast robust automated brain extraction. *Hum Brain Mapp*. 2002 Nov;17(3):143-55.
- Sparing R, Buelte D, Meister IG, Paus T, Fink GR. Transcranial magnetic stimulation and the challenge of coil placement: a comparison of conventional and stereotaxic neuronavigational strategies. *Hum Brain Mapp*. 2008 Jan;29(1):82-96.
- Sparing R, Hesse MD, Fink GR. Neuronavigation for transcranial magnetic stimulation (TMS): where we are and where we are going. *Cortex*. 2010 Jan;46(1):118-20.
- Stephan KE. On the role of general system theory for functional neuroimaging. *J Anat*. 2004 Dec;205(6):443-70.
- Stephan KE, Harrison LM, Kiebel SJ, David O, Penny WD, Friston KJ. Dynamic causal models of neural system dynamics: current state and future extensions. *J Biosci*. 2007 Jan;32(1):129-44.
- Stephan KE, Penny WD, Daunizeau J, Moran RJ, Friston KJ. Bayesian model selection for group studies. *Neuroimage*. 2009 Jul 15;46(4):1004-17.

- Stephan KE, Penny WD, Moran RJ, den Ouden HE, Daunizeau J, Friston KJ. Ten simple rules for dynamic causal modeling. *Neuroimage*. 2010 Feb 15;49(4):3099-109.
- Stinear CM, Barber PA, Smale PR, Coxon JP, Fleming MK, Byblow WD. Functional potential in chronic stroke patients depends on corticospinal tract integrity. *Brain*. 2007 Jan;130(Pt 1):170-80.
- Stinear CM, Byblow WD. Role of intracortical inhibition in selective hand muscle activation. *J Neurophysiol*. 2003 Apr;89(4):2014-20.
- Suppa A, Bologna M, Gilio F, Lorenzano C, Rothwell JC, Berardelli A. Preconditioning repetitive transcranial magnetic stimulation of premotor cortex can reduce but not enhance short-term facilitation of primary motor cortex. *J Neurophysiol*. 2008 Feb;99(2):564-70.
- Takeuchi N, Chuma T, Matsuo Y, Watanabe I, Ikoma K. Repetitive transcranial magnetic stimulation of contralesional primary motor cortex improves hand function after stroke. *Stroke*. 2005 Dec;36(12):2681-6.
- Takeuchi N, Tada T, Toshima M, Chuma T, Matsuo Y, Ikoma K. Inhibition of the unaffected motor cortex by 1 Hz repetitive transcranial magnetic stimulation enhances motor performance and training effect of the paretic hand in patients with chronic stroke. *J Rehabil Med*. 2008 Apr;40(4):298-303.
- Talagala SL, Noll DC. Functional MRI using steady-state arterial water labeling. *Magn Reson Med*. 1998 Feb;39(2):179-83.
- Talelli P, Greenwood RJ, Rothwell JC. Arm function after stroke: neurophysiological correlates and recovery mechanisms assessed by transcranial magnetic stimulation. *Clin Neurophysiol*. 2006 Aug;117(8):1641-59.
- Talelli P, Greenwood RJ, Rothwell JC. Exploring Theta Burst Stimulation as an intervention to improve motor recovery in chronic stroke. *Clin Neurophysiol*. 2007 Feb;118(2):333-42.
- Talelli P, Rothwell J. Does brain stimulation after stroke have a future? *Curr Opin Neurol*. 2006 Dec;19(6):543-50.
- Tanji J, Hoshi E. Premotor Areas. In: Binder MD, Hirokawa N, Windhorst U, editors. *Encyclopedia of Neuroscience*. Berlin Heidelberg: Springer; 2009. p. 925-33.
- Taub E, Miller NE, Novack TA, Cook EW, 3rd, Fleming WC, Nepomuceno CS, et al. Technique to improve chronic motor deficit after stroke. *Arch Phys Med Rehabil*. 1993 Apr;74(4):347-54.
- Terao Y, Ugawa Y, Sakai K, Miyauchi S, Fukuda H, Sasaki Y, et al. Localizing the site of magnetic brain stimulation by functional MRI. *Exp Brain Res*. 1998 Jul;121(2):145-52.
- Thickbroom GW, Byrnes ML, Archer SA, Mastaglia FL. Motor outcome after subcortical stroke: MEPs correlate with hand strength but not dexterity. *Clin Neurophysiol*. 2002 Dec;113(12):2025-9.
- Thielscher A, Wichmann FA. Determining the cortical target of transcranial magnetic stimulation. *Neuroimage*. 2009 Oct 1;47(4):1319-30.
- Thulborn KR, Chang SY, Shen GX, Voyvodic JT. High-resolution echo-planar fMRI of human visual cortex at 3.0 tesla. *NMR Biomed*. 1997 Jun-Aug;10(4-5):183-90.
- Tjandra T, Brooks JC, Figueiredo P, Wise R, Matthews PM, Tracey I. Quantitative assessment of the reproducibility of functional activation measured with BOLD and MR perfusion imaging: implications for clinical trial design. *Neuroimage*. 2005 Aug 15;27(2):393-401.
- Tomassini V, Jbabdi S, Klein JC, Behrens TE, Pozzilli C, Matthews PM, et al. Diffusion-weighted imaging tractography-based parcellation of the human lateral premotor cortex identifies dorsal and ventral subregions with anatomical and functional specializations. *J Neurosci*. 2007 Sep 19;27(38):10259-69.

- Traversa R, Cicinelli P, Bassi A, Rossini PM, Bernardi G. Mapping of motor cortical reorganization after stroke. A brain stimulation study with focal magnetic pulses. *Stroke*. 1997 Jan;28(1):110-7.
- Traversa R, Cicinelli P, Oliveri M, Giuseppina Palmieri M, Filippi MM, Pasqualetti P, et al. Neurophysiological follow-up of motor cortical output in stroke patients. *Clin Neurophysiol*. 2000 Sep;111(9):1695-703.
- Trompetto C, Assini A, Buccolieri A, Marchese R, Abbruzzese G. Motor recovery following stroke: a transcranial magnetic stimulation study. *Clin Neurophysiol*. 2000 Oct;111(10):1860-7.
- Turton A, Wroe S, Trepte N, Fraser C, Lemon RN. Contralateral and ipsilateral EMG responses to transcranial magnetic stimulation during recovery of arm and hand function after stroke. *Electroencephalogr Clin Neurophysiol*. 1996 Aug;101(4):316-28.
- Ugawa Y, Day BL, Rothwell JC, Thompson PD, Merton PA, Marsden CD. Modulation of motor cortical excitability by electrical stimulation over the cerebellum in man. *J Physiol*. 1991 Sep;441:57-72.
- Uludag K, Muller-Bierl B, Ugurbil K. An integrative model for neuronal activity-induced signal changes for gradient and spin echo functional imaging. *Neuroimage*. 2009 Oct 15;48(1):150-65.
- Van Der Werf YD, Paus T. The neural response to transcranial magnetic stimulation of the human motor cortex. I. Intracortical and cortico-cortical contributions. *Exp Brain Res*. 2006 Nov;175(2):231-45.
- Vickery RM, Morris SH, Bindman LJ. Metabotropic glutamate receptors are involved in long-term potentiation in isolated slices of rat medial frontal cortex. *J Neurophysiol*. 1997 Dec;78(6):3039-46.
- Walsh V, Cowey A. Transcranial magnetic stimulation and cognitive neuroscience. *Nat Rev Neurosci*. 2000 Oct;1(1):73-9.
- Wang LE, Fink GR, Diekhoff S, Rehme AK, Eickhoff SB, Grefkes C. Noradrenergic enhancement improves motor network connectivity in stroke patients. *Ann Neurol*. 2011 Feb;69(2):375-88.
- Ward NS, Brown MM, Thompson AJ, Frackowiak RS. Neural correlates of motor recovery after stroke: a longitudinal fMRI study. *Brain*. 2003a Nov;126(Pt 11):2476-96.
- Ward NS, Brown MM, Thompson AJ, Frackowiak RS. Neural correlates of outcome after stroke: a cross-sectional fMRI study. *Brain*. 2003b Jun;126(Pt 6):1430-48.
- Ward NS, Newton JM, Swayne OB, Lee L, Frackowiak RS, Thompson AJ, et al. The relationship between brain activity and peak grip force is modulated by corticospinal system integrity after subcortical stroke. *Eur J Neurosci*. 2007 Mar;25(6):1865-73.
- Ward NS, Newton JM, Swayne OB, Lee L, Thompson AJ, Greenwood RJ, et al. Motor system activation after subcortical stroke depends on corticospinal system integrity. *Brain*. 2006 Mar;129(Pt 3):809-19.
- Wassermann EM. Risk and safety of repetitive transcranial magnetic stimulation: report and suggested guidelines from the International Workshop on the Safety of Repetitive Transcranial Magnetic Stimulation, June 5-7, 1996. *Electroencephalogr Clin Neurophysiol*. 1998 Jan;108(1):1-16.
- Wassermann EM, McShane LM, Hallett M, Cohen LG. Noninvasive mapping of muscle representations in human motor cortex. *Electroencephalogr Clin Neurophysiol*. 1992 Feb;85(1):1-8.
- Wassermann EM, Wang B, Zeffiro TA, Sadato N, Pascual-Leone A, Toro C, et al. Locating the motor cortex on the MRI with transcranial magnetic stimulation and PET. *Neuroimage*. 1996 Feb;3(1):1-9.
- Weder B, Knorr U, Herzog H, Nebeling B, Kleinschmidt A, Huang Y, et al. Tactile exploration of shape after subcortical ischaemic infarction studied with PET. *Brain*. 1994 Jun;117 (Pt 3):593-605.
- Weiller C, Chollet F, Friston KJ, Wise RJ, Frackowiak RS. Functional reorganization of the brain in recovery from striatocapsular infarction in man. *Ann Neurol*. 1992 May;31(5):463-72.

- Weimar C, Ziegler A, König IR, Diener HC. Predicting functional outcome and survival after acute ischemic stroke. *J Neurol*. 2002 Jul;249(7):888-95.
- Weishaupt D, Köchli VD, Marincek B, editors. *Wie funktioniert MRI?* Heidelberg: Springer; 2006.
- Werhahn KJ, Conforto AB, Kadom N, Hallett M, Cohen LG. Contribution of the ipsilateral motor cortex to recovery after chronic stroke. *Ann Neurol*. 2003 Oct;54(4):464-72.
- Westlake KP, Nagarajan SS. Functional connectivity in relation to motor performance and recovery after stroke. *Front Syst Neurosci*. 2011 Mar;16;5:8.
- Weyh T, Siebner HR. Hirnstimulation – Technische Grundlagen. In: Siebner HR, Ziemann U, editors. *Das TMS-Buch*. Heidelberg: Springer; 2007. p. 17-26.
- White LE, Andrews TJ, Hulette C, Richards A, Groelle M, Paydarfar J, et al. Structure of the human sensorimotor system. I: Morphology and cytoarchitecture of the central sulcus. *Cereb Cortex*. 1997 Jan-Feb;7(1):18-30.
- Williams DS, Detre JA, Leigh JS, Koretsky AP. Magnetic resonance imaging of perfusion using spin inversion of arterial water. *Proc Natl Acad Sci U S A*. 1992 Jan 1;89(1):212-6.
- Wilson SA, Thickbroom GW, Mastaglia FL. Comparison of the magnetically mapped corticomotor representation of a muscle at rest and during low-level voluntary contraction. *Electroencephalogr Clin Neurophysiol*. 1995 Oct;97(5):246-50.
- Wintermark M, Sesay M, Barbier E, Borbely K, Dillon WP, Eastwood JD, et al. Comparative overview of brain perfusion imaging techniques. *Stroke*. 2005 Sep;36(9):e83-99.
- Wittenberg GF, Chen R, Ishii K, Bushara KO, Eckloff S, Croarkin E, et al. Constraint-induced therapy in stroke: magnetic-stimulation motor maps and cerebral activation. *Neurorehabil Neural Repair*. 2003 Mar;17(1):48-57.
- Wohlschläger A, Kellermann T, Habel U. Datenanalyse: Vorverarbeitung, Statistik und Auswertung. In: Schneider F, Fink GR, editors. *Funktionelle MRT in Psychiatrie und Neurologie*. Heidelberg: Springer; 2007. p. 133-39.
- Wong EC, Buxton RB, Frank LR. Quantitative imaging of perfusion using a single subtraction (QUIPSS and QUIPSS II). *Magn Reson Med*. 1998 May;39(5):702-8.
- Woolrich MW, Ripley BD, Brady M, Smith SM. Temporal autocorrelation in univariate linear modeling of fMRI data. *Neuroimage*. 2001 Dec;14(6):1370-86.
- Worsley KJ, Evans AC, Marrett S, Neelin P. A three-dimensional statistical analysis for CBF activation studies in human brain. *J Cereb Blood Flow Metab*. 1992 Nov;12(6):900-18.
- Ye FQ, Smith AM, Yang Y, Duyn J, Mattay VS, Ruttimann UE, et al. Quantitation of regional cerebral blood flow increases during motor activation: a steady-state arterial spin tagging study. *Neuroimage*. 1997 Aug;6(2):104-12.
- Yongbi MN, Fera F, Yang Y, Frank JA, Duyn JH. Pulsed arterial spin labeling: comparison of multisection baseline and functional MR imaging perfusion signal at 1.5 and 3.0 T: initial results in six subjects. *Radiology*. 2002 Feb;222(2):569-75.
- Yousry TA, Schmid UD, Alkadhi H, Schmidt D, Peraud A, Büttner A, et al. Localization of the motor hand area to a knob on the precentral gyrus. A new landmark. *Brain*. 1997 Jan;120 (Pt 1):141-57.
- Zappe AC, Pfeuffer J, Merkle H, Logothetis NK, Goense JB. The effect of labeling parameters on perfusion-based fMRI in nonhuman primates. *J Cereb Blood Flow Metab*. 2008 Mar;28(3):640-52.
- Ziemann U. Improving disability in stroke with RTMS. *Lancet Neurol*. 2005 Aug;4(8):454-5.

- Ziemann U, Chen R, Cohen LG, Hallett M. Dextromethorphan decreases the excitability of the human motor cortex. *Neurology*. 1998a Nov;51(5):1320-4.
- Ziemann U, Lonnecker S, Steinhoff BJ, Paulus W. The effect of lorazepam on the motor cortical excitability in man. *Exp Brain Res*. 1996a Apr;109(1):127-35.
- Ziemann U, Rothwell JC, Ridding MC. Interaction between intracortical inhibition and facilitation in human motor cortex. *J Physiol*. 1996b Nov 1;496 (Pt 3):873-81.
- Ziemann U, Tergau F, Wassermann EM, Wischer S, Hildebrandt J, Paulus W. Demonstration of facilitatory I wave interaction in the human motor cortex by paired transcranial magnetic stimulation. *J Physiol*. 1998b Aug 15;511 (Pt 1):181-90.

8 Acknowledgements

I would like to thank my supervisor PD Dr. Christian Grefkes for the trust that he placed in me, as well as his ongoing encouragement, guidance, and support, which enabled me to conduct this research. I also owe my gratitude to Professor Dr. Gereon Fink and Professor Dr. Ansgar Büschges for professional advice and fruitful discussions. I am indebted to many others who contributed to this work: Professor Dr. Kamil Uludağ, Dr. Mustafa Cavuşoğlu, Dr. Marc Tittgemeyer, Professor Dr. Yves von Cramon, Professor Dr. Roland Sparing, Eva-Maria Hohl, Kurt Wittenberg, Jochen Michely, Ricarda Strunk, Dr. Anne Kathrin Rehme, Corina Melzer, Dr. Ling Wang, and Simone Steinmeier. In particular, I would like to thank Dr. Anna-Sophia Sarfeld – without her I would not have been able to complete this research. I am thankful to Franziska Flick, Melanie Hoffmann, Sabine Maier, and Simone Zander for advice and distractions from research. I am deeply grateful to my parents, who encouraged me to go my own way and made a high *degree of efficiency* possible. My deepest thanks go to Christoph Krebs for his patient love, which makes me live here and now.

9 Erklärung

Ich versichere, dass ich die von mir vorgelegte Dissertation selbständig angefertigt, die benutzten Quellen und Hilfsmittel vollständig angegeben und die Stellen der Arbeit – einschließlich Tabellen, Karten und Abbildungen –, die anderen Werken im Wortlaut oder dem Sinn nach entnommen sind, in jedem Einzelfall als Entlehnung kenntlich gemacht habe; dass diese Dissertation noch keiner anderen Fakultät oder Universität zur Prüfung vorgelegen hat; dass sie – abgesehen von unten angegebenen Teilpublikationen – noch nicht veröffentlicht worden ist sowie, dass ich eine solche Veröffentlichung vor Abschluss des Promotionsverfahrens nicht vornehmen werde. Die Bestimmungen der Promotionsordnung sind mir bekannt. Die von mir vorgelegte Dissertation ist von Herrn PD Dr. Christian Grefkes betreut worden.

Teilpublikation:

Diekhoff S, Uludağ K, Sparing R, Tittgemeyer M, Cavuşoğlu M, von Cramon DY, Grefkes C (2011) Functional localization in the human brain: Gradient-Echo, Spin-Echo, and arterial spin-labeling fMRI compared with neuronavigated TMS. *Hum Brain Mapp* 32(3):341-57.

Köln, den 22.08.2011